

The Effects of Temperature on the Growth and Competition of Phytoplankton

Philipp Siegel

A thesis submitted for the degree of
Doctor of Philosophy in Biological Sciences

School of Life Sciences

University of Essex

April 2020

Thesis Abstract

With aquatic environments changing in the Anthropocene at unprecedented rates, phytoplankton are under enormous abiotic pressure to cope with environmental conditions they did not encounter in the past. In this thesis, I investigated the growth and competitive response of algae to changes in temperature and nitrogen concentrations across high resolution temperature gradients. The first three data chapters of this thesis concentrated on the response of isolated algae species to changes in their thermal environment. Focus lay on whether thermal adaptations could occur when culturing algae for extended periods of time at elevated temperatures. My results showed that warming does not necessarily lead to thermal adaptation and that the responses will not be as simple as a mere shift in thermal performance curves towards warmer temperatures. For the last two data chapters I focused on mixed populations of the diatoms *Phaeodactylum tricornutum* and *Thalassiosira pseudonana* and how they compete across stable and fluctuating temperatures under high and low nitrate concentrations. I could show that under stable thermal conditions, the outcome of competition could be well predicted; both in nutrient-replete and nitrogen-limited conditions, but those predictions became less reliable under fluctuating temperatures. This thesis provides further insight into adaptation and competition in phytoplankton communities faced with environmental change. The gained knowledge can provide a better understanding of some of the uncertainties and limitations surrounding the prediction of future phytoplankton community composition from single species responses and teaches us to be cautious when it comes to extrapolating experimental results from the laboratory to natural environments.

Statement of Authorship

I hereby declare that I wrote this PhD thesis myself without sources other than those indicated herein.

Ph. Siegel

Colchester, 20.4.2020

Philipp Siegel

Acknowledgements

First and foremost I would like to thank my supervisors Richard Geider and Etienne Low-Décarie for accepting me as their PhD student and guiding my scientific life through the past years. Your knowledge and help has always been impressive.

I would also like to say a big thank you to Kirralee Baker who has basically been my third supervisor and this thesis would not be the same without her.

Thank you to all the laboratory technicians at Essex University who have helped me to get my experiments up and running and for fixing all the things that I broke. Specifically I would like to thank Tania Cresswell-Maynard, Amanda Clements, Sue Corbett, John Green, and Phil Davey.

Thank you to the nice people at TomAlgae who have given me the chance to work with them and allowed me to live in Belgium and taught me how to apply my research knowledge on an industrial scale and showed me what can be done with algae other than laboratory experiments.

Thank you to my family, all the good friends, housemates, and people in general that I have met throughout this PhD and made the time enjoyable.

Table of Contents

Thesis Abstract	ii
Statement of Authorship	iii
Acknowledgements	iv
Table of Contents	v
List of Figures	ix
List of Supplementary Figures	xiv
List of Tables.....	xviii
List of Supplementary Tables	xix
Declaration of the Contribution to Each Chapter	xx
1. CHAPTER 1: GENERAL INTRODUCTION.....	1
1.1 Phytoplankton communities	1
1.2 Changing aquatic environments	2
1.3 Phytoplankton response to changing environmental conditions	5
1.3.1 Responses to individual drivers	6
1.3.2 Responses to multiple drivers.....	11
1.3.3 Evolutionary adaptation to environmental change.....	13
1.4 Phytoplankton Competition and Nutrient Availability.....	14
1.4.1 Physiological models explaining competitive success	17
1.5 Research Objectives and Thesis Outline.....	22
2. CHAPTER 2: THE SEARCH FOR THERMAL ADAPTATION IN LONG-TERM PHYTOPLANKTON CULTURES.....	25
2.1 Abstract	25
2.2 Introduction.....	26
2.3 Materials & Methods	31
2.3.1 Culturing of algae	31
2.3.2 Measurement of Algal Growth	32

2.3.3 Thermal Performance Curves	33
2.4 Results.....	37
2.4.1 Test of thermal adaptation in long-term culture lines from the Essex culture collection	37
2.4.2 Previously evolved lines of <i>T. pseudonana</i> (positive control)	40
2.4.3 Comparison of imposed selection on species.....	41
2.5 Discussion.....	43
2.5.1 Thermal niche of studied species	43
2.5.2 Effect of culturing methods on thermal adaptation.....	45
2.5.3 Limitations of the Study.....	47
2.6 Conclusion	48
2.8 Supplementary Material	49
2.8.1 AIC scores for TPC model fits to growth rate data of different species	49
3. CHAPTER 3: RATE MEASUREMENTS OF ALGAL RESPIRATION AND PHOTOSYNTHESIS AS INDICATORS OF THERMAL ADAPTATION.....	51
3.1 Abstract.....	51
3.2 Introduction.....	52
3.3 Materials & Methods	54
3.3.1 Long-term algal cultures	54
3.3.2 Rate measurements of Photosynthesis and Respiration.....	54
3.3.3 Statistical Testing	56
3.4 Results.....	57
3.5 Discussion.....	59
3.6 Conclusion	63
4. CHAPTER 4: HIGH PREDICTABILITY OF DIRECT COMPETITION BETWEEN MARINE DIATOMS UNDER DIFFERENT TEMPERATURES AND NUTRIENT STATES	64
4.1 Abstract.....	64
4.2 Introduction.....	65
4.3 Material & Methods.....	68
4.3.1 Competition Experiments	68
4.3.2 Chlorophyll Fluorescence.....	74

4.3.3 Mixed Population Species Frequency Counts.....	75
4.3.4 NO _x -Assay (Total nitrite/nitrate analysis)	75
4.3.5 Flow Cytometry	75
4.3.6 Data Analysis	76
4.4 Results	82
4.4.1 Differences in temperature and nutrient response between species in monoculture ...	82
4.4.2 Competition across assay temperatures	87
4.4.3 Predictability of change in competitive ability	90
4.5 Discussion	92
4.5.1 Reduced nitrogen impacts competition across temperatures	92
4.5.2 Predictability of competition under environmental change	95
4.5.3 Wider implications of the study	97
4.6 Conclusion	98
4.7 Supplementary Material	99
4.7.1 Supplementary Tables	99
4.7.2 Supplementary Figures	108
5. CHAPTER 5: INFLUENCE OF TEMPERATURE FLUCTUATIONS ON THE STABLE COEXISTENCE OF TWO COMMON PHYTOPLANKTON SPECIES.....	125
5.1 Abstract	125
5.2 Introduction.....	126
5.2.1 Jensen’s Inequality & Scale Transition Theory.....	126
5.2.2 Phytoplankton in Fluctuating Thermal Environments	128
5.3 Material and Methods	131
5.3.1 Competition Experiments	132
5.3.2 Competition Coefficients	136
5.4 Results	139
5.4.1 Pre-fluctuation period.....	139
5.4.2 Fluctuation period.....	139
5.4.3 Post-fluctuation period	142
5.5 Discussion	142
5.5.1 Limitations of the study	146
5.5.2 Implications of Findings	148
5.6 Conclusion	150

5.7 Supplementary Material	151
5.7.1 Power analysis to determine experimental design	151
5.7.2 Supplementary Figures	153
6. CHAPTER 6: GENERAL DISCUSSION.....	163
6.1 Future Responses and the Role of Adaptations.....	164
6.2 Phytoplankton Competition Under Future Climate Change	169
6.3 Consequences for Ecosystem Functioning.....	173
6.4 Conclusion & Future Directions	180
7. LITERATURE CITED IN THIS THESIS.....	183

List of Figures

- Figure 1.1:** Schematic illustration of resource competition and competitive exclusion in relation to nutrient supply. Solid lines indicate zero net growth isoclines (ZNGIs) for species A (blue lines) and species B (orange lines), indicating the minimum concentrations of nutrients X (Vertical lines) and Y (horizontal lines) that they require to grow at a rate where population increases and decreases cancel each other out and equilibrium conditions exist. In equilibrium conditions cell death rate (cell loss) equals out the cell growth rate and the isocline does not move. Under non-equilibrium conditions, for instance if the cells are growing exponentially, the isocline can move up for nutrient X, and to the right for nutrient Y. If loss rate decreases (i.e. growth conditions are beneficial and growth rates are high), minimum nutrient requirements will become lower. Circled numbers indicate nutrient supply points. (A) Three different nutrient supply scenarios are presented. Species A has the lower nutrient requirements for both nutrients X and Y. At nutrient supply level 1, concentrations of X and Y are too low for neither species to grow. At nutrient level 2, nutrient levels are too low for species B, but A can survive. At concentration level 3, the nutrient supply concentration is also high enough for species B to survive. However species A would deplete the concentration below a level that is suitable for B, causing its extinction. (B) In this scenario, the ZNGIs of both species are altered and each of them has the lowest resource requirement for one of the two nutrients (X for species A, and Y for species B). At nutrient supply level 1, both species can once again not thrive because supply concentrations are too low. At nutrient supply levels 2, only species A, whereas at level 3 only species B would thrive. Nutrient levels 5 and 6 are high enough for both species to survive if they would be in isolation. As mixed cultures, species A would however outcompete species B over time at supply level 5, and vice versa at supply level 6. At nutrient supply level 4 enough nutrients would be present for both species to co-exist. Illustration adapted from Begon et al. (2006).16
- Figure 1.2:** Graphical representation of the Monod equation. S = substrate concentration, μ_S = growth rate at substrate concentration S , μ_{max} = maximum growth rate, K_S = half saturation constant for growth. The equation describes the relationship between external substrate concentrations and growth rates of microorganisms. The higher the ambient concentration of a substrate S , the larger will be its steady state growth rate, until a horizontal asymptote for μ_{max} is approached.....18
- Figure 2.1:** Typical thermal performance curve along a temperature gradient. T_{opt} = Optimum Temperature, CT_{min} = Critical minimum temperature, CT_{max} = Critical maximum temperature. Adapted from Krenek et al. (2012).....27
- Figure 2.2:** Conceptual figure of potential changes in thermal performance curves. Original curve (blue) could extend its growth range (red), shift as a whole towards other temperatures (orange), or change its slope around cardinal temperatures (green).....28

Figure 2.3: Mean thermal performance of 3 phytoplankton species with experimental lines grown at 15°C (blue) and 20°C (orange) source temperatures. Model fits and the corresponding optimum temperatures predicted from those model fits are depicted for *D. tertiolecta* lines (A & B), for *P. provasolii* lines (C & D), and for *C. mulleri* lines (E & F). Single points underlying the TPC plots are single growth rates measured along the investigated assay temperature gradient. Grey-shaded area around the mean TPC of each line denotes one standard deviation, calculated from single replicate model fits. For the optimum growth temperatures of the *P. provasolii* lines, a significant difference was found that did not follow the expectation of lines having their T_{opt} closer to their source environment. For the other two species, no significant differences were found.....40

Figure 2.4: Mean thermal performance of *T. pseudonana* lines evolved under cold assay temperatures at 15°C (blue), normal initial culture temperatures 22°C (green), and warm assay temperature 26°C (orange). (A) Mean TPCs of lines grown in a tube thermoblock. Single points are measured growth rates at the assay temperatures onto which the growth models were fit. Colour-shaded areas indicate one standard deviation calculated from single replicate model fits around the mean TPC. (B) Optimum temperatures estimated from model fits.41

Figure 2.5: (A) Comparison of TPCs of the parent lines of *D. tertiolecta*, *C. mulleri*, *P. provasolii*, and *T. pseudonana*. (B) Imposed selection pressure on the species in % of their daily growth rates.....42

Figure 3.1: Measurements of respiration and net photosynthesis in 4 phytoplankton species with two culture lines each (15 °C and 20 °C) (n = 4 for each line). Blue boxplots denote results of the lines coming from a 15 °C source environment, red boxplots those coming from a 20 °C source environment. All lines were tested for their oxygen consumption (respiration) and net oxygen production (net photosynthesis), measured both at 15 °C (blue-shaded areas) and 20 °C (red-shaded areas) to investigate whether lines would have higher rates at their source temperature. In all species, significant differences were found between the rates measured in the dark (respiration) and in the light (net photosynthesis). However, within one light regime no significant differences were found for any of the lines or species. Note the difference in scale on the y-axis, as species had varying overall rates.....58

Figure 3.2: Conceptual figure to illustrate the idea that attempting to detect thermal adaptation at specific assay temperatures might be flawed. In this example a rate Y was measured at an assay temperature X. The measured rate at supra-optimal temperatures in a non-adapted TPC (pink) might be the same as the rate in an adapted TPC (green) where X would constitute a sub-optimal temperature. The fact that thermal adaptation had occurred by a shift of the TPC towards warmer temperatures would not be detected, as rate measurements would remain the same.61

Figure 4.1: Simulation of semi-continuous cultures for obtaining and maintaining (A) nutrient replete (high N scenario) and (B) nutrient-limited (low N scenario) cultures. Simulation assumes cultures are already acclimated to the nutrient replete growth under defined

temperature, irradiance, etc. Assumes logistic growth with the nutrient replete growth rate = 1.4 d^{-1} , and carrying capacity = 1. Dilution is approximately a 10-fold in the high N scenario and 1.25-fold in the low N scenario. Solid lines are the culture density. In (A), the solid lines are interrupted to signify that for each dilution step, an aliquot of the assay culture was taken and pipetted into a fresh tube, whereas in (B) the assay culture remained in the same tube for the duration of the whole experiment, whereby 20% of culture was removed from an assay tube on a daily basis and topped up with fresh low N f/2 medium. Dashed line is the culture density that would be obtained in a batch culture undergoing logistic growth. Note that (A) is on a log-scale to represent that high N exponential cultures were kept at low densities far from reaching stationary phase, whereas (B) is on a linear scale.....70

Figure 4.2: Average temperature response curves depicting acclimated growth rates of *P. tricornutum* (red circles and solid line) and *T. pseudonana* (black squares and dashed line) under (A) high nitrate conditions ($n = 4$ and 3 respectively) and (B) of the initial acute growth rate (days 0 – 4) under low N conditions ($n = 2$ for both species). Shaded area denotes standard deviation of the average model calculated from replicate model fits. Symbols in (A) represent the growth rates from distinct biological replicates and were calculated from the average growth rates across dilution steps after the diatoms had acclimated to growth under assay conditions. Dotted line in (B) indicates $\ln(1/0.8)$, the dilution rate in these semi-continuous cultures; cell abundance would have declined in cultures with growth rates below this value which equates to a growth rate of 0.22 d^{-1} due to the daily dilution that was imposed by the sampling regime. Raw data used to calculate growth rates in the high nitrate ($882 \mu\text{M NO}_3^-$) medium (A) can be seen in Suppl. Fig. 4.1, data used to calculate growth rates in the low N ($55 \mu\text{M NO}_3^-$) medium (B) can be seen in Suppl. Fig. 7. Nonlinear model outputs of the single replicate models used to calculate the average model can found in Suppl. Tables 4.2 and 4.3, and single model fits on the individual growth replicates can be found in Suppl. Fig. 4.2 A and B.83

Figure 4.3: Comparison of (A) cardinal temperatures, and (B) maximum growth rates from thermal performance curve model fits for growth rates between *P. tricornutum* and *T. pseudonana* under high N and low N growth conditions. For *P. tricornutum* $n = 4$ in high N and $n = 2$ in low N. For *T. pseudonana* $n = 3$ in high N and $n = 2$ in low N.....84

Figure 4.4: (A) Temperature response curves of carrying capacity of *P. tricornutum* (red circles and solid line) and *T. pseudonana* (black squares and dashed line) under nitrogen-depleted conditions in the N-limited phase of semi-continuous culturing in the low N medium ($n = 2$ for both species). Shaded area denotes standard deviation of the average model calculated from replicate model fits. Symbols show the carrying capacities from distinct biological replicates across the assay temperature range. Raw data used to calculate carrying capacities can be seen in Suppl. Fig. 4.8. (B) Forward scatter (FSC) from flow cytometry data of the low N experiment across assay temperatures. FSC measurements depicted here were taken on the last day of replicate monocultures before they were mixed together for the competition experiment. The solid and dashed

lines are LOESS lines to visualise the U-shaped trend of the data across assay temperatures ($R^2 = 0.85$, and $RSE = 4.503$ for *P. tricornutum*; $R^2 = 0.97$, and $RSE = 3.378$ for *T. pseudonana*). LOESS was not used as a model to predict the relationship between temperature and cell size. Dotted line at 30 °C indicates the critical maximum temperature for *P. tricornutum* beyond which it could not sustain growth. (C) Correlation between carrying capacity K and log(FSC) for both species. Solid and dashed lines are linear models of the regression. Nonlinear model outputs of the single replicate models used to calculate the average model can be found in Suppl. Table 4.4 and single model fits on the individual growth replicates can be found in Suppl. Fig. 4.2C.85

Figure 4.5: Comparison of (A) cardinal temperatures, and (B) maximum carrying capacities from thermal performance curve model fits for carrying capacities between *P. tricornutum* and *T. pseudonana* in low N conditions ($n = 2$ for both species).86

Figure 4.6: Predicted (lines) and observed (symbols) competition coefficients between *P. tricornutum* and *T. pseudonana* across assay temperatures in (A) high N conditions, and (B) low N conditions. A coefficient of 0 indicates no competitive advantage for either species, and predicts stable co-existence under the assay conditions. At coefficients greater than 0, *P. tricornutum* has the competitive advantage, at coefficients below 0 *T. pseudonana* has the advantage. The further the competition coefficient deviates from 0, the stronger is the competition between the two species. In (A) the solid black line indicates predictions for competition coefficients made from monoculture growth rates. The solid blue line is the LOESS smooth to visualise the progression of all observed high N competition coefficients across temperatures ($R^2 = 0.97$, $RSE = 0.047$). Observed coefficients were calculated from changes in species frequencies over time in mixed cultures (data from Suppl. Fig. 4.10), calculated with equation [5]. Closed symbols represent the competition coefficients that were started when stock cultures were transferred to the temperature-gradient-block, open symbols those that were started two weeks later to investigate the potential effects of temperature acclimation. In (B) solid black line indicates predictions made from the initial exponential growth rate in low N medium for monocultures, whereas the dashed line indicates predictions made from monoculture carrying capacities across the temperature gradient. The solid blue line is the LOESS smooth to visualise the progression of all observed low N competition coefficients across temperatures ($R^2 = 0.86$, $RSE = 0.051$). Observed coefficients were calculated from changes in species frequencies over time in mixed cultures (data from Suppl. Fig. 4.11), calculated with equation [5]. Closed symbols represent competition replicates that were started at the onset of N-limitation, open symbols those that were started from monocultures that were cultured under N-limitation for an additional seven days.88

Figure 5.1: Schematic illustration for Jensen’s inequality / scale transition theory on a hypothetical environmental performance curve. When performance across an environmental gradient is non-linear, performance P2 at the average environment E2, is

not going to be the average value of performances P1 at environment E1 and P3 at environment E3.....127

Figure 5.2: Schematic timeline of the fluctuation experiments. The chronological set-up was the same for the high N and low N experiment. The only aspect that differed between the two experiments was the temperature at which both species could coexist, which was found to be 18.6 °C under high N conditions, and 25.2 °C under low N conditions. The experiments started off with a 10 day period during which *P. tricornutum* and *T. pseudonana* were cultured as mixed populations. This period was used to determine whether the two species could coexist and whether mixed populations could be considered as stable over time in regards to their species abundance ratios. After this initial period, temperature was fluctuated for 20 days (10 up and 10 down fluctuations). Temperature was changed every 24 hours. After the fluctuation period, temperature was re-stabilised for another 10 days to investigate whether the species abundance ratio at the end of the fluctuation period would remain stable.134

Figure 5.3: Predicted (lines) and observed (symbols) competition coefficients across fluctuation amplitudes in high N conditions (A) and low N conditions (B). Depending on which species would be predicted to win or would actually win, based on equations [1] and [2], competition coefficients could take on positive or negative values. Positive values would indicate *P. tricornutum* as the winning species, negative values would indicate *T. pseudonana* as the winning species. In (A), solid line is a locally estimated scatter plot smoothing (LOESS) line, and indicates predictions for competition coefficients calculated from monoculture growth rates with equation [1a]. Symbols are the observed competition coefficients calculated with equation [2]. Vertical dotted line distinguishes fluctuation amplitudes for which temperatures did not drop below a lethal cold temperature for *T. pseudonana* on the cold cycles from those that did (determined based on monoculture TPCs). In (B), solid LOESS line indicates predictions made from exponential phase of growth in low N medium, dashed LOESS line indicates predictions made from carrying capacities. Predictions were made with equations [1a] and [1b] respectively. Symbols indicate the observed competition coefficients in a fluctuating environment in low N medium calculated with equation [2]. Vertical dotted line in (B) separates fluctuation amplitudes that stayed below the critical lethal temperature determined from monoculture growth rates TPCs of *P. tricornutum* on the warm fluctuation days from those that did not, and dashed line indicates the same based on monoculture TPCs for carrying capacity, which indicated a lower CT_{max} . Grey shaded area indicates the region in which all *P. tricornutum* cells died after one 24-hour-cycle, based on Fv/Fm measurements of monocultures. In this fluctuation amplitude range only *T. pseudonana* was alive in mixed cultures after one day of fluctuations for the remainder of the competition experiment. Variations in competition coefficients in the grey-shaded area are therefore caused by manual counting error (see section 5.5.1 “Limitations of the study”). Note that although both scenarios (A) and (B) had the same assay fluctuation amplitudes, the mean temperatures from which fluctuations started were different, to

account for the fact that the temperature at which the two diatoms could co-exist stably over time depended on the amount of N in the growth medium. In high N conditions, the midpoint of the fluctuations lay at 18.6 °C, in the low N scenario it was at 25.2 °C. Also note the difference in y-axis scale between (A) and (B).....140

List of Supplementary Figures

Supplementary Figure 2.1: AIC scores of model fits to growth rate data of <i>D. tertiolecta</i>	49
Supplementary Figure 2.2: AIC scores of model fits to growth data of <i>P. provasolii</i>	49
Supplementary Figure 2.3: AIC scores of model fits to growth data of <i>C. mulleri</i>	50
Supplementary Figure 2.4: AIC scores of model fits to growth data of <i>T. pseudonana</i>	50
Supplementary Figure 4.1: Average $\ln(F_0)$ of exponentially growing <i>P. tricornutum</i> (n = 4) (red) and <i>T. pseudonana</i> (n = 3) (black) in the high N medium measured at the indicated assay temperatures across the temperature gradient. Individual slopes represent single dilution phases. Grey error bars denote 1 standard deviation.	108
Supplementary Figure 4.2: (A) Single TPC model fits for the two diatom species <i>P. tricornutum</i> in red (n = 4) and <i>T. pseudonana</i> in black (n = 4) from which average growth models for Figure 4.2A were calculated. The one <i>T. pseudonana</i> replicate that was omitted in the final analysis is plotted in blue. (B) Single TPC model fits for the two diatom species <i>P. tricornutum</i> in red (n = 2) and <i>T. pseudonana</i> in black (n = 2) from which average growth models for Figure 4.2B were calculated. (C) Single TPC model fits for the two diatom species <i>P. tricornutum</i> in red (n = 2) and <i>T. pseudonana</i> in black (n = 2) from which average carrying capacity models across temperatures for 4.4A, were calculated. Single non-linear model parameters for these model fits can be found in Supplementary Tables 4.2 – 4.4.	109
Supplementary Figure 4.3: Visual representation of the competition experiments to better understand when the various growth and competition replicates were collected.	110
Supplementary Figure 4.4: (A) Growth progression over time for <i>P. tricornutum</i> and <i>T. pseudonana</i> grown in f/2 medium with different nitrate concentrations (882 μ M (red), 220.5 μ M (green), 110.25 μ M (blue), 55.13 μ M (purple)). (B) Dependence of carrying capacity (K) on nitrogen concentration in the growth medium. (C) Dependence of exponential growth rate r on nitrogen level in the growth medium.	111
Supplementary Figure 4.5: Average (n = 2) nitrate plus nitrite concentrations in monocultures across all assay temperatures in the low N medium over time for <i>P. tricornutum</i> and <i>T. pseudonana</i> . Grey error bars denote standard deviation from two	

replicates. At the cold and warm ends of the temperature gradient, it can be seen that values for the NO_x concentration do not drop as quickly as towards the optimum temperatures. This is because especially for *P. tricornutum* at the warm end and *T. pseudonana* at the cold end, the cells did not grow as rapidly and it took them more time to deplete the available nitrogen stocks.112

Supplementary Figure 4.6: Average (n = 2) F_0 fluorescence in low N monocultures across all assay temperatures over time for *P. tricornutum* and *T. pseudonana*. Grey error bars denote standard deviation from two replicates.....113

Supplementary Figure 4.7: Average (n = 2) F_0 measured by FRRf per cell across all assay temperatures for *P. tricornutum* and *T. pseudonana* in low N medium. Flow cytometry counts were taken for monocultures in the first 14 days of the experiment before mixing cultures together to start competition experiments. Grey error bars denote standard deviation from two replicates.....114

Supplementary Figure 4.8: Example flow cytometry (FC) data that was collected for *P. tricornutum* and *T. pseudonana* monocultures at the end of the first experimental day of the low N experiment, and after the diatoms had been cultured in low N medium for 15 days. After 15 days, N levels were depleted below the detection limit of the utilised NO_x assay. The dotted red and turquoise lines were roughly drawn through the mean forward scatter (FSC) values (used as proxies for cell size) of the starting day cultures. It could be observed that cell size declined after being cultured under N-limitation for two weeks, which can be derived from the fact that the dotted lines do not intersect the middle of the FC clouds at day 15. The average cell size has shifted to the left on the FSC-axis, i.e. cells became smaller.115

Supplementary Figure 4.9: Mean slopes of $\ln(F_0)$ across temperatures for *P. tricornutum* (n = 2) and *T. pseudonana* (n = 2) during the first four days of the low N scenario. Single replicate slopes were used to calculate the acute exponential growth response across temperatures, to which a daily growth rate of 0.22 d^{-1} was added to account for the daily dilution rates. Single growth replicate rates can be seen in Fig. 5.2 B. Grey error bars denote 1 standard deviation.....116

Supplementary Figure 4.10: Average (n = 2) cells per ml across all assay temperatures for *P. tricornutum* and *T. pseudonana* in low N medium. Flow cytometry counts were taken for monocultures in the first 14 days of the experiment before mixing cultures together to start competition experiments. Grey error bars denote standard deviation from two replicates. Dashed line in each facet panel is the average carrying capacity for each monoculture growth duplicate from day 5 onwards across assay temperatures.117

Supplementary Figure 4.11: All AIC values across models from the models fits of high N growth rates (blue symbols), low N growth rates (green symbols), and low N carrying capacities (red symbols) across temperatures for (A) *P. tricornutum* and (B) *T. pseudonana*. AIC scores for *T. pseudonana* replicate 2 are excluded as it was not taken into consideration for the final data analysis.118

Supplementary Figure 4.12: Log₂ over time *P. tricornutum*-to-*T. pseudonana* cell abundance ratio in high N mixed cultures. Blue lines are the first 2 competition replicates that were started directly at the beginning of the experiment. Red lines are the temperature acclimated competition replicates that were started after the first competition was completed.119

Supplementary Figure 4.13: Log₂ over time of the *P. tricornutum*-to-*T. pseudonana* cell abundance ratio in low N mixed cultures. Blue lines are the first 2 competition replicates that were started two weeks after growing monocultures in N-limited conditions. Red lines are competition replicates that were started after the first competition was completed and monocultures had been starved for nitrate even longer.120

Supplementary Figure 4.14: (A) LOESS fits of single competition replicates across temperatures on competition coefficients from observed changes in species frequency ratios (Supplementary Figure 5.7). (B) Average temperatures (n = 2) of unacclimated and acclimated inflexion points of competitive advantage. The ANOVA output test for a significant difference between the two groups can be found in Supplementary Table 5.5. .121

Supplementary Figure 4.15: Average F_v/F_m values of exponentially growing *P. tricornutum* (n = 4) (red) and *T. pseudonana* (n = 3) (black) measured in the high N medium at the indicated assay temperatures across the temperature gradient. Grey error bars denote 1 standard deviation.122

Supplementary Figure 4.16: Average (n = 2) F_v/F_m in low N monocultures across all assay temperatures over time for *P. tricornutum* and *T. pseudonana*. Grey error bars denote standard deviation from two replicates.123

Supplementary Figure 4.17: Average (n = 2) daily growth rate in the low N medium calculated from daily changes of F_0 (pre-dilution on day t divided by post-dilution on day t-1) in monocultures across all assay temperatures over time for *P. tricornutum* and *T. pseudonana*. Grey error bars denote standard deviation from two replicates. At temperatures above 30°C, *P. tricornutum*, did not grow, so that panels were left blank. The line parallel to the time axis at a growth rate of 0.22 d⁻¹ is the dilution rate: growth rate equals dilution rate when cultures are in N-limited steady state.....124

Supplementary Figure 5.1: Average (n = 4) ln(F_0) of exponentially growing mixed cultures of *P. tricornutum* and *T. pseudonana* across temperature fluctuation amplitudes. Blue data indicate the period prior to the start of the fluctuations, red data indicate the fluctuation period, and black data indicate the period after fluctuations. Each panel represents an assay fluctuation amplitude around the mean temperature of 18.6 °C.153

Supplementary Figure 5.2: Average (n = 4) F_v/F_m of exponentially growing mixed cultures of *P. tricornutum* and *T. pseudonana* across temperature fluctuation amplitudes. Blue data indicate the period prior to the start of the fluctuations, red data indicate the fluctuation period, and black data indicate the period after fluctuations. Each panel represents an assay fluctuation amplitude around the mean temperature of 18.6 °C. Note how at the highest fluctuation temperatures (17 °C and above), a general drop in values in comparison to the pre-fluctuation period (blue) can be observed in the first three to five

days of the fluctuation period (red). During this time, *P. tricornutum* encountered conditions close to its physiological limits on the warm cycles, and *T. pseudonana* on the cold cycles. As the fluctuation period progressed and *P. tricornutum* was fully or almost fully displaced from the mixed cultures at high fluctuation amplitudes, this drop in values could only be observed every second day of the experiment. This is because *T. pseudonana* encountered unfavourable conditions on cold days, but not on warm days, and *P. tricornutum* did not influence the F_v/F_m signal anymore.154

Supplementary Figure 5.3: Average ($n = 4$) $\ln(F_0)$ of N limited mixed cultures of *P. tricornutum* and *T. pseudonana* across temperature fluctuation amplitudes. Blue data indicate the period prior to the start of the fluctuations, red data indicate the fluctuation period, and black data indicate the period after fluctuations. Each panel represents an assay fluctuation amplitude around the mean temperature of 25.2 °C.155

Supplementary Figure 5.4: Average ($n = 4$) F_v/F_m of N limited mixed cultures of *P. tricornutum* and *T. pseudonana* across temperature fluctuation amplitudes. Blue data indicate the period prior to the start of the fluctuations, red data indicate the fluctuation period, and black data indicate the period after fluctuations. Each panel represents an assay fluctuation amplitude around the mean temperature of 25.2 °C.156

Supplementary Figure 5.5: Progression of $\log_2(\text{frequency } P.\text{tricornutum} : \text{frequency of } T.\text{pseudonana})$ species ratio over time in high N mixed cultures at 18.6 °C before temperature fluctuations were started. Each panel displays 4 replicate cultures and the fluctuation amplitude they were exposed to after this 10 day pre-fluctuation period. \log_2 was utilised in this figure, and in the following 5 Supplementary Figures, as a biologically relevant depiction of species frequency change over time, whereby a doubling or halving in the abundance ratio translates to one unit on the \log_2 scale.157

Supplementary Figure 5.6: Progression of $\log_2(\text{frequency } P.\text{tricornutum} : \text{frequency of } T.\text{pseudonana})$ species ratio over time in low N mixed cultures at 25.2 °C before temperature fluctuations were started. Each panel displays 4 replicate cultures and the fluctuation amplitude they were exposed to after this 10 day pre-fluctuation period.158

Supplementary Figure 5.7: Progression of $\log_2(\text{frequency } P.\text{tricornutum} : \text{frequency of } T.\text{pseudonana})$ species ratio over time in mixed cultures at different fluctuation amplitudes during the fluctuation period of the high N experiment. Each panel represents an assay fluctuation amplitude around the mean temperature of 18.6 °C.159

Supplementary Figure 5.8: Progression of $\log_2(\text{frequency } P.\text{tricornutum} : \text{frequency of } T.\text{pseudonana})$ species ratio over time in mixed cultures at different fluctuation amplitudes during the fluctuation period of the low N experiment. Each panel represents an assay fluctuation amplitude around the mean temperature of 25.2 °C.160

Supplementary Figure 5.9: Progression of $\log_2(\text{frequency } P.\text{tricornutum} : \text{frequency of } T.\text{pseudonana})$ species ratio over time in mixed cultures at different fluctuation amplitudes after the fluctuation period of the high N experiment. Each panel represents an assay fluctuation amplitude around the mean temperature of 18.6 °C that the mixed cultures were exposed to during the temperature fluctuation period.161

Supplementary Figure 5.10: Progression of $\log_2(\text{frequency } P.\text{tricornutum} : \text{frequency of } T.\text{pseudonana})$ species ratio over time in mixed cultures at different fluctuation amplitudes after the fluctuation period of the low N experiment. Each panel represents an assay fluctuation amplitude around the mean temperature of 25.2 °C that the mixed cultures were exposed to during the temperature fluctuation period.162

List of Tables

Table 4.1: Parameters for linear models ($y = ax + b$) correlating predicted (x) and observed competition coefficients (y) across assay temperatures. Significant correlations (alpha level of 0.05) that conclude a relationship between predictions and observations are marked in bold and with an asterisk. 91

Table 6.1: Table summarising the findings on thermal adaptation in selected studies on eukaryotic microorganisms, mainly phytoplankton. 166

List of Supplementary Tables

Supplementary Table 4.1: Equations that can be used to describe thermal performance across temperatures from Low-Décarie et al. (2017). The experimental growth rate and carrying capacity were fitted to Equations 4 – 15 (shaded in green) with the R package “temperatureresponse” in this study. Equations 1 – 3 (shaded in blue) can only be used to cover a sub- or supra-optimal range of temperatures, but not the whole gradient, and were therefore not utilised in this study. In all model equations, small letters <i>a</i> to <i>f</i> are model parameters, <i>R</i> is the universal gas constant, <i>T</i> is the assay temperature at which a growth rate μ was measured, μ_0 the starting growth rate, E_A the activation energy of metabolism, T_{min} and T_{max} are the minimum and maximum temperatures beyond which no growth occurs for the organism under observation, and T_{ref} is the reference temperature at which a reference μ was measured in the cited study.	99
Supplementary Table 4.2: Non-linear model outputs of single replicate TPC growth models for <i>P. tricornutum</i> (<i>n</i> = 4) and <i>T. pseudonana</i> (<i>n</i> = 3) in the high N scenario.	101
Supplementary Table 4.3: Non-linear model outputs of single replicate TPC growth models for <i>P. tricornutum</i> (<i>n</i> = 2) and <i>T. pseudonana</i> (<i>n</i> = 2) in the low N scenario.	103
Supplementary Table 4.4: Non-linear model outputs of single replicate TPC carrying capacity models for <i>P. tricornutum</i> (<i>n</i> = 2) and <i>T. pseudonana</i> (<i>n</i> = 2) in the low N scenario.	104
Supplementary Table 4.5: One-way ANOVA output of comparison of competition inflexion point temperature between unacclimated and acclimated competition replicates in the high N scenario.	105
Supplementary Table 4.6: Two-way MANOVA output table for comparison between growth rate Thermal Performance Curve (TPC) fits of <i>P. tricornutum</i> and <i>T. pseudonana</i> . Dependent variables that were compared were μ_{max} , CT_{50min} , CT_{50max} , and T_{opt} . Individual ANOVA test statistics wrapped within this MANOVA are found in Supplementary Tables 5.7 – 5. 10.	105
Supplementary Table 4.7: Two-way Individual ANOVA output table from MANOVA for CT_{50min}	105
Supplementary Table 4.8: Two-way Individual ANOVA output table from MANOVA for T_{opt}	105
Supplementary Table 4.9: Two-way Individual ANOVA output table from MANOVA for CT_{50max}	106
Supplementary Table 4.10: Two-way Individual ANOVA output table from MANOVA for μ_{max}	106
Supplementary Table 4.11: One-way ANOVA output table of CT_{50min} from K model fits.	106
Supplementary Table 4.12: One-way ANOVA output table of T_{opt} from K model fits.	106
Supplementary Table 4.13: One-way ANOVA output table of CT_{50max} from K model fits.	107
Supplementary Table 4.14: One-way ANOVA output table of K_{max} from K model fits.	107
Supplementary Table 4.15: One-way ANOVA output table for differences between high N and low N inflexion points.	107

Declaration of the Contribution to Each Chapter

My supervisors and Kirralee Baker gave me substantial feedback and guidance throughout chapters 1 to 5.

Chapter 1

I conceived and wrote this introductory chapter.

Chapter 2

All data of this chapter were collected at Essex University. Thank you to Katrin Schmidt who provided the thermally adapted *T. pseudonana* cultures. Culturing and FRRf measurements were carried out by myself. I had some partial help with the optical densities measurements by the student helper Amelia White. Data analysis was carried out by myself.

Chapter 3

All data of this chapter were collected at Essex University. I conducted the rate measurements and analysed the data myself.

Chapter 4

All data of this chapter were collected at Essex University. I conceived the experimental design and conducted the experimental work. Data analysis was carried out by myself.

Chapter 5

All data of this chapter were collected at Essex University. Kirralee Baker and I conceived the experimental design and I conducted the experimental work. Data analysis was carried out by myself.

Chapter 6

I conceived and wrote this discussion chapter.

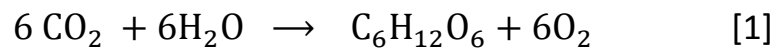
Chapter 1: General Introduction

1.1 Phytoplankton communities

Phytoplankton is the term used to refer to free-floating algae that can be found in almost all of the world's water bodies (Lalli and Parsons, 2006). Phytoplankton is a taxonomically diverse group that consists of thousands of species, ranging from prokaryotic cyanobacteria to unicellular eukaryotes like diatoms and coccolithophores that form beautiful and complex cell walls out of silica or calcium carbonate, respectively (Suthers and Rissik, 2009). Even colonial organisms like *Volvox*, and free-floating macroalgae like *Sargassum* form a part of phytoplankton (Beardall et al., 2009). Phytoplankton communities can be comprised of several dozens to thousands of species (Lalli and Parsons, 2006), and these communities form the basis of aquatic food webs and global biogeochemical cycles in oceans, rivers and lakes. Phytoplankton species are commonly microscopic and have a high level of inter and intra-specific genetic variability (Schaum et al., 2018). They are often regarded as good model organisms to study ecological and evolutionary questions because they can display short generation times (e.g. several hours under optimum growth conditions), and because some species are relatively easy to culture under laboratory conditions, in flasks or on petri dishes. Furthermore algae are increasingly gaining relevance for biotechnological applications so that interest in their ecology and physiology is growing not only in the scientific community, but also in industry (Andersen, 2005).

As photoautotrophic organisms, phytoplankton take up large quantities of atmospheric carbon dioxide (CO₂) in the sun-lit surface layers of water bodies and roughly account for half of the

world's oxygen production (Suthers and Rissik, 2009) by converting inorganic carbon with the energy from sunlight into organic compounds through photosynthesis [1].



Being such important organisms with a wide-ranging influence on the biotic and abiotic environments, alterations amongst phytoplankton communities have the potential to affect the Earth's aquatic ecosystems (Crowder and Norse, 2008; Falkowski et al., 1998; Thomas et al., 2012). For instance, changes in competitive dynamics between species would change community composition and would consequently lead to altered ecosystem functioning (Thomas et al., 2012). This is because different algal groups and assemblages sequester carbon differently, photosynthesize at varying rates, or take up nutrients with different efficiencies (Prézelin et al., 2004). Altered community composition would therefore have large-scale implications and affect global biogeochemical cycles and aquatic food webs (Han and Furuya, 2000; Karl et al., 2001; Prézelin et al., 2004).

In order to predict and prepare for such potentially influential changes, it is crucial to understand how temperature changes and alterations in nutrient concentrations will influence aquatic systems and impact phytoplankton, from single species to simple and complex communities. This thesis provides new information to help fill some of the knowledge gaps to further our understanding and predictive capability on the responses of phytoplankton communities to future environmental change.

1.2 Changing aquatic environments

Anthropogenically induced climate change is a reality beyond any scientific doubt. Currently, ecosystems on our planet are changing rapidly under the pressure of the Anthropocene in a

complex combination of man-made and natural drivers (Duarte, 2014), and these changes are exerting their influence on aquatic systems (IPCC, 2013). In natural environments, organisms are constantly under the influence of multiple environmental parameters changing at the same time, which can lead to non-linear and unpredictable responses (Folke et al., 2004; Lawson et al., 2015). Predictions of the conditions in a future ocean include an overall warming of sea surface temperatures, a more stratified water column and a reduction of sea ice coverage (Berdahl et al., 2014; Bopp et al., 2013; Yoshiyama et al., 2009). As a consequence of more stratified water columns decreased nutrient loadings of nitrogen and phosphorus are expected (Iglesias-Rodríguez et al., 2002). In contrast, coastal waters in some areas are predicted to increase in their nutrient load due to run-off from human activities (Lemley et al., 2019; Shuler et al., 2019). Surface water $p\text{CO}_2$ is expected to decrease and pH to decrease, which will also lead to a reduced uptake of CO_2 from the atmosphere (Bopp et al., 2013; Gruber, 2011). As hypoxic areas are expected to expand, O_2 contents of surface waters are forecasted to fall on a global scale (Bopp et al., 2013).

These changes will exert their influence on phytoplankton by impacting their physiology and consequently ecology. Changes in temperature for example can alter the rate at which a biological reaction increases or decreases for every 10 °C temperature change (this is known as the Q_{10} , which is species specific) so that the abilities to take up and store nutrients are always determined by external conditions (Fujimoto et al., 1997). Warming in already warm habitats where species live close to their maximum temperature may for instance shift community composition in a direction where only species that can sustain warmer temperatures would survive, with other community members dying off if there is no potential for migration or adaptation. Even though fluctuations in abiotic parameters might allow for periodic relief of

environmental pressures, overall raised temperatures would likely lead to the disappearance of species that encounter their physiological limits. Whether a species is a thermal specialist with a narrow range of temperatures it can survive, or a generalist that can sustain a large range of temperatures at which it can grow will therefore play an important role (Listmann et al., 2016). A reduction in biodiversity as a consequence of warming or change in nutrient concentrations when species cannot cope with the changes would have the potential to severely reduce the functionality of primary producer communities, turning an area into a functional desert where ecosystem processes are not performed at former levels or disappear altogether (Ptacnik et al., 2008). The extent to which the environment will change and how much phytoplankton will be impacted by it will depend on the region (Joshi et al., 2011), and ultimately, how changes will affect the various life forms on our planet will depend on an individual's ability to adjust to their new environment, either through phenotypic plasticity and/or genetic adaptation.

Environmental changes will not necessarily be gradual and unidirectional throughout the coming decades either. Natural environments are heterogeneous in space (Cloern and Dufford, 2005; Tilman et al., 1982), and time (Litchman, 2000; Tilman et al., 1982), meaning that phytoplankton do not live in constant environments but within dynamic surroundings that change hourly, daily, and seasonally. Sea surface temperatures have seen a rise since the onset of the industrial revolution, but more and more studies point out that fluctuation intensities and frequencies are changing alongside an increase in the mean environment (Alexander et al., 2018; Huntingford et al., 2013; Lawson et al., 2015). It is therefore apparent that there is also an increasing need to assess biological processes under fluctuating environments. For example, since 1980 the interannual temperature variability in the Northern hemisphere has increased by more than 25%, although the exact magnitude is region specific (Huntingford et al., 2013).

Besides environmental changes having an influence on the primary producer community directly, they also bring indirect consequences by affecting all trophic levels in marine ecosystems such as microzooplankton and fish (Walther et al., 2002). Changes in predator communities can change top-down controls through altered directed grazing pressure on phytoplankton communities (Rose et al., 2009). With changes in water stratification patterns throughout an annual cycle, temporal peak abundances not just in phytoplankton, but also in zooplankton and fish larvae will be altered so that bottom-up and top-down controls will not be the same as under past and current environmental conditions (Edwards and Richardson, 2004). Alterations in the timing of annual blooms of phytoplankton will impact the trophodynamics of the marine food web and lead to asynchrony of established species succession and predator-prey dynamics (Asch et al., 2019; Edwards and Richardson, 2004). Due to these complexities, the scientific community is still struggling to accurately predict specific ecosystem responses to environmental changes as they will occur within complex communities and indirect and direct effects will exert their influence simultaneously, so that overall effects of environmental change are difficult to foresee.

1.3 Phytoplankton response to changing environmental conditions

When phytoplankton are faced with environmental changes, they have the potential to disperse to regions with more favourable conditions, to cope with the changes *in situ* through phenotypic plasticity or genetic adaptation, or face mortality (Gienapp et al., 2008). How species will ultimately respond is going to depend on the organism, the region they occur in, and community composition. As there is a plethora of environmental parameters that can change and influence phytoplankton, delving into all of them in detail could fill a book. Temperature and nutrient concentrations have been identified as two of the most important

drivers to phytoplankton growth (Elser et al., 2009; Follows et al., 2007; Toseland et al., 2013), and are the major aspects investigated in this thesis. Temperature rise has currently a global relevance in the light of climate change, and macronutrients such as nitrogen and phosphorus are often limiting to algal growth (Klausmeier et al., 2004), so that changes in their concentrations could lead to major restructuring of phytoplankton communities. Two other important aspects which were found to drive phytoplankton biomass change and functional diversity, that were however not covered in this thesis, are the direct and indirect effects of mixing of water masses (Perruche et al., 2010), as well as increasing CO₂ levels and the connected acidification of surface waters (Dutkiewicz et al., 2015).

1.3.1 Responses to individual drivers

Species diversity amongst phytoplankton is high and the response to environmental changes will be diverse (Litchman et al., 2010), as different species have different resource requirements (e.g. Tilman, 1977) and reaction norms (Thomas et al., 2012). The response of any species to environmental change will depend on the magnitude, time scale and frequency of the change. As a general trend however, species from natural environments were found to grow best under the temperature conditions they were isolated from, and were found to develop a tolerance to the water masses that they live in (Interlandi and Kilham, 2001; Suzuki and Takahashi, 1995).

Despite existing differences in responses to environmental changes between different species, reaction norms within a single species have been also found to vary substantially. In natural environments, individuals and populations of the same species can have “relevant physiological differences” although their genetic variation lies within the limits of being defined as one species (Rocap et al., 2003). These differences may be a result of inherent phenotypic variability within strains of the same phytoplankton species (Schaum, 2014), or due to variations amongst

different life cycle stages, for example the sexual and vegetative stages of diatoms (Chepurnov et al., 2004). Natural populations of the same species that display varying responses to the same environmental conditions can be classed as ecotypes. These specific ecotypes can give insights into the genetic variation of phytoplankton across varying habitats and can help to understand how phytoplankton may cope with different environmental conditions. The common marine cyanobacterium genus *Synechococcus* has been found to have about a dozen subclades with distinct physiological characteristics, displaying latitudinal differences in their distribution that are likely down to variations in thermal responses as well as nutrient concentration and light preferences (Pittera et al., 2014).

Like ecotypes from natural environments, laboratory cultures that have been kept for long enough time or under specific selective conditions, can differentiate into strains that react differently to the same treatment (Lakeman et al., 2009). As “strains” we classify individuals and populations from the same species that come from distinct spatial origin or have been kept as a specific lineage and cultured over a period of time through serial transfers (Lakeman et al., 2009). These laboratory lineages have the potential to change, as their genome can be altered over time in culture through random mutations causing physiological or morphological differences (Schaum et al., 2018), giving them properties that become unique to a specific laboratory and change environmental responses in comparison to the initially isolated individual. Exposing strains of one species to the same treatment can yield further insights about intra-specific genetic variation and the potential need for adaptations (Lakeman et al., 2009; Schaum, 2014).

Regardless of this inter and intra-species variability, research has attempted to draw generalised conclusions concerning ongoing climate change. Overall, phytoplankton community

biomass and composition are expected to change due to redistribution and differences in adaptive capabilities (Hallegraeff, 2010; Montes-Hugo et al., 2009; Winder and Sommer, 2012). Globally, the species composition within plankton communities is predicted to shift towards species adapted to higher average temperatures due to global warming (Dutkiewicz et al., 2015). Whereas at high latitudes algal biomass is expected to increase, potentially due to warming and migration, it is expected to decrease at middle to low latitudes, leading on average to a global decline in phytoplankton biomass (Boyce & Worm, 2015).

Changes in the nutrient contents of water masses are also expected to have significant influences on how future communities will be structured because of differing nutrient uptake rates amongst phytoplankton taxonomic groups (Davey et al., 2008; Heil et al., 2007; Tilman et al., 1982). A model that predicted the global distribution of diatoms, coccolithophores, and prasinophytes in the North Atlantic and North Pacific for instance found that depending on the system, increased N:P ratios in the water column will have direct and varying effects, but also interplay with other factors such as altered iron supply (Litchman et al., 2006). For the North Atlantic it was predicted that diatom biomass would be unaltered, whereas zooplankton and prasinophyte concentrations would increase significantly and coccolithophores would decrease. In contrast, in the North Pacific, no decreases relating to higher N:P ratios were found, but abundances of diatoms, prasinophytes and zooplankton were predicted to increase due to more nitrate and silicate in the upper ocean layers, while coccolithophore abundances in the North Pacific were not expected to decrease (Litchman et al., 2006). Modelling by Litchman et al. (2010) found that small cyanobacteria with high surface-to-volume (SA:V) ratios should outcompete larger phytoplankton species with lower SA:V ratios in oligotrophic nutrient conditions that are predicted in future oceans.

In contrast, under high nutrient conditions, larger cells such as those of green algae are expected to have the advantage in competition scenarios as they are not diffusion limited when nutrient concentrations are high and can achieve higher growth rates and biomass than smaller cells (Falkowski and Oliver, 2007; Shimoda et al., 2016). As an example, more stratified water columns with reduced nutrient concentrations will likely be disadvantageous to diatoms and their dominance in phytoplankton communities is predicted to decline, as nutrient-rich conditions are more beneficial to them (Bopp et al., 2005; Malviya et al., 2016). However, despite their reliance on high nutrient concentrations, diatoms were shown to prevail well in temporally heterogeneous environments and survive nutrient-depleted periods because they can store resources when nutrient concentrations are high (Tozzi et al., 2004). In addition to advantages or disadvantages emerging from differing SA:V between species under predicted lower surface layer nutrient contents and increased stratification of ocean layers due to warming, Iglesias-Rodriguez et al. (2002) concluded that diatoms would also be outcompeted by coccolithophorids in the future oceans because coccolithophores have a higher affinity for nitrogen.

As a confirmation of these modelling studies, nutrient loading in natural environments has indeed been found to shift a phytoplankton community to be dominated by larger cells (McAndrew et al., 2007). Nutrient pulses lead to phytoplankton communities being dominated by diatoms, especially pennate ones (Shimoda et al., 2016), and the overall Chl *a* concentration to increase (Alexander et al., 2015). Diatoms often dominate plankton communities in areas of upwelling (Irwin and Oliver, 2009; Tilstone et al., 2000). Decreases in silicate inputs to aquatic systems, in combination with anthropogenic N and P inputs have shifted or will in the future change the N and P to Si molar ratios, causing diatoms to be less abundant, with freshwater

and coastal communities becoming more dominated by flagellates which enter the freed-up niche space left behind by diatoms (Geider et al., 2014).

As the above-mentioned studies show, changes in body size play a crucial role under environmental change, and cell size alterations have ecological consequences that will be crucial in determining future community structure. A change in body size is directly linked to the SA:V ratio, and therefore a major determinant of how well phytoplankton can take up nutrients and compete (Morán et al., 2010). Body size also plays a role in determining grazing pressure. For instance, smaller phytoplankton species are grazed upon by microzooplankton, whereas larger cells are removed by mesozooplankton (Cermeño et al., 2008; Morán et al., 2010), resulting in top-down control of populations (Peter and Sommer, 2012), and freeing up niche space for species to become more abundant.

The temperature-size rule (TSR) links body size to temperature and states that the average size of individuals is inversely related to how warm it is (Peter and Sommer, 2012). This negative correlation has been shown to lead to higher cell densities as cells become smaller when temperatures rise (Li et al., 2006). Despite this general trend, the TSR was found to not be universal and different relationships between body size and temperature could be found in phytoplankton (Morán et al., 2010). Especially diatoms could have smaller cells when temperatures rise as warmer environments spur metabolic rates and therefore cell division, leading to a continuous reduction in cell size due to their unique silica cell walls (Peter and Sommer, 2012).

One ocean-wide study came to the conclusion that cell size in phytoplankton is not controlled by temperature directly as the TSR states, but through its interaction that it has with nutrient availability, light, and increased grazing pressure, which gets more intense as predator

metabolic rates rise when it gets warmer (Marañón et al., 2012). Untangling these interactive effects and determination of what role the TSR plays, will have to be elucidated further in the future (Chen and Liu, 2010).

Due to the complexity of abiotic and biotic parameters influencing phytoplankton ecology, not enough is known yet to make conclusive statements on the future abundance and distribution of species (Rost et al., 2008). Since aquatic environments are highly dynamic and varied, it is possible that there will always be sufficient niche space to sustain high biodiversity. It is therefore likely that species will still coexist in diverse communities, even if the abundance, distribution, and evenness within them will be different than under current conditions (Dutkiewicz et al., 2015). It has been predicted that due to all the expected shifts in phytoplankton competitive dynamics and maladaptation to novel climate conditions, the phytoplankton community composition in the North Atlantic will change by approximately 16% by the end of the 21st century (Barton et al., 2016). Communities will change in terms of their species composition and distribution, and species that have potentially never encountered each other before will meet and compete for resources (Barton et al., 2016). Hence understanding the response-variety of different phytoplankton groups and the individual characteristics of a system under observation is important for consolidating region-specific conditions and future responses.

1.3.2 Responses to multiple drivers

Response to changes in algal ecology and cell physiology along environmental gradients has often been investigated by growing cultures under controlled conditions and observing how they respond to alterations in isolated parameters (Baker et al., 2016; Boyd et al., 2013; Low-Décarie et al., 2011). These experimental findings are then incorporated into ecosystem models

to simulate current and future ecosystem functioning, nutrient cycles, and species dynamics (e.g. Dutkiewicz et al., 2015). Investigations on the effects of isolated parameter changes and single gradients provide a mechanistic understanding of species response to single drivers, which form the basis of understanding phytoplankton physiology. In contrast, in natural environments organisms are exposed to a multitude of changing abiotic parameters simultaneously, so that predictions made from isolated investigations are not necessarily representative of reality (Kordas et al., 2011; Kratina et al., 2012), and findings of single parameter studies cannot be simply extrapolated to answer scenario-based questions. More complex and informative experimental designs have to be found in order to bring predictions closer to reality (Boyd and Hutchins, 2012; Boyd et al., 2019, 2016; Kratina et al., 2012).

Responses to concurrent alterations in multiple parameters, such as temperature and nutrient levels jointly, may be different from when only one variable is altered, as the effects can be interactive (Dickman et al., 2006; Feng et al., 2010, 2009; Fu et al., 2007; Hare et al., 2007; Maddux and Jones, 1964). For instance, it was shown that the growth performance of the diatom *Thalassiosira pseudonana* along a temperature gradient depends on the amount of nitrogen present in the growth medium (Thomas et al., 2017). Shifts in community composition may become non-linear due to the interplay of antagonistic or synergistic effects which could not be predicted from the response to one variable in isolation (Christensen et al., 2006; Folke et al., 2004; Schlüter et al., 2014). The more parameters are altered, the more complex and diverse can the response become (Boyd, 2019; Strzepek et al., 2019). When conducting experimental studies of phytoplankton populations that assess the response to environmental changes, it is therefore important to attempt to replicate nature's complexity to gain a better understanding of how phytoplankton communities will respond under future environmental conditions. As two major structuring forces of community composition, it is therefore

worthwhile to combine the investigations of responses to thermal changes with responses to alterations in nutrient concentrations to uncover interactive effects.

1.3.3 Evolutionary adaptation to environmental change

The majority of aforementioned studies that aim to predict phytoplankton responses to environmental change assume that performance across gradients will be static through time and might not adapt to long-lasting environmental changes. Recent publications however suggest the opposite, so that predictions of future community composition might be offset through adaptations (e.g. Beckmann et al., 2019; Schaum et al., 2017).

Adapting to novel environmental conditions might bring a trade-off between competitive and adaptive ability in phytoplankton. Species that would be able to adapt to a new environment and thus ensure long-term survival under the new conditions, would potentially become less competitive at the conditions they were initially from (Litchman et al., 2012). For instance a study that investigated species dominance in a natural community showed that species persistence can change after a selection period. A community from a natural environment was cultured and species succession monitored over time. Single species from the community were isolated and adapted to higher temperatures for a year, after which the community was re-assembled. Diatoms that were rare and only present in low abundance in initial communities seemed to completely lose their competitive ability after being grown at elevated temperatures, whereas warming boosted the ability of already dominant diatom species to outcompete all other species faster than before the selection period (Tatters et al., 2013b).

A study that investigated the effects of disturbance frequency on the green algae *Chlamydomonas* found that the direction and manner of genotype adaptation was more predictable when disturbances were frequent than in environments where abiotic conditions

were disturbed less often (Collins and De Meaux, 2009). Other laboratory studies on experimental evolution have shown that adaptation to increased temperatures could be a common trait in phytoplankton species (Huertas et al., 2011; Padfield et al., 2015; Schaum et al., 2017; Schlüter et al., 2014). The full potential for rapid adaptation in phytoplankton to balance out adverse effects of oncoming climate change still remains to be elucidated and two of the chapters of this thesis are dedicated to the investigation of physiological adaptations as a consequence of increased temperature.

1.4 Phytoplankton Competition and Nutrient Availability

Understanding and predicting the response of isolated species to environmental changes is one aspect of phytoplankton ecology. However grasping how species react in mixed cultures is of crucial importance as well. Boyd and his colleagues (2013) for instance investigated the growth response to temperature of 25 algal strains in isolation from across the world, but acknowledged that in mixed communities growth of the strains might be altered when other algae are present.

Species in phytoplankton communities are in constant competition for a limited amount of resources. The most common resources limiting growth are nitrogen, phosphorus, silica, iron, light and carbon dioxide (Tilman et al., 1982). Traditional competition theory predicts that the species able to live at the lowest concentration of a common resource and able to maintain the highest production rate will outcompete all other competitors. This so-called resource-ratio hypothesis (R^* rule) predicts that the maximum species richness in an equilibrium community is set by the number of limiting resources (Interlandi and Kilham, 2001). It has been shown that the competitive outcome in direct species competition is defined by nutrient availability and the ability of a species to take up nutrients more efficiently (Sommer, 1989). The minimum

nutrient concentrations necessary for a species to survive can be visualised by plotting zero net growth isoclines (ZNGIs) across combinations of the minimum resource concentrations necessary to sustain growth without a decrease in population size (Fig. 1.1). Species competing for the same resources have ecological niche overlap (Letten et al., 2016), and the stronger the common requirement for an essential resource, the stronger will be the competition. Two species with the same or similar ecological niche cannot coexist if not separated geographically or through partitioning of resources (Begon et al., 2006; Ricklefs and Miller, 1999). However, if their ZNGIs overlap and both species in a two-species mixed population have the lower resource requirement for one of two limiting resources, stable co-existence can be achieved. For example, a phosphate-limited competitor and a silicate-limited competitor can co-exist in a stable equilibrium because each species has the lower R^* for a different nutrient, resulting in neither species being driven to extinction (Tilman, 1977, 1981) (Fig. 1.1). In natural environments, species can co-exist in the water column if they display a trade-off in light and nutrient competitive abilities, as with decreasing depth light levels decrease and nutrient levels usually increase, so that along those gradients multiple species can live (Klausmeier et al., 2007).

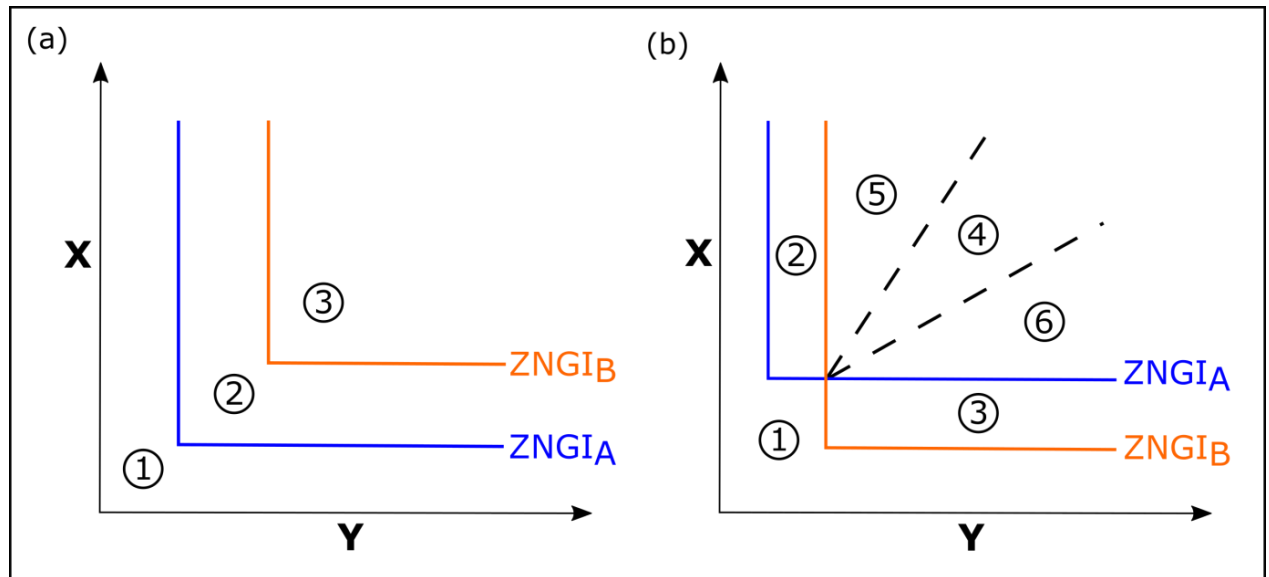


Figure 1.1: Schematic illustration of resource competition and competitive exclusion in relation to nutrient supply. Solid lines indicate zero net growth isoclines (ZNGIs) for species A (blue lines) and species B (orange lines), indicating the minimum concentrations of nutrients X (Vertical lines) and Y (horizontal lines) that they require to grow at a rate where population increases and decreases cancel each other out and equilibrium conditions exist. In equilibrium conditions cell death rate (cell loss) equals out the cell growth rate and the isocline does not move. Under non-equilibrium conditions, for instance if the cells are growing exponentially, the isocline can move up for nutrient X, and to the right for nutrient Y. If loss rate decreases (i.e. growth conditions are beneficial and growth rates are high), minimum nutrient requirements will become lower. Circled numbers indicate nutrient supply points. (A) Three different nutrient supply scenarios are presented. Species A has the lower nutrient requirements for both nutrients X and Y. At nutrient supply level 1, concentrations of X and Y are too low for neither species to grow. At nutrient level 2, nutrient levels are too low for species B, but A can survive. At concentration level 3, the nutrient supply concentration is also high enough for species B to survive. However species A would deplete the concentration below a level that is suitable for B, causing its extinction. (B) In this scenario, the ZNGIs of both species are altered and each of them has the lowest resource requirement for one of the two nutrients (X for species A, and Y for species B). At nutrient supply level 1, both species can once again not thrive because supply concentrations are too low. At nutrient supply levels 2, only species A, whereas at level 3 only species B would thrive. Nutrient levels 5 and 6 are high enough for both species to survive if they would be in isolation. As mixed cultures, species A would however outcompete species B over time at supply level 5, and vice versa at supply level 6. At nutrient supply level 4 enough nutrients would be present for both species to co-exist. Illustration adapted from Begon et al. (2006).

1.4.1 Physiological models explaining competitive success

The physiological basis for competition is based on the ability of a species to grow, acquire and store nutrients. Two mathematical models are commonly used to describe these abilities in algae and other microorganisms to predict competitive success. These are the Monod equation and the Variable Internal Stores Model (Droop's model), the former describing the ability to grow or take up nutrients in relation to their concentration in the surrounding of an algal cell, and the latter describing storage ability for nutrients once they have entered the cell (Tilman, 1977). In combination, the Monod equation and the Variable Internal Stores model form the basis of phytoplankton competition theory. According to these models, species compete by being better at utilizing a certain resource than others (Tilman, 1981).

The Monod equation has the same mathematical form as the Michaelis-Menten equation which had been initially developed for describing enzyme kinetics (Fig. 1.2). It can be used to describe a direct relationship between ambient resource concentration and the steady state growth rate at that concentration. The different abilities of phytoplankton to acquire nutrients are defined by a set of parameters, namely K_S , the half-saturation constant for nutrient limited growth, and μ_{max} , the maximum growth rate of a phytoplankton species, that together with the ambient substrate concentration S determine the growth rate of an algal cell (Fig. 1.2). Based on the Monod equation, Goldman and Carpenter (1974) derived a competition model, for small single-celled diatoms and chlorophytes, that predicted competitive outcome between two algal species as a function of temperature and their ability to take up nutrients. They came to the conclusion that both the ability to take up nutrients and temperature can influence the outcomes of competition between two species. The species with the lower K_S values would win competitions at low nutrient concentrations, but K_S values were found to change across temperatures leading to a shift in competitive advantage. Competitive strength along nutrient

gradients can therefore change if nutrient uptake rates and growth are influenced by nutrient concentrations as well as temperature.

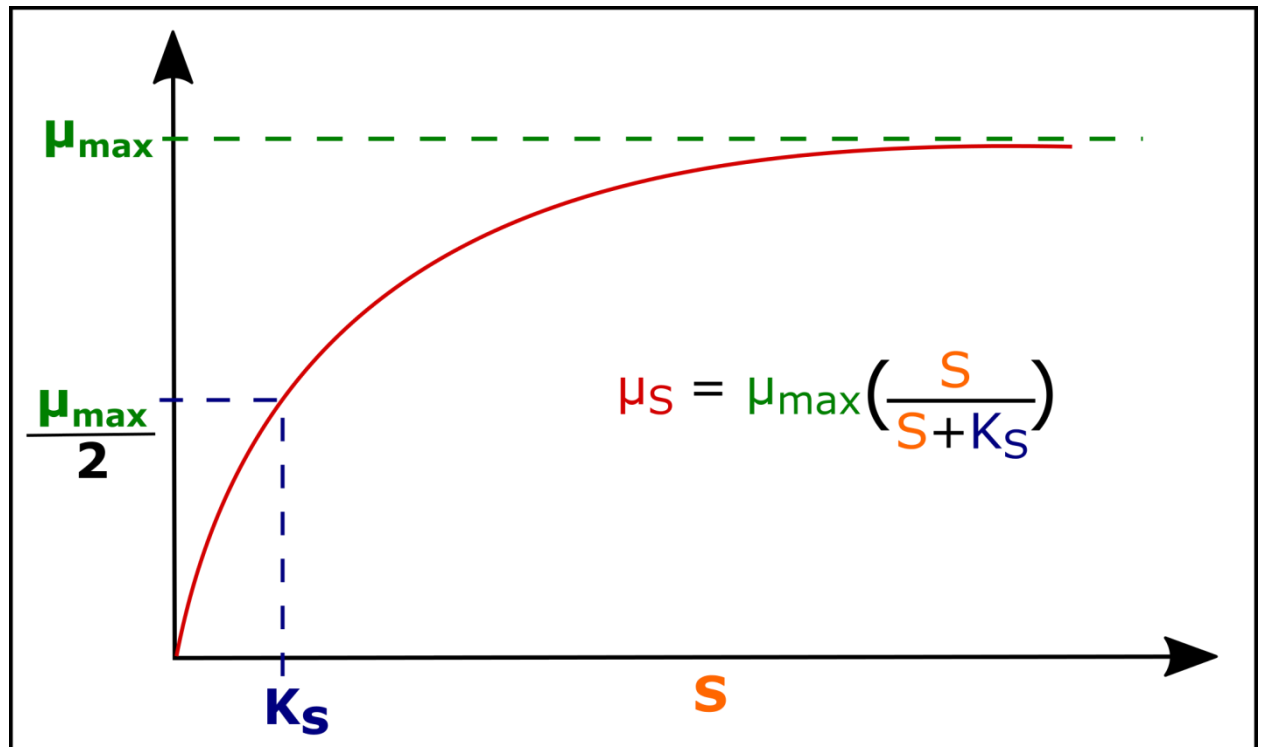


Figure 1.2: Graphical representation of the Monod equation. S = substrate concentration, μ_S = growth rate at substrate concentration S , μ_{\max} = maximum growth rate, K_S = half saturation constant for growth. The equation describes the relationship between external substrate concentrations and growth rates of microorganisms. The higher the ambient concentration of a substrate S , the larger will be its steady state growth rate, until a horizontal asymptote for μ_{\max} is approached.

Optimum temperatures for nutrient uptake and growth were found to differ, as optimum temperatures for enzyme reactions vary from those for growth (Raimbault, 1984). Nutrient uptake rates were furthermore found to vary within algae under the same external nutrient concentration depending on the physiological status of an algae cell (Morel, 1987). Morel (1987) could show that variations in the cell quota (the internal concentration of a limiting nutrient) would influence the nutrient uptake rates. He showed that the maximum nutrient

uptake rate V_{\max} increases as cells become nutrient limited, which leads to K_s , the half saturation constant for growth, being lower than the K_m , the half saturation constant for nutrient uptake. If algae have been nutrient starved over a period of time, acclimation processes within the cell can take place so that starved algae display much higher maximum uptake rates once nutrients are supplied than algae that were not nutrient starved, making the maximum uptake rate a variable parameter in the Michaelis-Menten equation (Smith et al., 2009). Nutrient starvation can heavily increase the demand for nutrients to sustain growth, ensuring that when nutrient-deficient cells come out of nutrient limitation or starvation, the algae are prepared to utilize fresh nutrients at a high rate as soon as they are supplied (Morel, 1987; Raimbault, 1984). This so-called surge uptake is a crucial process to ensure competitive success at times of nutrient pulses, as higher uptake rates and lower K_s values after a nutrient addition can be a sign of competitive strength (Fiksen et al., 2013). Increased surge uptake rates could ensure the survival of a species whilst simultaneously removing available nutrients for a direct competitor with potentially lower surge uptake rates.

Unlike in the Monod equation, the Variable Internal Stores model describes the steady state (equilibrium) growth of phytoplankton as a function of the intracellular quota of the limiting nutrient (Benavides et al., 2015, Morel, 1987). Thus, it accounts for the ability of single algal species to store and handle a resource once it has entered the cell (Fiksen et al., 2013). It is the original model that described phytoplankton growth as a function of intracellular nutrient concentrations, but other more complex models have been developed since (Flynn, 2008). Monod and Variable Internal Stores models are in contrast to each other, and conclusions for growth response can differ depending on which one is utilized. Monod equations would only be suitable to use under steady state conditions when nutrient supply is fixed (Sommer, 1991). If nutrient supply is varied or occurs in pulses, algae could be quick at taking up a resource, which

might however not translate into growth, as luxury uptake might occur. Good storage abilities for instance can lead to a decoupling between growth rates and resource availability for certain amounts of time (Sommer, 1991), enabling species to continue growing and outcompete others even if a resource stock has been depleted in the surrounding environment (Flynn, 2008). Likewise, a species might not be able to store nutrients as well as another, or not utilize it as effectively, even if it has the advantage on the uptake rates.

The theoretically weaker competitor for nutrient uptake and storage as described by simple mechanistic models does not always have to be the loser of a competition either. In interference competition, competition functions through interactions that inhibit or spur the growth or reproduction of competitors indirectly. For instance could an additional species prey on and suppress the abundance of a theoretically stronger direct competitor with lower values of R^* . This could allow an inferior resource competitor to still survive in a habitat (Tilman, 1987; Tilman and Sterner, 1984). Furthermore, competitive advantages could be gained via the excretion of toxic or beneficial chemicals. The red tide dinoflagellate *Karenia brevis* for instance has been shown to release allelochemicals to suppress the growth of other species it co-occurs with in natural communities, potentially explaining why it can at times form dominant blooms in the Gulf of Mexico (Kubanek et al., 2005). In facilitation scenarios, species can gain competitive advantages by affecting each other positively. In a study of an experimental phytoplankton community, diatoms seemed to rely heavily on the appearance of sufficient cyanobacteria to make nitrogen available, after which the diatoms then managed to dominate and outcompete all other species (Eggers et al., 2014). All these above-mentioned interactions could have never been predicted from knowing species growth rates or their physiological nutrient uptake kinetics in isolation. It is therefore important to combine predictive studies

with investigations of mixed populations to identify mismatches and patterns emerging from species interactions.

To complicate matters even further, phytoplankton competitive dynamics seem to not just be determined by the competing species and environmental aspects investigated, but also through a path-dependency effect. Species succession was found to be determined by the community composition of the inoculum community and therefore no general competitive response to laboratory manipulations might be determined because the response of species was found to depend not only on physiology, but also on abundance, evenness and frequency of initial community members (Sommer, 1983).

Because of this complexity, Trimborn et al. (2013) claimed that the outcome of multiple species competition cannot be well predicted from responses of monoculture due to the fact that allelochemical interactions and other unknown factors come into play when phytoplankton species interact. To account for more intricacy in species competition than just the ability to take up nutrients as a determinant of competitive outcomes, more complex models were developed to take into account initial population sizes, intraspecific factors such as death, cannibalism or other density-dependent effects (Schoener, 1976), as well as predation and interactions with other trophic levels. Contemporary niche theory for instance extended the traditional view of organisms competing for limiting resources, and added more complex interactions to explain species dynamics influenced by a multitude of factors (e.g. growth as a response to multiple stressors rather than just one), and how these are in turn influenced by that species (predator abundance, pathogens, or toxins) (Chase and Leibold, 2003).

More research is necessary to identify whether simple mechanistic models are ultimately suitable to predict competitive outcomes, as processes decoupled from cell physiology, single-

species growth, nutrient concentrations, and nutrient uptake and storage abilities, might play a role in determining species dominance within communities. Two chapters of this thesis are dedicated to better understand whether predictions about competitive outcomes can be made based on single species growth and physiology, as a successful determination would facilitate predictions on future phytoplankton community structures.

1.5 Research Objectives and Thesis Outline

Current physiological reaction norms, but also the capability of species to adapt to novel conditions will determine in what manner different phytoplankton groups will respond to changes in their abiotic environment. In order to better understand how phytoplankton populations and communities respond to environmental changes, I conducted experiments focussing on two aspects of performance across thermal gradients. Chapters 2 and 3, concentrate on the capacity for thermal adaptation within species. Chapters 4 and 5 studied direct competition between species across temperature gradients. Since the overarching aim of the thesis was to better understand responses of phytoplankton communities to future environmental change, the transition from single species to multi-species populations was aiming to improve our understanding of whether single species performance would be a suitable predictor of final community composition.

Chapters 2 and 3 investigated whether monocultures of laboratory phytoplankton populations can adapt to moderate temperature changes similar to those predicted in many marine systems for the coming century. In particular, chapter 2 investigated the growth response of different lines of the same species cultured at two different temperatures across a thermal gradient, whereas data chapter 3 studied the potential adaptation in respiration and

photosynthesis rates after the same lines were cultured at different temperatures for several years.

For Chapter 4, the focus shifted from investigating the response of isolated species to mixed cultures and direct species competition across a temperature gradient. To investigate whether the winner of direct competition in mixed cultures can be determined from knowing the performances of isolated cultures, I grew the laboratory model species *Phaeodactylum tricornutum* and *Thalassiosira pseudonana* as monocultures and mixed populations across temperature gradients to first of all observe whether predictions can be made, and second to see whether outcomes of competition would change across the gradient. In addition, I conducted competitions in nitrogen replete and deplete conditions as it has been shown previously that changes in multiple environmental parameters at a time can have interactive effects on monocultures of algae (Thomas et al., 2017). I wanted to investigate whether there would be an interactive effect on competition as well. I picked nitrogen concentration as the determining factor as it has often been found to be a limiting nutrient for growth in marine environments (Elser et al., 2007), so that it could be presumed that in natural environments, many competitive interactions would happen in N-deplete conditions rather than replete ones. Despite nitrogen often being limiting in natural environments, the role that its limitation would play in competition scenarios was however not previously investigated in depth until now.

In Chapter 5 I continued focussing on competition between the two diatoms *P. tricornutum* and *T. pseudonana*. My investigation in the preceding chapter showed that competition between the two diatoms across a stable temperature gradient changed and that there existed a potential stable equilibrium between the two under a specific combination of abiotic conditions, both in N-replete and N-deplete conditions. Leading on from this finding I

investigated whether it would be possible to create stable mixed cultures of the two diatoms that could be manipulated to answer questions on system stability. Focus lay on whether uniform temperature fluctuations of different magnitude could enhance or de-stabilise mixed populations.

Chapter 2: The Search for Thermal Adaptation in Long-Term Phytoplankton Cultures

2.1 Abstract

Future climate change is predicted to impact aquatic ecosystems and phytoplankton. Currently, warming of oceanic surface waters is happening at rates faster than ever recorded, with temperatures increasing on average by 0.2 °C per decade. Thermal adaptation may help phytoplankton to deal with rising temperatures. Lines from 3 species from 2 taxonomic groups (*Dunaliella tertiolecta*, *Pycnococcus provasolii*, *Chaetocerus mulleri*) were cultured at 15 °C and 20 °C for ~350 generations. Resulting selection lines were tested for thermal adaptation by measuring their growth across a high-resolution temperature gradient. None of the selection lines were found to differ significantly from the source line in accordance with the selection temperature, and it was concluded that none had adapted to their culture conditions in regards to their growth rates. Additionally, 3 strains of *Thalassiosira pseudonana*, previously found to have adapted to 9, 22 and 32°C, were re-examined for thermal adaptation. Significant differences in thermal performance among these lines were found and re-confirmed the previous conclusion. The results showed that phytoplankton cultured in the lab do not necessarily adapt to a new thermal environment if the selection pressure is not strong enough. Not all species seem to adapt at the same rates or possess the ability to keep up with ongoing environmental change, which will be a crucial aspect in determining future phytoplankton community composition.

2.2 Introduction

Temperature influences many biological processes. It drives metabolism on the level of single cells and the ecology of organisms. Thermal conditions directly impact and regulate parameters such as the speed of enzyme reactions, viscosity of fluids, or chronobiology in organisms (Krenek et al., 2012). It consequently determines growth ability, and as such influences the success of species to compete against one another, which ultimately determines community composition and ecosystem functioning (Sharp et al., 1979).

The rates at which biological processes occur across temperatures can be visualised through thermal performance curves (TPCs) (see Fig. 2.1), whereby growth or some other measure of fitness is measured along a temperature gradient (Krenek et al., 2012). A TPC can be used to predict cardinal points such as the optimum growth temperature (T_{opt}) or thermal limits at which cellular processes cease to function properly (CT_{min} and CT_{max}) (Mitz et al., 2017; Pörtner, 2002). At the optimal temperature of an organism or population, the sum of all catalytic reactions in a cell leads to the highest net growth. At temperatures where a TPC reaches 0, the particular organism's temperature limits are reached (Fig. 2.1). Although a "text book" TPC is predicted to have the same progression as depicted in Figure 2.1, with rates rising almost linearly with warming at sub-optimal temperatures, dropping off sharply at supra-optimal temperatures, the shape can differ significantly depending on the organism or trait under observation (Baker et al., 2016).

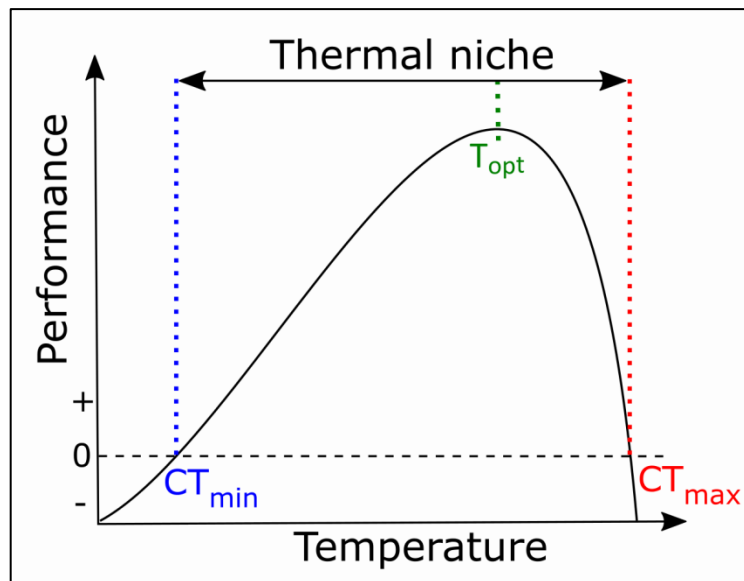


Figure 2.1: Typical thermal performance curve along a temperature gradient. T_{opt} = Optimum Temperature, CT_{min} = Critical minimum temperature, CT_{max} = Critical maximum temperature. Adapted from Krenek et al. (2012)

Shifts in thermal performance curves can occur due to alterations of cell physiology or changes in the abiotic environment. Temporary and reversible changes in performance caused by the organism encountering a novel condition are considered phenotypic plasticity or acclimation processes. These processes can be short-lived and be the result of biochemical alterations within a cell (such as changing the number of pigments or components of the photosynthetic apparatus) as a response to altered conditions (Moore et al., 2006; Reusch and Boyd, 2013). On the other hand, long-lasting modifications of performance that are the result of changes in the underlying genome are called adaptations (Schulte et al., 2011). TPCs can change by either shifting across the temperature gradient horizontally, expanding the growth range, by moving as a whole towards colder or warmer temperatures; or by changing vertically, becoming flatter or steeper (Fig. 2.2) (Schulte et al., 2011).

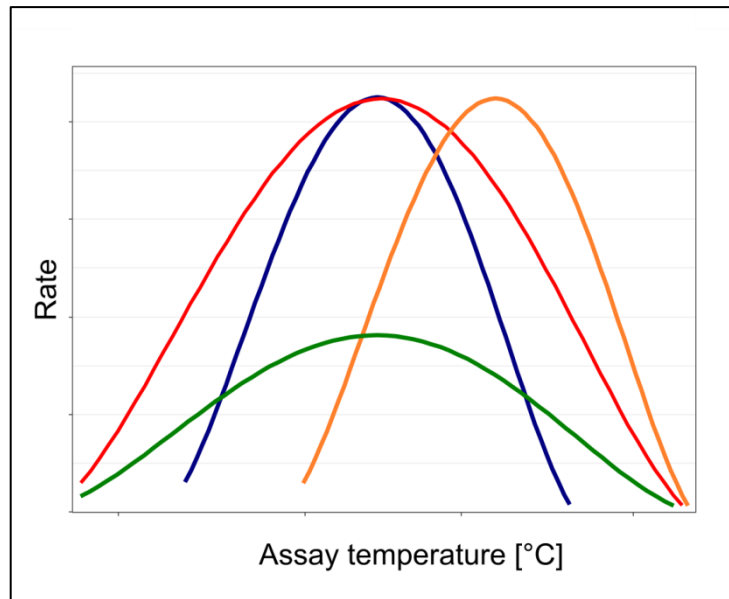


Figure 2.2: Conceptual figure of potential changes in thermal performance curves. Original curve (blue) could extend its growth range (red), shift as a whole towards other temperatures (orange), or change its slope around cardinal temperatures (green).

In the Anthropocene, scientific evidence predicts sea surface temperatures (SSTs) to rise at an average rate of up to 0.3 °C per decade (Collins et al., 2013; IPCC, 2013). Novel stratification patterns as a result of altered SSTs will lead to alterations of ocean currents and nutrient loadings of surface waters.

As single-celled microorganisms, phytoplankton are ectothermic and especially susceptible to such changes since they cannot regulate their organismal temperature and have no means of actively withstanding alterations in their environment. Their physiological performance is therefore directly linked to temperature (e.g. Geider, 1987). Like any other organism in aquatic environments phytoplankton are therefore faced with the challenge to either deal with the changing conditions by acclimating or adapting to them *in situ*, or shift in their distribution towards more favourable conditions. Factors that generally maximize the adaptive potential are high mutation rates, and a high selection pressure (Huertas et al., 2011), whereas limits to

acclimation or adaptation can be set via physiological or ecological processes. Physiological limits usually occur through mechanisms operating at the organismal level, like denaturing temperatures of proteins. Ecological limits on the other hand operate on populations levels through biotic factors such as a constant and strong high intra- and interspecific competitive pressure (Reusch and Boyd, 2013).

Phytoplankton populations have evolved to thrive in their local environments, growing best in water conditions in which they naturally occur in terms of water chemistry and temperature (Suzuki and Takahashi, 1995; Thomas et al., 2012). Optimum growth temperatures of different species have shown a co-variation with latitude, and co-vary with the mean annual temperature in the regions where they were initially isolated (Thomas et al., 2012). The ability to adapt to environmental changes is crucial for structuring future oceans (Chown et al., 2010), and unequal adaptive ability in combination with changes in spatial distribution is predicted to lead to major changes in composition of species assemblages, their interactions and ultimately the functioning of ecosystems (Barton et al., 2016). Whilst some species might be able to adapt to current rates of climate change, others may not. Some species might migrate to more favourable conditions when their current environment is altered, but especially for organisms living at or near conditions at the edge of their TPC's upper temperature limit, with little ability to migrate, lack of thermal adaptation might lead to extinction (Barton et al., 2016; Chown et al., 2010).

In the past decade, experimental evidence highlighting the potential for rapid thermal adaptation in phytoplankton has started to emerge, albeit still scarcely (e.g. Huertas et al., 2011; Schlüter et al., 2014). It has been shown to be a common occurrence across a diverse range of phytoplankton taxa, but different species were found to have varying adaptive

potential to the imposed stresses in the laboratory. Phytoplankton were shown to have the potential to adapt to changes in temperature even within the time span of around 450 asexual generations (Schlüter et al., 2014), or to a combination of temperature and altered CO₂ contents within 2700 generations (Listmann et al., 2016). One publication suggested that thermal adaptation can even occur within 100 generations (Padfield et al., 2015). What these publications all have in common is the suggestion that rapidly occurring thermal adaptation within relatively short time periods of a few months or years could enable species to keep up with the current rate of SST warming reported by many scientific studies (IPCC, 2013).

In a decade-long study of natural environments, phytoplankton shifted its mean niche optimum temperature by +0.45 °C, tracking a water temperature change of +0.73 °C (Irwin et al., 2015). Another study on decade-long warming in mesocosms discovered that increased temperatures lead to adaptive changes in physiological traits and shifts of TPCs in a common chlorophyte *Chlamydomonas reinhardtii* (Schaum et al., 2017). An analysis of niche plasticity in 12 diatom taxa over a 59-year-period in North Atlantic waters demonstrated that diatom species have the potential to adapt *in situ* and withstand SST changes over long periods of times. *Thalassiosira* species for instance were found to track colder waters and shift their distribution northwards away from warming waters, and displayed a significant negative correlation with northward moving isotherms (Chivers et al., 2017).

Many of the above-named experimental studies did however not assess the adaptive potential under an ecologically realistic change in the environmental parameter under observation. Adaptive responses were evoked through greater changes in temperature than predicted or with changes that would not occur on such order of magnitude in nature within such a short period of time, or by keeping cultures growing exponentially for hundreds of generations. To

test whether more moderate environmental alterations would also lead to thermal adaptation in phytoplankton cultures, lines of *Dunaliella tertiolecta*, *Chaetocerus mulleri*, and *Pycnococcus provasolli*, cultured at 15 and 20 °C, were tested for changes in growth along a temperature gradient. As a positive control of ability to detect adaptation, thermal performance was tested in 3 lines of *Thalassiosira pseudonana* in which thermal adaptation to temperature has been reported previously (lines were adapted at 9 °C and 32 °C from a 22 °C parent line) (Schmidt, 2017). It was hypothesized that culturing different lines of the above-mentioned algae over 6 years would lead to thermal adaptation detectable through a shift in their thermal growth performance and that this thermal adaptation would lead to a shift of the optimum temperatures towards the temperature of selection.

2.3 Materials & Methods

2.3.1 Culturing of algae

Lines of the algal species *Dunaliella tertiolecta* (CCAP1320), *Chaetocerus mulleri* (CCAP 1010/3), and *Pycnococcus provasolli* (CCMP 1203) were maintained at 15 °C and 20 °C and transferred once a month in f/2 medium (Guillard and Ryther, 1962; Guillard, 1975) for 6 years (~350 generations, depending on the species). Numbers of generations were calculated with equation [1].

$$g = \frac{(\log(N_2) - \log(N_1))}{\log(2)} * N_T \quad [1]$$

where N_1 is the number of cells ml⁻¹ after 1:36 dilution and at the onset of a new growth cycle, and N_2 is the number of cells before dilution of the cultures in stationary phase. N_T is the number of transfers, which was 72 for six years (6 years * 12 months).

Cryopreserved lines of *T. pseudonana* were gifted from Katrin Schmidt (University of East Anglia), which had been adapted to “cold” (9 °C), “ambient” (22 °C; parent culture), and “warm” (32 °C) conditions by maintaining cultures in exponential growth phase and diluting them every third day to a concentration of 1×10^5 cells ml⁻¹ for 2.5 years (300 generations) at their respective temperatures (Schmidt, 2017). Afterwards the cultures were defrosted at Essex University and cultured for 5 months in f/2 medium, to acclimate to f/2 medium and to dilute out the cryopreservant. Due to facility constraints, the cold and warm lines were maintained at 15 and 26 °C respectively (instead of 9 and 32 °C). Due to this circumstance, no stable temperature history could be guaranteed for the lines and it is unclear whether the new selection pressure of a shifted temperature led to a shift in thermal performance curves within the 5 months culturing period after bringing the cultures back from cryopreservation. The strains were tested for their thermal adaptation at Essex University to investigate whether results could be replicated and whether thermal adaptation remained through cryopreservation.

2.3.2 Measurement of Algal Growth

After the culturing period, species were tested for thermal adaptation by being grown along a temperature gradient. Two different thermal gradient blocks were used, depending on what facilities were available at the time.

For *T. pseudonana*, a temperature gradient was established with a 17 assay temperatures aluminium thermal gradient block, drilled to accommodate glass test tubes. Circulation immersion heater chillers (Grant Instruments, Cambridge, U.K.) at opposite ends maintained the temperature differential (± 0.2 °C per gradient position), monitored using a thermometer over the course of the experiment. Assay temperature ranged from 10 to 34 °C, and light levels

were set to $150 \pm \mu\text{mol m}^{-2} \text{s}^{-1}$. For all other species one microtiter thermoblock (18 assay temperatures for *P. provasolii* and *C. mulleri*) or two microtiter thermoblocks (36 assay temperatures for *D. tertiolecta*) were set-up, on which 24-well-plates were placed in succession (8 to 30 °C at $450 \pm 25 \mu\text{mol m}^{-2} \text{s}^{-1}$).

Changes in algae biomass over time were assessed via fast repetition rate fluorometry (FRRf) with an FRRf II Fastact Fluorometer (Chelsea Instruments, UK) at an excitation wavelength of 435 nm for samples grown in tubes, and from optical density (OD) measured at 450 nm with a FLUOstar Omega plate reader (BMG LABTECH, Germany) for samples grown in the microtiter plates. Chlorophyll *a* fluorescence and absorption were used as proxies for biomass. Exponential growth rates were calculated using linear models fitted onto the $\ln F_0$ (F_0 = minimum fluorescence yield) or $\ln OD$ (OD = optical density) measurements over time.

2.3.3 Thermal Performance Curves

The number of biological growth replicates per culture line that was collected for the statistical analysis differed between species. *D. tertiolecta* was the species with the highest amount of replicates with $n = 12$ per culturing line (meaning 12 replicates for the 15 °C line and 12 replicates for the 20 °C). In contrast and unfortunately, for *P. provasolii* and *C. mulleri* the amount of replication was very low with $n = 2$ per culture line. For the positive control species *T. pseudonana*, $n = 3$ per line and it was the only species that had three culture lines (the cold, the source temperature, and the warm selected lines), in comparison to only two for the other species (the source temperature, and the warm selected lines).

After growth data had been collected, the R package “temperatureresponse” was used to fit models of TPCs onto the obtained growth data across the temperature gradients (Low-Décarie et al., 2017). Twelve equations commonly used to model growth response to temperature were

fitted to the obtained growth data. The best fitting model for each species was picked based on the lowest Akaike Information Criterion (AIC) value where the equation could be fit to all replicates of the 15 °C and 20 °C lines. The AIC is an estimator of error and indicates the relative quality of statistical models. In general, the lower the AIC, the better does the data fit to a model. Sometimes a model had a lower AIC value but would not fit on all the growth replicates collected. The model chosen was then used to describe the growth response across the temperature gradient and to extract cardinal temperatures (see Suppl. Fig. 2.1 – 2.4 with AIC values for the four species, the table with all the single model equations as well as corresponding references can be found in the Supplementary Material to Chapter 4, where it was included as part of a peer-reviewed journal publication). Different equations were used for different species as species have evolved inherently different performances across temperature gradients. The equations all differ in their shapes, so that some might suit the thermal performance progression of a specific species better than others. For instance can a species have a more uniformly bell-shaped thermal performance, whereas another could be more skewed to the right or left. Therefore, not every model is equally suited for every species.

For *D. tertiolecta*, 12 replicates of two lines were grown in microtiter plates between 8 °C and 30 °C. Equation [2] taken from Heitzer et al. (1991) was found to best describe the performance along assay temperatures.

$$Rate = \frac{a \cdot \left(\frac{T}{298.15}\right) \cdot \exp\left(\frac{b}{R} \cdot \left(\frac{1}{298.15} - \frac{1}{T}\right)\right)}{1 + \exp\left[\frac{c}{R} \cdot \left(\frac{1}{d} - \frac{1}{T}\right)\right] + \exp\left[\frac{e}{R} \cdot \left(\frac{1}{f} - \frac{1}{T}\right)\right]} \quad [2]$$

whereby a , b , c , d , e , and f are model constants, T is the assay temperature, R the universal gas constant (Boltzmann constant).

Two replicates of two lines of *P. provasolii* were grown in microtiter plates between 12 °C and 30 °C, and the most suitable model was equation [3] from Ratkowsky et al. (1983).

$$Rate = [a \cdot (T - T_{min})]^2 \cdot [1 - \exp(b \cdot (T - T_{max}))]^2 \quad [3]$$

where a and b are model constants, T the assay temperature at which a rate was measured, and T_{min} and T_{max} where the estimated minimum and maximum temperatures (as estimated by the fitted model).

Also for *C. mulleri*, 2 replicates of two lines of were grown in microtiter plates between 8 °C and 30 °C, and equation [4] taken from Johnson et al. (1942) best described their thermal performance.

$$Rate = \frac{a \cdot T \cdot \exp\left(\frac{-b}{R \cdot T}\right)}{1 + \exp\left(\frac{-c}{R}\right) \cdot \exp\left(\frac{-d}{R \cdot T}\right)} \quad [4]$$

where the model parameters are the same as for equation [2].

Three lines with 3 replicates each of *T. pseudonana* were grown across an assay gradient of 8.6 °C to 33.6 °C to describe the TPCs. Equation [4], was also the most suitable model for them.

In order to test for significant differences in optimum growth temperatures (T_{opt}) between lines within each species, one-way ANOVAs with an alpha level of 0.05 were conducted. Significant differences would signify a signal of thermal adaptation. T_{opt} was the response variable, while source temperature was the independent variable. Because the TPCs of the two *P. provasolii* lines appeared to differ widely in their magnitude, the difference between their maximum growth rates (μ_{max}) was also tested for this species, with μ_{max} being the response, and source temperature the independent variable.

Only for *T. pseudonana* did the ANOVA compare the optimum temperature between 3 different groups. For all the other species the ANOVA compared only two groups, making it effectively a t-test, a special case of the ANOVA. Before the ANOVA could be performed, ANOVA assumption criteria for normal distribution of residuals and homogeneity of variance had to be tested. For groups that failed the ANOVA assumption tests on normality of residuals, a Kruskal-Wallis rank sum test was performed instead, to identify significant difference between culture lines. This was the case for the comparisons of T_{opt} between the *D. tertiolecta* lines, and for the comparison of maximum growth rates (μ_{max}) in *P. provasolii*. The tests for differences in the T_{opt} of the *P. provasolii*, *C. mulleri*, and *T. pseudonana* culture lines confirmed normality of residuals and equal variance. It has to be noted that these tests tend to pass when sample size is low, which was the case in this study. It would have been desirable to collect more growth replicates for the species that had only $n = 2$ per line. Since the ANOVA tested differences between 3 lines for the species *T. pseudonana*, post-hoc testing via Tukey's honest significance test was conducted to analyse the pairwise comparisons and identify where significant differences could be found. After TPCs had been modelled, it was also possible to calculate the amount of imposed selection pressure in terms of percentage of daily growth rate change that was imposed when the lines were transferred from their source environment to their selection environment. Once the ANOVA assumptions had been passed, it was tested via a two-way ANOVA, whether this percent change in daily growth rate (standardised to the μ_{max} at T_{opt} of each species), constituted a significant change. The independent variable was the percentage of daily growth rate relative to the μ_{max} , and the dependent variables were "species" and "culturing temperature".

All statistical analysis was conducted with R (version 3.3.1).

2.4 Results

2.4.1 Test of thermal adaptation in long-term culture lines from the Essex culture collection

Temperature response curve fits of all species revealed that culturing the lines at 15 or 20 °C meant that they had been cultured at sup-optimal temperatures (Fig. 2.3 A,C,E).

2.4.1.1 *Dunaliella tertiolecta*

Growing two lines of *D. tertiolecta* along the temperature gradient showed that TPCs were very similar (Fig. 2.3 A), and using the Kruskal-Wallis test, no significant differences in their optimum temperatures were found ($p = 0.97$) (Fig. 2.3 B). Optimum temperatures were estimated based on model fits at 28.8 ± 1.2 °C for the 15°C line and at 28.1 ± 2.4 °C for the 20°C line.

2.4.1.2 *Pycnococcus provasolii*

The 2 replicates of two lines of *P. provasolii* grown across the assay temperature gradient (Fig. 2.3 C) showed significant differences in their optimum temperatures existed ($F_{1,2} = 169.2$, $p < 0.01$) (Fig. 2.3 D). The signals obtained did however not align with their source environment (Fig. 2.3 C) and the 20 °C line had a colder optimum temperature with greater maximum growth rates (0.49 ± 0.01 day⁻¹ at 25.5 ± 0.1 °C) than the 15 °C line (0.34 ± 0.02 day⁻¹ at 28.0 ± 0.2 °C).

This striking difference in the μ_{max} between the two lines was tested statistically as well. However, the statistical analysis with the Kruskal-Wallis test yielded that the observed difference was not statistically significant ($p = 0.12$). A higher amount of replication and potential ANOVA testing, if the ANOVA assumptions would be consequently met, could potentially have resulted in finding a significant difference.

2.4.1.3 *Chaetocerus mulleri*

Growing lines of *C. mulleri* along the assay temperature gradient (Fig. 2.3 E) showed that there were once again no significant differences in their optimum temperatures ($F_{1,2} = 2.54$, $p = 0.25$) (Fig. 2.3 F). Optimum temperatures were estimated based on model fits at 29.6 ± 0.6 °C for the 15°C line and at 28.9 ± 0.2 °C for the 20°C line.

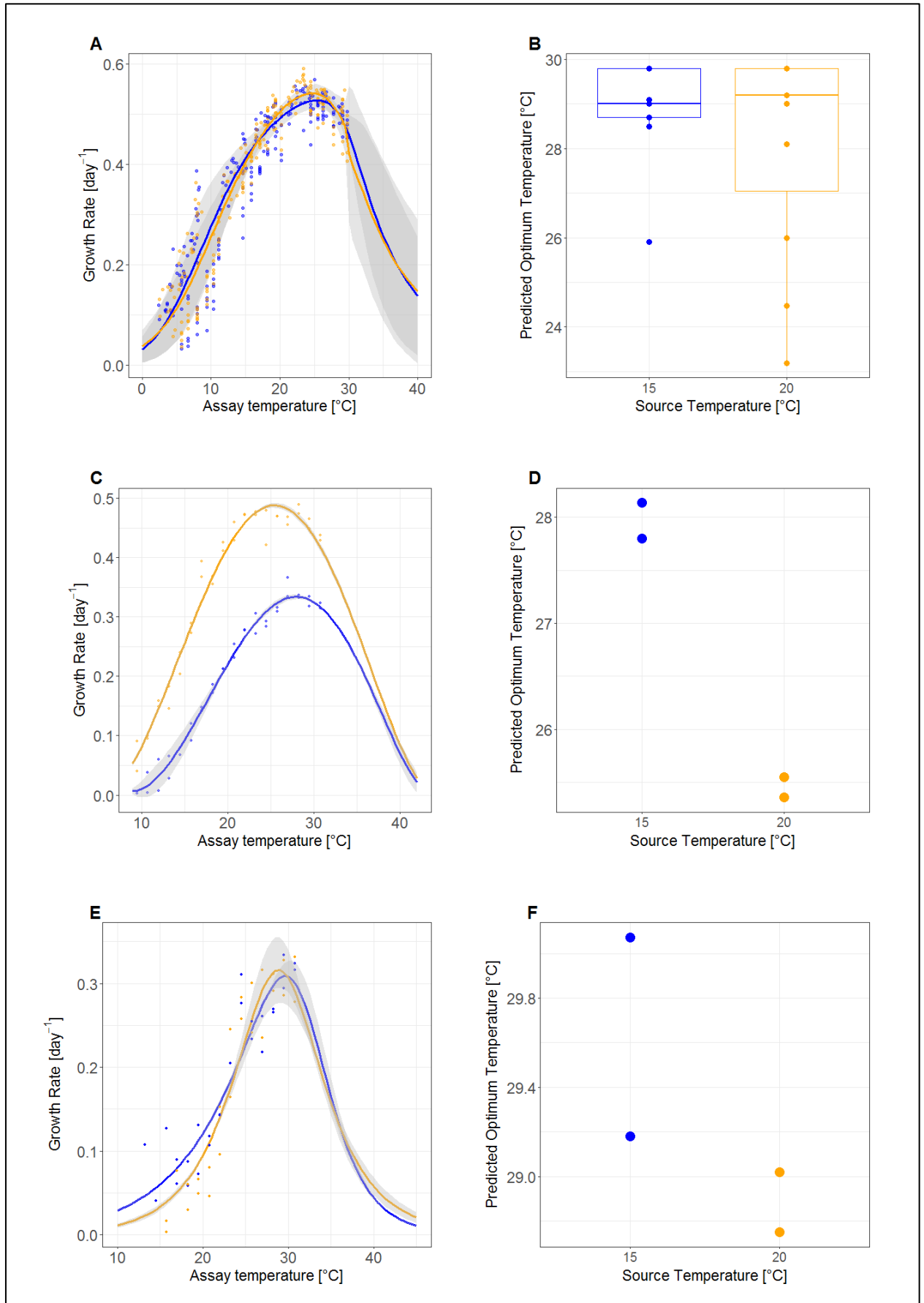


Figure 2.3: Mean thermal performance of 3 phytoplankton species with experimental lines grown at 15°C (blue) and 20°C (orange) source temperatures. Model fits and the corresponding optimum temperatures predicted from those model fits are depicted for *D. tertiolecta* lines (A & B), for *P. provasolii* lines (C & D), and for *C. mulleri* lines (E & F). Single points underlying the TPC plots are single growth rates measured along the investigated assay temperature gradient. Grey-shaded area around the mean TPC of each line denotes one standard deviation, calculated from single replicate model fits. For the optimum growth temperatures of the *P. provasolii* lines, a significant difference was found that did not follow the expectation of lines having their T_{opt} closer to their source environment. For the other two species, no significant differences were found.

2.4.2 Previously evolved lines of *T. pseudonana* (positive control)

Previously adapted lines of *T. pseudonana* were used as a positive control to test whether the used methods were adequate for finding thermal adaptation. Growth performance of these three *T. pseudonana* lines across the temperature gradient showed that the thermal performance curves differed for each individual strain (Fig. 2.4 A) and that significant changes in optimum growth temperatures existed and had persisted through cryopreservation (Fig. 2.4 B) ($F_{2,7} = 8.23$, $p < 0.05$). Tukey's post-hoc testing revealed a significant difference between the 15 °C and the 26 °C line, i.e. the coldest and warmest *T. pseudonana* lines ($p < 0.05$). Between the other pairs the difference in optimum temperatures was however not significant (comparison between 15 °C and 22 °C line had a p-value of 0.31, and comparison between 22 °C and 26 °C line had $p = 0.07$). Optimum growth temperatures had shifted in accordance with expectations and corresponded to the source temperatures that the lines were cultured at. For the 15°C line, the average optimum temperature was $22.5 \pm 0.8^\circ\text{C}$, for the 22°C it was $23.8 \pm 1.5^\circ\text{C}$, and for the 26 °C it was found to be $26.0 \pm 0.4^\circ\text{C}$.

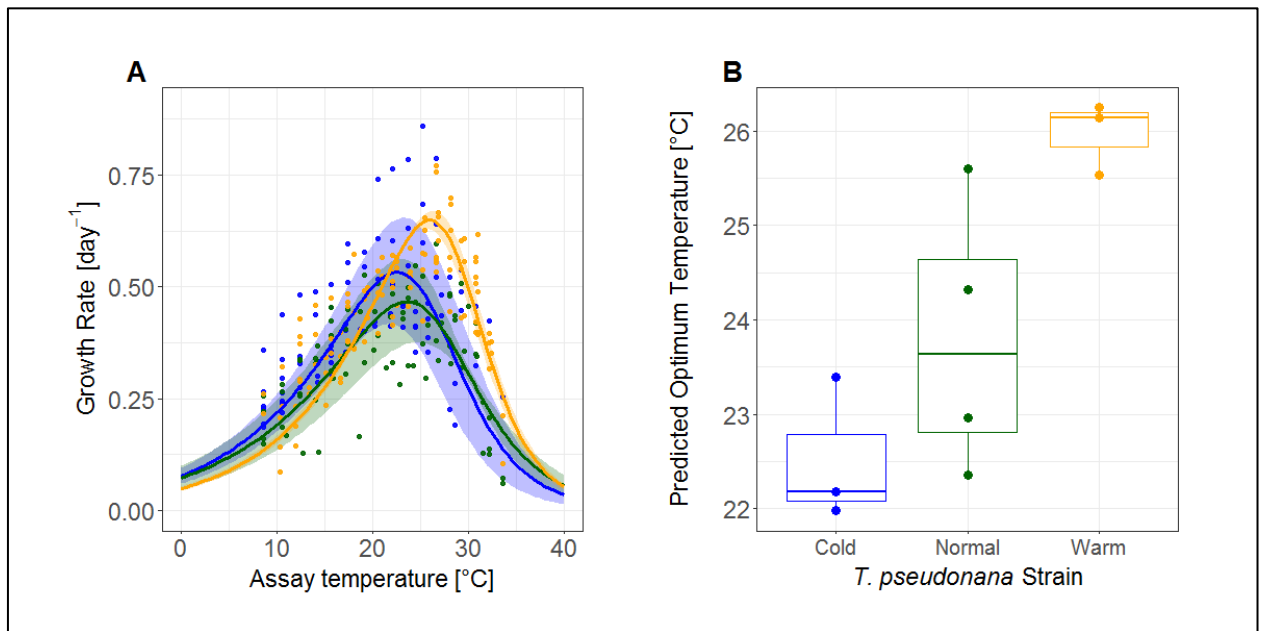


Figure 2.4: Mean thermal performance of *T. pseudonana* lines evolved under cold assay temperatures at 15°C (blue), normal initial culture temperatures 22°C (green), and warm assay temperature 26°C (orange). (A) Mean TPCs of lines grown in a tube thermoblock. Single points are measured growth rates at the assay temperatures onto which the growth models were fit. Colour-shaded areas indicate one standard deviation calculated from single replicate model fits around the mean TPC. (B) Optimum temperatures estimated from model fits.

2.4.3 Comparison of imposed selection on species

Comparing the TPCs of the ancestral lines (the 15 °C lines for the species from the Essex collection, and the 22 °C line for *T. pseudonana* from UEA) of the investigated species showed that their growth ranges were overlapping, however absolute growth rates and CT_{\min} and CT_{\max} temperatures differed (Fig. 2.5 A). For instance did *D. tertiolecta* display the highest overall growth rates and the widest thermal niche, whereas *C. mulleri* had the lowest growth rates and narrowest niche.

The selection pressure, quantified as the imposed change in daily growth rate that was exerted on the selection lines at the selection temperature (which was 20 °C for the Essex lines, and 9 or 32 °C for *T. pseudonana*) was compared between all species. For the lines from Essex, a 5 °C

change for the initial source temperature meant less selection pressure than the 10 °C or 13 °C change that was imposed upon the *T. pseudonana* lines. A change of 5 °C for *D. tertiolecta* meant that the imposed selection was a change of 15.1 ± 4.3 % of its daily growth rate. A similar value was reached for *C. mulleri* with 19.6 ± 1.8 %. For *P. provasolii* the selection pressure was higher with 38.2 ± 4.9 %, and for the positive control *T. pseudonana* the selection pressure was estimated at 53.2 ± 11.7 % (Fig. 2.5 B). For all species, the changes in terms of their percentage of daily growth rate constituted a significant difference ($F_{1,26}=133.75$, $p < 0.001$). The values for *D. tertiolecta* and *C. mulleri* were lower because the slopes of their TPCs at the imposed selection temperatures were flatter than for *P. provasolii*, so that a temperature change would have had less of an impact in terms of change in growth rates. For *T. pseudonana*, the exerted pressure was the highest, with the selection temperature of 32 °C being several degrees warmer beyond the estimated optimum temperature of 23.8 ± 1.5 °C.

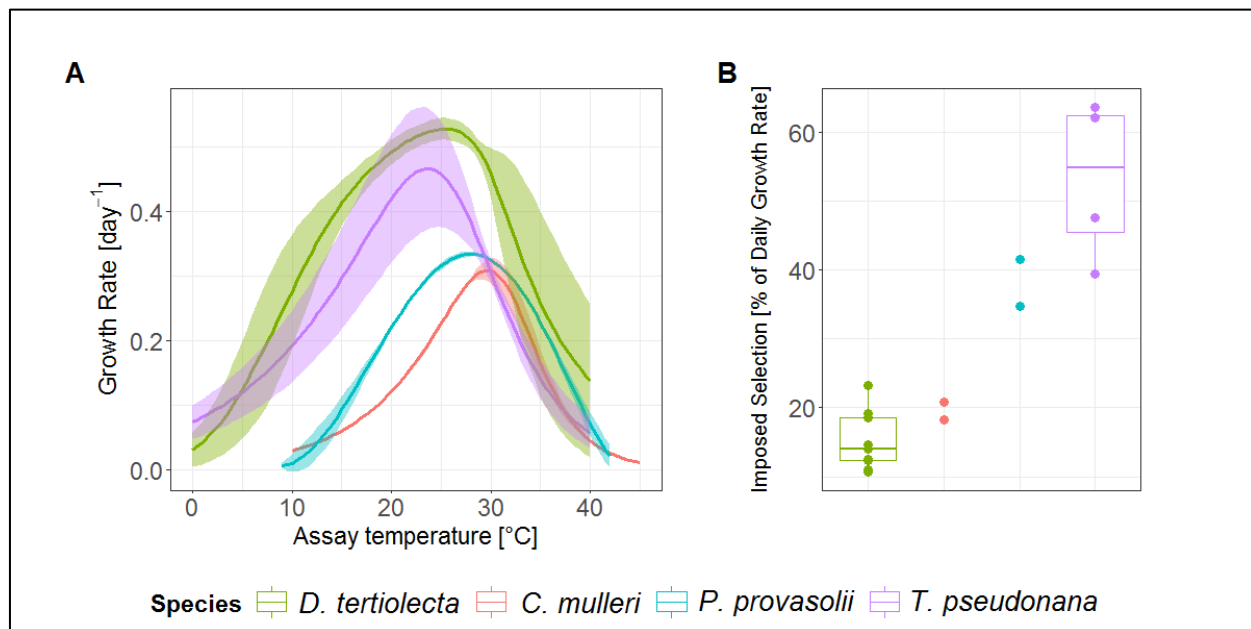


Figure 2.5: (A) Comparison of TPCs of the parent lines of *D. tertiolecta*, *C. mulleri*, *P. provasolii*, and *T. pseudonana*. (B) Imposed selection pressure on the species in % of their daily growth rates.

2.5 Discussion

2.5.1 Thermal niche of studied species

The aim of this study was to identify whether thermal adaptation had occurred in experimental lines of phytoplankton. The investigation of the selection lines did not result in findings of thermal adaptation and the results showed that the applied environmental change of 5 °C did not impose a significant enough pressure to lead to thermal adaptation within ~350 generations.

The circumstance that thermal adaptation could be detected with the used experimental set-up was demonstrated by growing *T. pseudonana* lines which had previously been adapted in another laboratory and confirming these findings. Although these donated algae were adapted at a higher selection pressure than the investigated algae from the Essex collection (see Fig. 2.5), the findings confirm the suggestion that the ubiquitous *T. pseudonana* might be able to track changes in surface water temperatures *in situ*, as it seems to be able to adapt to temperature changes within several hundred generations. Whether this diatom species will keep up with the predicted changes (IPCC, 2013) at sufficient rates, remains unclear as the selection pressure that evoked a shift in thermal performance was substantially higher than the predicted changes (10 °C selection pressure vs 3 °C predicted change).

For the cultures from the Essex collection, the question remains whether these species have the capability to adapt to warming conditions or not. Potentially through a longer culturing period or a further increase in culturing temperature, as is the case in other studies (Listmann et al., 2016; Schlüter et al., 2014; Schmidt, 2017), optimum temperatures or slopes in TPCs around T_{opt} or towards the critical maximum temperature (CT_{max}) might change as a consequence of phytoplankton adapting to altered abiotic conditions (Baker et al., 2018). The

fact that no improvement in growth rates as a response to culturing conditions occurred in the currently investigated species does not necessarily mean that no adaptation to the changed environment occurred. It is possible that adaptation occurred in other traits that were not measured in this study. Growth performance is by far not the only trait that can adapt and adaptive changes might occur in traits other than growth capabilities that could lead to competitive advantages under warming conditions. For instance could the production of toxins, the chemical composition of the cells, or cell size be altered, which would affect susceptibility to predation or direct competition within phytoplankton community members (Reusch and Boyd, 2013).

In order to make conclusive statements whether any genetic adaptation has occurred as a response to altered source temperatures, genetic analysis would be necessary. Due to budgetary restraints, this was however not performed. If such an investigation would be performed, modifications in genes that are usually associated with processes that result in better growth ability (carbon sequestration and respiration, improved photosynthetic efficiency, etc.) could then be positively identified and presumed to be a response to the culturing environment. The type of potential genetic modifications can be diverse (exchange of single nucleotides, duplication or loss of chromosomes, insertions, deletions), and consequently the genetic basis for altered growth ability might differ depending on the species even, if the resulting TPC shift might be comparable (Rengefors et al., 2017). Based on the current findings in this study however, it needs to be assumed that no adaptation occurred and that if temperatures were to rise in waters where these species occur and grow closely to their CT_{max} , they would die off or be outcompeted and replaced by species which can grow beyond that temperature.

2.5.2 Effect of culturing methods on thermal adaptation

This study contrasted species and lines that have been continuously kept in exponential growth phase to evoke a thermal adaptive response (*T. pseudonana*) and some that have been cultured mainly in stationary growth phase (all other investigated species). In most of the studies that investigated the adaptive potential for shifted thermal tolerances, phytoplankton cultures were kept in exponential growth phase throughout the adaptation period (e.g. Schlüter et al., 2014). This is supposedly done to increase the amount of generations within a shorter amount of times and to sustain the algae under ideal conditions and in good health.

However, in natural environments phytoplankton rarely grow exponentially for prolonged periods of time, even less so for years without interruption, spending their life cycle in stationary as well as exponential growth phases (Padfield et al., 2015). Whether similar rates of thermal adaptation would occur in nature as under laboratory conditions should be tested in further mesocosm or field experiments. Natural mechanisms operate on different scales of time and complexity than experimental ones. Environmental variations such as temperature changes might appear over years and even natural nutrient pulses do rarely occur within a few hours or days but on longer time scales. Adaptations in natural populations could be diluted due to an influx of new population members that did not acquire the thermal adaptation or adapted individuals might be carried away. In addition, grazing pressure, changes in nutrient-availability as well as other fluctuations in the abiotic environment might change the rate at which natural populations can adapt to a changing environment (Irwin et al., 2015; Sommer, 2002). All of these multiple biotic and abiotic stressors interact and exert an influence on phytoplankton simultaneously whereas in the lab, environmental changes are investigated in isolation. Observed adaptive rates in laboratory set-ups might therefore occur to be higher than they are in nature where less resources and energy can be solely allocated for the adaptation to

the thermal environment when the organism has to deal with a plethora of external pressures. In addition, as the investigated cultures were not clonal at the beginning of the experiment, it is also likely that the inherent genetic variability within the investigated long-term algae cultures provided a larger amount of genotypes capable of dealing with altered external conditions, so that adaptive rates might have been further reduced overall if enough genotypes were present in the population to cope with the 5 °C temperature increase without adapting and shifting T_{opt} towards warmer temperatures (Reusch & Boyd, 2012).

Most species that were investigated in experimental studies on thermal adaptation would be considered laboratory cultures that were purchased from professional culture collections (such as the investigated cultures in this study), or were in culture for many years after they had been isolated from natural environments. Such cultures are usually not kept in exponential phase but rather transferred on a monthly basis to keep them alive, until the decision is made to use them for experimentation, upon which they are suddenly cultured in exponential growth and get exposed to a whole new set of abiotic conditions and culturing schedules. Laboratory environmental manipulations where cultures are continuously grown exponentially and in nutrient replete conditions at optimum light levels can therefore exert an adaptive pressure that is very different to a natural environment (Sommer, 2002). It could be possible that in comparison to investigations that kept their cultures growing exponentially for extended periods of time, the investigated algal cultures from this study could be slightly more representative of natural plankton populations due to their schedule of exponential growth when cultures were freshly transferred each month (simulating dilution and nutrient pulses from natural environments), and extended periods of stationary growth when nutrients were used up (simulating oligotrophic natural conditions). It would have been ideal to have also kept

the lines in continuous exponential growth for the same amount of time to compare potential changes in thermal performance. Before conclusive statements about the adaptive potential of marine communities subject to environmental change can be made, a general discussion about the methods of how experimental evolution is investigated and detected and which approach to studying evolutionary responses is most appropriate might help the research community to a) standardize the methods of investigation and b) identify which experimental laboratory set-ups best represent and closest mimic natural dynamics.

2.5.3 Limitations of the Study

Although overall model fits onto the growth rate data across temperatures for species grown in microtiter plates yielded good results, the variation in growth rates captured due to biological variation or physical variations of the experimental set-up might have obscured evidence of thermal adaptations in the investigated species. Possibly the set-up used was not adequate to uncover small but important differences between the lines. There were for example re-occurring inconsistencies with the temperature gradient for the microtiter plate-based thermoblocks. Water was used to flood the thermoblocks to improve thermal conductivity. As this water evaporated continuously, it was impossible to keep a precise stable temperature gradient. The measured growth rates were therefore mean rates of assay temperatures that occurred at a specific well position throughout the experimental run. Although not huge, these fine differences are however important and need to be detected, as slight variations in TPCs could lead to crucial ecological differences in natural environments (Low-Décarie et al., 2017). This also begs the question as to what is the best modelling approach for thermal performance and whether using specific models may reinforce the expectation bias to find a positive result. Depending on what equation was used (not necessarily the one with lowest AIC) and whether

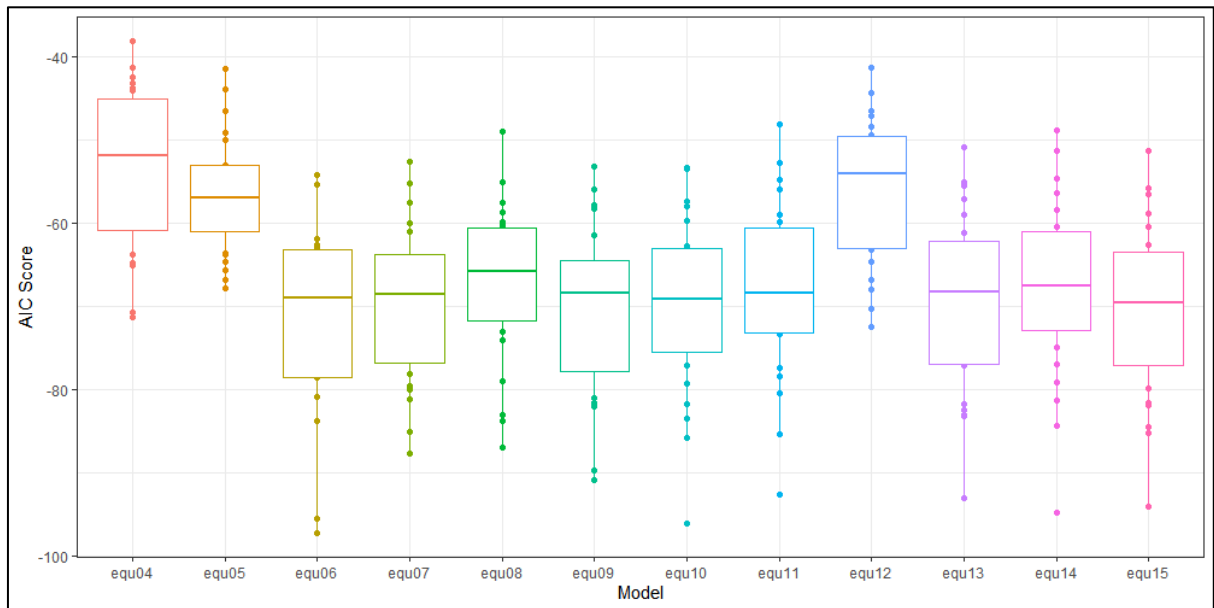
models were fit on single dilution phases (pseudo-replication), single replicates or averages, significant differences could be found if the data would have been analysed differently. It is therefore of utmost importance for studies investigating thermal adaptation to openly identify how data were pooled or bootstrapped and how equations were fit (Low-Décarie et al., 2017).

2.6 Conclusion

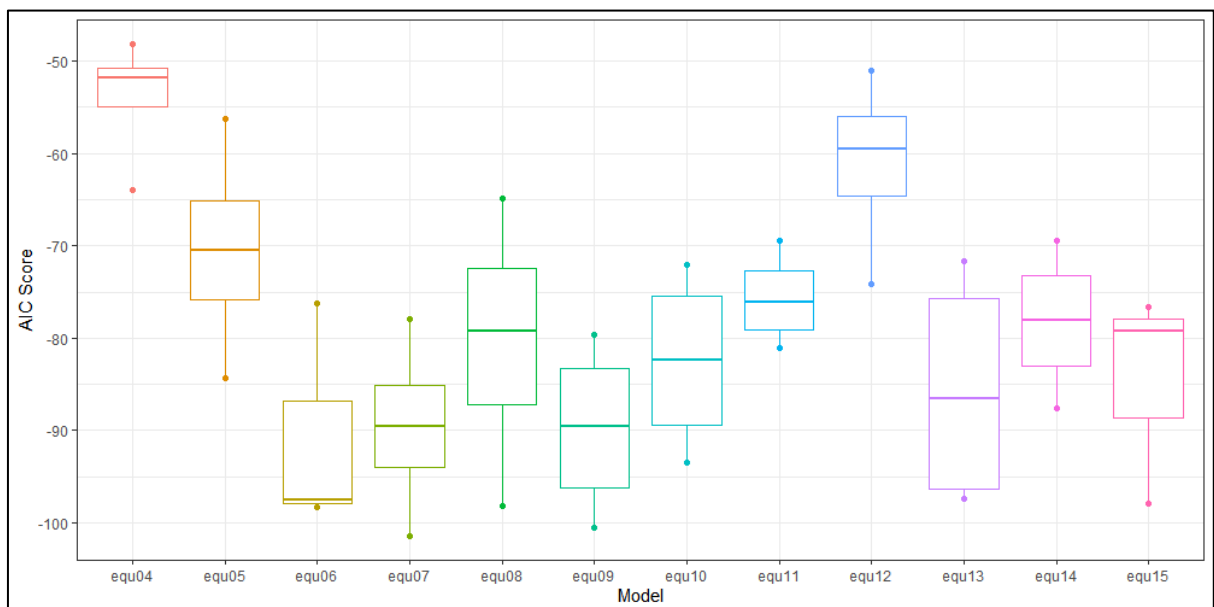
Like all marine species, the species in this study will most likely be affected by warming water temperatures as a result of climate change in the coming decades. Testing multiple species from varying taxonomic groups indicated that adaptation to temperature under laboratory conditions in a relative short amount of time is not necessarily the norm, as previously suggested by some of the studies mentioned in the introductory section of this chapter. This investigation however showed that the amount of temperature change, as well as culturing method seem to play a major role in evoking an adaptation response. As natural conditions are much more complex than controlled laboratory set-ups, the question remains whether thermal adaptation in marine phytoplankton will occur in coming decades, and if so, whether adaptations will ensure the same temporal variations in community structures, and ecosystem functionalities as under current conditions. Adaptive rates might change when multiple abiotic factors are altered simultaneously or adaptation might be hampered altogether. Future investigations of thermal adaptation should therefore focus on replicating realistic scenarios instead of trying to find thermal adaptation by exposing phytoplankton to unrealistic conditions. Furthermore it is essential to investigate whether thermal adaptations can have an effect on species interactions and competition and how varying rates of adaptation in different strains or species might affect community structure, as adaptations that would be overall neutral in a complex ecosystem would be less relevant to study.

2.8 Supplementary Material

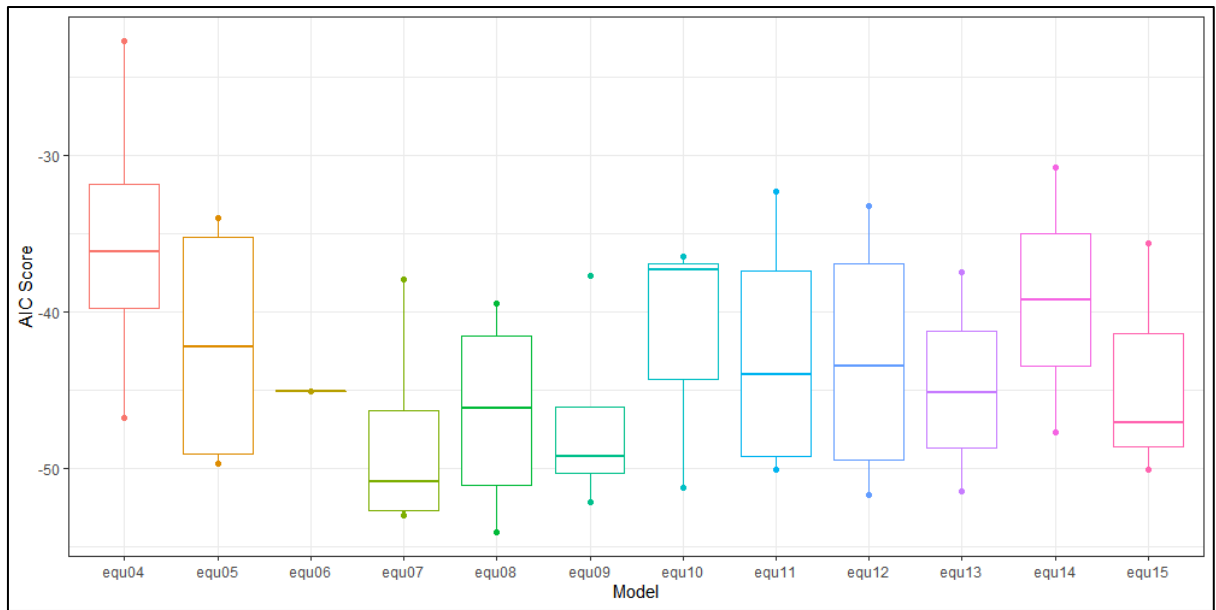
2.8.1 AIC scores for TPC model fits to growth rate data of different species



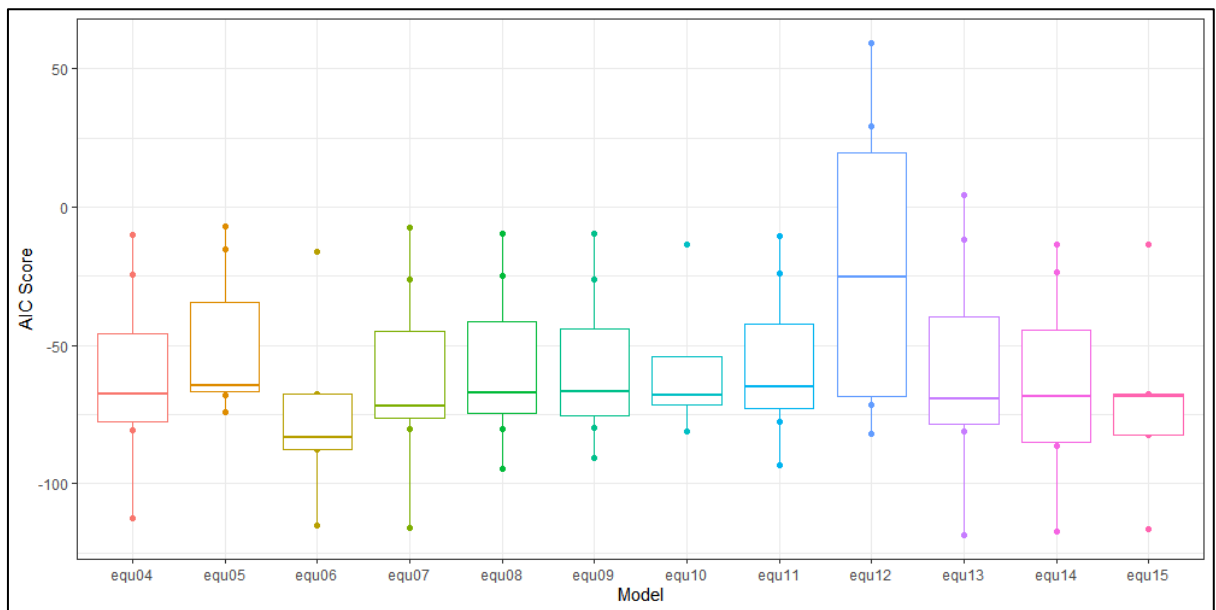
Supplementary Figure 2.1: AIC scores of model fits to growth rate data of *D. tertiolecta*.



Supplementary Figure 2.2: AIC scores of model fits to growth data of *P. provasolii*.



Supplementary Figure 2.3: AIC scores of model fits to growth data of *C. mulleri*.



Supplementary Figure 2.4: AIC scores of model fits to growth data of *T. pseudonana*.

Chapter 3: Rate Measurements of Algal Respiration and Photosynthesis as Indicators of Thermal Adaptation

3.1 Abstract

Respiration and photosynthesis are essential processes in phototrophic organisms that ensure correct cell functioning and growth. In the face of environmental change, these processes need to be able to acclimate and adapt to ensure continued cell health in phytoplankton. This chapter examined the respiration and net photosynthesis rates of 4 species from 3 different taxa of phytoplankton (*Dunaliella tertiolecta*, *Pycnococcus provasolii*, *Isochrysis galbana*, and *Phaeodactylum tricornutum*) cultured in 2 different thermal environments. Lines of these species were cultured at 15 and 20 °C for 6 years and tested for thermal adaptation afterwards. The results indicated no thermal adaptation in the rates of any of the investigated species. This finding suggests that were a 5 °C temperature increase to occur in natural environments over several years, rates of respiration and photosynthesis would not track the change. The consequences of these traits being seemingly conserved, and the role for ecosystem dynamics under environmental change, remain to be elucidated.

3.2 Introduction

Photosynthesis and respiration are temperature-dependent processes in photosynthetic organisms (Robarts and Zohary, 1987). Photosynthesis is the process that uses energy from sunlight to produce intracellular organic carbon sources from atmospheric CO₂, which can be used for cell growth or other C-requiring processes and results in the evolution of O₂ (Garcia-Carreras et al., 2018). Respiration on the other hand consumes organic carbon and oxygen, allowing the energy stored within carbon molecules to be used to drive cellular processes (Williams, 1998). The two processes are therefore an indicator of growth, and crucial in controlling marine carbon cycling and the surface water response to eutrophication (Falkowski and Owens, 1980; Giorgio, 1992). Hence, it is necessary to understand how these processes will be altered by climatic changes such as increased temperatures or increased atmospheric CO₂ (McKinnon et al., 2017). The rates of respiration and photosynthesis can be assessed by measuring oxygen evolution in the light and oxygen consumption in the dark. Whereas photosynthesis occurs only in the light, respiration is happening at all times so that measured rates of O₂ production in the light are net rates of gross photosynthesis minus respiration (McKinnon et al., 2017).

When abiotic conditions change, so does phytoplankton performance of most physiological traits, including respiration or photosynthesis, which can have subsequent impacts on aquatic ecosystems in general (Staehr and Sand-Jensen, 2006). Although photosynthesis and respiration are processes tightly correlated with cell functioning (Davison, 1991), their performance across a temperature gradient does not necessarily follow the same thermal performance curve (TPC) as for growth (Baker et al., 2016). It has been additionally demonstrated that TPCs of these two processes can be highly dynamic and change within short periods of time; acclimation of photosynthesis and respiration to novel temperature conditions

can occur quickly within the time span of a few generations (Coles and Jones, 2000), or even minutes to a few hours (Geider et al., 1996). Whether long-term adaptations occur and prevail to alter the performance of phytoplankton is however still unclear. Adaptations could be an important process to buffer responses to environmental change and ensure continued ecosystem productivity (Padfield et al., 2015).

A study on the diatom *P. tricornutum* focussed on identifying thermal adaptation in rates of RUBPCase enzyme activities, carbon assimilation, and bulk protein synthesis rates, which are tightly connected to photosynthesis and respiration (Li and Morris, 1982), without measuring these two processes directly. Another study on the macroalgae *Laminaria saccharina* tested changes in photosynthetic rates and carbon fixation, but conditioned the cultured at different temperatures for only a month (Davison, 1987). To our knowledge, respirometry has never been used on long-term cultures of microalgae to test for thermal adaptation through measuring changes in oxygen content of the surrounding medium directly as a proxy for net rates of photosynthesis and respiration. To investigate whether rates of photosynthesis and respiration in algal cultures could adapt to a temperature increase of 5 °C, lines of 4 species of phytoplankton spanning 3 taxonomic groups (2 chlorophytes, 1 diatom, 1 haptophyte) were maintained at 15 °C and 20 °C for over 6 years and investigated via a reciprocal transplant experiment. Each line's rates of respiration and net photosynthesis were measured at both 15 and 20 °C to test the hypothesis that thermal adaptation to source conditions would optimise net photosynthesis or respiration rates in its source environment relative to that of the line adapted to a different temperature.

3.3 Materials & Methods

3.3.1 Long-term algal cultures

Lines of the algal species *Dunaliella tertiolecta* (CCAP1320), *Pycnococcus provasolii* (CCMP 1203), *Phaeodactylum tricornutum* (CCMP 2561), and *Isochrysis galbana* (CCMP 1323) were maintained at 15 and 20 °C in f/2 medium (Guillard and Ryther, 1962; Guillard, 1975) for approximately 6 years at $\sim 100 \mu\text{mol photons m}^{-2} \text{ s}^{-1}$ (~ 350 generations, depending on the species, see Chapter 2 for calculation of generations). The stock culture conditions and maintenance was the same as for the cultures used in Chapter 2. Experimental cultures were inoculated 1 week prior to the onset of rate measurements by transferring 1 ml of dense stock culture into 35 ml of fresh f/2 medium so that cultures would be in exponential growth at the time of measurement. Each species had four biological replicates from each source temperature.

3.3.2 Rate measurements of Photosynthesis and Respiration

Oxygen production and consumption rates were measured with Clark-type electrodes (Digital Oxygen System Model 10, Rank Brothers Ltd., UK) at two assay temperatures (15 °C and 20 °C). To increase signal strength at time of measurement, 10 ml of culture were concentrated by centrifugation at 5000 RPM for 5 minutes and re-suspended in 2 ml f/2 medium. A two-point calibration was carried out at 15 and 20 °C with air-saturated distilled water (100% O₂) and O₂-depleted water with sodium hydrosulfite (0% O₂). Using distilled water rather than artificial sea water for the calibration, is a shortcoming of this investigation, as oxygen solubility will be altered depending on the amount of ions present in the water. As all calibrations across species and replicates were done with the same water, the results are nonetheless comparable to each other. The analog data output (change in voltage) from the electrodes was digitized using a PicoScope 3424 PC Oscilloscope (pico Technology Ltd., UK) prior to being recorded with the

Software Picoscope 6 (pico Technology Ltd., UK). Polarising voltage was set to 700 ± 2 mV for both electrodes. Samples were acclimated to the assay temperature for 15 minutes in complete darkness to measure the response to acute temperature variation (based on Padfield et al., 2015). After acclimatisation, oxygen consumption in the dark was recorded for 10 minutes, after which light emitting diodes (LEDs) were switched on to illuminate the samples with 1000 ± 100 $\mu\text{mol photons m}^{-2} \text{sec}^{-1}$. Oxygen evolution was then recorded for another 12 minutes of which the first 2 minutes were discarded to allow for rate acclimation due to the abrupt switch from total darkness to high light levels. From each species, 4 replicate cultures of the 15 °C line and 4 replicates of the 20 °C line were measured. Because two electrodes were utilised to register changes in oxygen content, for each culture line, half of the replicates were measured at one electrode ($n = 2$) and half of the replicates at the other ($n = 2$ as well), to even out potentially confounding effects of the equipment (resulting in a total of $n = 4$ per culture line). Respiration and photosynthetic rates were calculated by converting measured changes in voltage per minute into changes of O_2 per minute, and normalized by dividing by the total amount of chlorophyll *a* (Chl *a*) to calculate the rate of change of O_2 per unit chlorophyll per hour.

Samples for measuring chlorophyll concentrations were obtained by pipetting 1 ml of sample into 9 ml of 100% methanol (final concentration 90% (v/v)) after each dark-light cycle. After extraction in methanol-water for at least 14 hours at 4 °C in the dark, absorbance spectra were obtained from 360 nm to 800 nm with a methanol:water baseline in a UV-Vis Spectrophotometer (Genesys 10S, Thermo Scientific, USA). Total Chl *a* concentrations were calculated with formula [1] for methanol Chl *a* extractions according to Ritchie et al. (2008).

$$\text{Chl } a = -2.078 * A_{630} - 6.5079 * A_{652} + 16.2127 * A_{665} - 2.1372 * A_{696} (\pm 0.007) \quad [1]$$

Where A_{nnn} is the absorbance of the extract solution at the wavelength nnn .

3.3.3 Statistical Testing

To test whether thermal adaptation had occurred in net photosynthetic and respiration rates within each species, three-way ANOVAs with an alpha level of 0.05 were used to identify significant differences between the average maximum rates (response variable) of the tested lines. The three independent variables were “source temperature” with two levels to differentiate the two lines from 15 and 20 °C, “assay temperature” which also had two levels to test whether significant rate differences would occur depending on the experimental temperature, and “rate type” to clarify the two rate measurement levels “respiration” and “net photosynthesis”. However, before ANOVA testing could be performed, normality of residuals and equal variance testing had to be performed.

For the normality of residuals, these tests failed for *D. tertiolecta*, *P. tricornutum*, and *P. provasolii*. Equal variance of the distributions was not given in *I. galbana*. Effectively, none of the species could be analysed with the envisaged test. As an alternative to the three-way ANOVA, a Kruskal-Wallis rank test was performed when normality of residuals was not given. For tests in which the assumption of equal variances was not met, an ANOVA was performed that allowed to drop this assumption, the so-called Welch one-way test. The downside of both, the Kruskal-Wallis test and the ANOVA test without the assumption of equal variances, is that the effects of the single independent variables cannot be separately reported but only the hypothesis tested and the p-value returned. Therefore, a rank-based post-hoc test had to be performed when a significant difference was found. In this case it was the Dunn-test, which

does pairwise comparisons on rank-based data and adjusts the p-value for multiple testing to avoid Type 1 errors. Another curiosity with these rank-based tests is that degrees of freedom can appear as decimal numbers.

All the above-mentioned statistical analysis was conducted with R (version 3.3.1).

3.4 Results

Rates of respiration and net photosynthesis did not show the hypothesized pattern of a line having higher rates at its source temperature than the corresponding line (Fig. 3.1). As expected across all species, rates of respiration were registered as a decline in oxygen over time, whereas rates of net photosynthesis were recorded as an increase in oxygen content over time. Across all species and their separate culture lines, the differences between rates of respiration and rates of photosynthesis were significantly different (at least a p-value of < 0.05). Within each respirometry type (either respiration or net-photosynthesis), the expected pattern that a culture line would display higher rates at its source environment than the reciprocal one, was not confirmed (Fig. 3.1). Instead, it could be seen visually that one of the two lines within each species had higher pronounced rates than the other line at both assay temperatures. Although these differences in the rates of respiration and photosynthesis could be seen, the Dunn post-hoc test did not identify significant differences between lines of one species among either rates of photosynthesis or respiration ($p > 0.05$ for all comparisons). Thus the conclusions that had to be drawn were that i) a line did not perform better in its source environment than the a line from the other environment, and ii) not only did they not perform better, but there was no statistical difference among lines so that it has to be concluded that thermal adaptation did not occur in any of the species.

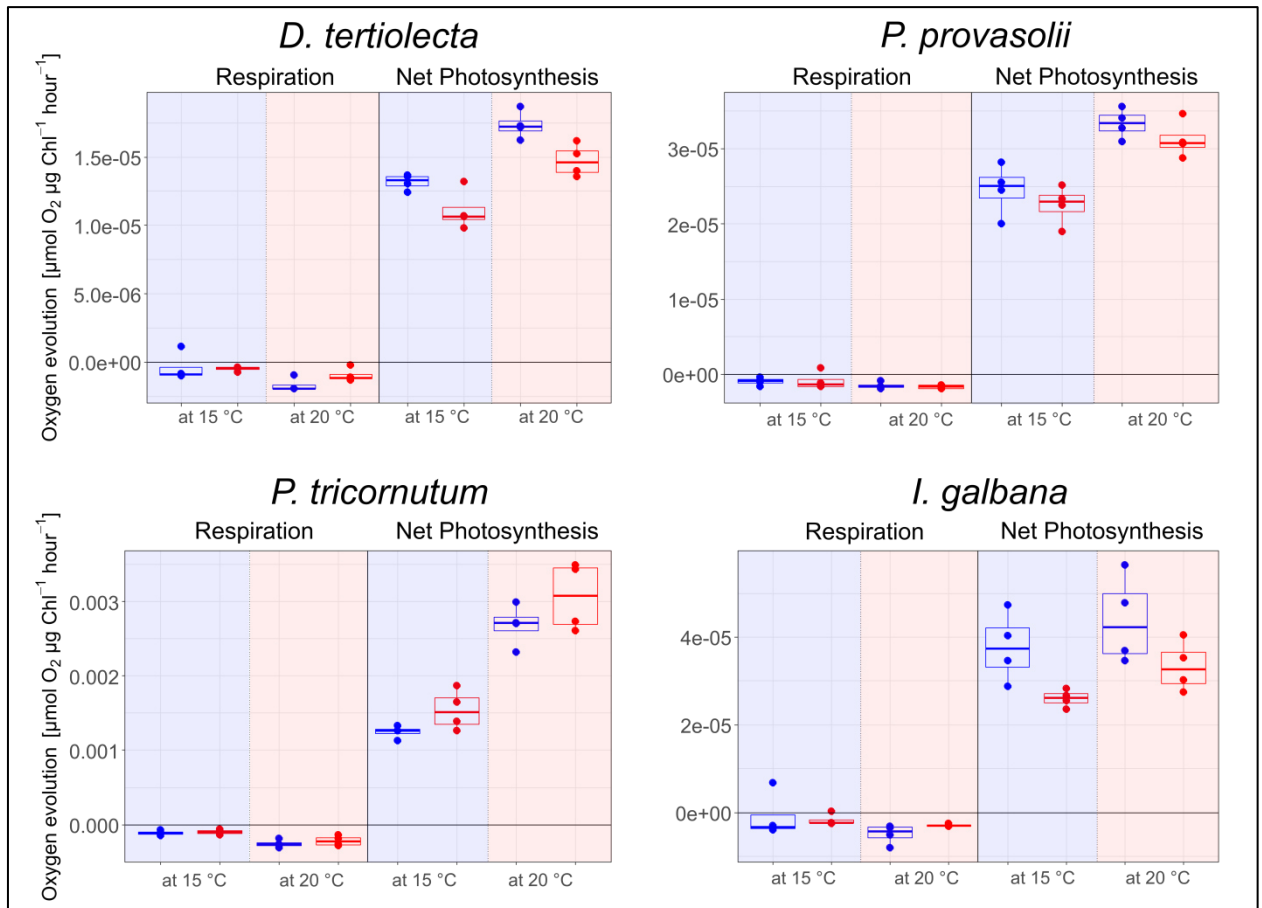


Figure 3.1: Measurements of respiration and net photosynthesis in 4 phytoplankton species with two culture lines each (15 °C and 20 °C) ($n = 4$ for each line). Blue boxplots denote results of the lines coming from a 15 °C source environment, red boxplots those coming from a 20 °C source environment. All lines were tested for their oxygen consumption (respiration) and net oxygen production (net photosynthesis), measured both at 15 °C (blue-shaded areas) and 20 °C (red-shaded areas) to investigate whether lines would have higher rates at their source temperature. In all species, significant differences were found between the rates measured in the dark (respiration) and in the light (net photosynthesis). However, within one light regime no significant differences were found for any of the lines or species. Note the difference in scale on the y-axis, as species had varying overall rates.

3.5 Discussion

Measurements of respiration and net photosynthesis in all cases did not indicate adaptation to the source environment. Apart from the significant differences in rates of respiration and photosynthesis, rates between lines within a species and at the two assay temperatures did not differ from each other. It could be that this lack of differences could be down to the statistical tests employed and the relatively low number of replication, as it could be observed visually that, within each species, one of the lines always had higher rates at both source temperatures in comparison to the other. It is possible that being cultured at 15 °C or 20 °C for a long period of time might down or up-regulate the metabolism of a specific line in general, and that 15 minutes of acclimation to temperatures may not have been sufficient to reverse this response.

Previous studies found that exposure to a colder temperature over extended periods of time would lead to overall higher maximum rates of carbon fixation in comparison to a line that was grown at a warmer temperature (Davison, 1987; Li and Morris, 1982). These current findings hint towards the idea that being cultured at a specific temperature can down or up-regulate metabolism in general, causing overcompensation through more activated rates of respiration and photosynthesis (Li and Morris, 1982). Apart from *P. tricornutum*, 15 °C lines were tending to display higher rates than their 20 °C counterparts across all species, whereas in the diatom it was the 20 °C line that had overall higher rates. The finding for *P. tricornutum* is surprising as past research has shown that a population of this diatom grown at colder temperatures should exhibit compensatory dynamics and more activity than a population from a warmer source environment to counterbalance the reduction in performance that is expected at colder temperatures because of slower metabolism (Li & Morris, 1982). This difference in activated metabolism, rather than higher pronounced rates at the specific source temperature can be a

sign of thermal adaptation in phytoplankton (Li & Morris, 1982). I point out clearly once more, that these visually seen differences were however not statistically significant. It could be that a longer period of adaptation, as well as a stronger selection pressure and different experimental culturing regime, as discussed in Chapter 2, could evoke variations that would pass the test for statistical significance. In addition and in order to confirm this presumption, work to identify whether the genes responsible for the regulation of the metabolic pathways for respiration and photosynthesis would be expressed differently between the lines would also be necessary. It could be that even though the observed differences were not statistically significant, trends in altered gene expression would already emerge. Similar to the previous chapter, this genomic analysis was however not performed, so that the identified trends can only be regarded as a start into the investigation of respirometry as an indicator of thermal adaptation. Identification of genes that are responsible for patterns of thermal adaptation is still in its infancy and the scientific community is lacking knowledge about the genes that play a role in thermal adaptation of phytoplankton (Rengefors et al., 2017).

Measuring rates at two assay temperatures in the pursuit to discover thermal adaptation might be insufficient to detect thermal adaptation. It is possible that the optimum temperatures for measured rates of photosynthesis and respiration might have shifted during the culturing period, which would potentially not be detected in the rate measurement if one was done at a sub-optimum temperature for one line, and at supra-optimum temperature for another. Rates might appear the same, although overall the response across the whole temperature gradient might have adapted (Fig. 3.2). Comparing these results to the investigation in Chapter 2, it is however unlikely that such a pronounced adaptive shift in thermal response happened, as 5 °C was shown to not be a strong enough selective pressure to evoke thermal adaptation in a

culture regime that was based on monthly transfers. Other studies investigating potential adaptations might however want to pay attention to this detail in their experimental design and analysis, as adaptations might be overlooked if the resolution of measured assay parameters is not high enough.

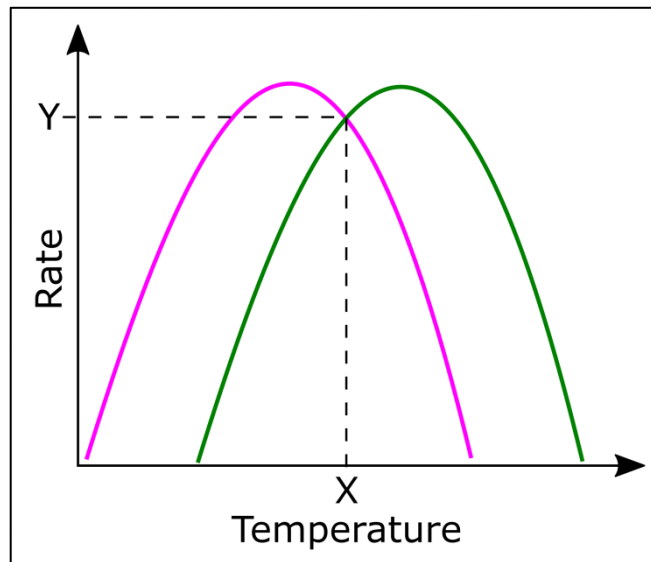


Figure 3.2: Conceptual figure to illustrate the idea that attempting to detect thermal adaptation at specific assay temperatures might be flawed. In this example a rate Y was measured at an assay temperature X . The measured rate at supra-optimal temperatures in a non-adapted TPC (pink) might be the same as the rate in an adapted TPC (green) where X would constitute a sub-optimal temperature. The fact that thermal adaptation had occurred by a shift of the TPC towards warmer temperatures would not be detected, as rate measurements would remain the same.

In addition to thermal history, light history has also been found to affect the response of photosynthetic rate parameters (Jassby and Platt, 1976). As both the 15 °C and 20 °C lines were grown in different incubators, a lack of adaptation could also be down to different environmental pressure combinations of light and temperature that potentially did not evoke a detectable response. Although this is unlikely and it is virtually impossible to guarantee exact equal culture conditions when different models of incubators are used and cultures are being shifted around so that all scientists sharing an incubator are accommodated for space.

Light, temperature, respiration, and photosynthesis are not always directly coupled (Baker et al., 2016; Rhee, 1982). Under specific light and temperature combinations, dissolved organic carbon can be released and not be utilised for growth (up to 40%) (Collins and Boylen, 1982). Additionally, the measurements were done at light levels far higher than the source incubator conditions ($\sim 1,000$ in comparison to $\sim 100 \mu\text{mol photons m}^{-2} \text{s}^{-1}$) in order to register enough of a response that could be picked up by the utilised method. Consequently, the observed responses should also be potentially considered as the acute response of a 15 °C or 20 °C line to changed light levels rather than changed assay temperatures.

Dynamic responses of rates to changed temperature regimes are important to consider for estimating ocean primary production and respiration (Anning et al., 2001; Geider et al., 1997). It is therefore crucial to further understand how species acclimate and adapt to temperature as responses do not seem to follow the simple idea that a species does best in its source environment, but the responses seem to be more nuanced, species specific, and do not appear to be a straightforward vertical shift of TPCs across the temperature axis. Short-term responses of photosynthesis do not necessarily correlate with long-term responses or optimum temperatures for growth, which can be several °C removed from optimum temperatures for net photosynthesis (Davison, 1991). Photosynthesis is not the sole factor responsible for growth, as growth is the resulting response of all cellular processes combined (enzyme reactions, transport of molecules and nutrients, etc.), so that a disconnection between the two should not be surprising (Kuebler et al., 1991). In past research, positive rates of photosynthesis were even observed at temperatures beyond the maximum limits for growth so that measurements of respiration and net photosynthesis are potentially not a good indicator of thermal adaptation if measurements are taken in the short-term as a response to changed assay conditions or only over the course of several minutes or hours (Davison, 1991).

3.6 Conclusion

The investigated lines of four species of phytoplankton did not show thermal adaptations of respiration and net photosynthesis to their source temperature that could be found in reciprocal transplant measurements. However, generally up-regulated or down-regulated metabolisms in lines from differing source environments could be a sign of thermal adaptation. Respiration and net photosynthesis are complex mechanisms and their long-term responses to changes in the thermal environment are not fully understood. More knowledge on the physiology of these two processes is therefore necessary if their rate measurements are to be used as indicators of thermal adaptation.

Chapter 4: High Predictability of Direct Competition Between Marine Diatoms Under Different Temperatures and Nutrient States

Accepted and published in the journal "Ecology and Evolution" as: Siegel P, Baker K, Low-Décarie E, Geider R. 2020. „High predictability of direct competition between marine diatoms under different temperatures and nutrient states." Ecology and Evolution, 10(14), 7276 - 7290. doi.org/10.1002/ece3.6453.

4.1 Abstract

The distribution of marine phytoplankton will shift alongside changes in marine environments, leading to altered species frequencies and community composition. An understanding of the response of mixed populations to abiotic changes is required to adequately predict how environmental change may affect the future composition of phytoplankton communities. This study investigated the growth and competitive ability of two marine diatoms, *Phaeodactylum tricornutum* and *Thalassiosira pseudonana*, along a temperature-gradient (9 °C to 35 °C) spanning the thermal niches of both species under both high-nitrogen nutrient-replete and low-nitrogen nutrient-limited conditions. Across this temperature gradient, the competitive outcome under both nutrient conditions at any assay temperature, and the critical temperature at which competitive advantage shifted from one species to the other, was well predicted by the temperature dependencies of the growth rates of the two species measured in monocultures. The temperature at which the competitive advantage switched from *P. tricornutum* to *T. pseudonana* increased from 18.8 °C under replete conditions to 25.3 °C under nutrient-limited conditions. Thus *P. tricornutum* was a better competitor over a wider temperature range in a low N environment. Being able to determine the competitive outcomes from physiological responses of single species to environmental changes has the potential to

significantly improve the predictive power of phytoplankton spatial distribution and community composition models.

4.2 Introduction

Competition plays an important role in shaping biological communities in terrestrial and aquatic ecosystems (Tilman, 1987). Interspecific competition within communities occurs when two or more species possess the same or similar resource requirements (Clements and Shelford, 1939). For phytoplankton, the most important resources are macronutrients (N, P, Si), micronutrients (trace elements), organic nutrients (vitamins), CO₂, and light (Riebesell, 2004; Tilman et al., 1982). If demand for a depletable resource by the organisms within an ecosystem is high, the abundance or concentration of the resource will decline. When the concentration of a resource becomes too low, it can fall below the minimum requirement of a species to support its temperature and light-dependent maximum growth rate (μ_{\max}), and therefore become limiting (Andersen, 2005).

In equilibrium communities, the minimum resource concentration that supports net population growth, and for which uptake rates by the population and supply rates by the environment are in balance, is called R* (Tilman, 1981). Assuming that all species compete for the same limiting resource and ignoring the effects of interference or apparent competition, the species with the lowest R* should outcompete all other species and dominate a community (resource ratio theory or R*-theory; Tilman et al., 1982). Theoretically, the number of species that can stably coexist in a system is therefore equal to the number of limiting resources, if different species are limited by different resources. The fact that most communities of primary producers usually

display higher species diversity than the number of limiting resources (Cloern and Dufford, 2005; Sommer, 1984) indicates that natural communities are often not in equilibrium or that the ability of a species to exploit resources is not the only factor that regulates a community's diversity and the outcome of competition. Apart from limiting nutrients, species diversity is governed by other major regulating forces which can be biotic (e.g. differential grazing pressure or various forms of symbiosis such as mutualism or parasitism) or abiotic (e.g. temperature, pH, salinity) (Begon et al., 2006; Cloern and Dufford, 2005).

Whether the effect of environmental change on the outcome of competition can be predicted from the performance of isolated species and whether these predictions align with classical competition models or single species performance is unclear because experiments that examine direct species interactions along environmental gradients are scarce (Kordas et al., 2011). Only a few studies have previously found evidence to suggest that this is possible. For example Huisman et al. (1999) showed that the ability of isolated algae species to survive at the lowest light level determined their competitive success in mixed communities. Bestion et al. (2018a) showed that phosphorus uptake rates of monocultures at different temperatures correctly predicted the competitive outcome between pairs of 6 phytoplankton species in the majority (71%) of the cases.

Simultaneous changes in multiple abiotic factors such as those predicted to occur under climate change (e.g. rising sea surface temperatures in conjunction with changes in nutrient inputs), may also complicate predictions, as abiotic factors may interact (e.g. antagonistic or multiplicative), and organisms may respond in a way that is not accounted for from the responses to gradients of individual factors operating in isolation (Harley et al., 2017; Thomas et al., 2017). For instance nutrient concentration was shown to interact with temperature to

influence phytoplankton growth rates (Rhee and Gotham, 1981), and the cardinal temperatures (e.g. thermal optimum) of thermal performance curves (TPCs) (Bestion et al., 2018b; Thomas et al., 2017; van Donk and Kilham, 1990). In particular, N-limitation can significantly lower the thermal optimum of the diatom *Thalassiosira pseudonana* towards colder temperatures (Thomas et al., 2017). Given this shift in thermal performance due to nutrient limitation, *T. pseudonana* may become less competitive in warm N-limited waters. In contrast, *Phaeodactylum tricornutum*, is known to be a good competitor for inorganic nitrogen when this nutrient is scarce because it can take up nitrate when abundant, and store it for times of depletion (Cresswell and Syrett, 1982). Thus, the outcome of interspecific competition for inorganic nutrients might be expected to depend on temperature if the interaction of nutrient limitation with temperature is species specific. For example, *P. tricornutum* has been found to outcompete *T. pseudonana* and other species in maricultural ponds (Nelson et al., 1979) despite not being a dominating species in marine phytoplankton communities (Guillard and Kilham, 1977), which may be a reflection of nutrient availability or temperature characteristics in different systems. An early study on the competition between *P. tricornutum* and *T. pseudonana* showed that competition is indeed temperature-dependent and that the thermal environment influences the competitive outcome in stationary phase cultures (Goldman and Ryther, 1976). Specifically, *P. tricornutum* was found to be a good invader and dominant species under cold to intermediate temperatures (< 20 °C), whereas it could not establish itself as an invasive species in warmer temperatures.

Here, the interaction of temperature and nitrate availability on direct competition between *P. tricornutum* and *T. pseudonana* was investigated along a temperature gradient. To test whether temperature and nutrient status have an interactive effect on the outcome of competition, experiments were conducted in both nutrient-replete high N conditions and low N

conditions (whereby nitrate limited yield). Specifically, it was hypothesised that (i) the species with the higher growth rate or carrying capacity at a given temperature and nutrient level as a monoculture would have the competitive advantage in mixed cultures, and that (ii) greater absolute differences in growth rate between species at a specific assay temperature would determine how quickly the poorer competitor would be displaced.

4.3 Material & Methods

Stock cultures of *P. tricornutum* (CCMP 2561) and *T. pseudonana* (CCMP 1335) were maintained in the University of Essex algal culture collection at 15.5 ± 1.0 °C, in f/2 medium (Guillard and Ryther, 1962) prepared in artificial sea water (Berges et al., 2001; Harrison et al., 1980) and grown on a 12:12 hour light and dark cycle at a photosynthetic photon flux density (PPFD) of approximately $60 \mu\text{mol photons m}^{-2} \text{s}^{-1}$, which is close to optimum light levels for *P. tricornutum* (Geider et al., 1986), and approximately 30% of the optimum light level for *T. pseudonana* (Geider et al., 1998; Geider et al., 1997). Stock cultures were transferred monthly as 1:36 dilutions.

4.3.1 Competition Experiments

4.3.1.1 High N competition experiment

Prior to experimentation, *P. tricornutum* and *T. pseudonana* were maintained in exponential growth for two weeks (approximately 10 to 14 generations) under stock culture conditions at 15.5 ± 1.0 °C by transferring cultures into fresh f/2 medium once cell densities reached 500,000 cells ml^{-1} for *P. tricornutum* and 250,000 cells ml^{-1} for *T. pseudonana* (equivalent to about 5 % of each species' carrying capacity).

Experiments using an aluminium temperature-gradient block were conducted to assess (i) thermal performance curves (TPCs) for growth rate of monocultures of the two diatoms and (ii) temperature dependence of competition between these species. The aluminium block was heated at one end and cooled at the other to generate a temperature gradient from 8.8 °C at the cold end to 35 °C at the hot end. The block provided 4 rows with 17 columns (assay temperatures) in each row. Temperature within each column was controlled to within 0.2 °C, providing approximately 1.5 °C increments along the temperature gradient. Illumination was provided from below by light emitting diodes (LEDs). PPFD was set to $150 \pm 15 \mu\text{mol photons m}^{-2} \text{s}^{-1}$ and illumination was provided on a 12:12 hour light and dark cycle.

Aliquots from stock cultures of each of the diatoms were used to inoculate 17 autoclaved borosilicate test tubes (5 ml assay volumes), which were distributed along the same 17-assay-temperature gradient described above. To assess the growth rate TPCs, *in vivo* chlorophyll *a* minimum fluorescence yield (F_0) was used as a proxy for biomass (see section 4.3.2 below). Initial cell densities were approximately $160,000 \text{ cells ml}^{-1}$ for *P. tricornutum*, and $80,000$ for *T. pseudonana*, corresponding to similar F_0 values for both species. The monocultures were kept in exponential phase by diluting whenever an assay culture reached F_0 values equivalent to cell densities corresponding to about 5 % of each species' carrying capacity, approximately $500,000 \text{ cells ml}^{-1}$ for *P. tricornutum* and $250,000 \text{ cells ml}^{-1}$ for *T. pseudonana* (Fig. 4.1A & Suppl. Fig. 4.1).

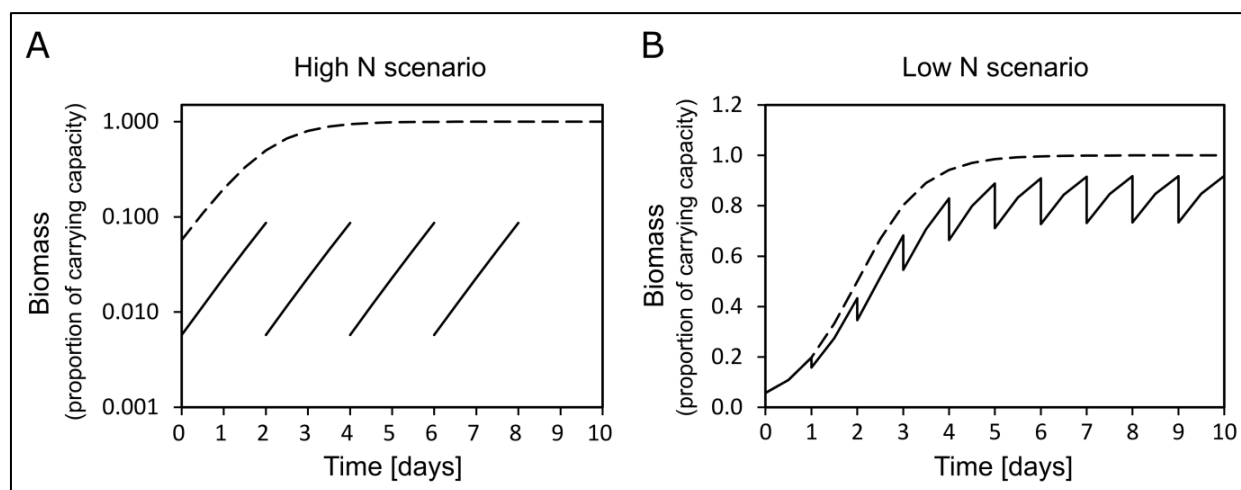


Figure 4.1: Simulation of semi-continuous cultures for obtaining and maintaining (A) nutrient replete (high N scenario) and (B) nutrient-limited (low N scenario) cultures. Simulation assumes cultures are already acclimated to the nutrient replete growth under defined temperature, irradiance, etc. Assumes logistic growth with the nutrient replete growth rate = 1.4 d^{-1} , and carrying capacity = 1. Dilution is approximately a 10-fold in the high N scenario and 1.25-fold in the low N scenario. Solid lines are the culture density. In (A), the solid lines are interrupted to signify that for each dilution step, an aliquot of the assay culture was taken and pipetted into a fresh tube, whereas in (B) the assay culture remained in the same tube for the duration of the whole experiment, whereby 20% of culture was removed from an assay tube on a daily basis and topped up with fresh low N f/2 medium. Dashed line is the culture density that would be obtained in a batch culture undergoing logistic growth. Note that (A) is on a log-scale to represent that high N exponential cultures were kept at low densities far from reaching stationary phase, whereas (B) is on a linear scale.

At the same time, to assess competition between these species, aliquots from the stock monocultures were combined to create a mixed culture with equal cell densities of $100,000 \text{ cells ml}^{-1}$ in a 1:1 species ratio (50,000 cells of each species). The starting ratio could only be approximated, as cell densities were estimated from the relationship between cell density and F_0 determined at $15.5 \text{ }^\circ\text{C}$, but fluorescence per cell is not constant as it varies between species and with assay temperature. This mixed culture was then used to inoculate 34 autoclaved borosilicate test tubes (5 ml assay volumes), which were distributed in duplicates along the same 17-assay-temperature gradient to assess the acute effect of temperature on competition. After mixed cultures had been established and distributed across the temperature

gradient, 200 μL were removed daily from each mixed culture tube and preserved with Lugol's solution for cell frequency counts, i.e. relative species abundances of the mixed cultures over time. 200 μL of fresh f/2 medium was added to keep the culture volume constant. As with the monocultures, F_0 measured daily was used as an index of community biomass. The mixed cultures were kept in exponential growth by diluting when F_0 reached values corresponding to about 5% of the carrying capacity.

After a further two weeks, the monocultures from each assay temperature that had been used to assess the growth rate TPCs of the two species were mixed together in an equal cell density ratio to investigate the effect of thermal acclimation on competition. Here, 2 mixed cultures to monitor competition were created at each assay temperature and aliquots were sampled daily to monitor changes in relative species frequencies.

Following completion of the competition experiment, triplicate monocultures of each species were grown across the gradient to increase the total replication for determining the TPC for growth rate of each monoculture to $n = 4$. However, in the final analysis, one of the *T. pseudonana* growth replicates was omitted as an outlier because the TPC was significantly different to the remaining three replicates (Suppl. Fig. 4.2A).

The above experimental design enabled the examination of (i) the TPCs for growth of *P. tricornutum* ($n = 4$) and *T. pseudonana* ($n = 3$), and (ii) the acute interspecific competition along the temperature gradient in the two weeks following the transfer from their 15.5 ± 1.0 °C source environment ($n = 2$), and of cultures acclimated for two weeks to temperatures of 8.8 °C to 35 °C ($n = 2$). A more visual representation of the experimental chronology can be found in Supplementary Figure 4.3.

4.3.1.2 Low N competition experiment

Cultures were acclimated as a batch culture for two weeks in low N f/2 medium (starting concentration 55 μM in comparison to 882 μM in full f/2). As shown in Supplementary Figure 4.4, this NO_3 concentration reduced carrying capacity, and ensured that cultures would reach the stationary growth phase at cell densities that did not saturate the fast repetition rate fluorometry (FRRf) signal, allowing to track the culture growth from the onset of the exponential growth phase all the way through to stationary phase. The starting NO_3 concentration of 55 μM was picked after pre-tests were conducted during which the two diatoms had been grown in f/2 medium with 4 different NO_3 -starting-concentrations (882, 220.5, 110.25, and 55.13 μM) (Suppl. Fig. 4.4). After acclimation, two monoculture replicates of each species were inoculated from early stationary phase stock cultures and grown in 5-ml-volumes across the 17 assay temperatures in the temperature-gradient-thermoblock (9.1 to 33.8°C) in the low N (55 μM) f/2 medium. The light regime was kept consistent with that used for the high N competition experiment and once again set to a PPFD in the range of $150 \pm 15 \mu\text{mol photons m}^{-2} \text{s}^{-1}$ on a 12:12 hour light and dark cycle.

The cultures were maintained in semi-continuous growth by removing 20% of the culture volume (1 mL) daily (used for determining cell abundance and nitrate concentration) and replacing this volume with fresh medium to maintain a total volume of 5 ml. This way cultures could be grown until cell abundance (yield) was limited by the concentration of nitrate provided in the growth medium and daily population growth rate was set by the dilution rate (Fig. 4.1B). Although the daily sampling regime was different from the high N scenario to account for the necessities of culturing microorganisms in nutrient-limited conditions, the results of the two nutrient scenarios can be compared as the same species were used and cultures were treated otherwise equally during the competition experiment.

The removed 1 ml samples were centrifuged at 5000 *g* for 7 minutes at 4 °C. A subsample of the supernatant (300 µL) was transferred to a flat-bottom 96-well plate (Thermo Scientific Nunclon, USA) and stored at -20°C to measure the sum of nitrate plus nitrite (NO_x) at a later time (see section 4.3.4 below). The cell pellet was re-suspended in the remaining volume (700 µL), fixed with formaldehyde (final concentration 1%) and stored at -20°C until cell abundances were estimated with flow cytometry (see section 4.3.5 below).

After growing in monocultures for two weeks, inorganic nitrogen concentrations in all treatments were depleted below the detection limit of the NO_x-assay (i.e. <0.5 µM; see Suppl. Fig. 4.5). At this point the fluorescence signals had stabilized or were declining, indicating that the yield was N-limited (see Suppl. Fig. 4.6). Following this determination, one of the two monocultures of each species at each assay temperature was used to inoculate two mixed cultures for the competition phase of the experiment. Each mixed culture tube received 2 ml assay volumes from each monoculture, for a total volume of 4 ml, which was then topped up with 1 ml of low N f/2 medium to maintain a constant assay volume of 5 ml (competition replicates across assay temperatures at this point in time *n* = 2). The need to use 2 ml assay volume of each monoculture to not break with the 20% daily dilution had the consequence that the desired 1:1 species ratio at the start of mixed cultures could not always be reached. As in the high N experiments, 200 µL of the sampled volume were preserved with Lugol's solution for cell frequency counts. The remaining 800 µL volume was treated the same way as low N monocultures, with samples being centrifuged, and 300-µL-aliquots stored for NO_x analysis.

One week later, the second N-limited semi-batch monoculture replicate of each species was used to inoculate another set of two mixed cultures tubes at each assay temperature for a second duplicate competition experiment (increasing the amount of competition replicates to

n = 4). Mixed cultures were kept in the same semi-continuous regime as monocultures with 20% of sample volume being harvested and replaced with fresh medium on a daily basis.

The above experimental design enabled the examination of (i) the thermal niche of *P. tricornutum* (n = 2) and *T. pseudonana* (n = 2) under low N conditions, and (ii) the acute interspecific competition along the temperature gradient at the onset of N-limitation (n = 2), and of cultures that were cultured in isolation for an additional 7 days at 9.1 to 33.8 °C (n = 2). As for the high N competition, the Supplementary Figure 4.3 provides a more visual representation of the experimental set-up and explains when the different monoculture and mixed culture replicates were collected.

4.3.2 Chlorophyll Fluorescence

In vivo chlorophyll *a* minimum fluorescence F_0 (minimum fluorescence yield), used as a proxy for biomass, as well as photosynthetic efficiency F_v/F_m , were measured daily via FRRf with a FastTracka II fluorometer and Fast Act laboratory system (both CTG Ltd, West Molesey, UK). Photosynthetic efficiency was calculated via the formula $(F_m - F_0)/F_m$ (F_m = maximum fluorescence yield) by the FastPro software (version 1.0.55) used to attain and record FRRf measurements. Peak excitation was at 435 nm and fluorescence emission measured at 680 nm (with a 25 nm bandwidth). The measuring protocol was set to 24 sequences per acquisition with a 100 ms sequence interval and a 20 s acquisition pitch.

Measurements were taken on cells that were dark acclimated for 30 minutes at their assay temperature and profiles of fluorescence emission were fitted within the Fast Pro 8 software (version 1.0.55) (Chelsea Technologies, UK).

4.3.3 Mixed Population Species Frequency Counts

Frequency counts for the high N and low N experiment were carried out to monitor the relative abundance of each species in the mixed populations over time. Flow cytometry could not be used to discriminate between the two species as their forward scatter (FSC) and chlorophyll-*a* fluorescence overlapped. As such, Lugol's preserved cells were allowed to settle to the bottom of the well-plate wells (approximately 3 hours) before frequency counts were performed using an Olympus inverted microscope at 200X magnification. In each fixed sample, a minimum of 400 cells was counted in order to calculate a *P. tricornutum*-to-*T. pseudonana* cell abundance ratio.

4.3.4 NO_x-Assay (Total nitrite/nitrate analysis)

NO_x, the sum of nitrite and nitrate, concentration was measured using the method of Schnetger and Lehnert (2014) to track the monocultures to nitrogen depletion before mixing them together for the low N competition experiment. The 300 µL frozen aliquots were defrosted on ice, and a 150 µL volume was transferred to a fresh 96 well-plate and 75 µL of the NO_x reagent was added. The reagent was mixed with the assay volume by pipetting up and down several times and incubated at 45 ± 5 °C for 60 minutes before measuring absorbance at 540 nm in a FLUOstar Omega plate reader (BMG Labtech, Germany).

4.3.5 Flow Cytometry

For the low N experiment only, flow cytometry data were used to confirm that cell densities had stabilized, despite F_0 fluorescence declining, as cell physiology continued to adjust to N-limitation. Cellular chlorophyll content is known to decline under N-limitation (Parkhill et al., 2001) and as a consequence the ratio of F_0 to cell density also declines (Suppl. Fig. 4.7). Because

cellular physiology was stable in exponentially growing cultures of the high N experiment, flow cytometry was not required.

Previously collected samples (as described above in section 4.3.1.2) were defrosted on ice and quantified with an Accuri C6 flow cytometer (BD Biosciences, USA) equipped with a blue laser (488 nm). Diatom populations were discriminated based on chlorophyll-*a* fluorescence (>670 nm) and forward scatter (FSC). FSC was used as a proxy for cell size to observe potential changes across assay temperatures after 15 days of monoculture growth in the low N medium. After counting cells within 45 μ L of sample volume per sample, population statistics were calculated using particle counts within gates with the supplied BD Accuri C6 Analysis Software (Version 1.0.264.21). Gates were kept stable for the same experimental day, but had to be slightly adjusted over time to account for the fact that cell size within the populations decreased the longer the cells were N-limited. Gates were therefore extended or moved along the FSC-axis towards smaller values the further the experiment progressed. To see example gates and example flow cytometry results, and to get an idea of how cell size changed over time for the two species under N-limitation, see Supplementary Figure 4.8.

4.3.6 Data Analysis

4.3.6.1 Growth rates and carrying capacities

Growth rates (μ) in high N medium (starting nitrate concentration of 882 μ M) were calculated for each monoculture replicate and dilution phase as the slope of the linear regression of the natural log of F_0 over time (Suppl. Fig. 4.1). The growth rate calculated for the 1st dilution phase was not used as the cultures had not yet acclimated to assay conditions. Growth rates from all subsequent dilution phases were used to fit the TPCs (see section 4.3.6.2 below).

The initial exponential growth rates during the nutrient replete phase in low N semi-continuous cultures (with a starting nitrate concentration of 55 μM) were calculated using FRRf data from the first four days of culturing before the exponential increase in F_0 slowed (see Suppl. Fig. 4.6 & 4.9). Growth rates were calculated with equation [1] as

$$\mu = k + \ln\left(\frac{1}{0.8}\right) \quad [1]$$

where k is the slope of $\ln(F_0)$ over time, and $\ln\left(\frac{1}{0.8}\right)$ (natural logarithm of 100% medium (i.e. 1.0) over 80% medium (i.e. 0.8)) was added to k to account for the dilution by the daily volume removed (1 ml) from the 5 ml culture.

Cell densities increased to a maximum by day 5 that was sustained thereafter (see Suppl. Fig. 4.10). The carrying capacity, K , under the imposed dilution rate of 0.22 d^{-1} was calculated for each replicate and at each assay temperature from the average cell densities measured after experimental day 4.

4.3.6.2 Thermal performance curves

All twelve equations available in the R package “temperatureresponse” (Low-Décarie, 2017) were fitted to the temperature-dependent data of growth and carrying capacities obtained from monocultures of *P. tricornutum* and *T. pseudonana* (Suppl. Table 4.1). For the growth model fitting in high N cultures, data from all dilution phases, except dilution phase 1, which was regarded as the growth phase in which the cultures acclimated to assay conditions, was used. The average growth rate across dilution phases was calculated for each species and replicate at each assay temperature, and the temperature dependence was modelled based on these average growth rates. For the low N scenario, thermal performances were modelled on

the acute growth rates obtained from the first 4 days of low N growth (Suppl. Fig. 4.9), and on the thermal response of carrying capacities across assay temperatures (Suppl. Fig. 4.10).

The most appropriate equation for each species was selected based on a visual inspection of the data in combination with Akaike Information Criterion (AIC) values (see Suppl. Fig. 4.11). Visual inspection was necessary as AIC values alone did not always predict the equation that best described the temperature-dependent data, especially at sub-optimal temperatures. For *P. tricornutum*, equation [2] from Ratkowsky et al. (1983) was found to be the best model across all replicates.

$$Rate = [a \cdot (T - T_{min})]^2 \cdot [1 - \exp(b \cdot (T - T_{max}))]^2 \quad [2]$$

where a and b are model parameters, T is the assay temperature at which growth rate or carrying capacity was measured, and T_{min} and T_{max} are the maximum and minimum temperatures that *P. tricornutum* would be predicted to grow at.

For *T. pseudonana* equation [3] from Montagnes et al. (2008) was found to best describe the thermal performance.

$$Rate = a + b \cdot T + c \cdot T^2 \quad [3]$$

Where a , b , and c are model parameters and T is once again the assay temperature at which growth rate and carrying capacity were measured.

The fitted TPCs were used to obtain the optimum temperature for growth (T_{opt}), the maximum growth rate (μ_{max}) at this temperature, and the low and high temperatures at which $\mu = 0.5 \mu_{max}$

(CT_{50min} and CT_{50max}). Single parameters of non-linear model fits can be found in Supplementary Tables 4.2 – 4.4.

To investigate whether the thermal niche differed significantly between (i) the two species, and (ii) two nutrient scenarios, a two-way MANOVA was used to examine the 4 dependent variables (T_{opt} , CT_{50min} , CT_{50max} , and μ_{max}). The two independent variables were “species” (levels: *P. tricornutum* and *T. pseudonana*) and “nutrient scenario” (levels: high N and low N). Sample size was $n = 11$ (4 *P. tricornutum* replicates in high N, and 2 in low N, as well as 3 *T. pseudonana* replicates in high N and 2 in low N), and significance levels were set to a p-value of 0.05. By conducting a MANOVA we could assess all pairwise comparisons to determine which cardinal temperatures (i) changed significantly in the overall thermal niche, and (ii) were affected by a “species” and “nutrient scenario” interaction.

To test whether the thermal dependency of carrying capacities under low N conditions differed between the two species, individual one-way ANOVAs were conducted with “species” as the independent variable on the four dependent parameters T_{opt} , CT_{50min} , CT_{50max} , and maximum carrying capacity (K_{max}). MANOVA testing was not possible due to the replication number of $n = 2$ for the monocultures grown in low N conditions. p-values of the single ANOVAs were adjusted for multiple testing with a Bonferroni correction and reported as q-values.

4.3.6.3 Predicted competition coefficients

Competition coefficients across assay temperatures in high N and low N conditions were predicted from the mean growth rates (equation [4a]) or mean carrying capacities (equation [4b]) of each species calculated from the fitted TPCs.

$$\textit{Predicted competition coefficient } (T) = (\mu_1)_T - (\mu_2)_T \quad [4a]$$

where $(\mu_1)_T$ and $(\mu_2)_T$ are the growth rates of species 1 and species 2 at temperature T .

$$\textit{Predicted competition coefficient } (T) = (K_1)_T - (K_2)_T \quad [4b]$$

where $(K_1)_T$ and $(K_2)_T$ are the carrying capacities of species 1 and 2 at temperature T .

Since competition coefficients are traditionally calculated from growth rates (e.g. Low-Decarie et al., 2011; Segura et al., 2011), coefficients calculated from carrying capacities must be treated with caution, as the relationship between K and competitive outcome is not established for steady-state nutrient limited conditions. Higher K does not necessarily signify better competition ability. Under steady-state nutrient limitation, it is R^* that determines competitive outcome (Tilman, 1981), but because the NO_x concentrations were below the detection limit of our assay, we could not measure R^* in our experiment.

The predicted temperature dependence of competition coefficients was modelled with a local estimated scatter plot smoothing (LOESS) from the R core package “stats” (R Core Team, 2016). LOESS fits a smoothing curve into data that is distributed on a scatter plot to graphically represent the relationship between an independent and a dependent variable. It is a suitable method for visualising complex non-linear relationships. The final smoother curve is the result of many local regression curves fit together (Isnanto, 2011; Jacoby, 2000). As such, it is a tool for predicting specific points on a regression, such as the inflexion point of competition, and to explore data. To display the strength of how closely our LOESS smoother followed the calculated competition coefficients, we reported R^2 -values and residual standard errors (RSE) in the results.

4.3.6.4 Observed competition coefficients

Changes in the ratio of the abundances of the two species through time (Suppl. Fig. 4.12 & 4.13) were used to calculate observed competition coefficients. The competition coefficient was calculated as the slope of the change in the natural logarithm of species frequency over time. Competition coefficients were calculated with equation [5] for mixed high N cultures and mixed low N cultures.

$$\text{Competition coefficient} = \frac{\ln\left(\frac{N_{P. \text{tricornutum}}:N_{T. \text{pseudonana}}(t)}{N_{P. \text{tricornutum}}:N_{T. \text{pseudonana}}(0)}\right)}{t} \quad [5]$$

where N = species abundance, and t = time. At the temperature at which competition coefficients are 0, stable co-existence of the two species is expected.

As described above (Section 4.3.1), each nutrient scenario had 4 competition replicates across the temperature gradient. In the final analysis of competition under high N conditions the acute and acclimated competition replicates were pooled because we did not find an effect of temperature acclimation and could not observe a significant difference in the temperatures at which the competitive advantage switched from *P. tricornutum* to *T. pseudonana* ($F_{1,2} = 4.337$, $p = 0.173$) (Suppl. Fig. 4.14, and Suppl. Table 4.5). Due to a lack of an effect of temperature acclimation on the progression of competition across temperatures, we did not structure the competition replicates into acclimated and non-acclimated in the low N scenario and focussed on culturing the monocultures to N limitation, pooling the four competition replicates as well.

In order to determine whether nutrient regime significantly changed the temperature at which *P. tricornutum* and *T. pseudonana* co-existed (i.e. the inflexion point temperature at which the competition coefficient equalled 0), we conducted a one-way ANOVA with the temperature of

competition inflexion as the response variable, and “nutrient regime” as the independent variable. Significance levels were set to a p-value of 0.05

All data analysis and calculations mentioned above were carried out with the statistical software R (version 3.3.1) (R Core Team, 2016).

4.4 Results

4.4.1 Differences in temperature and nutrient response between species in monoculture

When *P. tricornutum* and *T. pseudonana* were grown as monocultures, the thermal niches of the two species differed significantly from one another irrespective of nitrogen conditions (2-way-MANOVA, $F_{1,7} = 134.97$, $p < 0.001$) (Fig. 4.2, Suppl. Table 4.6). The contrasting thermal niches between the two species were evident in differing cardinal temperatures (CT_{50min} , T_{opt} , CT_{50max}) (Fig. 4.3A), and μ_{max} (Fig. 4.3B). *P. tricornutum* occupied a cooler thermal niche than *T. pseudonana*, characterised by lower cardinal temperatures (Fig. 4.3A), and could not sustain growth when temperature was in excess of 30 °C (Fig. 4.2). In contrast, *T. pseudonana* occupied a warmer thermal niche and was able to grow across the whole range of tested assay temperatures. However, towards the lowest assay temperatures (10 °C and below), the growth rate of *T. pseudonana* approached 0 d⁻¹, indicating that the thermal tolerance minimum of this *T. pseudonana* strain was almost reached (Fig. 4.2).

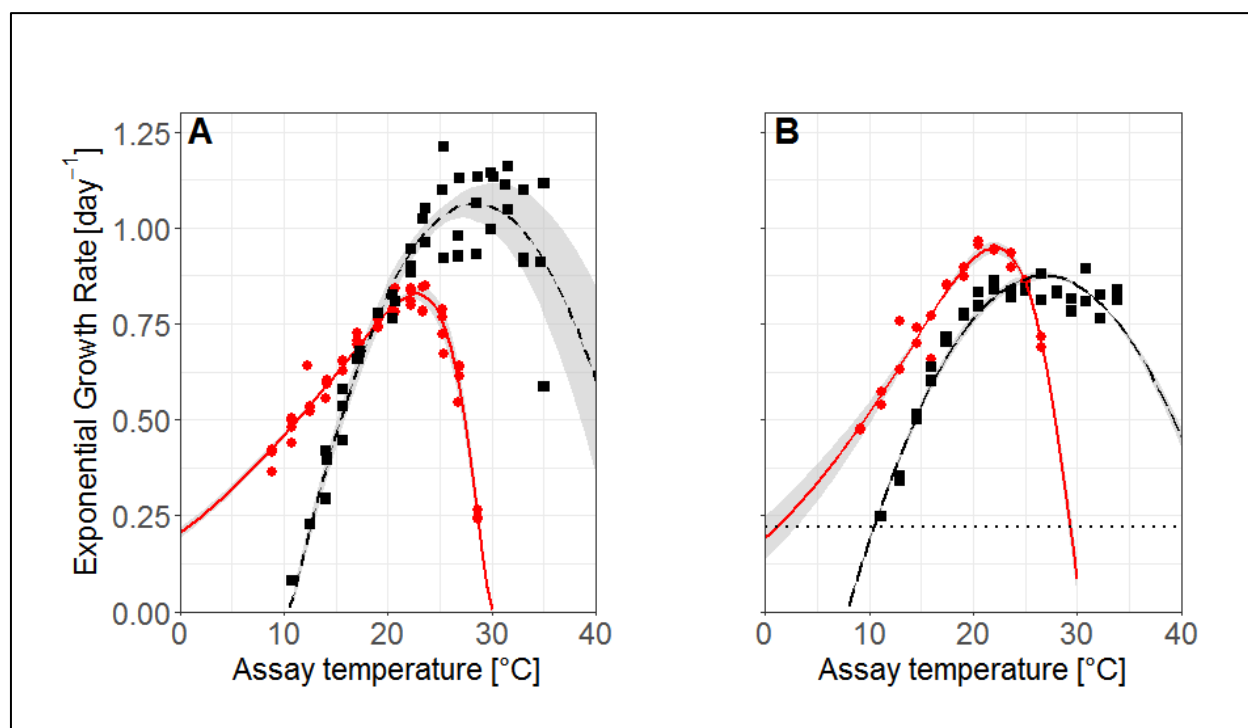


Figure 4.2: Average temperature response curves depicting acclimated growth rates of *P. tricornutum* (red circles and solid line) and *T. pseudonana* (black squares and dashed line) under (A) high nitrate conditions ($n = 4$ and 3 respectively) and (B) of the initial acute growth rate (days 0 – 4) under low N conditions ($n = 2$ for both species). Shaded area denotes standard deviation of the average model calculated from replicate model fits. Symbols in (A) represent the growth rates from distinct biological replicates and were calculated from the average growth rates across dilution steps after the diatoms had acclimated to growth under assay conditions. Dotted line in (B) indicates $\ln(1/0.8)$, the dilution rate in these semi-continuous cultures; cell abundance would have declined in cultures with growth rates below this value which equates to a growth rate of 0.22 d^{-1} due to the daily dilution that was imposed by the sampling regime. Raw data used to calculate growth rates in the high nitrate ($882 \mu\text{M NO}_3^-$) medium (A) can be seen in Suppl. Fig. 4.1, data used to calculate growth rates in the low N ($55 \mu\text{M NO}_3^-$) medium (B) can be seen in Suppl. Fig. 7. Nonlinear model outputs of the single replicate models used to calculate the average model can be found in Suppl. Tables 4.2 and 4.3, and single model fits on the individual growth replicates can be found in Suppl. Fig. 4.2 A and B.

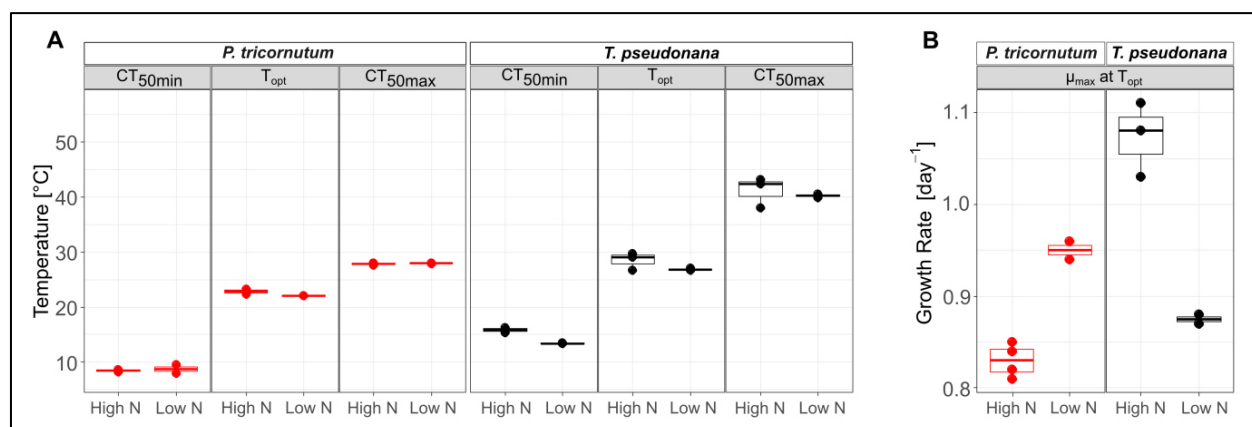


Figure 4.3: Comparison of (A) cardinal temperatures, and (B) maximum growth rates from thermal performance curve model fits for growth rates between *P. tricornutum* and *T. pseudonana* under high N and low N growth conditions. For *P. tricornutum* $n = 4$ in high N and $n = 2$ in low N. For *T. pseudonana* $n = 3$ in high N and $n = 2$ in low N.

N-limitation altered the thermal niche of both species (Fig. 4.2 & 4.3). The 2-way-MANOVA confirmed that nitrate levels had a significant effect on the cardinal temperatures of the TPCs of the two monocultures ($F_{1,7} = 9.38$, $p < 0.05$). However, the two diatoms responded differently to a reduction in N and consequently there was a significant interaction between “N regime” and “species” ($F_{1,7} = 33.87$, $p < 0.01$). Specifically, the thermal niche for *P. tricornutum* became slightly more narrow (increase in CT_{50min} by 0.31 °C), and μ_{\max} at T_{opt} increased by 14%. In contrast, thermal niche of *T. pseudonana* widened (CT_{50min} dropping by 2.42 °C), and the μ_{\max} of *T. pseudonana* decreased by 18% (isolated ANOVA results within the MANOVA test for each cardinal temperature can be found in Suppl. Tables 4.7 – 4.10).

Similar to the growth rate results, carrying capacities (K) also displayed a unimodal non-linear response along the assay temperature gradient and monocultures reached higher carrying capacities the closer the assay temperatures were to the species’ T_{opt} (Fig. 4.4A). All of the cardinal temperatures for carrying capacity differed significantly from one another between species (T_{opt}: $F_{1,2} = 545.9$, $q < 0.01$; CT_{50min}: $F_{1,2} = 78.28$, $q = 0.05$; CT_{50max}: $F_{1,2} = 743.1$, $q < 0.01$) (Fig. 4.5A). Similar to the growth trends in the high N scenario, these significant differences

arose because the thermal niche of *T. pseudonana* was shifted more towards warm temperatures than *P. tricornutum*. Despite differences in the thermal niches, the maximum carrying capacity at T_{opt} did not differ significantly between species ($F_{1,2}=6.96$, $q=0.48$) (Fig. 4.4B). Individual test statistics for the single one-way ANOVAs can be found in the Supplementary Material (Suppl. Tables 4.11 – 4.14).

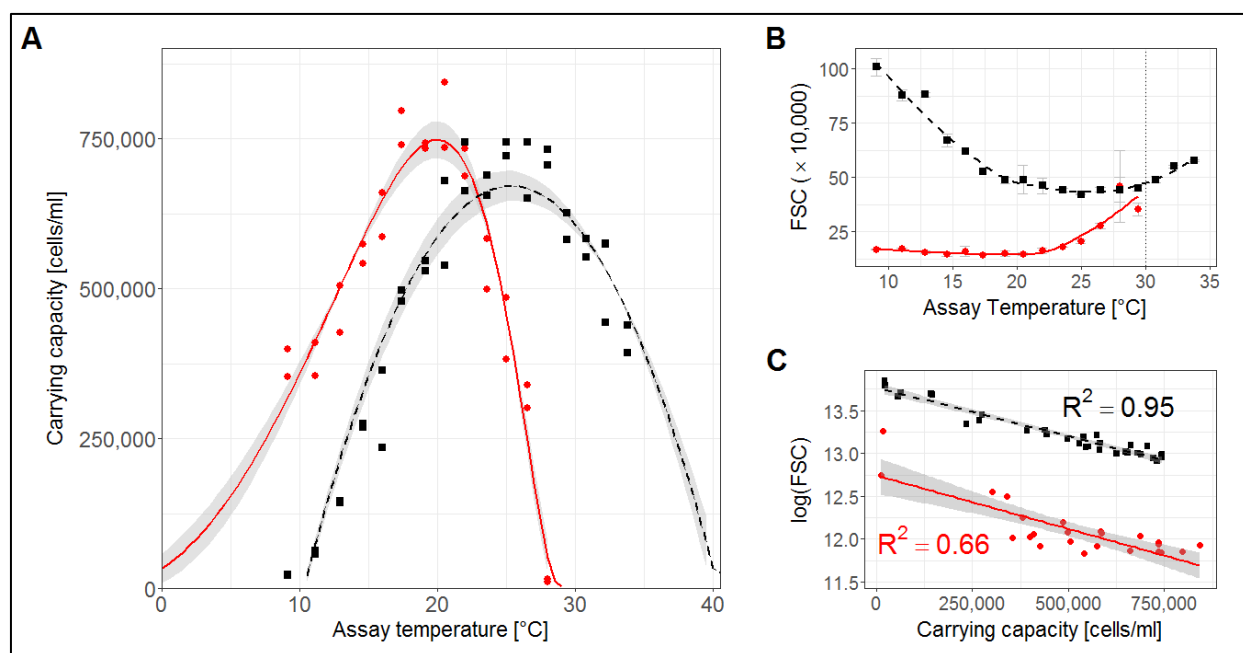


Figure 4.4: (A) Temperature response curves of carrying capacity of *P. tricornutum* (red circles and solid line) and *T. pseudonana* (black squares and dashed line) under nitrogen-depleted conditions in the N-limited phase of semi-continuous culturing in the low N medium ($n = 2$ for both species). Shaded area denotes standard deviation of the average model calculated from replicate model fits. Symbols show the carrying capacities from distinct biological replicates across the assay temperature range. Raw data used to calculate carrying capacities can be seen in Suppl. Fig. 4.8. (B) Forward scatter (FSC) from flow cytometry data of the low N experiment across assay temperatures. FSC measurements depicted here were taken on the last day of replicate monocultures before they were mixed together for the competition experiment. The solid and dashed lines are LOESS lines to visualise the U-shaped trend of the data across assay temperatures ($R^2 = 0.85$, and $RSE = 4.503$ for *P. tricornutum*; $R^2 = 0.97$, and $RSE = 3.378$ for *T. pseudonana*). LOESS was not used as a model to predict the relationship between temperature and cell size. Dotted line at 30 °C indicates the critical maximum temperature for *P. tricornutum* beyond which it could not sustain growth. (C) Correlation between carrying capacity K and $\log(FSC)$ for both species. Solid and dashed lines are linear models of the regression. Nonlinear model outputs of the single replicate models used to calculate the average model can be found in Suppl. Table 4.4 and single model fits on the individual growth replicates can be found in Suppl. Fig. 4.2C.

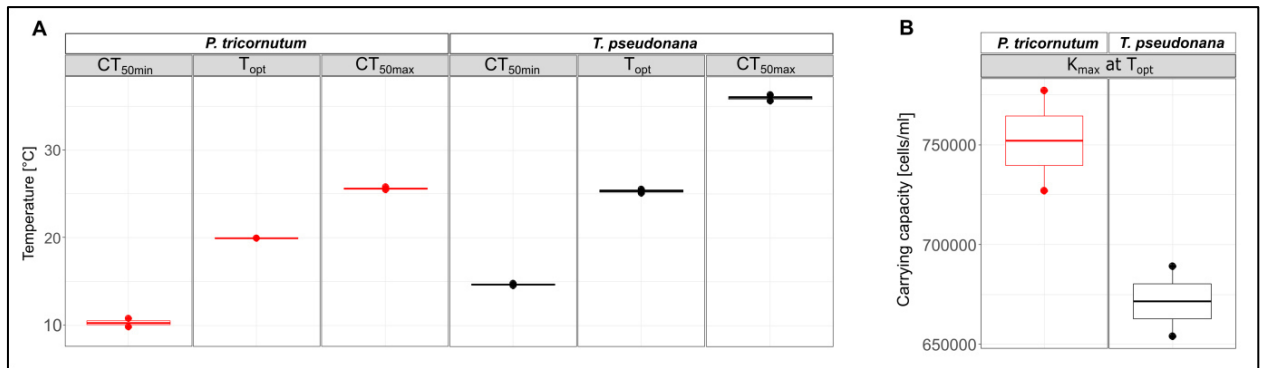


Figure 4.5: Comparison of (A) cardinal temperatures, and (B) maximum carrying capacities from thermal performance curve model fits for carrying capacities between *P. tricornutum* and *T. pseudonana* in low N conditions ($n = 2$ for both species).

After 15 days of growing the monocultures in the low N medium, cell size showed a U-shaped trend across assay temperatures with cell size increasing towards the coldest and warmest tested assay temperatures (Fig. 4.4B). There was a strong negative linear correlation between the logarithm of cell size and K (Fig. 4.4C), with the smallest cell sizes being observed at assay temperatures closest to each diatom's T_{opt} , meaning that cell size increased towards the diatoms' physiological limits.

4.4.2 Competition across assay temperatures

Monoculture TPCs were used to predict competition across assay temperatures. Under high N conditions, LOESS (represented by the solid black line in Fig. 4.6A, $R^2 = 0.998$, and $RSE = 0.021$) predicted an inflexion point at 18.7 °C (i.e. a competition coefficient equal to 0), indicating that *P. tricornutum* was predicted to outcompete *T. pseudonana* from the coldest assay temperature up to 18.7 °C. N limitation was predicted to alter the competition across assay temperatures whereby the inflexion point would shift horizontally across the temperature axis to 24.6 °C (5.9 °C warmer than under high N conditions; solid black line in Fig. 4.6B, $R^2 = 0.996$, and $RSE = 0.026$). Because K also showed a response across the assay temperature gradient, it was possible to make a second prediction of competition in the low N scenario based on K. Competition coefficients calculated from K predicted the switch at 22.9 °C (4.2 °C warmer than under high N conditions; dotted black line in Fig. 4.6B, $R^2 = 0.992$, and $RSE = 0.039$). Competition was predicted to be strongest at assay temperatures where the growth rates or carrying capacities in monocultures exhibited greatest divergence between species. Naturally, a species would lose the competition at an assay temperature where it could not sustain growth as an isolated species, having reached its physiological limits. Between the upper and lower temperature thresholds where both species could grow, the competitive outcomes were determined by the thermal growth performances of the species in isolation.

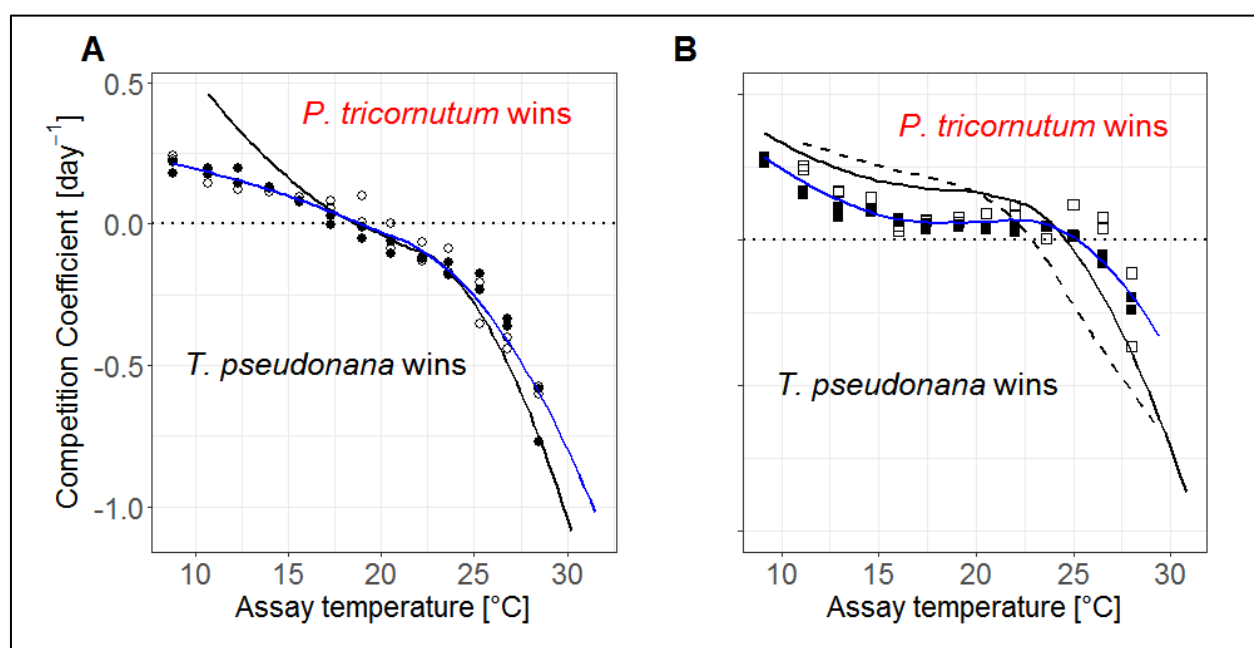


Figure 4.6: Predicted (lines) and observed (symbols) competition coefficients between *P. tricornutum* and *T. pseudonana* across assay temperatures in (A) high N conditions, and (B) low N conditions. A coefficient of 0 indicates no competitive advantage for either species, and predicts stable co-existence under the assay conditions. At coefficients greater than 0, *P. tricornutum* has the competitive advantage, at coefficients below 0 *T. pseudonana* has the advantage. The further the competition coefficient deviates from 0, the stronger is the competition between the two species. In (A) the solid black line indicates predictions for competition coefficients made from monoculture growth rates. The solid blue line is the LOESS smooth to visualise the progression of all observed high N competition coefficients across temperatures ($R^2 = 0.97$, $RSE = 0.047$). Observed coefficients were calculated from changes in species frequencies over time in mixed cultures (data from Suppl. Fig. 4.10), calculated with equation [5]. Closed symbols represent the competition coefficients that were started when stock cultures were transferred to the temperature-gradient-block, open symbols those that were started two weeks later to investigate the potential effects of temperature acclimation. In (B) solid black line indicates predictions made from the initial exponential growth rate in low N medium for monocultures, whereas the dashed line indicates predictions made from monoculture carrying capacities across the temperature gradient. The solid blue line is the LOESS smooth to visualise the progression of all observed low N competition coefficients across temperatures ($R^2 = 0.86$, $RSE = 0.051$). Observed coefficients were calculated from changes in species frequencies over time in mixed cultures (data from Suppl. Fig. 4.11), calculated with equation [5]. Closed symbols represent competition replicates that were started at the onset of N-limitation, open symbols those that were started from monocultures that were cultured under N-limitation for an additional seven days.

When the two diatoms were mixed together and competed against one another, the observed competition coefficients displayed a similar progression across assay temperatures as the predictions. In high N conditions, inflexion points occurred at 18.8 ± 1.2 °C (predicted at 18.7 °C) (Fig. 4.6A). As predicted, *P. tricornutum* won competitions across temperatures colder than the inflexion point, whereas *T. pseudonana* won competitions at temperatures warmer than the inflexion point. When the nitrate concentration was reduced, the competitive switch occurred at a warmer temperature, as predicted from the temperature dependencies of low N growth rates and carrying capacities (Fig. 4.6B). The average temperature for the inflexion point in low N medium was 6.5 °C greater than in high N medium and differed significantly ($F_{1,6} = 89.17$, $p < 0.001$) (Suppl. Table 4.15). The inflexion point was located at 25.3 ± 0.6 °C (predicted at 24.6 °C when growth rate was used to calculate the competition coefficients, or 22.9 °C when carrying capacity was used for the prediction). Pooling of mixed culture replicates for the final analysis due to a lack of a temperature acclimation signal in the high N scenario did not affect our interpretation of the conclusion that the competitive shift occurred at higher temperatures in the low N scenario.

4.4.3 Predictability of change in competitive ability

In both nutrient scenarios, the predicted and observed competition coefficients were strongly correlated (R^2 -values of 0.80 to 0.96), indicating that competition coefficients were very predictable from growth in monocultures (Table 4.1).

Progression of predicted and observed competition coefficients across temperatures was very similar, yet deviations existed between predictions and observations. For example in high N conditions, observed coefficients tended to be lower than predictions across the five lowest assay temperatures, and therefore observed competition was not as strong as predicted across the assay temperatures where *P. tricornutum* outcompeted *T. pseudonana* (competition coefficient > 0). Likewise, across the temperatures at which *T. pseudonana* was predicted to win (competition coefficient < 0), the strength of the competition coefficients was slightly overestimated and predicted to be more negative than observed values (Fig. 4.6A).

In low N conditions the predicted and observed coefficients aligned less strongly than in high N conditions, but correlation was still high (see R^2 in Table 4.1). Predictions were more accurate when they were made from low N growth rates than from carrying capacities (Fig. 4.6B). As with the high N experiment, the predicted coefficients were typically stronger than the observed. In addition, both low N predictions underestimated the temperature of the inflexion point and predicted the competitive advantage to switch at a lower assay temperature than it did in the experiment, therefore underestimating the temperature range at which *P. tricornutum* was the better competitor.

Table 4.1: Parameters for linear models ($y = ax + b$) correlating predicted (x) and observed competition coefficients (y) across assay temperatures. Significant correlations (alpha level of 0.05) that conclude a relationship between predictions and observations are marked in bold and with an asterisk.

Correlation	Linear Model parameters					
	R^2 of Correlation	Slope \pm 95%-confidence interval	y-Intercept \pm 95%-confidence interval	df	t-value	p-value of correlation
High N growth rates with competition coefficients (n=13)	0.96	0.67 ± 0.09	-0.06 ± 0.04	12	16.626	<0.001*
Low N growth rates with competition coefficients (n=13)	0.92	0.56 ± 0.11	0 ± 0.03	12	11.567	<0.001*
Low N carrying capacity with competition coefficients (n=13)	0.80	0.43 ± 0.14	0.03 ± 0.05	12	6.983	<0.001*

4.5 Discussion

In this study, competition between *P. tricornutum* and *T. pseudonana* was determined primarily by the growth performance of these species under specified thermal and nutrient regimes in isolation and indicated that they did not interact strongly in mixed populations. The results provide support for our hypotheses as we show that in relatively simple systems, prediction of competitive outcomes from isolated species performance across a thermal gradient is possible. The amount of N present in the mixed cultures influenced the competition across the temperature gradient and showed that alterations in nutrient concentrations have the potential to change the outcomes of competition with all else being constant. Further aligning with our hypothesis, the better growing species in isolation had the competitive advantage in mixed cultures, with the switch in competitive advantage occurring at or close to the temperature where the TPCs of the two species intercepted. The poorer competitor also lost the competition quicker when the absolute differences between monoculture thermal performances were the largest.

4.5.1 Reduced nitrogen impacts competition across temperatures

Under low N conditions, we observed *P. tricornutum* to be the better competitor across most of the tested assay temperatures. Although N-uptake rates were not measured in this experiment, the increased competitive success of *P. tricornutum* in low N conditions, and a warmer inflexion point of competitive advantage as a result thereof, could be attributed to its previously reported high affinity and high uptake rates for nitrogen (Goldman and Ryther, 1976; Grover, 1991; Sharp et al., 1979). This may have facilitated *P. tricornutum* to win competitions across most of the N-limited temperature gradient, including at assay temperatures up to 3.2 °C warmer than predicted (22.9 °C prediction from K across temperatures compared to warmest

observed inflexion point in low N conditions at 26.1 °C). To confirm that the increased competitive success can be explained through better nitrogen uptake rates and storage abilities, future experiments should quantify N-uptake rates of the two species under the assay conditions described in this study. Its good nitrogen uptake ability could help *P. tricornutum* to win competitions under N-limiting conditions at temperatures where other species can normally reach higher carrying capacities or grow faster when N is not limiting. However, the high N-affinity of *P. tricornutum* may be nullified in conditions where N-content of surface waters is high. For *T. pseudonana*, the reduction in μ_{\max} and shift of T_{opt} towards colder temperatures in low N conditions was in accordance with Grimaud et al. (2017) and confirmed the effect of nitrogen concentration on *T. pseudonana* growth rates. This change in thermal performance indicates that *T. pseudonana* may become less competitive in warm N-limited waters, but its competitive ability should be reinstated following the introduction of N into a system, e.g. in coastal up-welling zones.

Despite presumed better nitrogen uptake abilities, *P. tricornutum* did not win all competitions across the whole assay temperature gradient in low N conditions. This may be due to the fact that good N uptake ability was offset towards the warm assay temperatures by physiological limits for growth of this diatom. Past research has identified R^* across temperatures as a U-shaped function (Lewington-Pearce et al., 2019; Tilman, 1981) and warmer temperatures were found to increase nitrogen demand in phytoplankton (Toseland et al., 2013). Towards the growth limits, the minimum nutrient requirements for a species rise rapidly within a small temperature range as cells become stressed and need a larger internal nutrient content (cell quota) to survive while other physiological limits become more important (Rhee and Gotham, 1981; Thomas et al., 2017; Tilman, 1981). The circumstance that cell size was also found to

display a U-shaped trend with assay temperatures could have reinforced the observed patterns of competition across the assay temperature gradient. Cell size is known to play a role in competitive success and species dominance because larger, slower growing cells tend to have lower nutrient uptake rates relative to smaller cells with more beneficial surface-area-to-volume ratios (Gallego et al., 2019; Litchman and Klausmeier, 2008; Smith and Kalff, 1982). This study provides further support of this relationship, whereby cells growing towards their physiological limits (thermal extremes) were larger and grew slower, thus potentially amplifying the rate at which a species was losing competitions close to its physiological limits. As surface temperatures are expected to increase in aquatic systems worldwide, this temperature dependence of R^* and cell size might play a crucial role for population dynamics under warming scenarios in future marine systems (Bernhardt et al., 2018; Lewington-Pearce et al., 2019). Approaching physiological limits through warming might shift abiotic conditions in a direction in which a competitor might be at a loss although it is generally better at taking up nutrients in more moderate environments. Such an environmental change towards more critical conditions might offset the ability of a species to reduce nutrients to a concentration that is lower than the R^* of a direct competitor (McPeck, 2019).

The observed changes in species frequencies over time in the low N scenario may have been due to interspecific differences of the capacity for surge uptake, following the daily additions of fresh medium followed by extensive phases of nutrient starvation when this added nitrate was fully taken up. Greater capacity for surge uptake is commonly defined as higher values of the maximum velocity of nutrient uptake (V_{\max} in the Michaelis-Menten equation), induced in phytoplankton as a physiological adjustment to nutrient limitation (Morel, 1987). The species with the greater capacity to increase V_{\max} will sequester nutrients quicker, effectively depriving them from the competitor with a lower capacity to increase V_{\max} . Because we did not measure

nitrate uptake kinetics, we cannot conclude from our experiments whether the outcome of competition depended on the ability to sequester nitrate during surge uptake or the ability to use the low nitrate concentrations (interspecific differences in the half saturation constant for uptake, K_m of the Michaelis-Menten curve). The growth rates calculated from the increase in fluorescence during the first few days of the low N monocultures might be indicative of surge uptake playing a role in the competitive success under low N conditions. The predictions of competitive outcomes from the exponential growth phase in low N medium did align closer with the observed competitions than the predictions from carrying capacities (see Fig. 4.6B). However, using fluorescence based growth rates or maximum K under low N conditions as predictors of competition can be regarded as proxies at best. Confirmation of a role for surge uptake in competition between these two species requires further experiments. The determination of N uptake rates and residual nitrate concentrations using more sensitive methods (e.g. stable isotopes) may help improve predictions of competitive success.

4.5.2 Predictability of competition under environmental change

In this study, monoculture responses of phytoplankton were found to be good predictors of competitive outcomes. Previously they also have been identified as good predictors of phytoplankton biogeography (Barton et al., 2016; Thomas et al., 2012). Whether such culture-based measurements are ultimately suitable for forecasting shifts in phytoplankton communities in response to environmental change and whether the findings can be generalised for other species pairs or taxa remains to be tested. Predictability of competitive outcomes in complex communities still presents a major challenge (Pennekamp et al., 2019).

As the species in this study did not appear to influence one another in mixed cultures, it is likely that allelopathic interactions did not play a role in this competition scenario. Indeed, monoculture performance would cease to be a good predictor of competitive ability if one species had a toxic effect on the other in a two species competition. For example, dinoflagellates can inhibit growth of competitors by releasing toxins (e.g Kubanek et al., 2005), and some diatoms excrete chemicals that inhibit growth of other diatoms (Pichierri et al., 2017). A slower-growing species might be able to gain a competitive advantage through the excretion of allelopathic substances upon sensing another species in its surrounding. Such species-specific interactions may explain some of the uncertainty in modelling natural phytoplankton communities. Furthermore, TPCs for growth of the same species were found to vary slightly from lab to lab even when similar protocols were employed (Boyd et al., 2013). These differences could be driven in part by data quality and model fitting (Low-Décarie et al., 2017), but they still raise concerns that predictability of competition response, which is dependent on thermal niche parameters and μ_{max} , only remain valid within a specific setting. In addition, adaptive changes in nutrient requirements or physiological parameters could change competitive abilities and reduce predictability. Elucidating the role of evolutionary change and whether long-term interactions are affected by genotypic variability will therefore play a crucial role in understanding future phytoplankton community structure (Bernhardt et al., 2020).

Our observations in monocultures were suitable for predicting the inflexion points of competition, however the predictions commonly overestimated the magnitude of competition coefficients, and this increased the further the coefficients were from 0 (see Fig. 4.6). The mismatch between predicted and observed coefficients at the extreme temperatures may be due to the fact that light microscopy counts could not distinguish between viable and non-

viable cells. The outcome being that cell frequency counts overestimated the number of reproducing cells of the losing competitor and incorrectly tipping the competition coefficient in its favour. Future studies could employ the use of a cell viable stains to discriminate between live and dead cells (e.g. Baker et al., 2018) when conducting cell frequency counts.

4.5.3 Wider implications of the study

The nitrogen loads to many coastal waters are predicted to increase in the future due to agricultural run-off or other human activities (Beman et al., 2005; Nixon, 1995), and surface waters are expected to become more stratified as warming increases (Bestion et al., 2018b). The findings that competitive outcomes change across temperatures and are dependent on the amount of N present in the experimental system imply that environmental changes and alterations of marine environments will affect how phytoplankton communities will be structured in the future. Changes in species interactions could then have subsequent effects on ecosystem functioning since distinctively structured communities cycle nutrients and carbon differently or have varying nutritional value for higher trophic levels (Falkowski et al., 1998; Litchman et al., 2006; Schaum et al., 2012).

Regardless of the importance for natural ecosystems, the finding that competitive outcomes could be well predicted in a simplified system could be of relevance for large-scale pond maricultures or other algae biotechnological settings where simple model communities or monocultures are established for harvest or extraction of secondary metabolites. The ability to predict the population composition under a defined set of abiotic parameters could help to control growth dynamics or purity of a culture (Regan and Ivancic, 1984). By being able to

predict composition, parameters can be altered to potentially stabilize mixed cultures or purify them through changing temperature or nutrient loading.

4.6 Conclusion

The current study demonstrated that competition between two diatoms could be well predicted in a controlled laboratory system. The aquatic environments where these algae naturally occur are however exposed to fluctuations in light, nutrients, temperature, as well as changes in species compositions due to migrations and water currents. In order to achieve higher comparability with natural environments, further investigations should focus on the effects of temperature variations and other abiotic fluctuations and their effects on competition between these two diatoms. Other species combinations and more complex communities could also be investigated to verify the generality of the current findings. The ability to predict where inflexion points of species interactions lie across gradients and when multiple environmental stressors interact will bring the scientific community closer to understanding non-linear ecosystem responses and help to potentially find strategies to mitigate changes that are predicted to occur under future environmental scenarios.

4.7 Supplementary Material

4.7.1 Supplementary Tables

Supplementary Table 4.1: Equations that can be used to describe thermal performance across temperatures from Low-Décarie et al. (2017). The experimental growth rate and carrying capacity were fitted to Equations 4 – 15 (shaded in green) with the R package “temperatureresponse” in this study. Equations 1 – 3 (shaded in blue) can only be used to cover a sub- or supra-optimal range of temperatures, but not the whole gradient, and were therefore not utilised in this study. In all model equations, small letters *a* to *f* are model parameters, *R* is the universal gas constant, *T* is the assay temperature at which a growth rate μ was measured, μ_0 the starting growth rate, E_A the activation energy of metabolism, T_{min} and T_{max} are the minimum and maximum temperatures beyond which no growth occurs for the organism under observation, and T_{ref} is the reference temperature at which a reference μ was measured in the cited study.

Formula	Equ.	Number of Parameters	Reference
$k(T) = a \cdot \exp\left(\frac{-E_A}{R \cdot T}\right)$	1	2	Raven and Geider, 1988
$k(T) = k(T_{ref}) \cdot \exp\left[-\frac{E_A}{R} \left(\frac{1}{T} - \frac{1}{T_{ref}}\right)\right]$	2	2	e.g. Geider et al., 1997; Li et al., 1984
$\mu(T) = \mu_0 \cdot \exp(k \cdot T)$	3	2	Eppley, 1972
$Rate = a \cdot \exp\left(\frac{-b}{R \cdot T}\right) - c \cdot \exp\left(\frac{-d}{R \cdot T}\right)$	4	4	Li and Dickie, 1987 citing Hinshelwood, 1947
$Rate = \frac{a \cdot T \cdot \exp\left(\frac{-b}{R \cdot T}\right)}{1 + \exp\left(\frac{-c}{R}\right) \cdot \exp\left(\frac{-d}{R \cdot T}\right)}$	5	4	Li and Dickie, 1987 citing Johnson et al., 1942
$Rate = \frac{a \cdot \left(\frac{T}{298.15}\right) \cdot \exp\left(\frac{b}{R} \cdot \left(\frac{1}{298.15} - \frac{1}{T}\right)\right)}{1 + \exp\left[\frac{c}{R} \cdot \left(\frac{1}{d} - \frac{1}{T}\right)\right] + \exp\left[\frac{e}{R} \left(\frac{1}{f} - \frac{1}{T}\right)\right]}$	6	6	Heitzer et al., 1991
$Rate = \frac{a \cdot \left(\frac{T}{293.15}\right) \cdot \exp\left(\frac{b}{R} \cdot \left(\frac{1}{293.15} - \frac{1}{T}\right)\right)}{1 + \exp\left[\frac{c}{R} \cdot \left(\frac{1}{d} - \frac{1}{T}\right)\right]}$	7	4	Montagnes et al., 2008 citing Schoolfield et al., 1981

$Rate = a \cdot \exp \left[-0.5 \cdot \left(\frac{T - T_{ref}}{b} \right)^2 \right]$	8	3	Li and Dickie, 1987 citing Stoermer and Ladewski (1976)
$Rate = a \cdot \exp \left[-0.5 \cdot \left(\frac{abs[T - T_{ref}]^c}{b} \right) \right]$	9	4	Montagnes et al., 2008
$Rate = a \cdot \exp(c \cdot T) \left[1 - \left(\frac{T - T_{ref}}{b} \right)^2 \right]$	10	4	Thomas et al., 2012
$Rate = a + b \cdot T + c \cdot T^2$	11	3	Montagnes et al., 2008
$Rate = \frac{1}{1 + (a + b \cdot T + c \cdot T^2)}$	12	3	Montagnes et al., 2008 citing Flinn, 1991
$Rate = [a \cdot (T - T_{min})]^2 \cdot [1 - \exp(b \cdot (T - T_{max}))]^2$	13	4	Ratkowsky et al., 1983
$Rate = a \cdot \{1 - \exp[-b \cdot (T - T_{min})]\} \cdot \{1 - \exp[-c \cdot (T_{max} - T)]\}$	14	5	Kamykowski, 1986
$Rate = \mu_{max} \cdot \left\{ \sin \left[\pi \cdot \left(\frac{T - T_{min}}{T_{max} - T_{min}} \right)^a \right] \right\}^b$	15	5	Boatman et al., 2017

Supplementary Table 4.2: Non-linear model outputs of single replicate TPC growth models for *P. tricornutum* (n = 4) and *T. pseudonana* (n = 3) in the high N scenario.

Species	Equ.	replicate	term	estimate	std.err.	statistic	p.value
<i>P. tricornutum</i>	13	1	a	0.0230	0.005	4.463617	0.0021
		1	b	0.3550	0.154	2.309595	0.0497
		1	T _{opt}	22.27			
		1	μ _{max}	0.81			
		1	AIC	-32.23			
		1	BIC	-29.80			
		1	pseudoR ²	0.893			
		1	T _{50min}	8.15			
		1	T _{50max}	27.56			
		<i>P. tricornutum</i>	13	2	a	0.0233	0.002
2	b			0.360	0.048	7.499019	3.7E-05
2	T _{opt}			22.64			
2	μ _{max}			0.82			
2	AIC			-51.44			
2	BIC			-48.62			
2	pseudoR ²			0.980			
2	T _{50min}			8.66			
2	T _{50max}			27.86			
<i>P. tricornutum</i>	13			3	a	0.0212	0.001
		3	b	0.4520	0.038	12.00063	7.7E-07
		3	T _{opt}	23.18			
		3	μ _{max}	0.85			
		3	AIC	-60.78			
		3	BIC	-57.95			
		3	pseudoR ²	0.99			
		3	T _{50min}	8.35			
		3	T _{50max}	27.89			
		<i>P. tricornutum</i>	13	4	a	0.0222	0.002
4	b			0.4069	0.051	7.933699	2.37E-05
4	T _{opt}			23.03			
4	μ _{max}			0.84			
4	AIC			-51.84			
4	BIC			-49.01			
4	pseudoR ²			0.98			
4	T _{50min}			8.65			
4	T _{50max}			27.97			
<i>T. pseudonana</i>	11			1	a	-1.5631	0.4345
		1	b	0.1775	0.0372	4.770507	0.0006
		1	c	-0.0030	0.0008	-3.94688	0.0023
		1	T _{opt}	29.74			
		1	μ _{max}	1.08			
		1	AIC	-18.53			

		1	BIC	-15.97			
		1	pseudoR ²	0.85			
		1	T _{50min}	16.31			
		1	T _{50max}	43.16			
<i>T. pseudonana</i>	11	2	a	-0.5190	0.3768	-1.3774	0.1984
		2	b	0.0915	0.0309	2.955411	0.0144
		2	c	-0.0013	0.0006	-2.15604	0.0565
		2	T _{opt}	34.82			
		2	μ _{max}	1.07			
		2	AIC	-27.43			
		2	BIC	-25.17			
		2	pseudoR ²	0.85			
		2	T _{50min}	14.61			
		2	T _{50max}	55.03			
<i>T. pseudonana</i>	11	3	a	-1.7923	0.3958	-4.52877	0.0009
		3	b	0.2116	0.0339	6.245958	6.3E-05
		3	c	-0.0040	0.0007	-5.7643	0.0001
		3	T _{opt}	26.66			
		3	μ _{max}	1.03			
		3	AIC	-21.14			
		3	BIC	-18.58			
		3	pseudoR ²	0.81			
		3	T _{50min}	15.28			
		3	T _{50max}	38.04			
<i>T. pseudonana</i>	11	4	a	-1.5748	0.1220	-12.9132	8.63E-09
		4	b	0.1843	0.0114	16.10451	5.73E-10
		4	c	-0.003	0.0002	-12.7258	1.03E-08
		4	T _{opt}	29.09			
		4	μ _{max}	1.11			
		4	AIC	-47.50			
		4	BIC	-44.41			
		4	pseudoR ²	0.98			
		4	T _{50min}	15.88			
		4	T _{50max}	42.31			

Supplementary Table 4.3: Non-linear model outputs of single replicate TPC growth models for *P. tricornutum* (n = 2) and *T. pseudonana* (n = 2) in the low N scenario.

Species	Equ.	replicate	term	estimate	std.err	statistic	p.value
<i>P. tricornutum</i>	13	1	a	0.0320	0.0020	16.17818	2.14E-07
		1	b	0.2454	0.0299	8.200413	3.65E-05
		1	T _{opt}	22.04			
		1	μ _{max}	0.96			
		1	AIC	-65.32			
		1	BIC	-62.89			
		1	pseudoR ²	1.00			
		1	T _{50min}	9.54			
		1	T _{50max}	28.03			
<i>P. tricornutum</i>	13	2	a	0.0256	0.0072	3.557295	0.0074
		2	b	0.3012	0.1663	1.811701	0.1076
		2	T _{opt}	22.10			
		2	μ _{max}	0.94			
		2	AIC	-28.35			
		2	BIC	-25.92			
		2	pseudoR ²	0.87			
		2	T _{50min}	7.97			
		2	T _{50max}	27.87			
<i>T. pseudonana</i>	11	1	a	-0.8615	0.1434	-6.00656	4.4E-05
		1	b	0.12812	0.0135	9.487492	3.3E-07
		1	c	-0.0024	0.0003	-7.9881	2.27E-06
		1	T _{opt}	27.01			
		1	μ _{max}	0.87			
		1	AIC	-45.36			
		1	BIC	-42.27			
		1	pseudoR ²	0.93			
		1	T _{50min}	13.48			
<i>T. pseudonana</i>	11	2	a	-0.8858	0.1614	-5.48943	0.0001
		2	b	0.1329	0.0145	9.158956	9.17E-07
		2	c	-0.0025	0.0003	-8.10409	3.29E-06
		2	T _{opt}	26.60			
		2	μ _{max}	0.88			
		2	AIC	-46.76			
		2	BIC	-43.92			
		2	pseudoR ²	0.92			
		2	T _{50min}	13.32			
2	T _{50max}	39.89					

Supplementary Table 4.4: Non-linear model outputs of single replicate TPC carrying capacity models for *P. tricornutum* (n = 2) and *T. pseudonana* (n = 2) in the low N scenario.

Species	Equ.	replicate	term	estimate	std.err.	statistic	p.value
<i>P. tricornutum</i>	13	1	a	0.0398	0.0145	2.750692	0.0225
		1	b	0.1966	0.0855	2.298777	0.0471
		1	T _{opt}	19.96			
		1	μ _{max}	0.73			
		1	AIC	-26.93			
		1	BIC	-24.11			
		1	pseudoR ²	0.91			
		1	T _{50min}	9.78			
		1	T _{50max}	25.77			
		<i>P. tricornutum</i>	13	2	a	0.0474	0.0118
2	b			0.1925	0.0606	3.173647	0.0113
2	T _{opt}			19.97			
2	μ _{max}			0.77			
2	AIC			-33.83			
2	BIC			-31.00			
2	AICc			-25.26			
2	T _{50min}			10.75			
2	T _{50max}			25.47			
<i>T. pseudonana</i>	11			1	a	-1.1851	0.1654
		1	b	0.1438	0.0164	8.765961	4.65E-07
		1	c	-0.0028	0.0004	-7.50346	2.86E-06
		1	T _{opt}	25.57			
		1	μ _{max}	0.65			
		1	AIC	-34.05			
		1	BIC	-30.72			
		1	pseudoR ²	0.90			
		1	T _{50min}	14.79			
		1	T _{50max}	36.35			
<i>T. pseudonana</i>	11	2	a	-1.26407	0.1382	-9.14787	2.78E-07
		2	b	0.1556	0.0137	11.34796	1.91E-08
		2	c	-0.0031	0.0003	-9.89238	1.07E-07
		2	T _{opt}	25.11			
		2	μ _{max}	0.69			
		2	AIC	-40.15			
		2	BIC	-36.82			
		2	pseudoR ²	0.93			
		2	T _{50min}	14.56			
		2	T _{50max}	35.65			

Supplementary Table 4.5: One-way ANOVA output of comparison of competition inflexion point temperature between unacclimated and acclimated competition replicates in the high N scenario.

	Df	Sum Sq	Mean Sq	F value	Pr(>F)
Type	1	3.50	3.50	4.34	0.1727
Residuals	2	1.61	0.81		

High N and low N growth rate MANOVA fits

Supplementary Table 4.6: Two-way MANOVA output table for comparison between growth rate Thermal Performance Curve (TPC) fits of *P. tricornutum* and *T. pseudonana*. Dependent variables that were compared were μ_{max} , CT_{50min} , CT_{50max} , and T_{opt} . Individual ANOVA test statistics wrapped within this MANOVA are found in Supplementary Tables 5.7 – 5. 10.

	Df	Pillai	approx F	num Df	den Df	Pr(>F)
Intercept	1	1.00	2411.52	4	4	0.0000
Species	1	0.99	102.92	4	4	0.0003
N level	1	0.90	9.38	4	4	0.0261
Species : N level	1	0.97	33.87	4	4	0.0024
Residuals	7					

Supplementary Table 4.7: Two-way Individual ANOVA output table from MANOVA for CT_{50min} .

	Df	Sum Sq	Mean Sq	F value	Pr(>F)
Species	1	108.27	108.27	385.77	0.0000
N level	1	2.48	2.48	8.82	0.0208
Species : N level	1	4.69	4.69	16.72	0.0046
Residuals	7	1.97	0.28		

Supplementary Table 4.8: Two-way Individual ANOVA output table from MANOVA for T_{opt} .

	Df	Sum Sq	Mean Sq	F value	Pr(>F)
Species	1	75.94	75.94	90.72	0.0000
N level	1	3.50	3.50	4.18	0.0802
Species : N level	1	0.61	0.61	0.73	0.4220
Residuals	7	5.86	0.84		

Supplementary Table 4.9: Two-way Individual ANOVA output table from MANOVA for CT_{50max} .

	Df	Sum Sq	Mean Sq	F value	Pr(>F)
Species	1	455.72	455.72	207.37	0.0000
N level	1	0.37	0.37	0.17	0.6943
Species : N level	1	0.74	0.74	0.34	0.5808
Residuals	7	15.38	2.20		

Supplementary Table 4.10: Two-way Individual ANOVA output table from MANOVA for μ_{max} .

	Df	Sum Sq	Mean Sq	F value	Pr(>F)
Species	1	0.04	0.04	64.99	0.0000
N level	1	0.00	0.00	3.72	0.0950
Species : N level	1	0.06	0.06	99.19	0.0000
Residuals	7	0.00	0.00		

Low N carrying capacity ANOVA fits**Supplementary Table 4.11:** One-way ANOVA output table of CT_{50min} from K model fits.

	Df	Sum Sq	Mean Sq	F value	Pr(>F)
Species	1	19.45	19.45	78.28	0.0125
Residuals	2	0.50	0.25		

Supplementary Table 4.12: One-way ANOVA output table of T_{opt} from K model fits.

	Df	Sum Sq	Mean Sq	F value	Pr(>F)
Species	1	28.89	28.89	545.88	0.0018
Residuals	2	0.11	0.05		

Supplementary Table 4.13: One-way ANOVA output table of CT_{50max} from K model fits.

	Df	Sum Sq	Mean Sq	F value	Pr(>F)
Species	1	107.74	107.74	743.06	0.0013
Residuals	2	0.29	0.15		

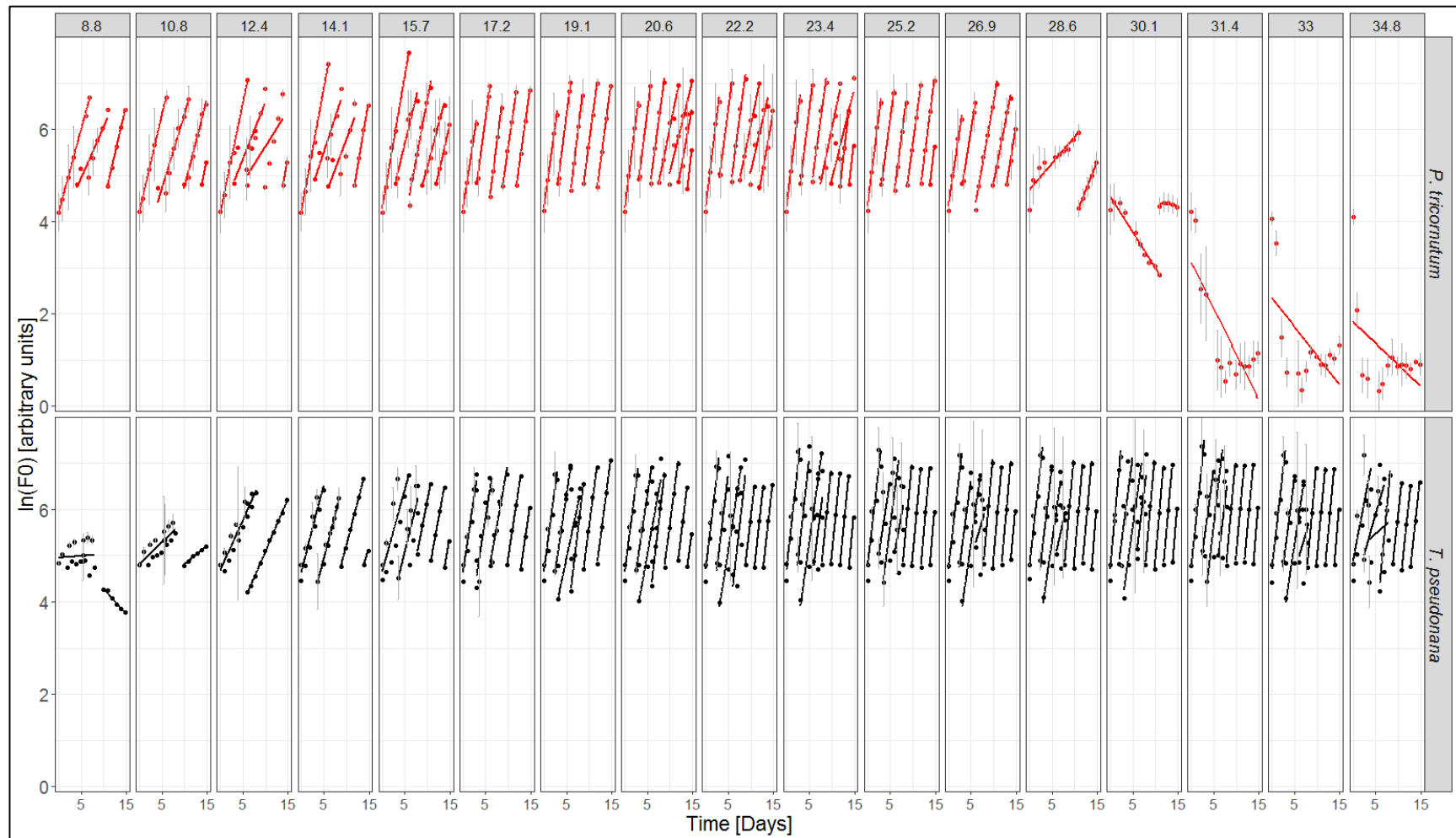
Supplementary Table 4.14: One-way ANOVA output table of K_{max} from K model fits.

	Df	Sum Sq	Mean Sq	F value	Pr(>F)
Species	1	0.65	0.65	6.96	0.1187
Residuals	2	0.19	0.09		

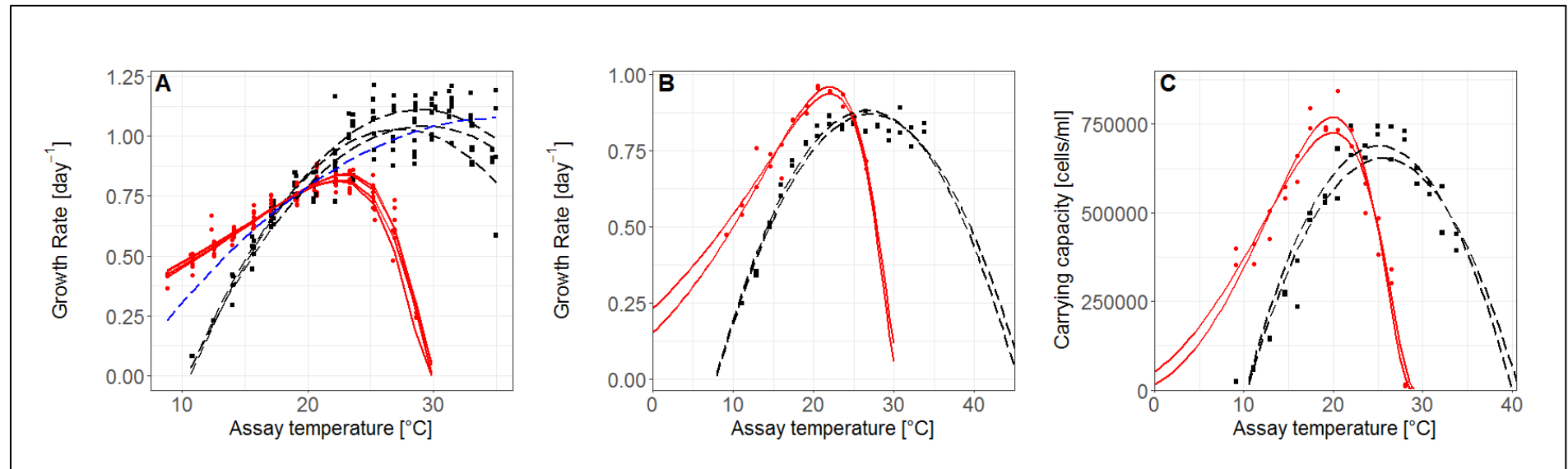
Observed inflexion point comparison**Supplementary Table 4.15:** One-way ANOVA output table for differences between high N and low N inflexion points.

	Df	Sum Sq	Mean Sq	F value	Pr(>F)
N level	1	85.59	85.59	89.17	0.0001
Residuals	6	5.76	0.96		

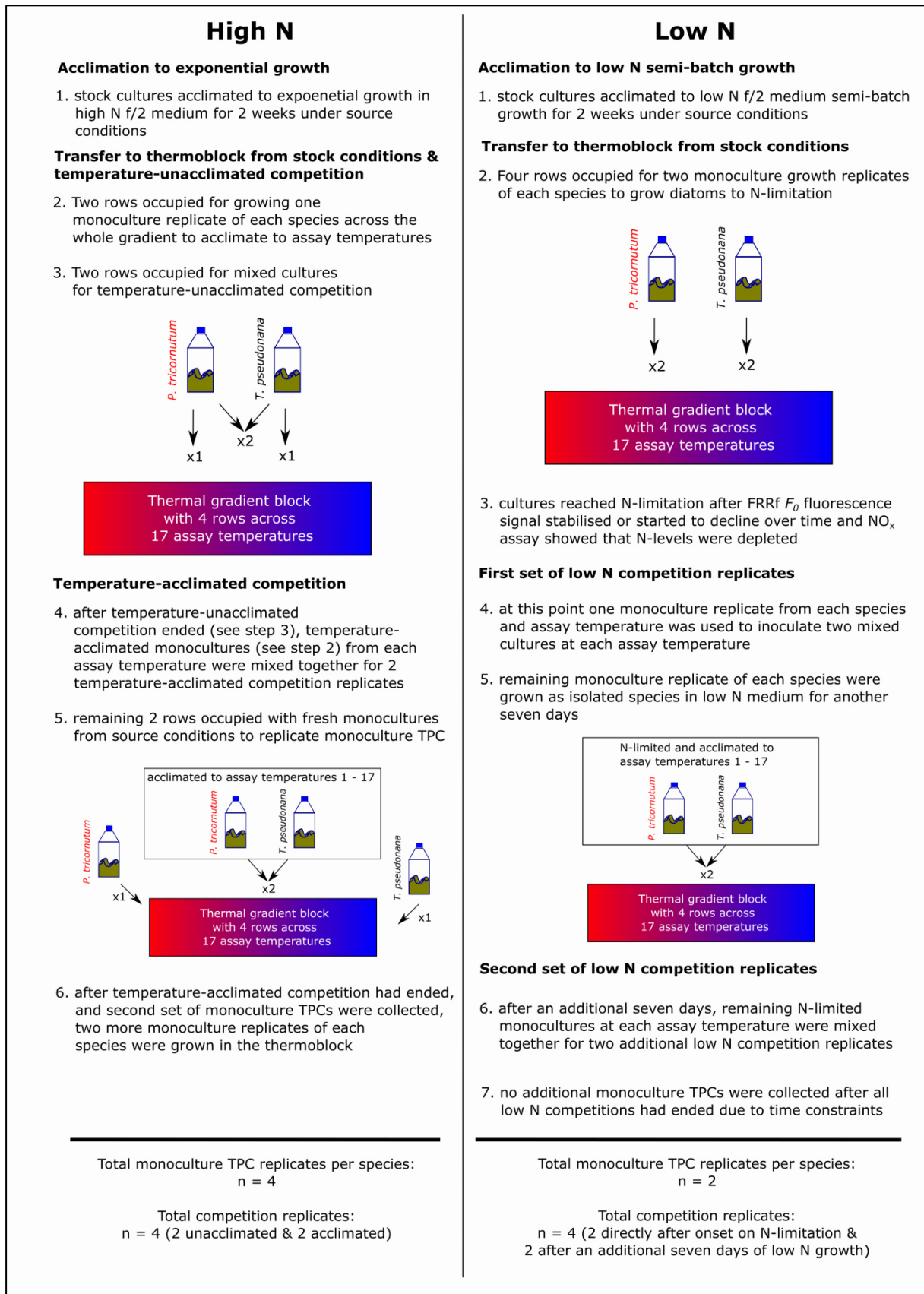
4.7.2 Supplementary Figures



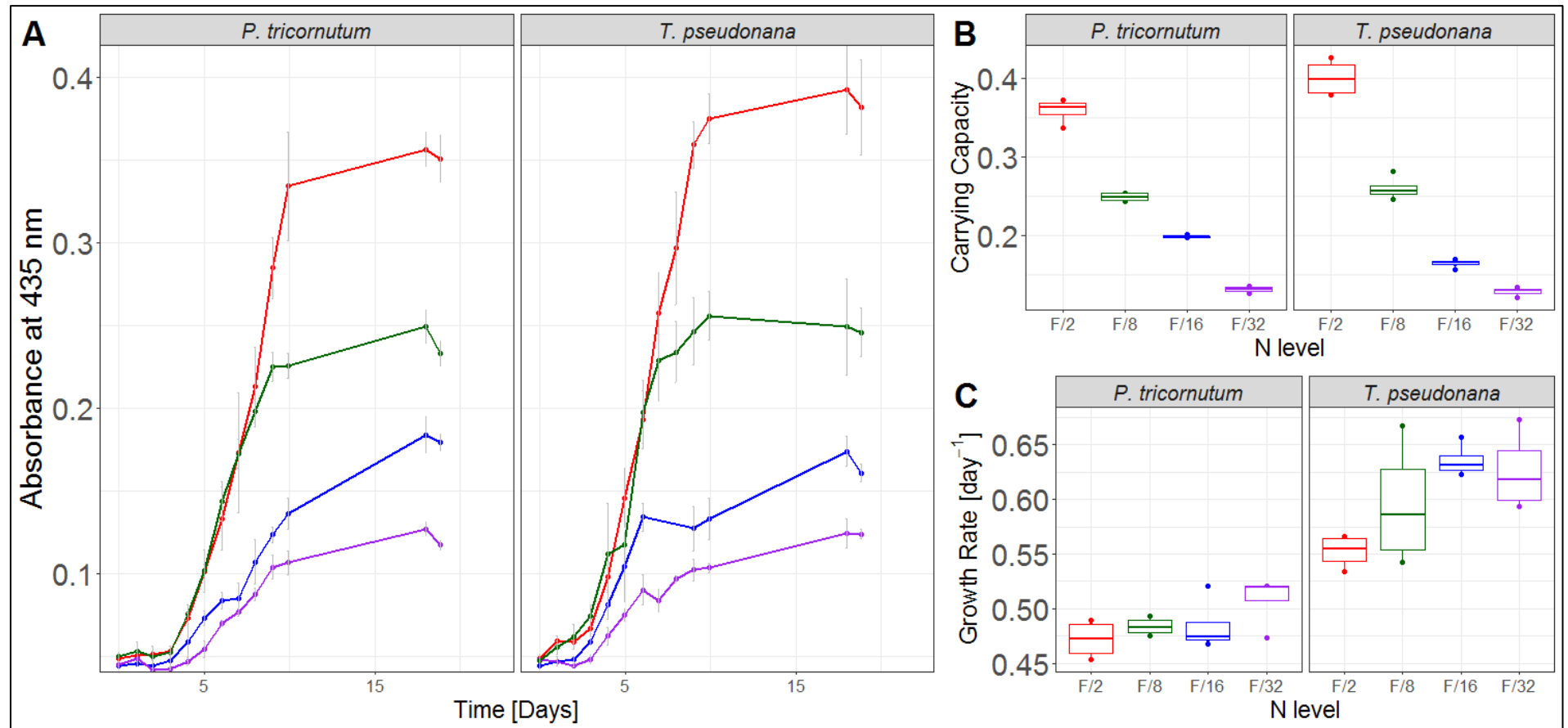
Supplementary Figure 4.1: Average $\ln(F_0)$ of exponentially growing *P. tricornutum* ($n = 4$) (red) and *T. pseudonana* ($n = 3$) (black) in the high N medium measured at the indicated assay temperatures across the temperature gradient. Individual slopes represent single dilution phases. Grey error bars denote 1 standard deviation.



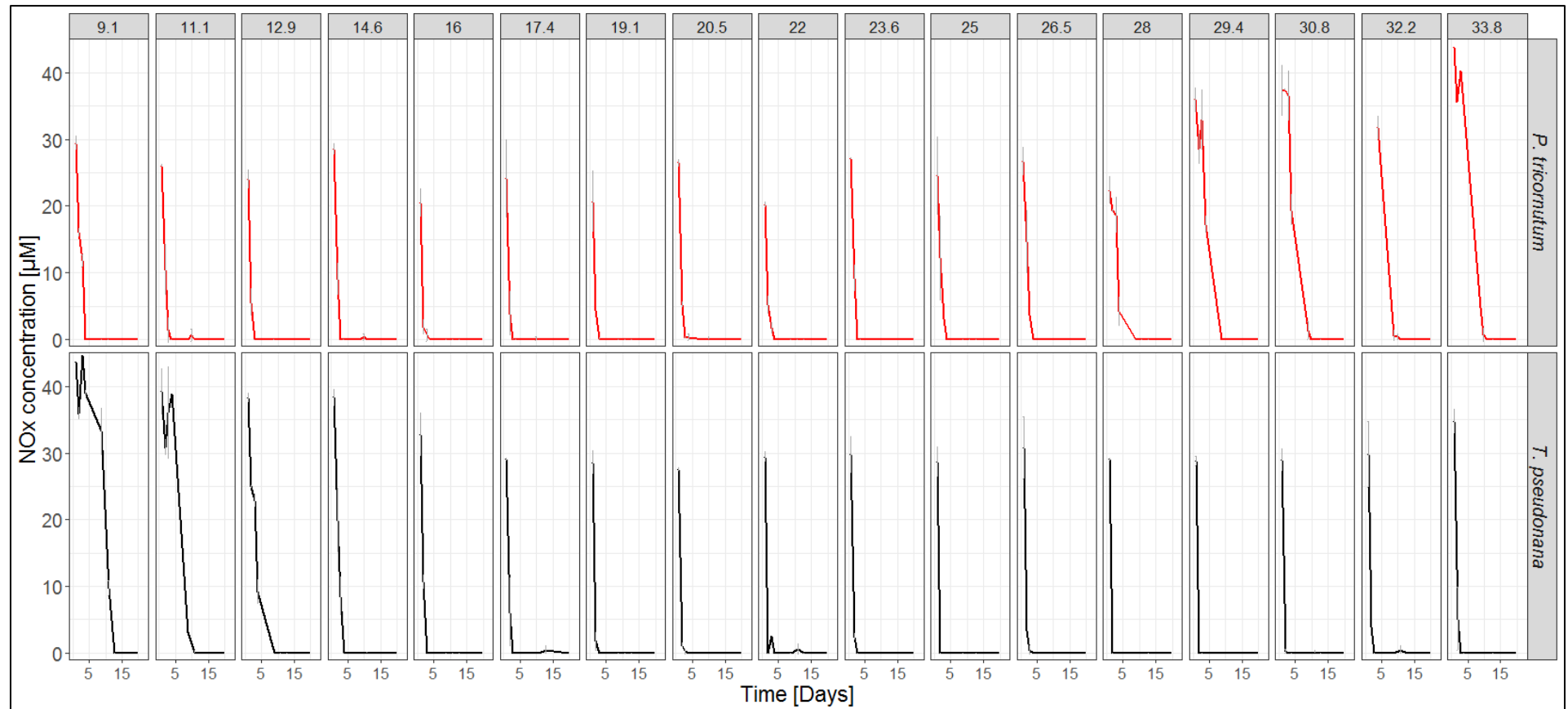
Supplementary Figure 4.2: (A) Single TPC model fits for the two diatom species *P. tricornutum* in red ($n = 4$) and *T. pseudonana* in black ($n = 4$) from which average growth models for Figure 4.2A were calculated. The one *T. pseudonana* replicate that was omitted in the final analysis is plotted in blue. (B) Single TPC model fits for the two diatom species *P. tricornutum* in red ($n = 2$) and *T. pseudonana* in black ($n = 2$) from which average growth models for Figure 4.2B were calculated. (C) Single TPC model fits for the two diatom species *P. tricornutum* in red ($n = 2$) and *T. pseudonana* in black ($n = 2$) from which average carrying capacity models across temperatures for 4.4A, were calculated. Single non-linear model parameters for these model fits can be found in Supplementary Tables 4.2 – 4.4.



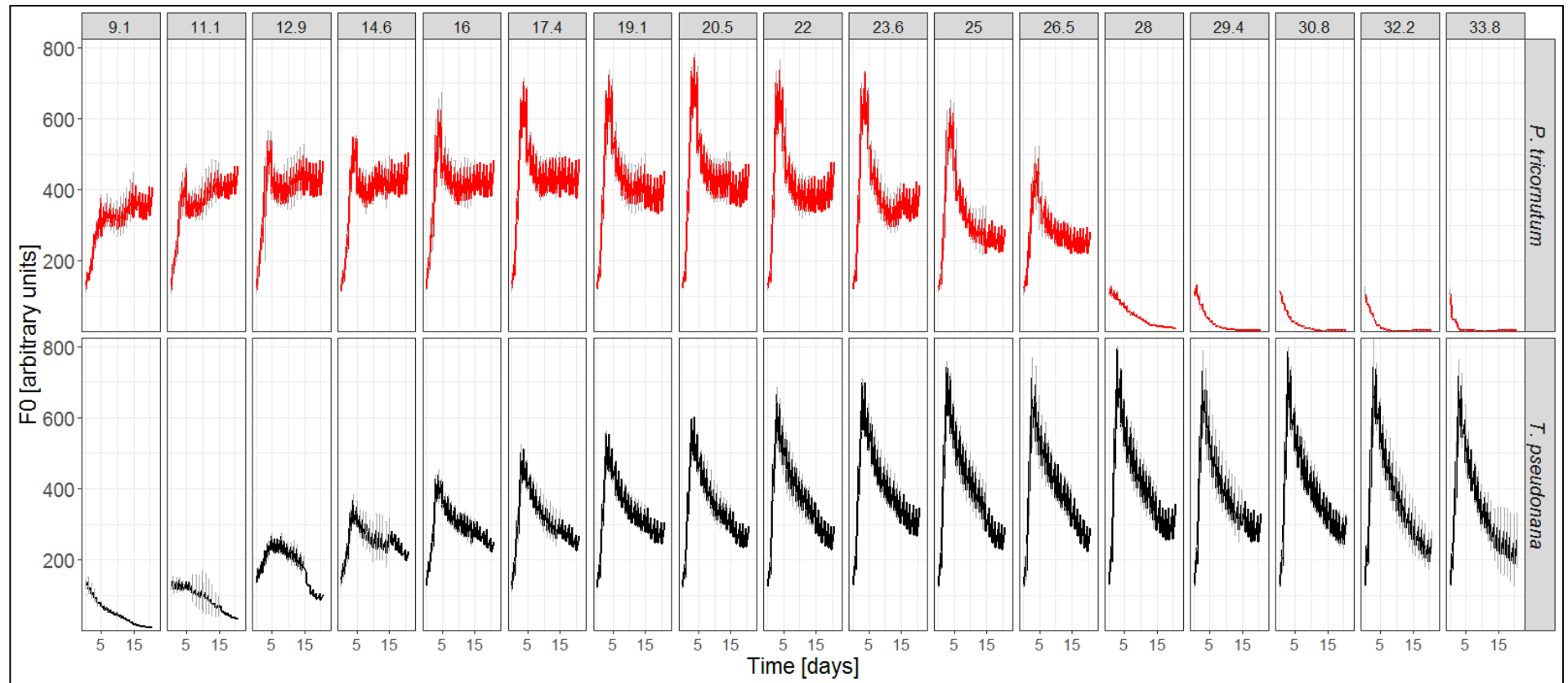
Supplementary Figure 4.3: Visual representation of the competition experiments to better understand when the various growth and competition replicates were collected.



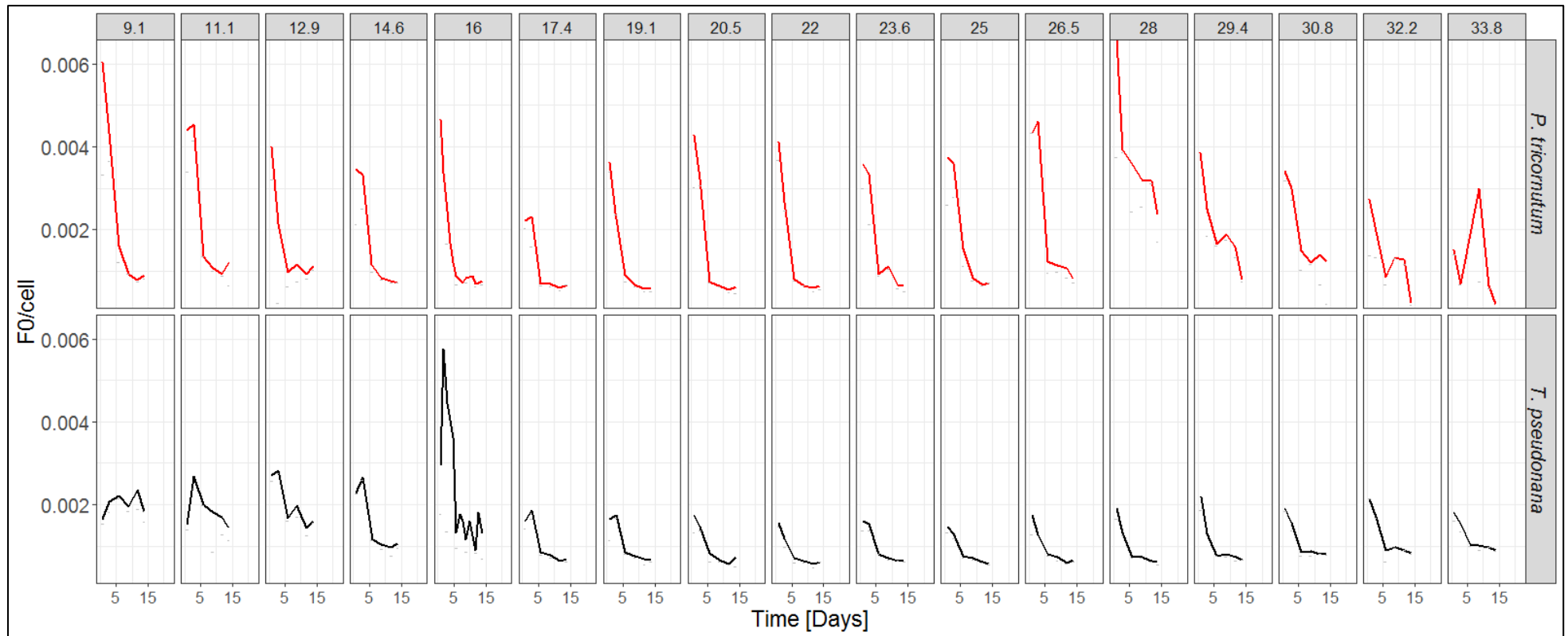
Supplementary Figure 4.4: (A) Growth progression over time for *P. tricornutum* and *T. pseudonana* grown in f/2 medium with different nitrate concentrations (882 μM (red), 220.5 μM (green), 110.25 μM (blue), 55.13 μM (purple)). (B) Dependence of carrying capacity (K) on nitrogen concentration in the growth medium. (C) Dependence of exponential growth rate r on nitrogen level in the growth medium.



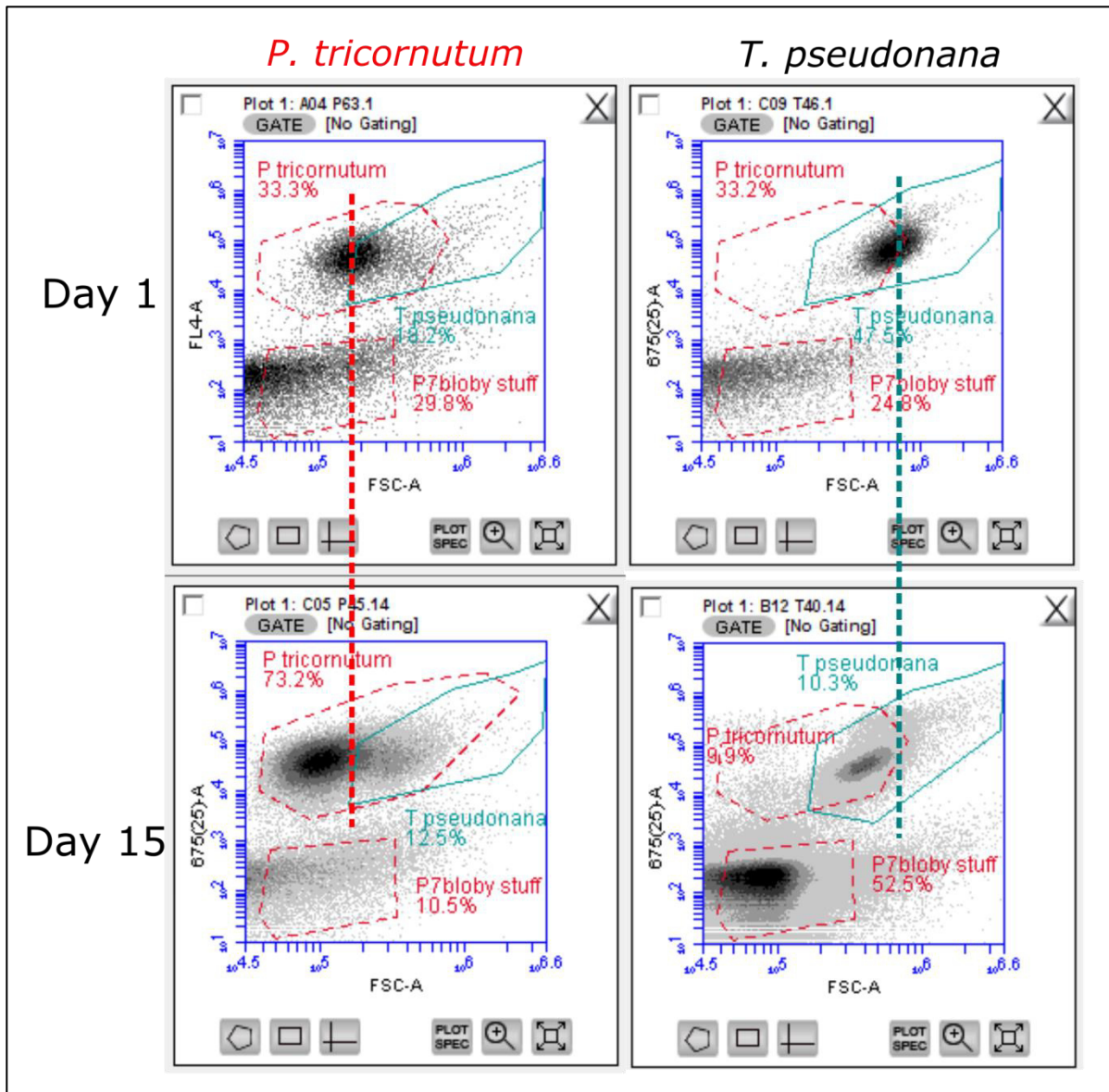
Supplementary Figure 4.5: Average ($n = 2$) nitrate plus nitrite concentrations in monocultures across all assay temperatures in the low N medium over time for *P. tricornutum* and *T. pseudonana*. Grey error bars denote standard deviation from two replicates. At the cold and warm ends of the temperature gradient, it can be seen that values for the NO_x concentration do not drop as quickly as towards the optimum temperatures. This is because especially for *P. tricornutum* at the warm end and *T. pseudonana* at the cold end, the cells did not grow as rapidly and it took them more time to deplete the available nitrogen stocks.



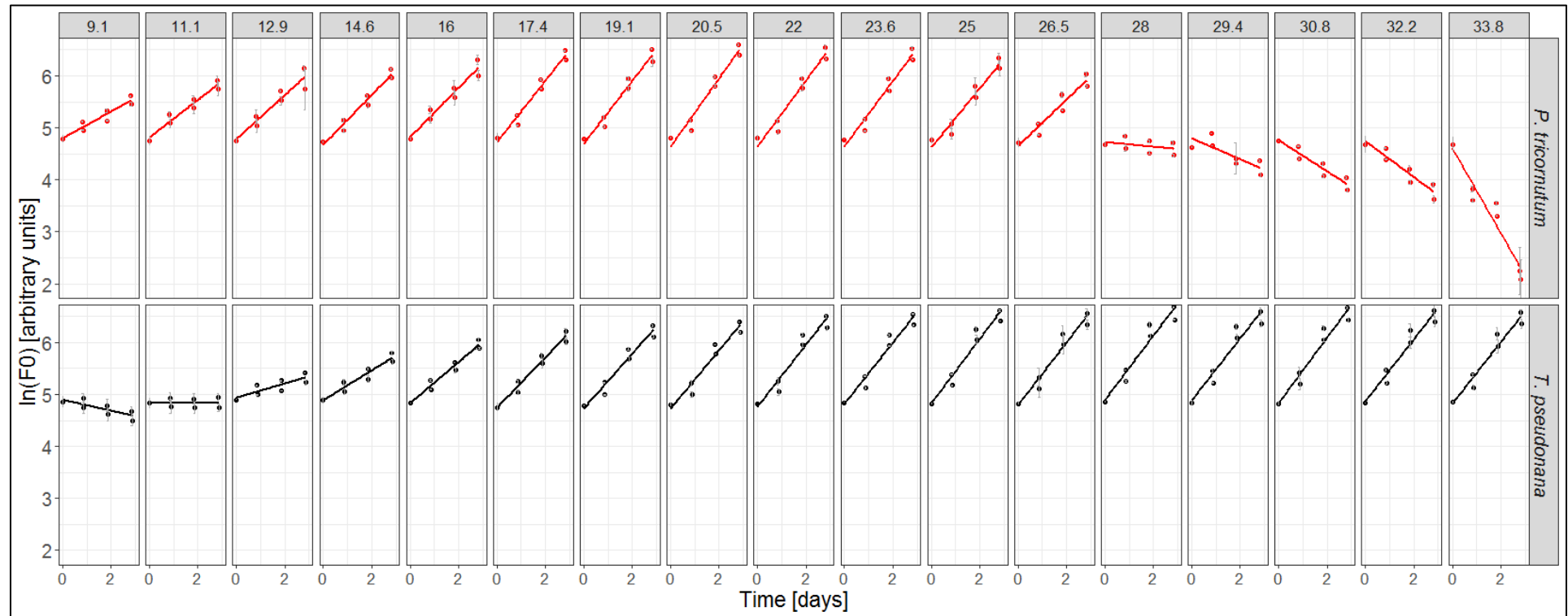
Supplementary Figure 4.6: Average ($n = 2$) F_0 fluorescence in low N monocultures across all assay temperatures over time for *P. tricornutum* and *T. pseudonana*. Grey error bars denote standard deviation from two replicates.



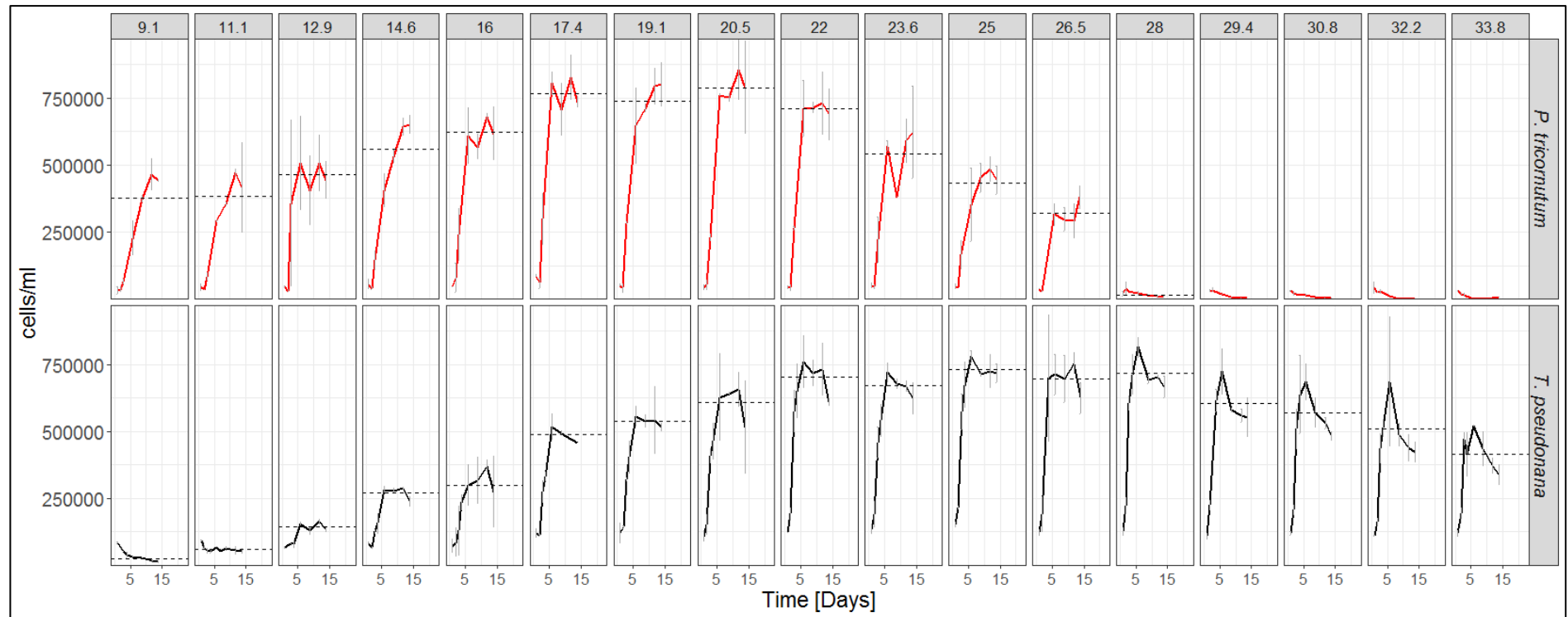
Supplementary Figure 4.7: Average ($n = 2$) F_0 measured by FRRf per cell across all assay temperatures for *P. tricornutum* and *T. pseudonana* in low N medium. Flow cytometry counts were taken for monocultures in the first 14 days of the experiment before mixing cultures together to start competition experiments. Grey error bars denote standard deviation from two replicates.



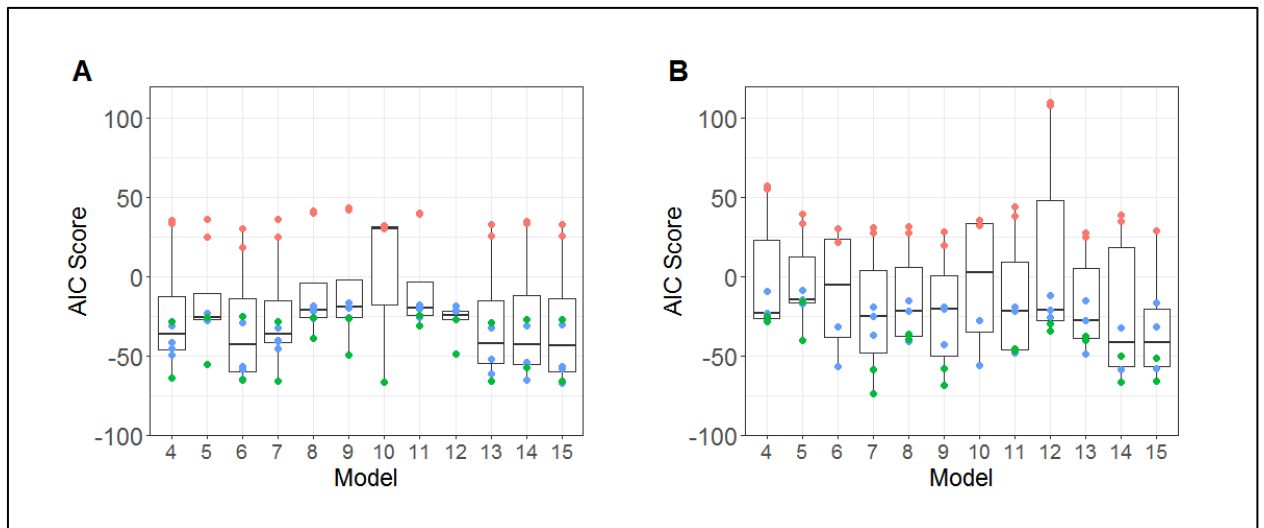
Supplementary Figure 4.8: Example flow cytometry (FC) data that was collected for *P. tricornutum* and *T. pseudonana* monocultures at the end of the first experimental day of the low N experiment, and after the diatoms had been cultured in low N medium for 15 days. After 15 days, N levels were depleted below the detection limit of the utilised NO_x assay. The dotted red and turquoise lines were roughly drawn through the mean forward scatter (FSC) values (used as proxies for cell size) of the starting day cultures. It could be observed that cell size declined after being cultured under N-limitation for two weeks, which can be derived from the fact that the dotted lines do not intersect the middle of the FC clouds at day 15. The average cell size has shifted to the left on the FSC-axis, i.e. cells became smaller.



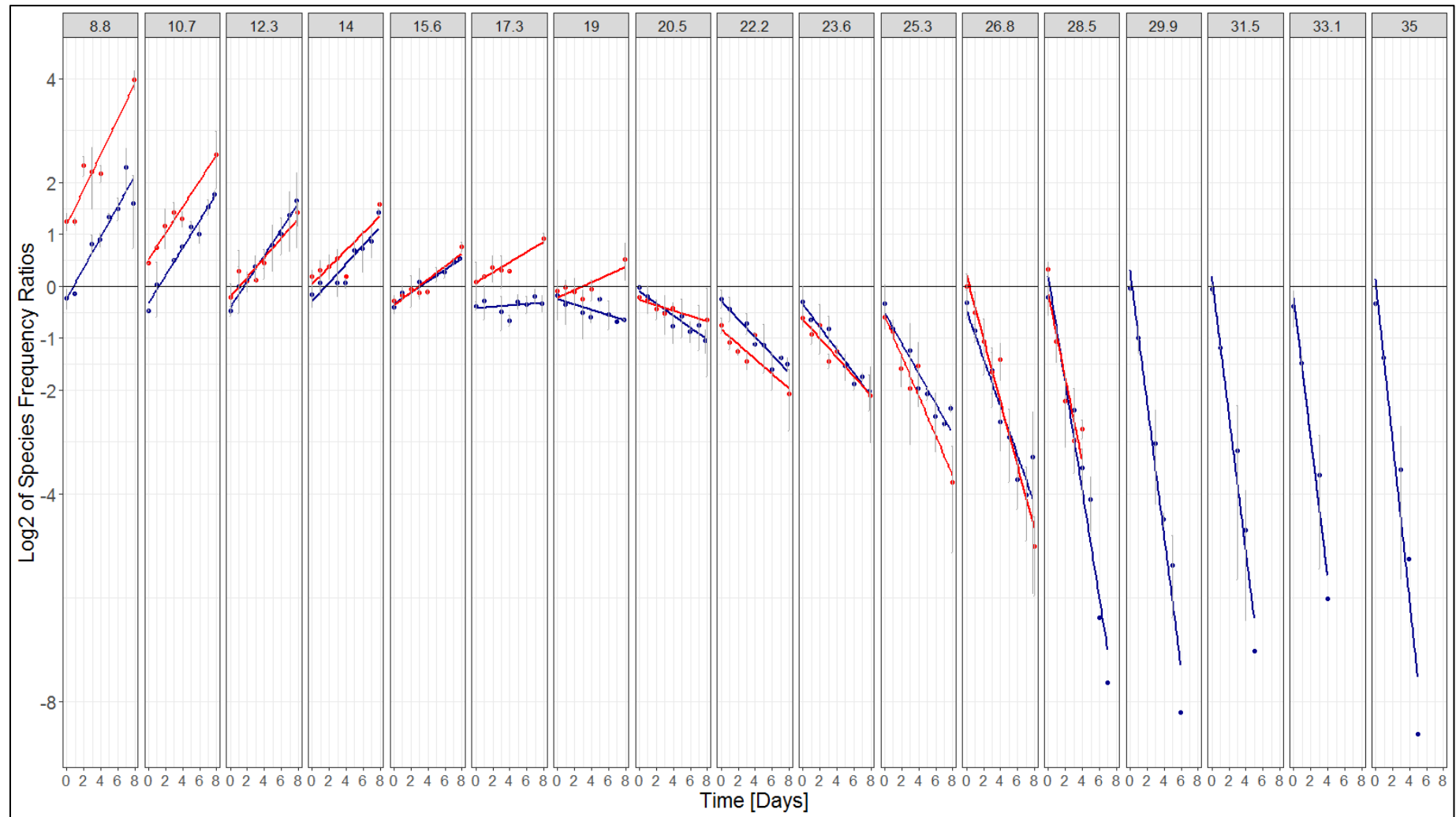
Supplementary Figure 4.9: Mean slopes of $\ln(F_0)$ across temperatures for *P. tricornutum* ($n = 2$) and *T. pseudonana* ($n = 2$) during the first four days of the low N scenario. Single replicate slopes were used to calculate the acute exponential growth response across temperatures, to which a daily growth rate of 0.22 d^{-1} was added to account for the daily dilution rates. Single growth replicate rates can be seen in Fig. 5.2 B. Grey error bars denote 1 standard deviation.



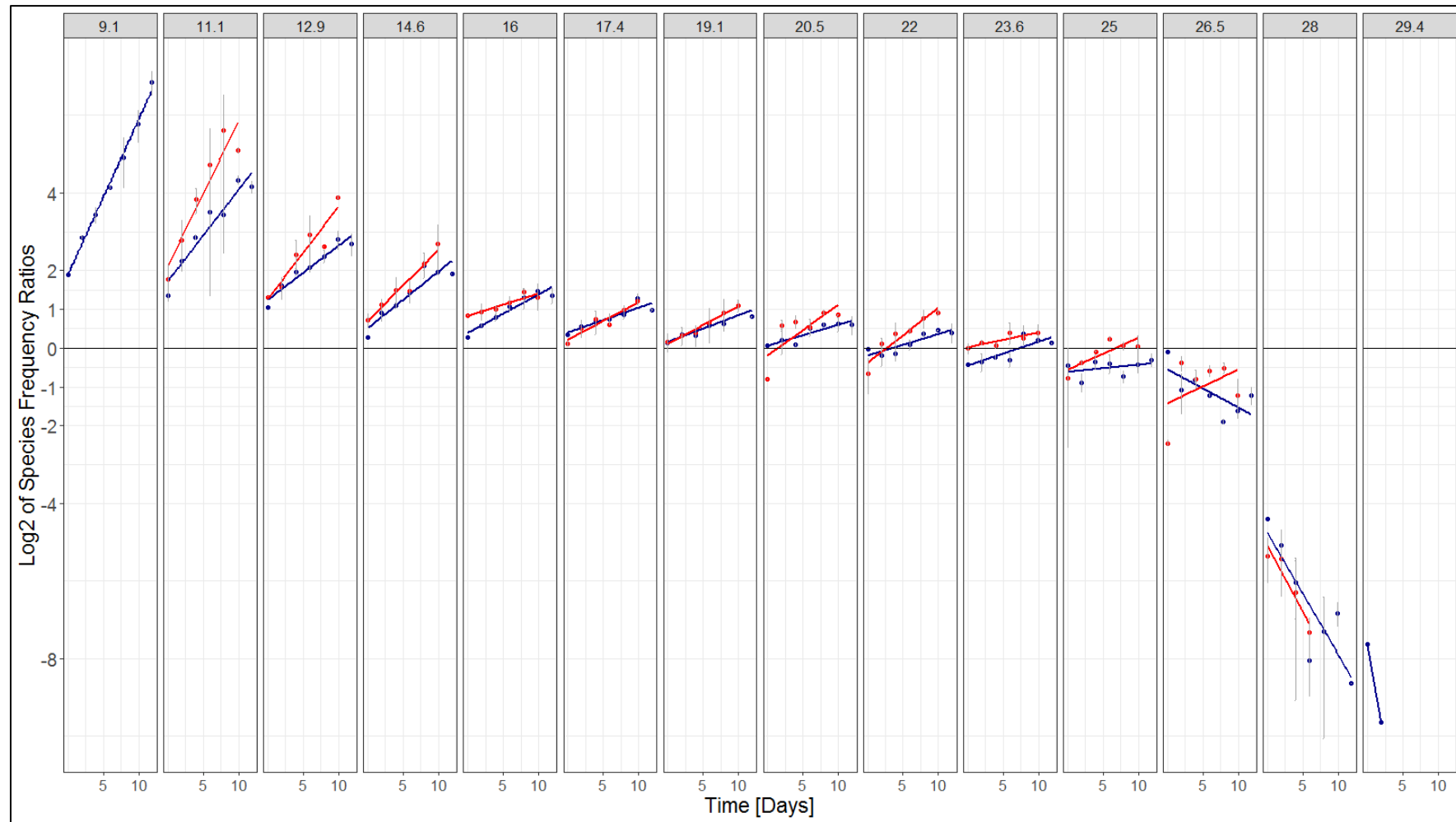
Supplementary Figure 4.10: Average ($n = 2$) cells per ml across all assay temperatures for *P. tricornutum* and *T. pseudonana* in low N medium. Flow cytometry counts were taken for monocultures in the first 14 days of the experiment before mixing cultures together to start competition experiments. Grey error bars denote standard deviation from two replicates. Dashed line in each facet panel is the average carrying capacity for each monoculture growth duplicate from day 5 onwards across assay temperatures.



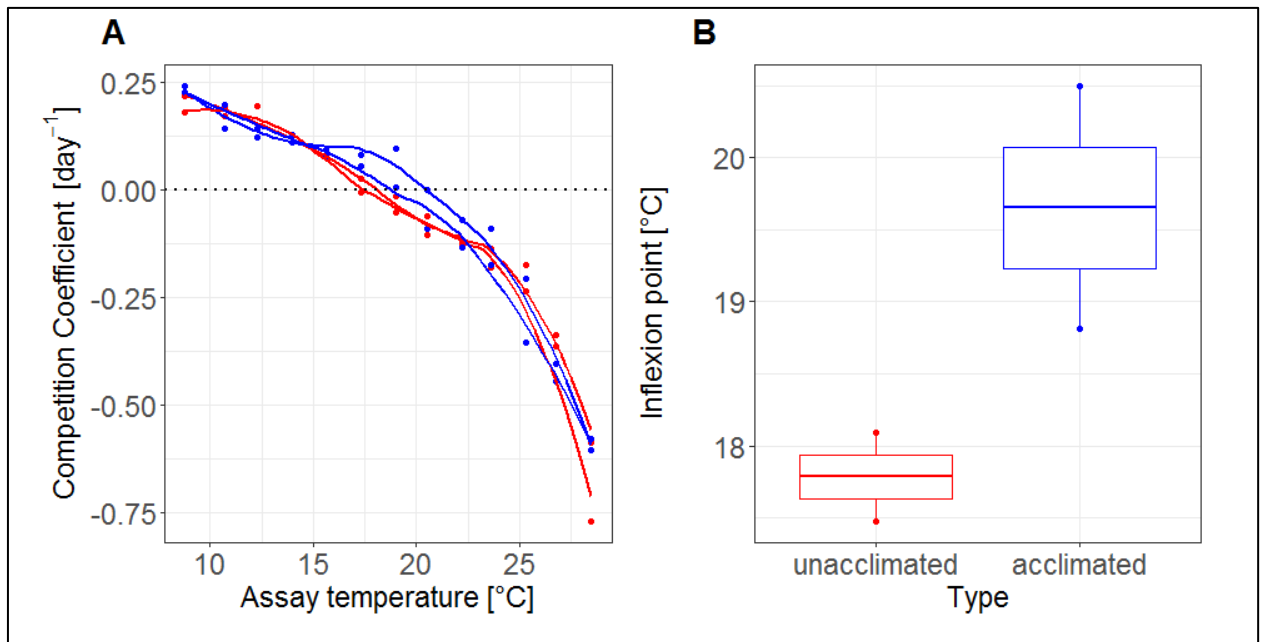
Supplementary Figure 4.11: All AIC values across models from the models fits of high N growth rates (blue symbols), low N growth rates (green symbols), and low N carrying capacities (red symbols) across temperatures for (A) *P. tricornutum* and (B) *T. pseudonana*. AIC scores for *T. pseudonana* replicate 2 are excluded as it was not taken into consideration for the final data analysis.



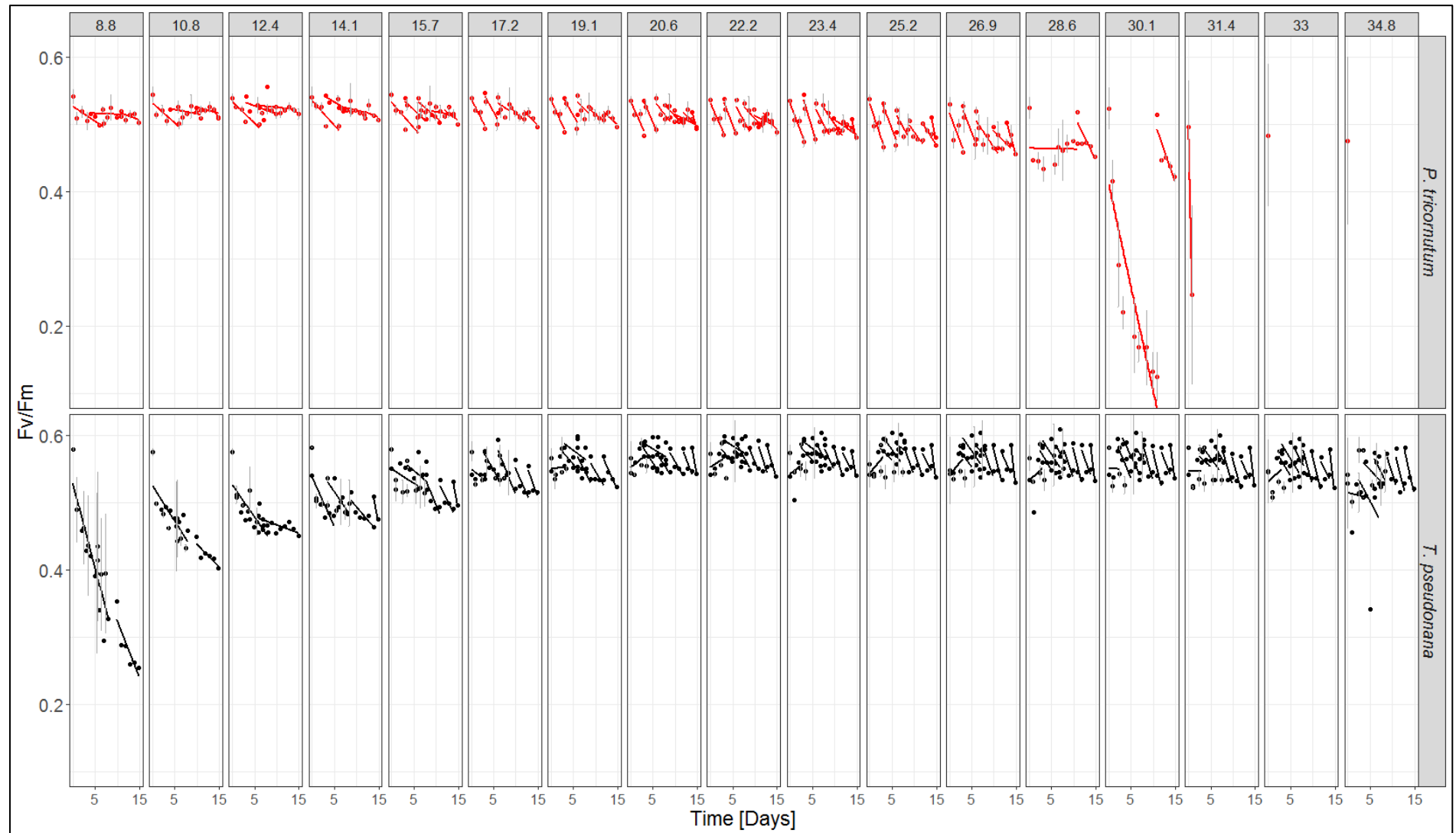
Supplementary Figure 4.12: Log_2 over time *P. tricornutum*-to-*T. pseudonana* cell abundance ratio in high N mixed cultures. Blue lines are the first 2 competition replicates that were started directly at the beginning of the experiment. Red lines are the temperature acclimated competition replicates that were started after the first competition was completed.



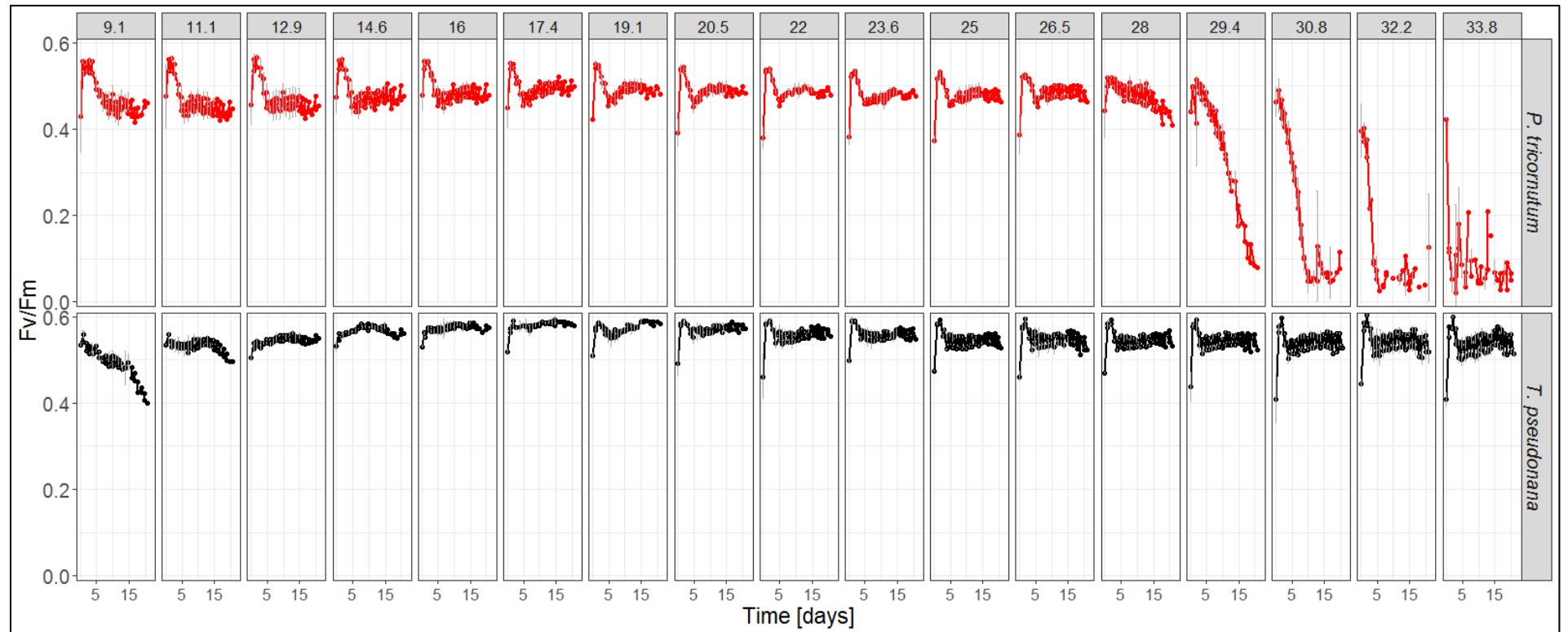
Supplementary Figure 4.13: \log_2 over time of the *P. tricornutum*-to-*T. pseudonana* cell abundance ratio in low N mixed cultures. Blue lines are the first 2 competition replicates that were started two weeks after growing monocultures in N-limited conditions. Red lines are competition replicates that were started after the first competition was completed and monocultures had been starved for nitrate even longer.



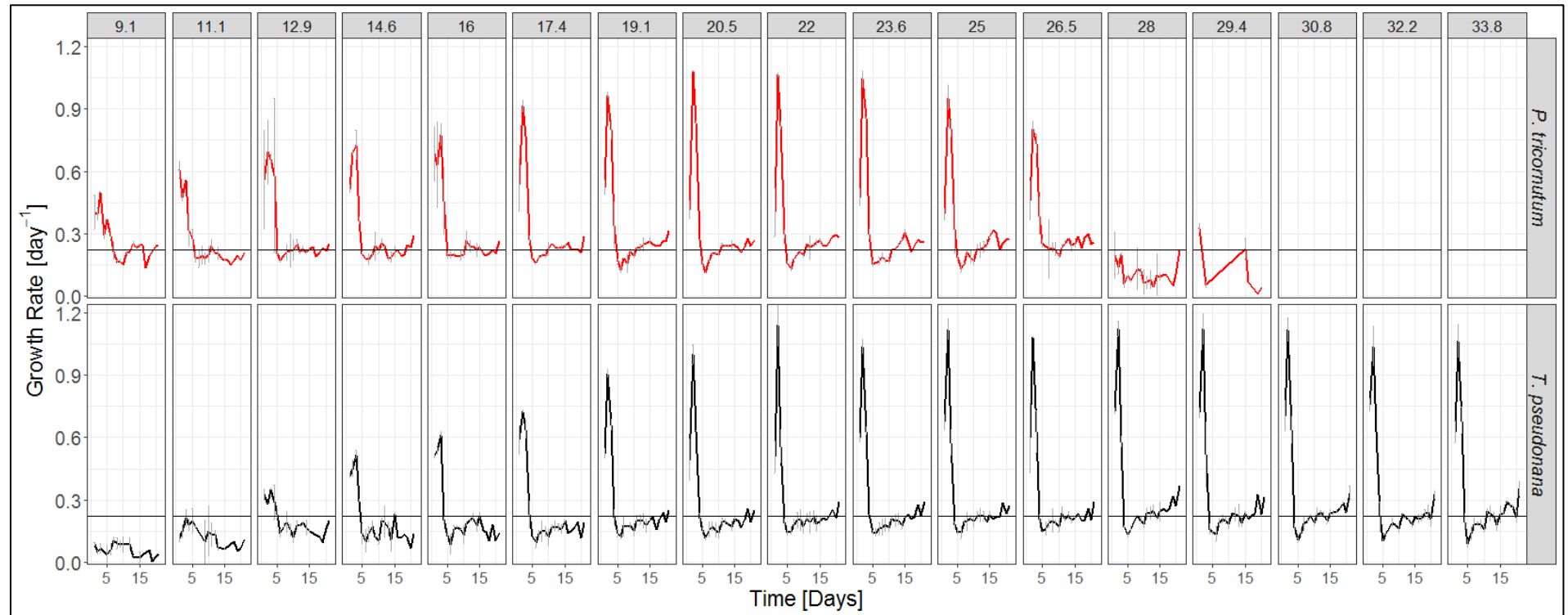
Supplementary Figure 4.14: (A) LOESS fits of single competition replicates across temperatures on competition coefficients from observed changes in species frequency ratios (Supplementary Figure 5.7). (B) Average temperatures ($n = 2$) of unacclimated and acclimated inflexion points of competitive advantage. The ANOVA output test for a significant difference between the two groups can be found in Supplementary Table 5.5.



Supplementary Figure 4.15: Average F_v/F_m values of exponentially growing *P. tricornutum* ($n = 4$) (red) and *T. pseudonana* ($n = 3$) (black) measured in the high N medium at the indicated assay temperatures across the temperature gradient. Grey error bars denote 1 standard deviation.



Supplementary Figure 4.16: Average ($n = 2$) F_v/F_m in low N monocultures across all assay temperatures over time for *P. tricornutum* and *T. pseudonana*. Grey error bars denote standard deviation from two replicates.



Supplementary Figure 4.17: Average ($n = 2$) daily growth rate in the low N medium calculated from daily changes of F_0 (pre-dilution on day t divided by post-dilution on day $t-1$) in monocultures across all assay temperatures over time for *P. tricornutum* and *T. pseudonana*. Grey error bars denote standard deviation from two replicates. At temperatures above 30°C , *P. tricornutum*, did not grow, so that panels were left blank. The line parallel to the time axis at a growth rate of 0.22 d^{-1} is the dilution rate: growth rate equals dilution rate when cultures are in N-limited steady state.

Chapter 5: Influence of Temperature Fluctuations on the Stable Coexistence of Two Common Phytoplankton Species

5.1 Abstract

Environmental variability is a common feature of all natural systems and continuously influences members of biotic communities. As many responses of species across environmental gradients are not linear, there is no reason to assume that their interactions with other community members would be. Outcomes of competition between species in a variable environment can therefore not be presumed to be the average of species interactions determined in stable conditions. Stable mixed cultures of the laboratory model organisms *Phaeodactylum tricornutum* and *Thalassiosira pseudonana* in high N and low N conditions were exposed to 17 uniform temperature fluctuations with amplitudes between 2.8 °C and 22.8 °C around the temperature of coexistence (18.6 °C in high N medium and 25.2 °C in low N medium), to investigate whether coexistence could persist in a variable environment. The results showed that although the mean temperature of all treatments was the same within a specified nutrient regime, continued stable coexistence was rarely observed. Nutrient conditions of the growth medium also changed how the two species competed under a fluctuating thermal environment. More knowledge on how environmental variations of different magnitudes influence community dynamics will help to improve predictions for ecosystems in general, but also allow to understand how future predicted climate variability will affect phytoplankton communities.

5.2 Introduction

5.2.1 Jensen's Inequality & Scale Transition Theory

In ecological studies, rates are often calculated for an average response of an organism or system in the average environment where they occur. This assumption poses a problem however, as ecological performance across temperature gradients is rarely linear and the average of two rates does not equate to the rate that would be encountered in the average environment. The mathematical generalisation of this phenomenon has been coined Jensen's inequality (Denny, 2017), named after Danish mathematician Johan Jensen who provided proof of this case in 1906 based on convex functions.

The extension of Jensen's inequality to ecology and ecophysiology has been termed scale transition theory (Chesson et al., 2005; Dowd et al., 2015), which predicts that the performance of a species in a fluctuating environment is not the average of the performances in constant environments (Fig. 6.1), necessitating that an additional correction term needs to be added or subtracted from the average performance to quantify the actual response in a variable environment (Koussoroplis et al., 2017).

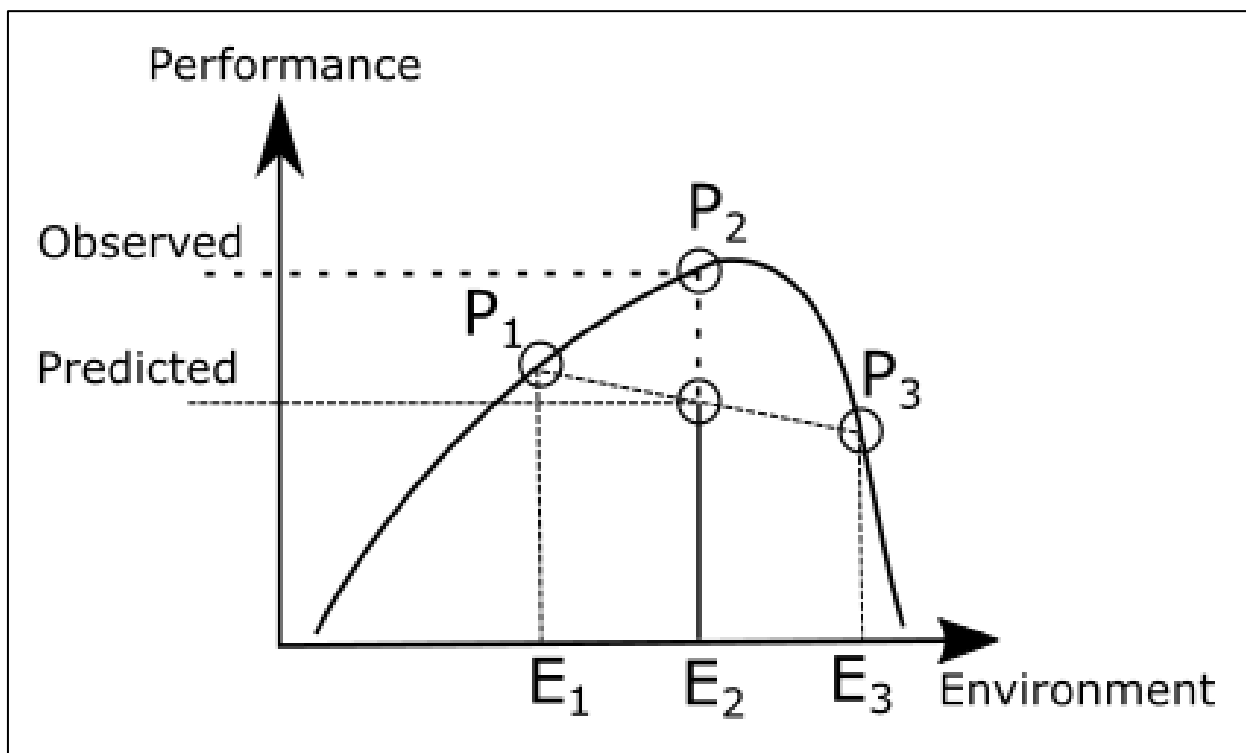


Figure 5.1: Schematic illustration for Jensen's inequality / scale transition theory on a hypothetical environmental performance curve. When performance across an environmental gradient is non-linear, performance P_2 at the average environment E_2 , is not going to be the average value of performances P_1 at environment E_1 and P_3 at environment E_3 .

Although individuals of any natural population encounter abiotic fluctuations during their lifetime, the outcomes of species interactions and competition are often predicted based on measurements conducted under stable laboratory conditions (Dowd et al., 2015). These predictions do not take into account the potential effects that fluctuations in abiotic parameters could have on the shape of the TPC of an organism (Bernhardt et al., 2018). Such assumptions are currently necessary due to a lack of better knowledge on how thermal performance of single organisms change across a parameter's range when the environment is not stable (Bernhardt et al., 2018). Changes in TPCs and the predictions that we make based on them would however determine conclusions on how species compete against each other. As climate variability is predicted to increase globally (Romero et al., 2018), it will therefore be crucial to further the understanding of variation, as environmental fluctuations have been

suggested as a major mechanism that affect the structure of natural communities and allow for high species diversity (Chattopadhyay, 2007; Descamps-Julien and Gonzalez, 2005; Sommer, 1984).

Environmental variability could provide temporal and spatial refuges for species to recover from adverse conditions and ensure that environmental stresses are distributed across all species within a system. This would provide enough room for more species to thrive side by side than predicted by traditional competition theory. Variability in fluctuating environments could enable populations of single species to temporally outgrow a competitor while favoured by a temperature fluctuation, creating enough population buffer to prevail once conditions become disadvantageous (Chesson, 2000). This proposed “storage effect” has been suggested as one of the reasons for high species diversity persisting in natural populations (Chesson, 2000).

5.2.2 Phytoplankton in Fluctuating Thermal Environments

In aquatic systems, temperature changes can occur within the duration of a few minutes depending on irradiation and mixing of water column, between day and night, throughout seasons, but may also constitute extreme events (Dowd et al., 2015; Kling et al., 2020; Lawson et al., 2015). Especially in lakes, environmental fluctuations can have crucial impacts on the functioning of the ecosystem (Rasconi et al., 2017; Woolway et al., 2016). The smaller the lake, the more intense will the daily temperature range fluctuation be (up to 15 °C temperature range in a single day), demanding high physiological flexibility of the organisms contained within (Woolway et al., 2016). In marine systems it is the very upper layer of sea surface water that is affected by fluctuations the most, whereas the effects become more buffered as depth increases (Shenoi et al., 2009). Apart from fluctuations in natural systems, open pond mass

algal culturing systems like raceway ponds or cascading raceways can also be prone to very high variability, as the culturing depth is usually quite shallow (< 30 cm deep) to allow light to penetrate all the way through the culture (James and Boriah, 2010; Ras et al., 2013). For phytoplankton, it has been empirically shown that growth rate at a given average temperature can vary substantially between populations grown under stable and those grown under fluctuating temperatures (Bernhardt et al., 2018; Wang et al., 2019), which is why the effects of thermal fluctuations need to be closer examined to be able to make more accurate predictions on their population dynamics.

Natural algae communities commonly display high diversity with often more than 30 species coexisting (Sommer, 1984). This is in stark contrast to traditional competition theory based on the resource-ratio hypothesis, which explains diversity in terms of competition for resources, and predicts that the number of species in a system should be equal to the number of their limiting resources. This contradiction has been coined Hutchinson's "Paradox of the plankton" (Hutchinson, 1961). Early theoretical and modelling approaches (Grenney et al., 1973), but also experiments with fluctuating nutrient levels (Sommer, 1984), concluded that continued coexistence of multiple species is not only possible through being limited by different nutrients, but through variability and temporal changes in nutrient supply. Even Hutchinson presumed that environmental variability could be the solution to his paradox (Hutchinson, 1961).

Like the relationship between growth rate and temperature, which depends not only on the average temperature, but also on the temperature range and the frequency distribution of temperatures within that range (Bernhardt et al. 2018), the outcomes of competition between species can be expected to be influenced by temperature variability as well. Despite the potential importance of this issue for global nutrient cycles, food web structures, and overall

ecosystem dynamics, experimental evidence of phytoplankton interacting in a fluctuating environment is scarce. The effect of temperature fluctuations on species interactions and competition in phytoplankton has, to our knowledge, only been investigated once experimentally (Descamps-Julien and Gonzalez, 2005). The study showed that two diatoms limited by one resource (Si) led to competitive exclusion in a stable thermal environment, but that they could coexist when temperature fluctuated.

In the previous chapter, the investigation of competition across a temperature gradient between *P. tricornutum* and *T. pseudonana* revealed that the two diatoms could coexist at 18.8 ± 1.2 °C in nutrient replete high N conditions, and at 25.3 ± 0.6 °C in low N conditions. The present study investigated how thermal variability around the temperature of stable coexistence affected competition between *P. tricornutum* and *T. pseudonana* under both high N and low N growth conditions. As growth rates around these cardinal temperatures do not change linearly and differ amongst these two species, uniform fluctuations around these temperatures will not necessarily lead to a response that ensures stable coexistence at the same average temperature in a fluctuating environment. Here, we asked whether uniform fluctuations with varying amplitudes around the temperature of stable coexistence would disrupt the long-term coexistence of these two species, and if stability would re-occur after the temperature was re-stabilized. In this context, stable coexistence was considered to be achieved when the relative abundances of the two species showed no statistically significant trend with time (Descamps-Julien and Gonzalez, 2005). In addition, we also wanted to investigate whether the starting species abundance ratios (i) would have an influence on the stable coexistence of the two species at the two aforementioned equilibrium temperatures, and (ii) whether competition between the two species would pan out differently depending on the species starting ratios. As mentioned in the introduction chapter of this thesis, abundance

and frequency of initial community members were found to play a role in determining final community structure in communities taken from a natural environment (Sommer, 1983). We therefore wanted to investigate whether this would also be the case in a relatively simplified and controlled system as ours. In order to explore this, mixed cultures had starting species ratios of 1:2, 1:1, and 2:1 (*P. tricornutum* : *T. pseudonana*), and changes in species frequencies over time were recorded.

5.3 Material and Methods

Stock cultures of *P. tricornutum* (CCMP 2561) and *T. pseudonana* (CCMP 1335) were maintained in the University of Essex algal culture collection at 15 to 16 °C, in f/2 medium (Guillard and Ryther, 1962) prepared in artificial sea water (Berges et al., 2001; Harrison et al., 1980), and grown on a 12:12 hour light and dark cycle at a photosynthetic photon flux density (PPFD) of about $60 \mu\text{mol m}^{-2} \text{s}^{-1}$. Stock cultures were transferred once a month as 1:36 dilutions. Cultures were acclimated to exponential growth in full f/2 medium for two weeks prior to the experiments conducted at high N. Similarly, for the low N experiment, cultures were acclimated for two weeks in f/2 medium with reduced N (final concentration 55 μM in comparison to 882 μM in full f/2). To assure exponential growth in the high N scenario, cultures were maintained at densities of $<500,000 \text{ cells ml}^{-1}$ for *P. tricornutum* and $<250,000 \text{ cells ml}^{-1}$ for *T. pseudonana* (equivalent to about 5 % of each species' carrying capacity).

In vivo chlorophyll *a* minimum fluorescence (F_0), used as a proxy for biomass, and the ratio of variable to maximum fluorescence (F_v/F_m), used as a proxy for photosynthetic efficiency, were measured daily via fast repetition rate fluorometry (FRRf) with a FastTracka II fluorometer and Fast Act laboratory system (both CTG Ltd, West Molesey, UK) (Supplementary Figures 5.1 – 5.4).

Photosynthetic efficiency was calculated via the formula $(F_m - F_0)/F_m$ (F_m = maximum fluorescence yield) by the FastPro software (version 1.0.55) used to attain and record FRRf measurements. Peak excitation was at 435 nm and fluorescence emission measured at 680 nm (with a 25 nm bandwidth). The measuring protocol was set to 24 sequences per acquisition with a 100 ms sequence interval and a 20 s acquisition pitch. Measurements were taken on cells that were dark acclimated for 30 minutes at their assay temperature in order to record F_0 when all reaction centres of PSII were open, and profiles of fluorescence emission were fitted within the Fast Pro 8 software (version 1.0.55) (Chelsea Technologies, UK).

5.3.1 Competition Experiments

5.3.1.1 High N competition experiment

For the high N scenario, 34 assay monocultures (each with a total volume of 5 mL) of each species were incubated in a tube-based temperature-gradient-thermoblock at 18.6 °C and $150 \pm 15 \mu\text{mol m}^{-2} \text{s}^{-1}$ PPFD to acclimate the algae to the assay conditions. This temperature was determined in pre-experiments to facilitate coexistence in a stable equilibrium under high N conditions.

After two days of acclimation in the temperature-gradient-thermoblock, the monocultures of *P. tricornutum* and *T. pseudonana* were mixed together. In order to investigate the influence of starting species ratios on the progression of competition, the species were mixed together at 1:1 (n=24), 1:2 (n=24), or 2:1 (n=20) relative cell abundance ratios. All mixed cultures were kept in exponential growth by re-diluting when necessary. As defined above for monocultures, this was the case when a fluorescence signal equal to about 5% of the carrying capacity was reached, in this case for the mixed population.

These mixed cultures were sampled every day for 10 days for assessing cell abundance ratios at 18.6 °C to ensure stable coexistence. Each day after FRRf measurements of F_0 and F_v/F_m , 200 μ L aliquots were extracted and stored in 96-well plates and fixed in 1%-Lugol's solution for cell ratio counts. In order to maintain a constant culture volume, the 200 μ L volume removed from each culture was replenished with the same volume of fresh f/2 medium. Ratio counts were carried out with an Olympus inverted microscope at 200x magnification. 400 cells were counted from each fixed sample to calculate a *P. tricornutum* : *T. pseudonana* cell abundance ratio.

On the 11th day of the experiment, temperature fluctuations were started. Fluctuations to high temperature were imposed by heating one end of the temperature-gradient-thermoblock, whilst the other was unchanged creating a thermal gradient of 20.0 °C to 30.0 °C. After 24 hours, the end of the thermoblock that had been heated the previous day was cooled, creating a gradient in the block of 17.2 °C to 7.2 °C. Half of the cultures were subjected to temperature fluctuations beginning on the first "hot" day, whilst the other half were subjected to temperature fluctuations starting one day later on the first "cold" day. The latter were transferred to a water bath that was also set to 18.6 °C and $150 \pm 15 \mu\text{mol m}^{-2} \text{sec}^{-1}$ PPFD for one day before being re-introduced to the temperature-gradient-thermoblock and exposed to the temperature fluctuations.

After 10 up and 10 down fluctuations (20 days), temperature was re-stabilized at 18.6 °C for an additional 10 days to investigate how species abundance ratios progressed after a prolonged period of thermal variability. The mixed cultures that started on the warm fluctuation were transferred to the external water bath so that the cultures that started on the cold period, could be exposed to a last 10th warm period. The next day all cultures were put in the temperature-gradient-thermoblock at 18.6 °C. A schematic representation of the chronology of

the experiment can be seen in Figure 5.2, in which the three distinct experimental phases described above are represented.

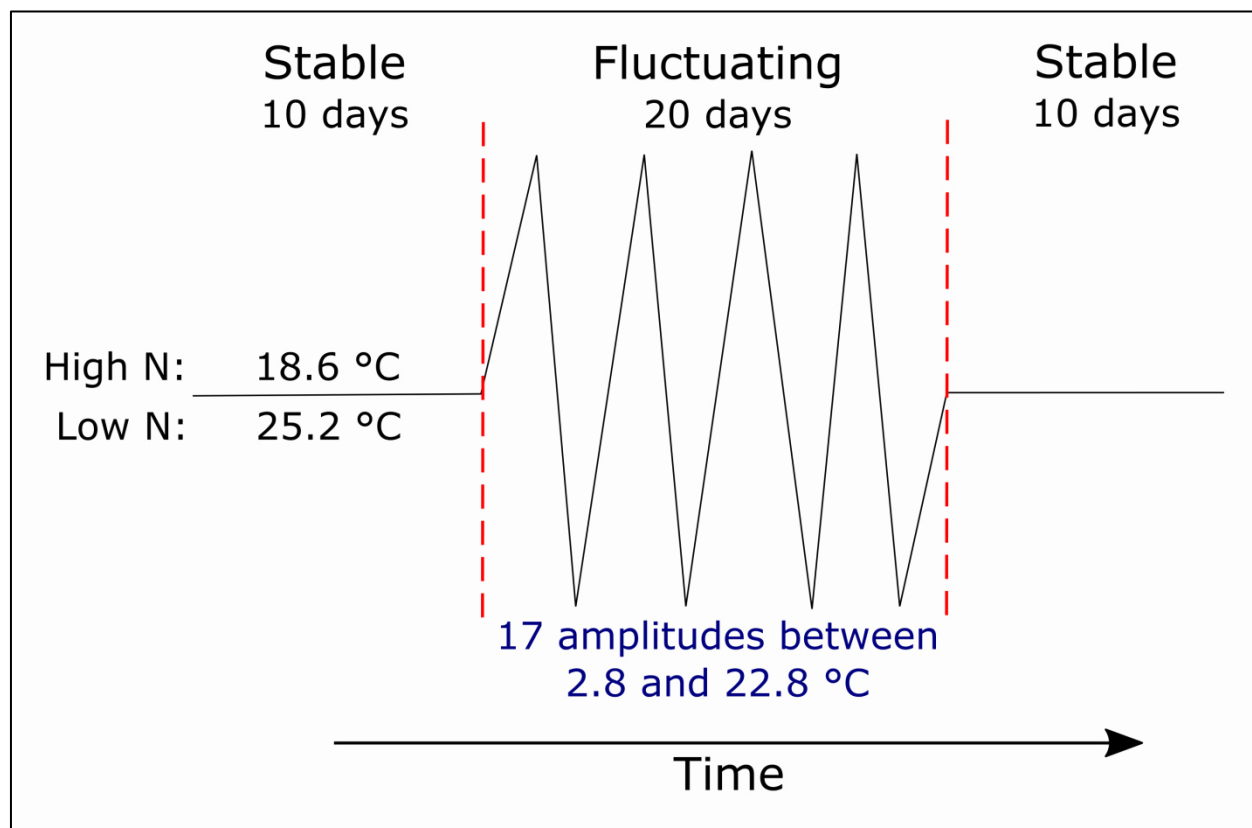


Figure 5.2: Schematic timeline of the fluctuation experiments. The chronological set-up was the same for the high N and low N experiment. The only aspect that differed between the two experiments was the temperature at which both species could coexist, which was found to be 18.6 °C under high N conditions, and 25.2 °C under low N conditions. The experiments started off with a 10 day period during which *P. tricornutum* and *T. pseudonana* were cultured as mixed populations. This period was used to determine whether the two species could coexist and whether mixed populations could be considered as stable over time in regards to their species abundance ratios. After this initial period, temperature was fluctuated for 20 days (10 up and 10 down fluctuations). Temperature was changed every 24 hours. After the fluctuation period, temperature was re-stabilised for another 10 days to investigate whether the species abundance ratio at the end of the fluctuation period would remain stable.

5.3.1.2 Low N competition experiment

Under low N conditions, a temperature of 25.2 °C and $150 \pm 15 \mu\text{mol m}^{-2} \text{sec}^{-1}$ PPFD was determined by pre-experiments to be the temperature of stable-coexistence. 34 monocultures of *P. tricornutum* and 34 of *T. pseudonana* were transferred from their stock cultures to assay tubes and cultured at 25.2°C until the onset of N-depletion. 20% of the culture medium were removed daily for monitoring N-drawdown. The removed medium was replenished with fresh low N f/2 medium. In contrast to the high N sampling schedule, cultures were not diluted after reaching a certain F_0 value to allow them to grow until reaching N-limited stationary growth phase. The onset of N-depletion was determined via FRRf as the point at which the fluorescence signal (F_0) did not increase between two consecutive days. At that point, the sum of nitrate plus nitrite (NO_x) was below the detection limit of 0.5 μM in samples from all monocultures, confirming N-depletion (Schnetger and Lehnert, 2014). Once N-depletion was confirmed, which was the case after 4 culturing days, mixed cultures were established. Like in the high N mixed populations, the monocultures were mixed together so that starting species ratios were either 1:1 (n=24), 2:1 (n=24) or 1:2 (n=20) *P. tricornutum* : *T. pseudonana* for a total assay volume of 4.0 ml, which was then topped up with 1.0 ml of low N f/2 medium to a volume of 5.0 ml to not break with the daily sampling routine.

To not break with the low N culturing regime, mixed cultures were then grown semi-continuously by removing 1.0 ml daily after FRRf measurements were made, and replenishing with 1.0 ml of low N medium to maintain an assay volume of 5.0 ml. This imposed a daily growth rate of $\ln(5/4) = 0.22 \text{ d}^{-1}$. From the removed 1 ml sample volume, 200 μL subsamples were then fixed in 1%-Lugol's solution for cell counts.

Like in the high N competition, cultures were kept at the temperature of stable coexistence for 10 days. After 10 days, temperature fluctuations were imposed for 20 days, with the mean being set at 25.2 °C, but the amplitudes of the fluctuations being equal to the ones from the high N conditions (17 fluctuation amplitudes ranging between 2.8 °C and 22.8 °C). After 10 up and down fluctuations, temperature was once again stabilised at 25.2 °C for 10 days. In terms of experimental progression over time, the low N experiment had the exact same set-up as the high N experiment (Figure 5.2), so that the two nutrient scenarios could be compared.

5.3.2 Competition Coefficients

5.3.2.1 Predictions of competition

The growth rates (r) measured in stable thermal environments across a temperature gradient from 8.8 to 35 °C (see Chapter 4) were used to calculate predicted competition coefficients for the high N experiment in the fluctuating thermal regimes. The predicted competition coefficient of a “fluctuation temperature pair”, for instance 17.2 °C and 20.0 °C (1.4 °C down and 1.4°C up from the temperature of stable coexistence which was 18.6 °C in high N conditions), was calculated with equation [1a]. This calculation assumes that the predicted growth rate is the average of the growth rates at the two temperature extremes, and that the step changes in temperature between these two limits was instantaneous; as such, it follows Jensen’s inequality (see Figure 5.1) and conforms to the non-linear averaging used by Bernhardt et al. (2018).

$$\text{Predicted competition coefficient } (A) = \left(\frac{r_1(T_1) + r_1(T_2)}{2} \right) - \left(\frac{r_2(T_1) + r_2(T_2)}{2} \right) \quad [1a]$$

where A is the fluctuation amplitude, r_1 and r_2 are the growth rates of species 1 and 2, at the coldest (T_1) and the warmest (T_2) assay temperatures of the fluctuation amplitude between

which temperature was fluctuated. If species 1 would have a higher average growth rate than species 2, species 1 would be predicted to be the winner of the competition scenario. As a consequence, the predicted competition coefficient would turn out to be a positive value. If however species 2 would have a higher average growth rate, it would be predicted to win the competition. In that case the greater average growth rate of species 2 would be subtracted from the smaller average growth rate of species 1, rendering the predicted competition coefficient negative. Therefore, both positive and negative values of competition coefficients can occur. The algebraic sign in front of the competition coefficient indicates the winning species. In this study, *P. tricornutum* was determined to be species 1, whereas *T. pseudonana* was species 2, meaning that every time the predicted competition turned out to be positive, *P. tricornutum* was predicted to win, and if it would turn out negative, it was predicted to lose.

For the low N experiment, predicted competition coefficients were calculated from both the initial exponential growth rates (r) and N-limited carry capacities (K) measured in stable thermal environments across a temperature gradient (Chapter 4), using equations [1a] and [1b] respectively.

$$\text{Predicted competition coefficient } (A) = \left(\frac{K_1(T_1) + K_1(T_2)}{2} \right) - \left(\frac{K_2(T_1) + K_2(T_2)}{2} \right) \quad [1b]$$

Where A is once again the fluctuation amplitude, K_1 and K_2 are the carrying capacities of species 1 and 2, and T_1 and T_2 are the coldest and warmest assay temperatures of the fluctuation amplitude.

Predictions of competition coefficients under high N and low N conditions could only be made in a fluctuation amplitude range for which the fluctuations did not exceed the lethal temperature for *P. tricornutum* or *T. pseudonana*, as we did not calculate death rates. Growth

rates reaching the lethal range of a species would all be set to $r = 0$ regardless of investigated assay temperature and predictions could not be calculated as averages between a lethal and a non-lethal temperature.

5.3.2.2 Observed Competition

Observed competition coefficients in the high N and low N scenarios were determined with equation [2] by calculating the slope of the change in species frequency ratios of *P. tricornutum* : *T. pseudonana* over time.

$$\text{Competition coefficient} = \frac{\ln\left(\frac{N_{P. tricornutum}:N_{T. pseudonana}(t)}{N_{P. tricornutum}:N_{T. pseudonana}(0)}\right)}{t} \quad [2]$$

Where N = species abundance, and t = time.

As was the case for the predicted competition coefficients, negative and positive values of competition coefficients were indicating the winning species. If the relative abundance of *P. tricornutum* was increasing over time in mixed cultures, the resulting slope in equation [2] would be positive, indicating that it would win. If its relative abundance in comparison to *T. pseudonana* would decline, the slope would turn out to be negative and so would the resulting competition coefficient. In that case *P. tricornutum* would lose the competition.

All calculations of linear models to determine stability of mixed cultures, predicted and observed competition coefficients, as well as the visualisation of species progressions in mixed populations, were carried out with the statistical software R (R Core Team, 2016).

5.4 Results

5.4.1 Pre-fluctuation period

According to our definition of stability, all mixed cultures, except one in the low N set up, were found to be stable in their abundance ratios over time in both nutrient scenarios during the 10 day pre-fluctuation period. Starting species abundance ratios did not have an effect on stability, mixed populations remained stable throughout the pre-fluctuation period regardless of whether the initial species ratios were 1:2, 1:1, or 2:1 (*P. tricornutum* : *T. pseudonana*) (Supplementary Figures 5.5 & 5.6).

5.4.2 Fluctuation period

When temperature fluctuations were imposed on the high N mixed cultures, most cultures at fluctuation amplitudes below 6.2 °C were considered stable according to our definition (i.e. mixed cultures with no significant change in their species frequency ratio). Overall, stable coexistence was observed at fluctuation amplitudes up to 14.4 °C (Fig. 5.3A). However, most cultures at amplitudes of 6.2 °C or higher displayed a significant trend in change of species frequency ratios and cultures that did not change significantly were not the norm once fluctuation amplitudes reached 6.2 °C or more, as most (9 out of 12 mixed populations between fluctuation amplitudes of 6.2 °C and 14.4 °C) were showing significant trends in the change in species abundance ratios over time. Above 14.4 °C all mixed cultures displayed a significant trend (Supplementary Figure 5.7). In general, the larger the fluctuation amplitude, the more did the competitive ability of *P. tricornutum* decline (Fig. 5.3A).

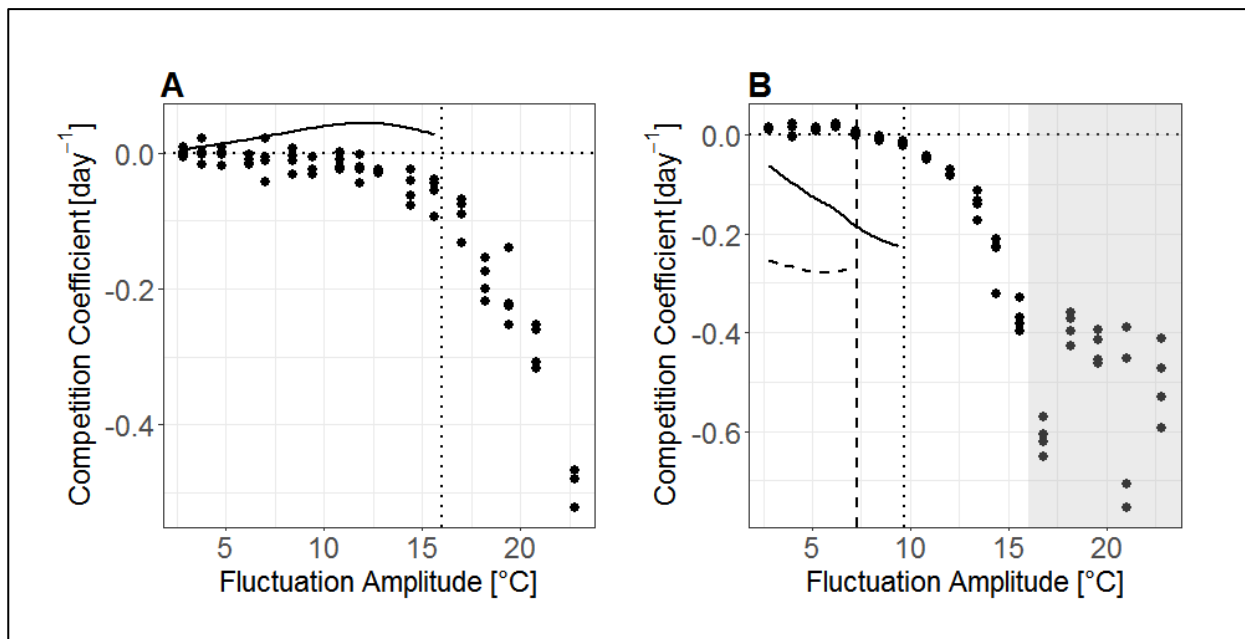


Figure 5.3: Predicted (lines) and observed (symbols) competition coefficients across fluctuation amplitudes in high N conditions (A) and low N conditions (B). Depending on which species would be predicted to win or would actually win, based on equations [1] and [2], competition coefficients could take on positive or negative values. Positive values would indicate *P. tricornutum* as the winning species, negative values would indicate *T. pseudonana* as the winning species. In (A), solid line is a locally estimated scatter plot smoothing (LOESS) line, and indicates predictions for competition coefficients calculated from monoculture growth rates with equation [1a]. Symbols are the observed competition coefficients calculated with equation [2]. Vertical dotted line distinguishes fluctuation amplitudes for which temperatures did not drop below a lethal cold temperature for *T. pseudonana* on the cold cycles from those that did (determined based on monoculture TPCs). In (B), solid LOESS line indicates predictions made from exponential phase of growth in low N medium, dashed LOESS line indicates predictions made from carrying capacities. Predictions were made with equations [1a] and [1b] respectively. Symbols indicate the observed competition coefficients in a fluctuating environment in low N medium calculated with equation [2]. Vertical dotted line in (B) separates fluctuation amplitudes that stayed below the critical lethal temperature determined from monoculture growth rates TPCs of *P. tricornutum* on the warm fluctuation days from those that did not, and dashed line indicates the same based on monoculture TPCs for carrying capacity, which indicated a lower CT_{max} . Grey shaded area indicates the region in which all *P. tricornutum* cells died after one 24-hour-cycle, based on Fv/Fm measurements of monocultures. In this fluctuation amplitude range only *T. pseudonana* was alive in mixed cultures after one day of fluctuations for the remainder of the competition experiment. Variations in competition coefficients in the grey-shaded area are therefore caused by manual counting error (see section 5.5.1 “Limitations of the study”). Note that although both scenarios (A) and (B) had the same assay fluctuation amplitudes, the mean temperatures from which fluctuations started were different, to account for the fact that the temperature at which the two diatoms could co-exist stably over time depended on the amount of N in the growth medium. In high N conditions, the midpoint of the fluctuations lay at 18.6 °C, in the low N scenario it was at 25.2 °C. Also note the difference in y-axis scale between (A) and (B).

Predictions of competition for the high N fluctuation temperatures from monoculture data did not align closely with the observed pattern. The predictions based on differences in the average growth rates of the two diatoms did predict competitive advantages for *P. tricornutum*, whereas such an advantage was never observed in the mixed cultures. This mismatch between prediction and observation results from the fact that the competition coefficients across a stable temperature gradient (see Fig. 4.6A in Chapter 4) had a steeper slope at temperatures below the coexistence temperature of 18.6 °C in the favour of *P. tricornutum*, than at higher temperatures in the favour of *T. pseudonana*. In the actual competition experiment however, the predicted competitive advantage was offset because presumably overall metabolic rates were reduced in cold conditions in comparison to warm conditions. Predictions of competition could only be made until fluctuation amplitudes of 15.6 °C, because temperature dropped below the cold end lethal temperature for *T. pseudonana* at higher fluctuation amplitudes.

In the low N scenario, a fluctuation amplitude of 8.4 °C evoked stable coexistence over time as 3 of the 4 competition replicates exposed to that fluctuation amplitude showed no significant trend in the species ratio (Fig. 5.3B, Supplementary Figure 5.8). At fluctuation amplitudes below 8.4 °C a general competitive advantage for *P. tricornutum* was observed, whereas at amplitudes larger than 8.4 °C the competition advantage increased strongly in *T. pseudonana*'s favour (symbols in Fig. 5.3B). Our predictions based on the initial exponential growth rate and carrying capacities in low N monocultures did not forecast a competitive advantage for *P. tricornutum* at any fluctuation amplitude (LOESS lines in Fig. 5.3B). As in the high N scenario, predictions of competition could only be made where both the cold and warm temperatures that fluctuations reached were in the non-lethal temperature range for both species, based on monoculture TPCs for growth and carrying capacities in low N medium. In the temperature range where

predictions could be made, the observed and predicted coefficients did not correlate well (Fig. 5.3B).

5.4.3 Post-fluctuation period

When the stable coexistence temperature was re-established after the fluctuation period in the high N scenario, 90% of all mixed cultures in which *P. tricornutum* had not been fully outcompeted (54 out of 60 remaining cultures) were found to be stable again in their species abundance ratios. Only six cultures showed a significant positive trend after fluctuations had ended (p-values ranging from $p=0.038$ to $p<0.001$), with competition coefficients in the range of 0.03 to 0.10 d^{-1} (Supplementary Figure 5.9).

After fluctuations in the low N scenario, 43 mixed cultures remained that still contained both species. Of these, 26 showed a significant trend in their frequency ratios over time and 17 were considered stable. Significant trends that were observed were largely in favour of *P. tricornutum* taking up a relative greater abundance in the species mix over time (Supplementary Figure 5.10).

5.5 Discussion

This study showed that the imposed thermal variability did not necessarily disrupt the stability of the coexistence between the two diatoms *P. tricornutum* and *T. pseudonana* and that the effect of temperature fluctuations was dependent on the concentration of inorganic N in the growth medium.

The stability of the species abundance ratios during the pre-fluctuation periods confirmed the findings of Chapter 4, and indicated that the science is replicable and reliable. The two diatoms

were indeed able to coexist stably at the determined coexistence temperatures in high N and low N conditions. The starting species abundance ratio did not appear to influence this observation at all. This should not come as a surprise under high N conditions, as the species grow at the same daily rate at 18.6 °C. Therefore regardless of the starting abundance, the ratio is expected to remain the same over time. Under low N conditions, this observation becomes a bit harder to explain. In the mixed cultures that did not have a 1:1 starting ratio, one would assume that the species with the lower starting abundance would increase in its abundance over time until the ratio reaches 1:1. This would be in accordance with Tilman's classical R* theory, which states that the superior competitor for a resource would outcompete the other species. In our case, the assay conditions were able to sustain both species stably in equal cell abundances, as was demonstrated through the stable low N mixed populations that started at 1:1. Therefore, one could expect the abundance of the species with greater starting numbers to decline, while the abundance of the species with smaller starting numbers would increase until the mixed population equilibrates at a 1:1 species ratio. The circumstance that this was not the case and stability was observed right from day 1 for mixed populations that did not start at a 1:1 species ratio, suggests that the N uptake rates of the species are of the same magnitude at the temperature of stable coexistence. Cells of both species supposedly take up the limiting nutrient at the same rate at 25.2 °C under our experimental conditions. To make this idea clearer, imagine two cells (one cell of each species) that are supplied with fresh nutrients after an addition of fresh medium. When both of the cells take up nutrients at the same rate, the resource is shared equally. Now imagine a starting population of three cells, with two cells of *P. tricornutum*, and one cell of *T. pseudonana*. Each individual cell of the three cells would still have the same uptake rate. The resource would be once again shared equally regardless of species identity. Neither species abundance would decline or increase. This presumed

explanation would also suggest that it is indeed N surge uptake rate, as suggested in Chapter 4, that determines competitive success under low N conditions. When temperatures are altered from the temperature of stable coexistence, N uptake rates between the two species would not be balanced anymore and one of two species would take up nitrogen quicker than the other. As a result thereof, we would see a change in species abundance ratios over time, based on R^* theory. The on average better nutrient competitor would be predicted to win. The results show the limitations of our predictions for nutrient-limited conditions. Under R^* theory, it is the concentration of the limiting nutrient relative to the half-saturation constant for growth that determines the outcome of competition under equilibrium conditions (Bestion et al., 2018a). However, we did not measure nutrient concentrations or half-saturation constants for growth, and as such could not make these predictions.

During the temperature fluctuation period in the high N scenario, continued coexistence over time was observed across temperature fluctuations up to 14.4 °C, but mainly up to fluctuations of 6.2 °C. The observed coexistence could possibly be attributed to the storage effect (Chesson, 2000). In Chapter 4 it was shown that *P. tricornutum* was a poor competitor against *T. pseudonana* at warm temperatures towards its physiological growth limit. However, *P. tricornutum* was able to persist longer in mixed cultures when adverse conditions alternated with more favourable low temperature conditions than when temperature was kept stable at unfavourably warm conditions. Fluctuations therefore created a “thermal refuge” during which abundances of the species favoured by the prevailing temperature could recover. In natural environments, fluctuations away from unfavourable conditions could provide a means to increase the length of time it takes to be outcompeted, potentially allowing a species’ population to be replenished via migration or mixing of the water column. Such fluctuations could also increase the time during which a superior competitor could potentially be preyed

upon or washed away. If the exclusion rate of one species is low and the immigration rate from an outer “source” environment is high, disadvantageous environmental conditions can be counterbalanced, as immigration increases spatial and temporal resilience (Gonzalez and Holt, 2002). This way it becomes possible that the ecological resilience of a diverse community of competitors can be fostered and high species diversity explained.

In low N conditions, such a potential storage effect was only observed at an intermediate fluctuation amplitude of 8.4 °C, whereas all other fluctuation amplitudes benefitted one of the two species. *P. tricornutum* having a competitive advantage over *T. pseudonana* in the low N experiment across the lowest fluctuation amplitudes could potentially be explained by its good nitrogen uptake abilities that rendered the N-concentration too low for *T. pseudonana* to grow well, regardless of the thermal environment. The fluctuation amplitude at which competitive advantage switched to *T. pseudonana* could indicate the point at which the effects of nutrient limitation and quicker nitrogen surge uptake rates which favoured *P. tricornutum* were offset by its physiological stresses imposed on this species during the warm periods of the fluctuation regime. We suggest that at high fluctuation amplitudes, *P. tricornutum* could not recover sufficiently from the thermal stress on cold fluctuation days due to lower overall growth rates.

The mismatch between predictions and observations of competition in both nutrient scenarios can potentially be explained by two factors. Firstly, a difference in physiological acclimation rates between the two species. Predictions were made on growth rates of acclimated cultures in a stable temperature environment and extrapolated to a variable environment. This approach did not account for acclimation to a new temperature on a daily basis, which could result in thermal performance of monocultures in a fluctuating environment differing from those in a stable environment, adding an error that was not accounted for in equations [1a] and

[1b]. Secondly, although the calculation of the average competition coefficient assumes an immediate temperature change between the high and the low point of the fluctuation amplitude, the temperature in the thermoblock did not change instantaneously when the temperature in the water baths changed. Instead it was a more gradual change as it took about one hour for the temperature block to warm or cool to the correct new temperature. Thus, for a short period of time the two species competed at intermediate temperatures between the two ends of the fluctuation amplitudes, which was also not accounted for in the predictions of competition using equations [1a] and [1b].

5.5.1 Limitations of the study

As the species could not be separated from each other during the time they were cultured together, it was impossible to assess the health of single species and how well each species coped with abiotic stress in mixed populations. Similar to Chapter 4, flow cytometry could unfortunately not be employed to distinguish between the two species in mixed populations as their gates would overlap due to similar size and fluorescence. It would however be interesting for future investigations to see if changes in the ratios between the two species could still be tracked reliably through the counts registered in the areas that did not overlap. Furthermore, it would be interesting to explore the use of a cell-viable stain to identify whether cells that were microscopically counted were viable or not, in order to assess single-species health. This would likely improve the precision of counts and align the observations of competition closer to the predictions.

Regardless of this shortcoming, it is however possible to make certain deductions based on knowing their physiological performance as monocultures, which were investigated in Chapter 4. Temperatures above 30 °C were lethal for *P. tricornutum*, consistent with the

observation that F_v/F_m declined to 0 over time in monocultures exposed to a range of 30 °C to 33 °C. Fluctuations to 33 °C or beyond would have killed *P. tricornutum* within one 24-hour-cycle, as F_v/F_m in monocultures dropped to 0 within one day in *P. tricornutum* monocultures at these temperatures. It can therefore be said with certainty that the manually counted cells of *P. tricornutum* in assay cultures reaching more than 33 °C were dead after one warm fluctuation cycle. The large scatter in the observations of competition that were made for fluctuation amplitudes that reached the lethal temperature range for *P. tricornutum* on warm days (grey-shaded are in Fig. 5.3B) is therefore concluded to be an artefact of counting error. Live and dead cells were not distinguishable in the manual Lugol's counts and small numbers of *P. tricornutum* cells could have influenced the calculated species ratios strongly.

Likewise, cold temperatures below 10 °C were stressful to *T. pseudonana*, and it must have been struggling to survive at this and lower temperatures. Further evidence of this can be seen in Supplementary Figure 5.2, where F_v/F_m in high N cultures dropped severely on every cold fluctuation cycle at fluctuation amplitudes of 17 °C or higher. At first this decrease in F_v/F_m values can be attributed to both species, as *P. tricornutum* reached critical temperatures on the warm fluctuations, and *T. pseudonana* on the cold ones. After *P. tricornutum* was fully displaced in those cultures, the decrease in F_v/F_m is only observed on the cold cycles, as the signal was fully influenced by *T. pseudonana*.

Towards the end of the low N experiment, particularly during the period after temperature fluctuations, empty frustules were sometimes observed and *T. pseudonana* cells began to aggregate in clumps the closer the experiment came to its end. This could be attributed to a general decline in cell health due to being cultured under nutrient limitation for 40 days (almost 6 weeks). The significant trends in species frequencies during the post-fluctuation period in

favour of *P. tricornutum* could be partially attributed to clumping of *T. pseudonana* cells (Suppl. Fig. 5.10). Single cells of *T. pseudonana* became less distinguishable and cell counts less accurate, underestimating the number of *T. pseudonana* cells present in the cultures. Therefore, it is possible that more cultures could have been considered stable again after fluctuations stopped, as in the case of the high N scenario, if cultures had not been struggling under the pressure of continuous N-depletion.

5.5.2 Implications of Findings

Assessing the dynamics of simple mixed communities can be important in biotechnological settings, for example in outdoor ponds or in greenhouses that are subject to diurnal, seasonal, and annual thermal fluctuations. Knowing how monocultures or mixed cultures react and perform in such systems will help to ensure more successful culturing of diatoms and aid to better assess whether culture crashes are imminent or how they can be prevented. Identifying fluctuation regimes that can stabilise the community could be beneficial for long-term projects. Now that the effects of uniform temperature fluctuations on competition are known, fluctuation regimes that would allow stable coexistence could potentially be identified by adjusting the time span that the cultures remain in the warm or cold cycle to account for different metabolic rates across temperatures. In this way mixed cultures could be kept stable in their species abundance ratios over longer time spans even if in the short term the prevailing temperature is disadvantageous for one of the two diatoms.

For natural environments, the implications of this study are relevant for the persistence of biodiversity in coming decades, during which overall lake and sea surface temperatures are predicted to rise, and temperature fluctuations are predicted to become more extreme and frequent (Boyd et al., 2016). This investigation showed that high amplitude fluctuations can

lead to changes in competition and extinction of competitors even though the average temperature of the environment is stable and still far away from critical maximum and minimum temperatures of the species that make up the community. The current study highlights the need to further our understanding not only of the implications of average changes in the abiotic environment, but also changes in the variability around the averages. Variance and skewness of environmental fluctuations are predicted to increase due to climate change, resulting in higher frequencies of extreme events (Vasseur et al., 2014). Theoretical studies on Jensen's inequality and fluctuating environment have made the call for more in-depth analyses of variability (Denny, 2017), but experimental evidence for the sensitivity to warming and extreme fluctuations is still scarce and has to be expanded upon. Because performance of species can be co-limited through multiple parameters changing at the same time (Koussoroplis et al., 2017) it will be necessary for future studies to focus on a range of parameters varying at the same time, such as light levels, pH, or other nutrient concentrations. This will improve certainty and predictive powers of models investigating the effects of abiotic changes when they occur in combination (Kratina et al., 2012). It will also be crucial to take into account potential species adaptations to changing means. Now that this stable model system was established, further questions on system stability can be addressed.

5.6 Conclusion

The experiments presented in this chapter showed that coexistence of two diatoms in a mixed population can persist or be destabilised depending on the amplitude of thermal variation around the temperature of stable coexistence. We also showed that the same thermal fluctuations can have different effects depending on the concentration of nitrogen present in the system. This laboratory model system provided experimental evidence that is relevant to the resolution of the “paradox of the plankton” and to the storage effect, both of which allow biodiversity to remain higher in a variable environment than is predicted for equilibrium conditions. More parameters and different species combinations have to be studied in order to be able to make conclusive statements about the co-existence of species under the influence of variability of environmental change that is predicted for the coming decades and centuries. As natural environments are continuously under the influence of environmental variations, this will help to improve our predictions of future community composition and ecosystem processes.

5.7 Supplementary Material

5.7.1 Power analysis to determine experimental design

Power analysis indicated that 10 days under each treatment was a long enough time period to determine statistically whether cultures can be considered stable or not. High N mixed populations were cultured for at least 10 generations to ensure that they were stable over time. Power analysis of linear model fits to the natural logarithm of species frequency over time of *P. tricornutum* in mixed cultures was carried out with an f2-test to identify stability. The obtained v value of the power test would indicate how many samples would need to be analysed to confirm a statistically significant trend in the change in species frequencies over time if the frequency count would happen every second day. The R package “pwr” was used to carry out the test with the following parameters:

$u = 1$, $f2 = 2.703704$, significance level = 0.05, power = 0.8

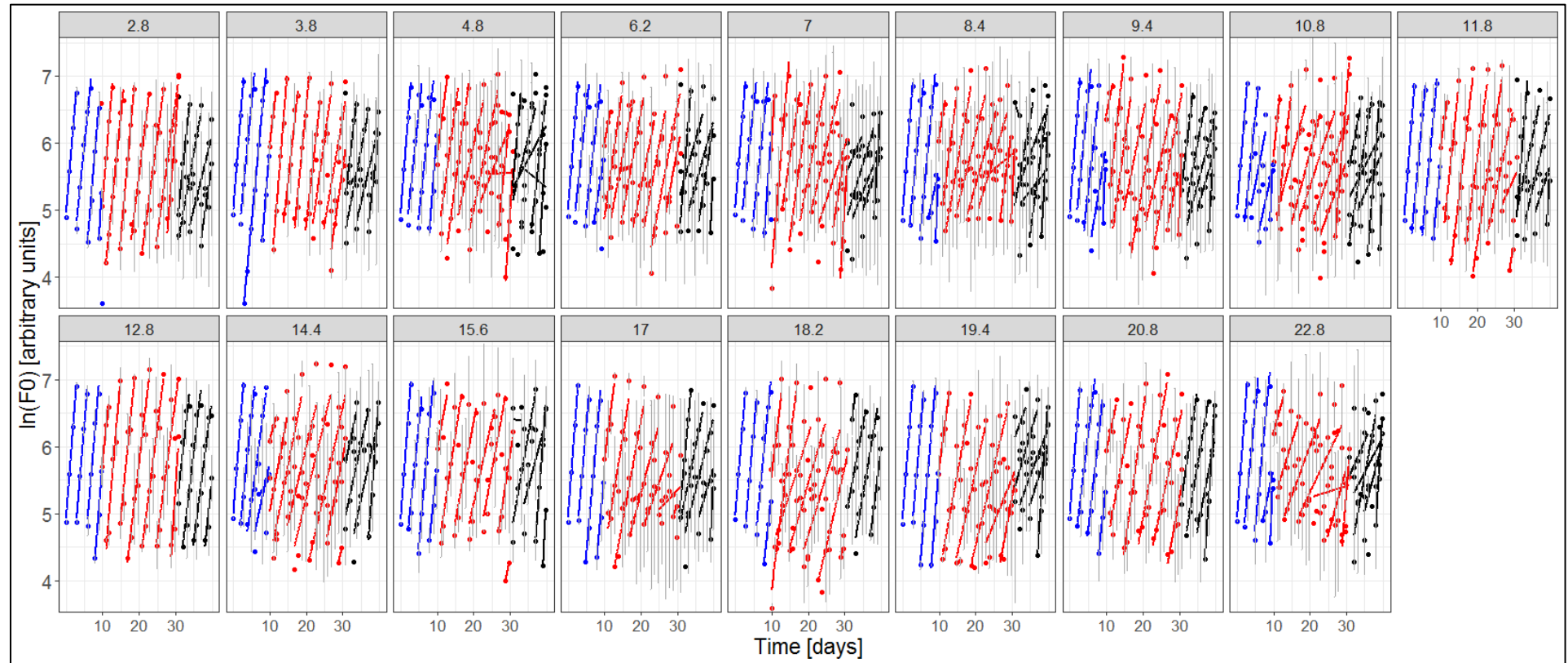
f2 was calculated as $R^2/(1-R^2)$, where R^2 was the average correlation coefficient of linear models across all competition replicates in the high N scenario from Chapter 5 ($R^2 = 0.72$). The resulting v value ($v = 3.628836$) yielded the number of data points necessary to identify a significant change in species frequency in mixed cultures of *P. tricornutum* and *T. pseudonana* in high N conditions with a power of 0.8 given the planned sampling routine. If after at least 5 frequency counts across 10 days (10 days yielded 10 generations or more for the high N algae cultures) linear models were still found to be insignificant, stability of mixed cultures over time was assumed.

For the power analysis in low N cultures, the parameters were set to

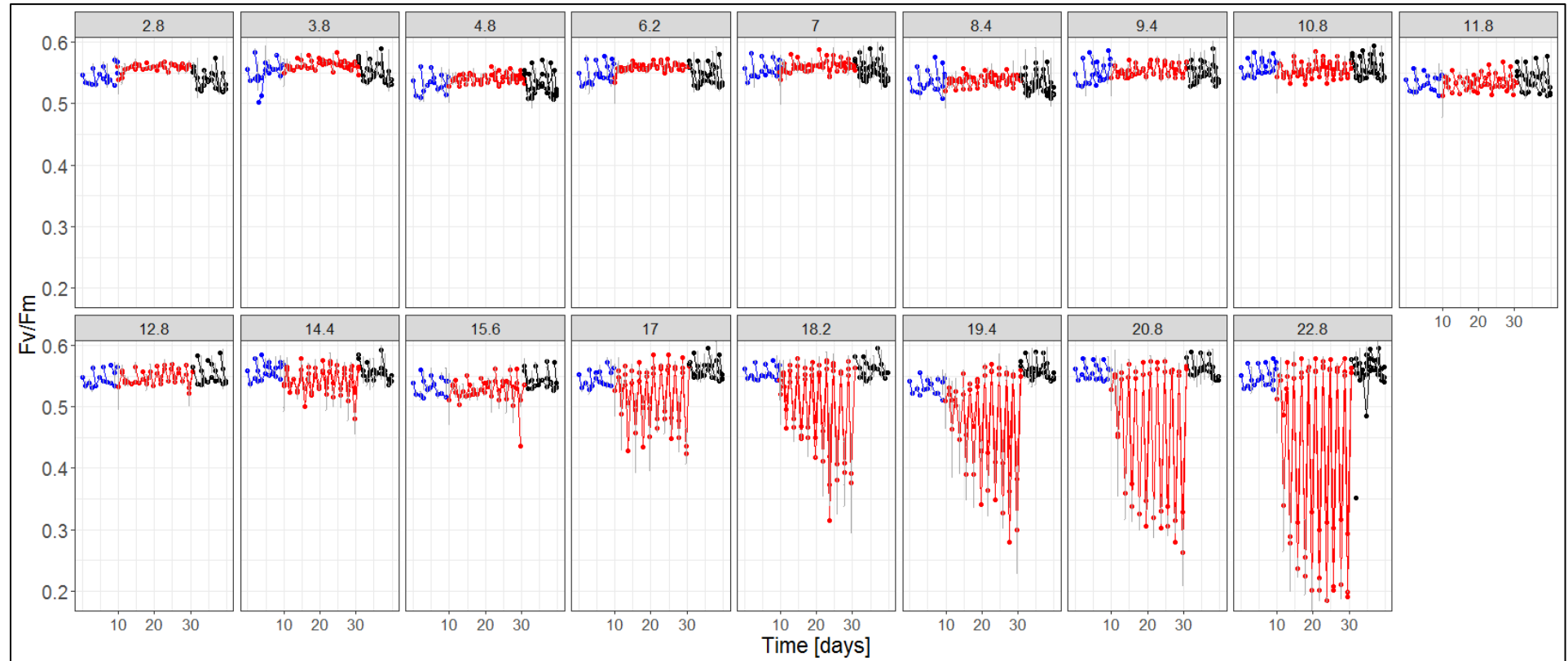
$u = 1$, $f2 = 2.225806$, significance level = 0.05, power = 0.8

f_2 was once more calculated as $R^2/(1-R^2)$, where R^2 was the average correlation coefficient of linear models across all competition replicates in the low N scenario from Chapter 5 ($R^2 = 0.69$). The power analysis yielded a v-value of 4.17, indicating that 5 samples were needed for enough statistical power to determine a trend of stability in mixed culture.

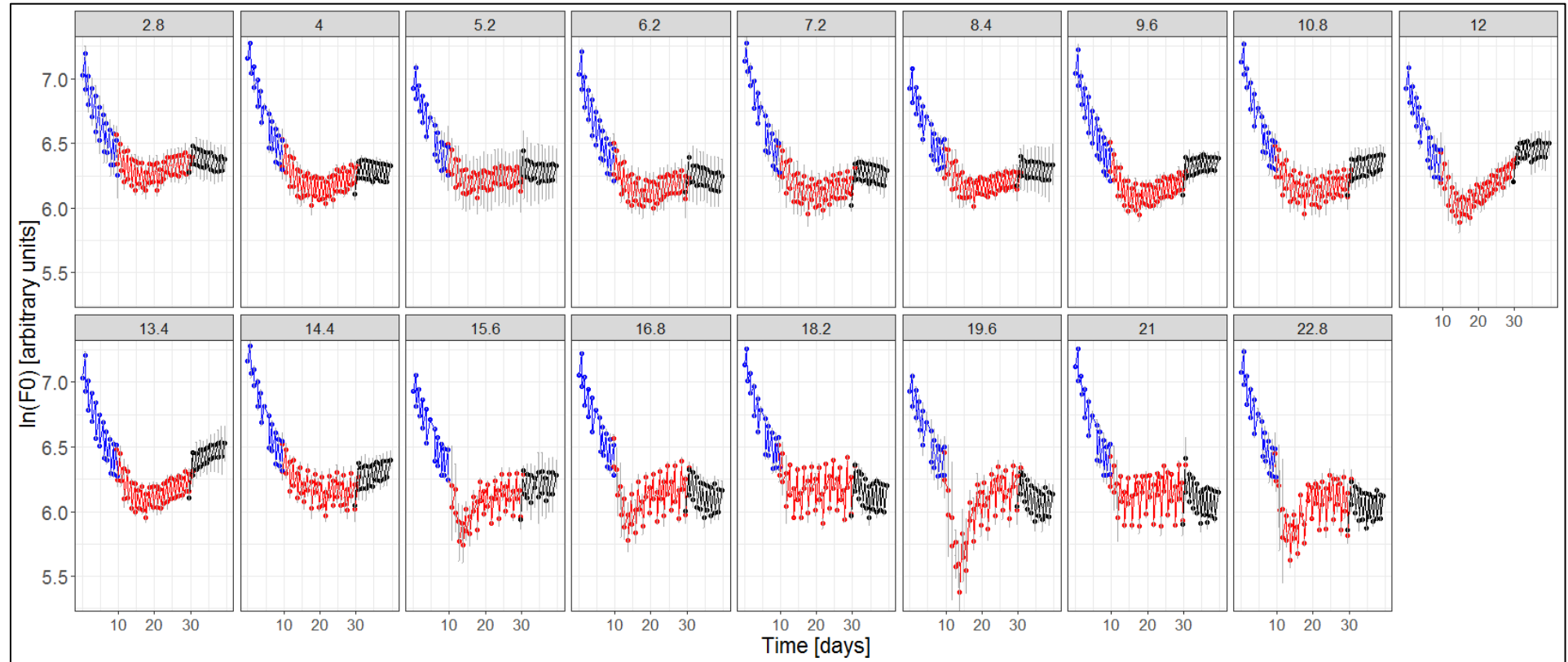
5.7.2 Supplementary Figures



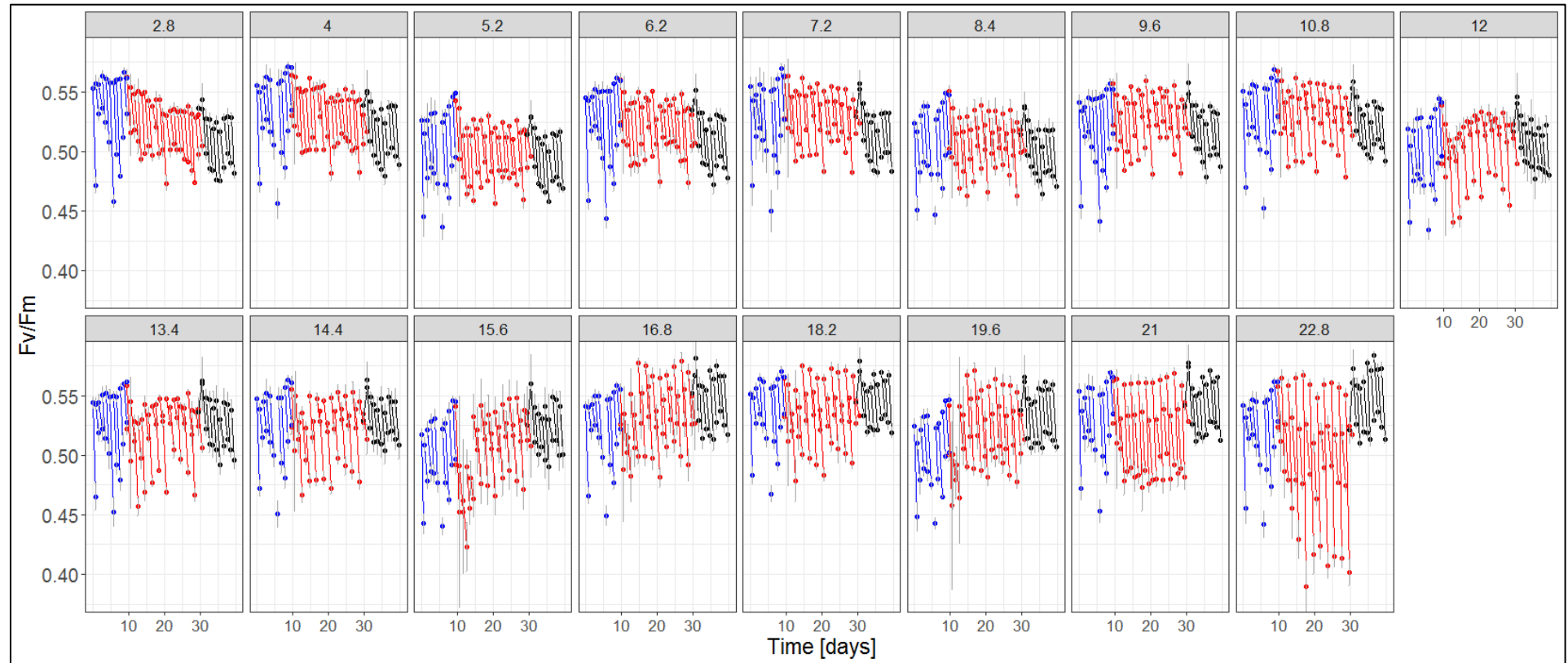
Supplementary Figure 5.1: Average ($n = 4$) $\ln(F_0)$ of exponentially growing mixed cultures of *P. tricornutum* and *T. pseudonana* across temperature fluctuation amplitudes. Blue data indicate the period prior to the start of the fluctuations, red data indicate the fluctuation period, and black data indicate the period after fluctuations. Each panel represents an assay fluctuation amplitude around the mean temperature of 18.6 °C.



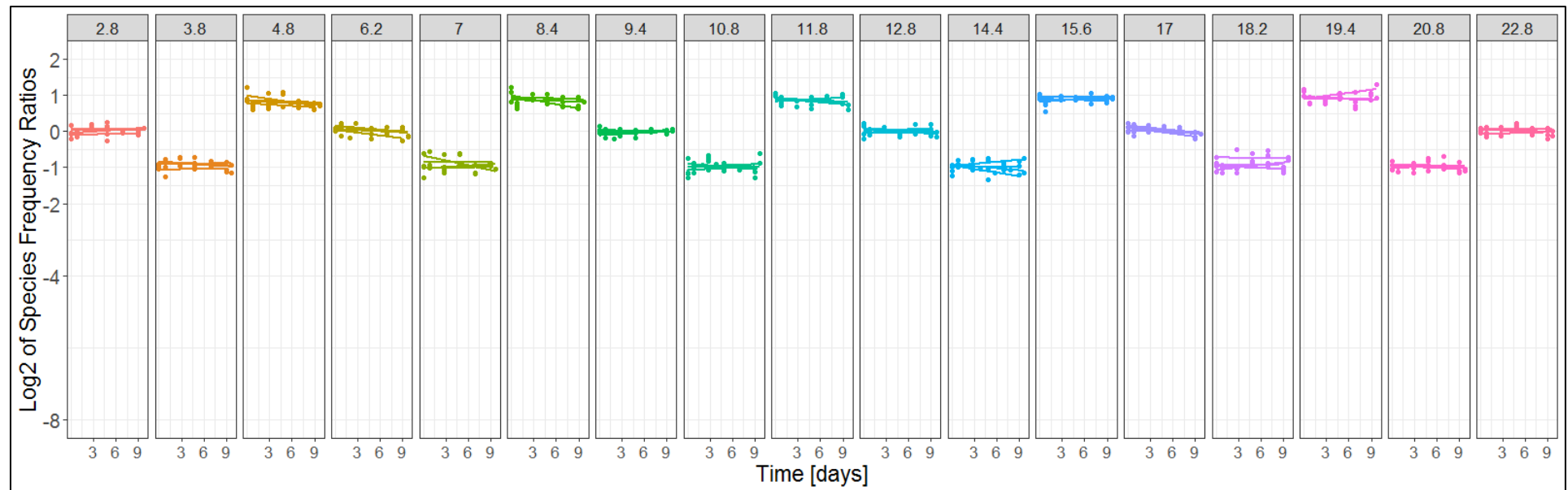
Supplementary Figure 5.2: Average ($n = 4$) F_v/F_m of exponentially growing mixed cultures of *P. tricornutum* and *T. pseudonana* across temperature fluctuation amplitudes. Blue data indicate the period prior to the start of the fluctuations, red data indicate the fluctuation period, and black data indicate the period after fluctuations. Each panel represents an assay fluctuation amplitude around the mean temperature of 18.6 °C. Note how at the highest fluctuation temperatures (17 °C and above), a general drop in values in comparison to the pre-fluctuation period (blue) can be observed in the first three to five days of the fluctuation period (red). During this time, *P. tricornutum* encountered conditions close to its physiological limits on the warm cycles, and *T. pseudonana* on the cold cycles. As the fluctuation period progressed and *P. tricornutum* was fully or almost fully displaced from the mixed cultures at high fluctuation amplitudes, this drop in values could only be observed every second day of the experiment. This is because *T. pseudonana* encountered unfavourable conditions on cold days, but not on warm days, and *P. tricornutum* did not influence the F_v/F_m signal anymore.



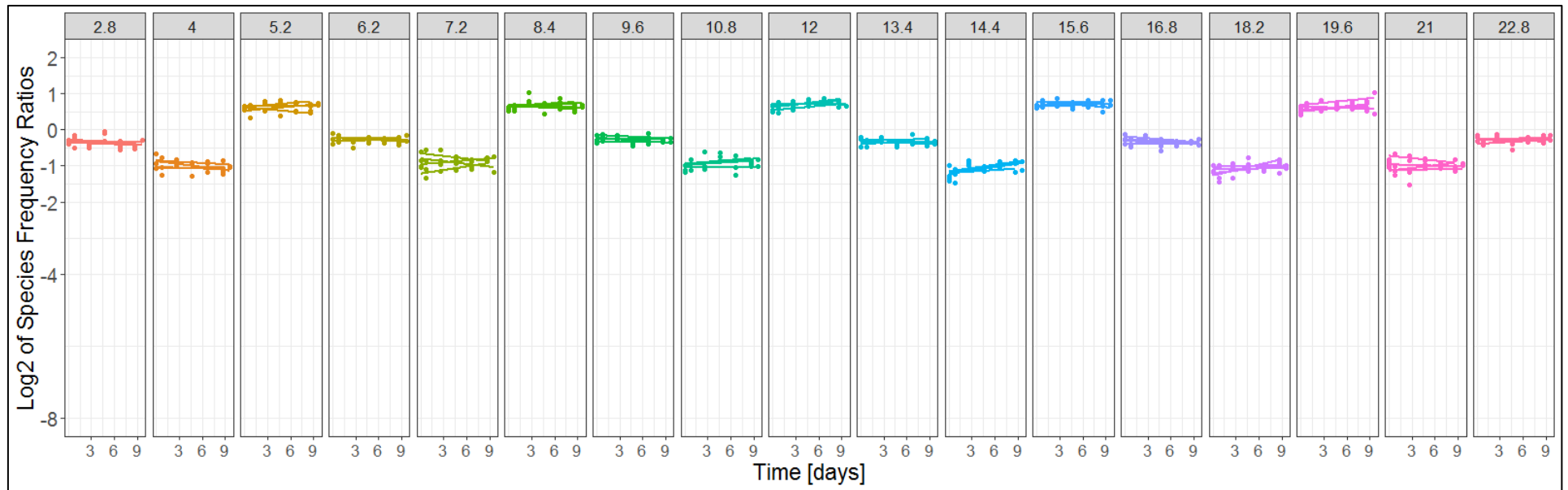
Supplementary Figure 5.3: Average ($n = 4$) $\ln(F_0)$ of N limited mixed cultures of *P. tricornutum* and *T. pseudonana* across temperature fluctuation amplitudes. Blue data indicate the period prior to the start of the fluctuations, red data indicate the fluctuation period, and black data indicate the period after fluctuations. Each panel represents an assay fluctuation amplitude around the mean temperature of 25.2 °C.



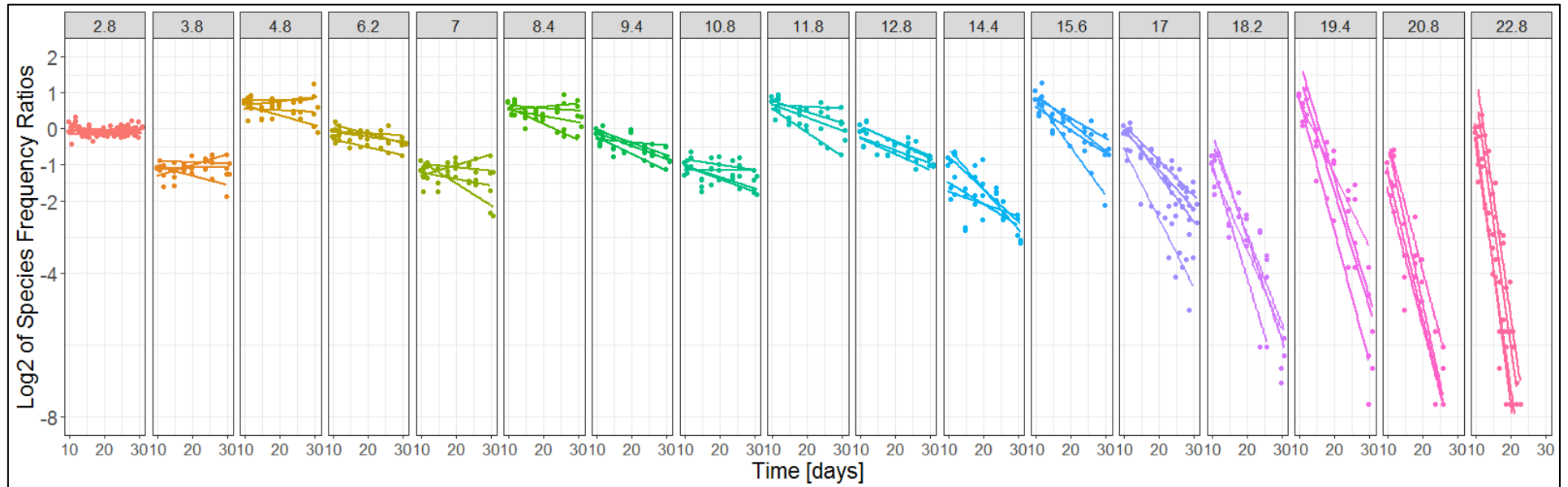
Supplementary Figure 5.4: Average ($n = 4$) F_v/F_m of N limited mixed cultures of *P. tricornutum* and *T. pseudonana* across temperature fluctuation amplitudes. Blue data indicate the period prior to the start of the fluctuations, red data indicate the fluctuation period, and black data indicate the period after fluctuations. Each panel represents an assay fluctuation amplitude around the mean temperature of 25.2 °C.



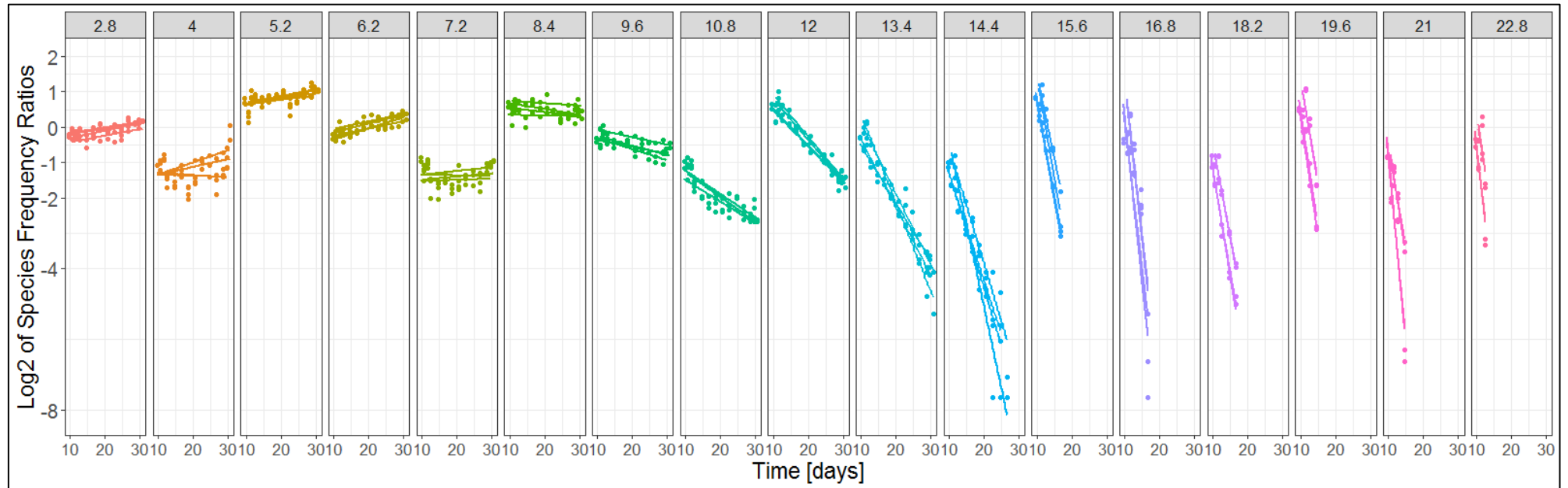
Supplementary Figure 5.5: Progression of $\log_2(\text{frequency } P.\text{tricornutum} : \text{frequency of } T.\text{pseudonana})$ species ratio over time in high N mixed cultures at 18.6 °C before temperature fluctuations were started. Each panel displays 4 replicate cultures and the fluctuation amplitude they were exposed to after this 10 day pre-fluctuation period. \log_2 was utilised in this figure, and in the following 5 Supplementary Figures, as a biologically relevant depiction of species frequency change over time, whereby a doubling or halving in the abundance ratio translates to one unit on the \log_2 scale.



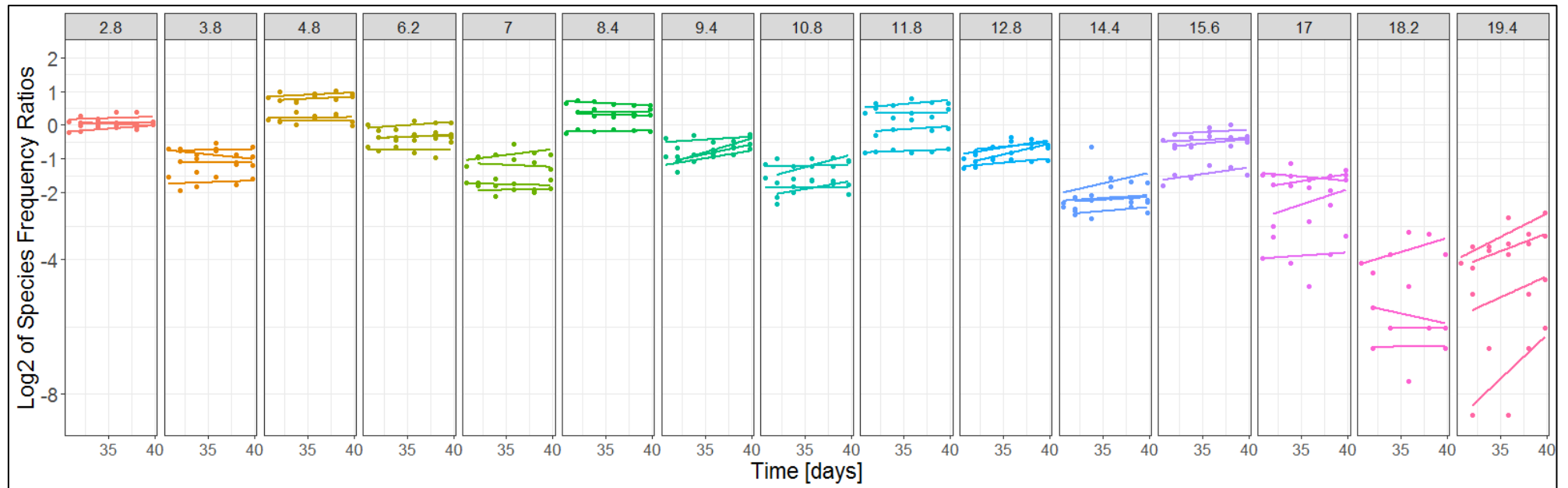
Supplementary Figure 5.6: Progression of $\log_2(\text{frequency } P.\text{tricornutum} : \text{frequency of } T.\text{pseudonana})$ species ratio over time in low N mixed cultures at 25.2 °C before temperature fluctuations were started. Each panel displays 4 replicate cultures and the fluctuation amplitude they were exposed to after this 10 day pre-fluctuation period.



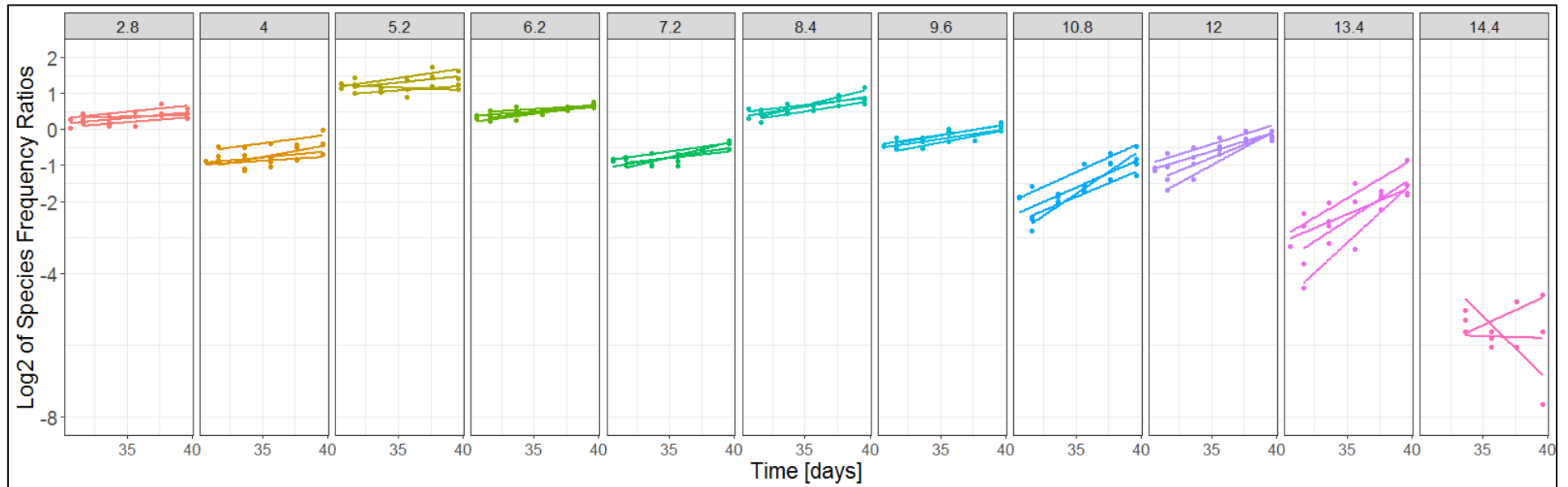
Supplementary Figure 5.7: Progression of $\log_2(\text{frequency } P.\text{tricornutum} : \text{frequency of } T.\text{pseudonana})$ species ratio over time in mixed cultures at different fluctuation amplitudes during the fluctuation period of the high N experiment. Each panel represents an assay fluctuation amplitude around the mean temperature of 18.6 °C.



Supplementary Figure 5.8: Progression of $\log_2(\text{frequency } P.\text{tricornutum} : \text{frequency of } T.\text{pseudonana})$ species ratio over time in mixed cultures at different fluctuation amplitudes during the fluctuation period of the low N experiment. Each panel represents an assay fluctuation amplitude around the mean temperature of 25.2 °C.



Supplementary Figure 5.9: Progression of $\log_2(\text{frequency } P.\text{tricornutum} : \text{frequency of } T.\text{pseudonana})$ species ratio over time in mixed cultures at different fluctuation amplitudes after the fluctuation period of the high N experiment. Each panel represents an assay fluctuation amplitude around the mean temperature of 18.6 °C that the mixed cultures were exposed to during the temperature fluctuation period.



Supplementary Figure 5.10: Progression of $\log_2(\text{frequency } P.\text{tricornutum} : \text{frequency of } T.\text{pseudonana})$ species ratio over time in mixed cultures at different fluctuation amplitudes after the fluctuation period of the low N experiment. Each panel represents an assay fluctuation amplitude around the mean temperature of 25.2 °C that the mixed cultures were exposed to during the temperature fluctuation period.

Chapter 6: General Discussion

Changes in the abiotic environment of phytoplankton are going to play an increasingly important role in continued functioning of aquatic ecosystems as yearly, seasonal and short-term means of abiotic parameters are shifting and frequencies and magnitudes of environmental variability are altered with climate change. We are still far away from gaining a holistic understanding of the responses of phytoplankton communities to these environmental changes. Precise predictions are still complicated because of the large variability in the responses among species, as well as the complexities and nonlinearities that come into play when species interact. There is a plethora of abiotic parameters that can influence communities and that need to be taken into consideration. Time to thoroughly assess the effects of a changing environment is however in short supply as ocean environments are changing ever quicker than previously assumed (Pörtner et al., 2019). If policy makers and aquatic stakeholders would like to mitigate or at least influence aquatic ecosystems in a direction that is beneficial to humans, more of the still existing knowledge gaps need to be closed, preferably within the coming decade. This thesis partially contributes to filling these gaps by further elucidating the role that temperature, as a stand-alone parameter, but also in interaction with nutrient concentrations, will play in determining the growth, adaptation, and competition in phytoplankton. All results of the conducted experiments in this thesis showed that temperature is a major factor in determining growth and competitive dynamics in phytoplankton, but that more needs to be investigated to fully understand its role in aquatic environments affected by climate change.

6.1 Future Responses and the Role of Adaptations

At the moment, the phytoplankton scientific community is working on fully understanding the responses of current phytoplankton performance to changes in the environment. Acclimation potential and environmental history will, without a doubt, play a crucial role for algae to respond to a changing environment. There are however limits to how flexible an alga can be and how much it can adjust its physiology and intracellular processes without new mutations and genomic changes. Adaptations to permanently changed conditions might become the key to surviving climate change. Novel genotypes might emerge within populations that have differing physiological performance across gradients and might show improved persistence in altered environments than current phenotypes. The extent to which adaptations will occur and at what rates are however still unresolved questions.

In Chapters 2 and 3, I focused on questions of potential thermal adaptation and what the consequences of such adaptations could be in the future. I was able to show that previous work on the potential for thermal adaptation in phytoplankton is likely overly optimistic when it comes to assuming thermal adaptation under future climate scenarios. Potential changes might not occur as easily as desired, especially since it is still largely unknown how optimum temperatures and thermal performance result from molecular cellular processes (Liang et al., 2019). I could show that a temperature change of 5 °C might not be sufficient to evoke thermal adaptation if algal cultures are not kept continuously in exponential phase and under optimal growth conditions while being exposed to a thermal change that would not occur in a natural environment. In Table 6.1 I have collated some research studies that were referred to throughout this thesis and compared the imposed thermal change and findings of thermal adaptation in their research to the temperature change in my Chapters 2 and 3. All of the

studies in Table 6.1, except my own work, found thermal adaptations in at least some of the investigated species. With a temperature change of +5 °C, my research lay at the lower end of selection pressure used to evoke thermal adaptation. More than half of the investigations chose a selection pressure much higher than what is realistically to occur in natural environments in coming decades, when compared to predictions made by the International Panel on Climate Change (IPCC, 2013). Even though these studies all focussed on thermal adaptation, their approaches and research methods differed. Some used freshly isolated species from natural communities (e.g. Tatters et al., 2013), others used laboratory cultures that had been kept in controlled environments for decades (e.g. Padfield et al., 2015), and one study conducted the selection experiment in outdoor mesocosms before isolating the species and testing their thermal performance (Schaum et al., 2017). As mentioned in my chapter discussions, there has to be a level of caution with statements generalising adaptive potentials of specific phytoplankton species and it should be once again stressed that it is important to elucidate them in the light of realistic environmental change conditions. Adaptations to temperature and nutrient concentrations will certainly play a crucial role in structuring future communities, however the direction and rate of these alterations is still unclear. Potentially uniform guidelines on investigations into thermal adaptation would help to reach more generalisable conclusions on phytoplankton responses of the future.

Table 6.1: Table summarising the findings on thermal adaptation in selected studies on eukaryotic microorganisms, mainly phytoplankton.

Study	Organism	Source Temperature [°C]	Selection Temperature [°C]	Temperature difference [°C]	Adaptation
Schaum et al., 2017	<i>C. reinhardtii</i>	18	22	+ 4	yes
This thesis	different phytoplankton species	15	20	+5	no, but maybe in rates of photosynthesis and respiration
Baker et al., 2018	<i>A. massartii</i>	25	30	+5	yes
Tatters et al., 2013	isolates from natural diatom community	14.8	14 and 19	+ 5	maybe, called newly found differences “conditioned”
Schmidt, 2017 (thesis)	<i>T. pseudonana</i>	22	9 and 32	- 13 and + 10	yes
Schlüter et al., 2014	<i>E. huxleyi</i>	15	26.3	+ 11.3	yes
Listmann et al., 2016	<i>E. huxleyi</i>	15	26.3	+ 11.3	yes, however adaptation evoked through combined increase of temperature and pCO ₂
Padfield et al., 2015	<i>C. vulgaris</i>	20	23, 27, 30, and 33	+ 3 to + 13	yes
Krenek et al., 2012	several clones of <i>P. caudatum</i>	22	7 – 35.5	-15 to + 13.5	yes, in some of the clones
Huertas et al., 2011	different phytoplankton strains isolated from various natural environments	22	30, 35, and 40	+ 8 to + 18	yes, but not all investigated species

Furthermore, even though adaptive rates of species might be unknown or differ, and even if a species is not directly threatened by extinction through a changed environment, different shapes of thermal performance curves and Q_{10} values (the rate of change of a biological or chemical reaction with a 10 °C temperature rise) at sub-optimum conditions could however mean that community dynamics and rates at which ecosystem processes are performed could change as temperatures rise. If a species would grow better under warmed conditions than under colder ones in comparison to a community member whose rates do not rise as quickly with warming, a new set of species could dominate the community that were previously present only in low abundances. The potential effects of environmental change on algae were reviewed in the introduction chapter of this thesis. In general, changes in abundances and distributions of algae are predicted world-wide, but will depend on region. Areas in which primary productivity occurs could shrink or move. However, these predictions do not take into account potential adaptations.

When predicting phytoplankton performance under future climate scenarios, two major assumptions concerning TPCs are often being made. The first one being that TPCs will remain static in terms of their width and overall shape and will be the same in the coming decades as they are under current conditions (Sinclair et al., 2016). The second one is that responses of biological communities to changes in abiotic parameters will be fixed (Baltar et al., 2019). On geological timescales it is well established that species do adapt to their environment, shown by distinct geographic distributions and community structures in different regions of the world. In comparison to static models and predictions, novel models are emerging that are trying to incorporate potential adaptive changes. More information about the various reaction norms and physiological responses from different taxonomic groups and species is however necessary

to bolster predictive powers (Beckmann et al., 2019). Modelling of whether phytoplankton thermal niches will be conservative and track the environment for favourable conditions or whether physiology will be plastic and resilient enough to cope with predicted climate change, showed that the response will depend on taxonomic group and species (Chivers et al., 2017). Even if species have shown the potential for adaptation under laboratory conditions, local extinction can still become a reality for them in natural environments. Rates of adaptation could be too slow because genetic variability might be low, populations small, abiotic conditions unfavourable and the selective pressure not high enough to cause an adaptation, leading to adaptation lag, and consequently decreases in fitness (Baltar et al., 2019). Mutations that would occur in a laboratory set-up could still become unique to this specific and over-simplified environment, with higher rates of adaptation occurring under ideal nutrient replete conditions than would be observed in natural environments. In comparison, when competing in nature against other algae, while being grazed upon by a predator under sub- or supra optimum abiotic conditions, adaptive rates and pressure might be very different leading to different outcomes. Furthermore, adaptations have a spontaneous and undirected nature to them, as different adaptations could occur in response to the same environmental change (Collins et al., 2020), further reducing predictability for natural environments. Future phytoplankton community composition therefore remains a complicated black box to predict.

Within-species variation of phytoplankton is creating further uncertainty around the performance of an algal species, as genetic diversity in populations of the same species allows for a variety of phenotypes to be expressed. The more genetic diversity a population possesses, the higher the likelihood that specific members within a community will be able to cope with *in situ* environmental conditions, but also the higher the potential for adaptation. Intra-species variability is a crucial aspect of phytoplankton diversity (Schaum, 2014) and has to be

considered when discussing the response to changing environments (Wood and Leatham, 1992). Godhe and Rynearson (2017) reviewed that clonal physiological variability in natural populations seems to be high enough to allow for a species to persist and dominate an ecosystem even when environmental conditions change, igniting questions on a species' ability to acclimate to an array of environmental conditions, but also questioning the necessity for adaptations in a rapidly changing environment and the extent of threat posed by, for instance, rising temperatures.

6.2 Phytoplankton Competition Under Future Climate Change

As species do not occur in isolation, competitive dynamics play a crucial role in determining future communities and ecosystem functioning. The role of temperature changes and nitrogen concentrations on competition could be partially elucidated with the work conducted in this thesis. Whether it is truly possible to predict competitive outcomes in nature from physiological performance of isolated species and whether predicted dynamics scale up to whole communities remains unclear, as not just growth would be the determinant factor to outcompete other community members (Ward et al., 2019). In Chapters 4 and 5, I investigated direct diatom competition between two common diatom species. I could expand on our knowledge of phytoplankton competition and showed that competition in stable environments could be well predicted from knowing the performance of monocultures. This work adds to a pool of just a few studies (e.g. Bestion et al., 2018), that show that traditional competition theory seems to be suitable to predict competitive outcomes in simple systems with pairs of species. In more diverse species assemblies predictions might also hold true (Pardew et al., 2018), but more knowledge is needed to make conclusive statements. As expected, temperature was found to play an important role in determining the outcomes, but nutrient

concentrations can interact with temperature to alter TPCs of algae and therefore how competition pans out. I could show that changes in abiotic parameters can interact with temperature to change the TPCs of species (nitrogen concentration in Chapter 4), and consequently the predictions we make about competitive outcomes from monoculture growth performance. In fluctuating environments the predictability of competitive outcomes already decreased although the experimental set-up was still relatively simple, indicating that the introduction of complexity increases non-linearity and quickly complicates understanding of competitive dynamics.

The conducted competition experiments did not yet attempt to assess what would happen to competitive outcomes if adaptation to assay conditions would occur during the experiment. Just as adaptations to the thermal environment or nutrient regimes are expected to influence and change the performance of isolated species, they will likely also play a role in competition scenarios and influence how future phytoplankton communities will be structured. If species in future aquatic systems adapt or change their physiology, their ecological fitness across environmental gradients will presumably change as well. Physiological traits that have been found to adapt or are used as tracers of evolution do however not necessarily correlate with fitness (Kremer and Klausmeier, 2017), and what makes a species successful when competing against other species remains unclear in many cases. One common trait that has been found to determine competitive success in equilibrium conditions is R^* and the correlating ability to live off a lower nutrient supply than a direct competitor (Bernhardt et al., 2020; Lewington-Pearce et al., 2019). Others still need to be elucidated, and as an example for the lack of insight, one can look at the mismatch between predictions and observations in Chapter 4 and especially Chapter 5 of this thesis to see that the understanding is far from complete.

If the competition experiments of this thesis would have lasted longer, adaptations to the local environment through spontaneous mutations could have potentially changed the observed patterns (Collins and Bell, 2004; Schaum et al., 2018, 2017). Gradual or spontaneous adaptations to assay conditions are more likely to accumulate as time passes. It has been shown that in fluctuating environments, a rescue event in *T. pseudonana* can lead to a population adapting to higher temperatures within 3 – 4 generations (Schaum et al., 2018). If such an event were to occur in one of the species while species co-exist in a stable equilibrium, the co-existence dynamics might be altered without changes in the abiotic environment. Similarly, it could also happen that a mutation would allow one of the species to cope better with temperature fluctuations, altering the competition coefficient that would be observed from unevolved monocultures. The algal cultures used in Chapters 4 and 5 for the experiments investigating the direct competition between *P. tricornutum* and *T. pseudonana* were not clonal but came from a semi-batch laboratory population that had been cultured over years. High genetic variability due to random mutations in the populations that occurred over years and went unnoticed were likely because laboratory cultures maintained at high densities can be expected to have at least one mitotic genetic mutation in each generation (Andersen, 2005). Genotypic variability can propagate in a laboratory culture that has been kept for many years (Lakeman et al., 2009). Although these mutations could be neutral and potentially be deleted in the future again, they could also lead to less or more competitiveness than the original genotype. As *P. tricornutum* and *T. pseudonana* are both species that can enter a sexual life stage, genetic variation can furthermore accumulate over time (Chepurnov et al., 2004). In addition, physiological differences despite morphological coherence were already observed since the early days of phytoplankton research into *P. tricornutum* and *T. pseudonana* strains (Guillard and Ryther, 1962; Wood and Leatham, 1992). Although for the current thesis inherent

genetic or phenotypic diversity within the investigated populations was not assessed and no sequencing of various isolates from the same culture was undertaken, the potential for within-species variability does add uncertainty about the ability to generalise the conducted work. It might be that standing stock culture genetic variation was high, and potentially two isolates from the same culture would display varying reaction norms to the same treatment (Lakeman et al., 2009; Schaum et al., 2012). Studies investigating the response of phytoplankton to environmental changes and competition might also gain different results from populations coming from different environments (Boyd et al., 2013). For instance two other *P. tricornutum* isolates from marine environments were found to possess optimum temperatures about 3 to 5 °C lower than the T_{opt} of the line used in this thesis (supplementary material from Thomas et al. (2012)). This would likely cause them to grow and compete differently across the investigated temperature gradients, if the growth response in isolation is used as a predictor for competition. It would therefore be interesting to investigate how dynamics between species can evolve over hundreds of generations and whether competition between a specific species pair, or a group of algae, is static under a specific set of abiotic parameters, or whether adaptations can lead an algae to display contrasting competitive abilities in comparison to its predecessor. Systems with the potential for adaptation might decrease our power to predict dynamics if we cannot assess whether competition based on current performance will persist under change (Petchey et al., 2015). Current observations of competitive performance across gradients should be considered as null models because they do not incorporate the time in which a species could potentially acclimate or even adapt, thus changing the currently measured competition in a stable and fluctuating environment (Dowd et al., 2015; Kordas et al., 2011).

6.3 Consequences for Ecosystem Functioning

If phytoplankton communities would fail to cope with current climate change and not be able to adapt adequately, dire consequences for ecosystems can be expected. In the introduction chapter, as well as the data chapters, it was highlighted that environmental changes will impact phytoplankton, changing physiology and consequently community composition. A lack of adaptation over time might slowly erode the ecological resilience of a system as members formerly performing certain functions or services are displaced and the buffer and redundancy within a community is decreased, making it more susceptible to extreme events and further changes in environmental conditions (Folke et al., 2004). Apart from influencing physiology and ecology directly, environmental changes will perpetuate and translate into changes in geochemical processes occurring on a local and global scale, as well as potentially change the provision of ecosystem services that could alter how other organisms and humans interact with phytoplankton and aquatic environments in general. Therefore, predictions looking into changes of phytoplankton due to environmental changes should consider not only how they will affect abundance, distribution and evenness of species, but also how they will affect functionality (Barton and Yvon-Durocher, 2019). Changes in community composition will likely result in shifted patterns of species succession and phytoplankton blooms (Mosser et al., 1972). Predicted changes in phytoplankton community structure, elemental composition, photophysiology, and growth rates will have consequences for functional traits dominant in surface waters and restructure aquatic communities, leading to changes in food quality for higher trophic levels, aquatic nutrient cycles, as well as the amount of carbon that can be sequestered and exported to the deep sea.

Possibly the most important aspect of changed phytoplankton ecology on a global scale will be the shift in biogeochemical fluxes of nutrients. If geochemical cycles are altered, the whole abiotic backbone of the planet's ecosystems is under threat to cease functioning in the way we know it, so that microscopic changes on the level of phytoplankton could have a knock-on effect for major nutrient dynamics that will affect sea, land and atmospheric processes. As mentioned in the thesis introduction, a shift towards warmer temperatures will likely cause a global shift towards smaller phytoplankton groups, affecting C, N, and Chl *a* contents of surface waters, and lowering them overall (Barton and Yvon-Durocher, 2019). Higher temperatures were found to correlate with increased intracellular C:P and N:P ratios, shifting phytoplankton phosphorus stoichiometry and consequently cycling and transport to higher trophic levels (Yvon-Durocher et al., 2015).

Phytoplankton's quality as a food source for zooplankton is predicted to decrease as higher carbon to nitrogen and carbon to phosphorus ratios will decrease the nutrient values of phytoplankton for higher trophic levels (Schaum et al., 2012). Changes in the C:N ratio in phytoplankton reflect changes in lipid and carbohydrate amounts relative to proteins and nucleic acids (Anderson and Hessen, 1995; Urabe et al., 2003). This is of importance for phytoplankton as a quality food source because more proteins indicate a desirable food source. While Yvon-Durocher et al. (2015) could show that C:N ratios were largely independent of temperature, other nutrient ratios are not. In the model diatom *T. pseudonana*, increased temperatures led to a decoupling of cell volume and frustule silification, indicating a reduction of C and Si incorporation, reducing the amounts of C and Si transferred to higher trophic levels and exports into deeper ocean layers (Baker et al., 2016). The shift away from diatom dominated communities towards dinoflagellates, due to decreased silicate inputs to aquatic

systems is also expected to reduce the nutritional value for grazers (Geider et al., 2014). Shifts in species elemental composition caused by changes in environmental parameters would therefore likely lead to altered aquatic food chains (Dickman et al., 2008).

Effects of altered phytoplankton community structure will most likely also perpetuate all the way to the highest trophic level as many zooplankters graze their prey selectively based on size or shape (Lee et al., 1966; Richman and Rogers, 1969). Alterations in the species composition of a phytoplankton community could therefore influence the health, distribution, and abundance of many animal populations higher up in the food chain (Mosser et al., 1972), with potential negative impacts for fisheries and food supply to humans (Ward et al., 2019). Just as phytoplankton, grazer populations are also expected to be influenced by climate change, altering the top-down pressure on phytoplankton (Boyce & Worm, 2015). This could lead to specific groups of phytoplankton becoming more or less abundant, with consequences feeding back into altered geochemical cycles. Decreases in phytoplankton biomass can have the consequence of reduced carrying capacities of ecosystems, which however could be counterbalanced if metabolic rates increased due to warming (Boyce and Worm, 2015).

Another potential consequence of climate change is the currently observed surge in harmful algal blooms (HABs) in coastal areas and freshwater systems worldwide. Increasing mean temperature and increased nutrient loadings in coastal areas have been linked to cause more toxic algae to thrive (Geider et al., 2014), affecting drinking water supplies and human health, killing fish, shellfish, seabirds, marine mammals, but also pet dogs that go for a swim in a lake.

Although this thesis did not investigate how changes in atmospheric CO₂ concentrations would impact phytoplankton, it is an important aspect to consider when discussing climate change impacts. Alterations in community structure due to changed physiology and competition across

temperature and nutrient gradients might influence the amount of carbon taken up and affect the ocean's carbon pump, as well as feed back into atmospheric carbon cycling. If the prediction that future oceans will be dominated more widely by small-sized phytoplankton species due to more common oligotrophic conditions would become a reality, then the oceans' ability as a carbon pump could be reduced and less carbon would be exported to deeper ocean depths (Falkowski et al., 1998). Litchman et al. (2006) presumed that decreases in diatom populations may lead to more CO₂ in the atmosphere and create a positive feedback loop of increasing carbon dioxide levels in the atmosphere, while less CO₂ would be taken up into the water column. Iglesias-Rodriguez et al. (2002) added that a future increase in CO₂ will be a disadvantage to carbon concentrating mechanisms in algae and that a decrease in the calcification potential in surface waters will decrease and influence the oceanic carbon pump. It has been suggested that in future oceans a lower total primary productivity can be expected (from 44 Pg C/yr at current CO₂ levels to 38.5 Pg C/yr at 4 times higher CO₂ levels (which are predicted to occur in 140 years in the classical CMIP II scenario of the IPCC)) due to a decline in diatom abundances (Bopp et al., 2005; IPCC, 2013). On the other hand it has been assumed that primary productivity will increase towards higher latitudes, which will however presumably be balanced out by a larger decrease of primary productivity at lower latitudes, resulting in no net change globally (Litchman et al., 2006). Higher ratios of respiration to photosynthesis predicted through the greater availability of phosphate would lead to shifted exchange rates of CO₂ between the oceans and the atmosphere and would therefore ultimately not only affect carbon cycles in the oceans, but also in the atmosphere, which would have a consequential effect on terrestrial ecosystems (Martinez-Garcia et al., 2010).

In addition to changes in the biotic and abiotic environment through anthropogenically caused climate change, it is furthermore important to notice that while many investigations focus on these changes, direct alterations by humans at the land-sea interface will further exert their influence on phytoplankton alongside all other discussed parameters. Agricultural practices and runoff, toxins from industry, habitat loss and coastal development, alteration of grazer communities through harvest, as well as introduction and replacement of species through ballast water will all interact with each other to influence phytoplankton (Cloern, 1996). There is for example evidence that phytoplankton biomass increases due to nutrient inputs from human activities in near-shore waters, shifting communities out of nutrient-limitation, which in turn can increase productivity of coastal fisheries on one side, but can in the worst case cause anoxic regions and dead zones (Boyce and Worm, 2015).

For a continuation of ecosystem functioning at desired levels, functional redundancy in source populations and communities will play a role in determining the response to changed environmental conditions. The diversity within and among species and the rare biosphere of species that can fulfil functionally similar roles will impact whether functionalities will persist or determine rates of adaptation. With sufficient redundancy, adaptations to changed environmental conditions might not be necessary in order to continue providing the same ecosystem services and performing processes at the usual rates (Baltar et al., 2019). Species that will not be able to adapt to new conditions might potentially disappear without a net effect on the ecosystem.

The sheer complexity of factors that will impact phytoplankton in future aquatic systems is daunting to tackle. Therefore it remains to be seen whether findings on phytoplankton's responses to changes in temperature or nutrient concentrations will hold true in natural

environments, and it is a question of future research to elucidate to what extent findings from laboratory experiments can be extrapolated to natural environments. Laboratory studies such as the ones in this thesis can only give an indication of how thermal performance and competition between species may pan out in uncontrolled natural environments that are heterogeneous in time and space. It was found in the past that the responses of controlled laboratory populations do not have to align with species dynamics observed in natural populations (e.g. Goldman and Ryther, 1976), and the ability to predict shifts in community composition and species succession in complex natural systems is still an unresolved question.

Phytoplankton will however not be the only organismal group influenced by climatic changes, and interactions within all ecosystems worldwide are complex and diverse. Synergistic and antagonistic effects could theoretically counterbalance each other, leading to no net change in response of phytoplankton communities, although this is unlikely (Boyce & Worm, 2015). Small physiological changes can have large impacts in natural communities as differences become larger over time (Geider et al., 2014; Low-Décarie et al., 2017). Complex systems have a tendency to behave non-linearly or almost counterintuitive when not all relevant parameters are considered (Begon et al., 2006; Bennett et al., 2003). From bacteria, to the highest trophic predators, from soil consistency to weather patterns, every aspect of the globe is influenced by a changing climate in the mid to long-term, but also by environmental changes in the short term. Knowing exactly what will happen in an ecosystem when the temperature rises by a certain amount will still be a complicated prediction for many years to come. However, phytoplankton is a crucial group in aquatic ecosystems without which our world would be in dire trouble. They are arguably worth the struggle to know more about and much more knowledge on how competitions and inter-species dynamics will be influenced by the oncoming

changes is necessary in a rapidly changing marine environment, as it will enable to improve prediction of dynamics in future marine systems (IPCC, 2013; Kordas et al., 2011). Studying algae and their response to changes in temperature and nutrient loadings holds great potential for biotechnological applications and the understanding of ecosystem dynamics, but how the knowledge from conducted research will ultimately be utilised is a matter for policy makers and entrepreneurs.

If phytoplankton will manage to adapt to ongoing and predicted environmental changes, it could however be that ecosystem processes will continue to occur at least partially under current rates. What can be stated with certainty is that in regards to phytoplankton and ecosystems, a change of some sort will occur. Alterations to phytoplankton ecology and physiology might ultimately translate into altered predator abundances, fish stocks, geochemical cycles, and the way humans can interact and live off the ocean (Stock et al., 2011), and all changes combined are likely to result in complex responses from marine socio-ecological systems. Earth and aquatic ecosystems will continue to persist in one form or another. Ecosystems and organisms will continue to thrive. However, in an anthropocentric world humankind would like ecosystems to continue to provide and perform services in a beneficial manner. At the moment they are under threat to continue persisting in a way that they support current species assemblies and ecosystem provisions that humans have learned to value, cherish, and live off. Changes to ecosystems and the values they hold are therefore defined according to the advantages they bring to humans, from production of oxygen to provision of food. Whether the changes in ecosystem processes that will result from novel community compositions will be beneficial to humans or accelerate the current decline in the ecosystems that we value remains to be seen.

6.4 Conclusion & Future Directions

Despite all the process that has been made on understanding phytoplankton physiological responses and competitive dynamics across environmental gradients, the scientific community still has a long way to go until community composition, outcomes of direct competition, and the resulting consequences for ecosystem processes can be comfortably and precisely predicted when the environment changes. During my PhD, I intermitted my studies to conduct an internship with a biotech company that was growing diatoms and turning them into aquaculture hatchery feed. It was during that internship that I realised that even without a full understanding of the complexities of phytoplankton, the research I was conducting had useful applications which can be expanded upon in the future. It all comes down to knowing your species well. If we know how isolated algae respond across environmental gradients with an adequate resolution of detail, we can utilise them to the advantage of ecosystems and humans. Being able to control species in isolation and as simple mixed populations will allow to advance their biotechnological applications.

With the successful establishment of stable mixed communities, many more questions on co-existence of species could now be addressed. Simple but controllable biological systems like the two species mixed populations containing *P. tricornutum* and *T. pseudonana* could be utilised to answer questions of system stability and resilience. Conditions which foster stability can be explored, as well as those that can break it. How much stress can a system endure until it is not functional anymore? Do alternate stable states exist within microalgae communities and can stability be achieved under differing combinations of abiotic parameters, or only under one specific condition at a time? When are potential tipping points reached and can a system in decline be recovered again? Hypotheses that could formerly only be tested in models based on

single species investigations or that could only be tested in prokaryotic communities could now be answered with a phytoplankton system.

A potential next step for the research that was conducted in this thesis is of course to combine direct competition experiments with experimentation on thermal adaptation. If species were to adapt to environmental changes as monocultures, would their new physiological performance be as good of a predictor for competitive outcomes as the old one and would it be possible to adapt and gain a competitive advantage at temperatures or nutrient concentrations that were formerly disadvantageous? How would competition change if adaptation were to occur while the species are already competing? What would happen if species competed or would be kept in stable mixed cultures for years? Could species adapt during an ongoing competition, potentially changing the competitive advantage or changing the point of stable co-existence because of a spontaneous mutation? Would the competitive success of a species against another remain always the same regardless of ecotypes under investigation having differing physiological responses or adaptations? Future research could investigate the outcomes when competing adapted and non-adapted strains against a common competitor to elucidate trade-offs of adaptation and investigate whether adaptive rates are similar between isolated species that are being adapted to new environments in isolation under ideal conditions in comparison to having to adapt while continuously competing. Are there adaptations that could be beneficial when a species is in isolation, but might lead to a competitive disadvantage when species are mixed together? What would happen if the complexity of the system would be increased to three species? Could a stable equilibrium be achieved in a non-fluctuating environment if each species is the winner to one and the loser to another species? Do adapted populations or communities perform ecosystem processes at differing rates and would rates of nutrient cycling, oxygen production or respiration, change?

There are many questions that remain to be answered when it comes to predicting phytoplankton community compositions of the future. The possible research directions that arose from this PhD are manifold and it will be interesting to see if it forms the basis for coming investigations. Concerning its relevance for natural species dynamics and predictive powers in models, the research conducted here is another small step in the ever increasing knowledge about our planet. Hopefully the science can be integrated into future models and studies in order to manage current ecosystem dynamics, and to also predict and alleviate potential changes that would be detrimental to functioning aquatic ecosystems.

Literature Cited in this Thesis

- Alexander, H., Rouco, M., Haley, S.T., Wilson, S.T., Karl, D.M., Dyrman, S.T., 2015. Functional group-specific traits drive phytoplankton dynamics in the oligotrophic ocean. *Proc. Natl. Acad. Sci.* 112, E5972–E5979. <https://doi.org/10.1073/pnas.1518165112>
- Alexander, M.A., Scott, J.D., Friedland, K.D., Mills, K.E., Nye, J.A., Pershing, A.J., Thomas, A.C., 2018. Projected sea surface temperatures over the 21st century: Changes in the mean, variability and extremes for large marine ecosystem regions of Northern Oceans. *Elem Sci Anth* 6, 9. <https://doi.org/10.1525/elementa.191>
- Andersen, R.A., 2005. *Algal Culturing Techniques*, 1st ed. Elsevier Academic Press.
- Anderson, T.R., Hessen, D.O., 1995. Carbon or nitrogen limitation in marine copepods? *J. Plankton Res.* 17, 317–331. <https://doi.org/10.1093/plankt/17.2.317>
- Anning, T., Harris, G., Geider, R., 2001. Thermal acclimation in the marine diatom *Chaetoceros calcitrans* (Bacillariophyceae). *Eur. J. Phycol.* 36, 233–241. <https://doi.org/10.1080/09670260110001735388>
- Asch, R.G., Stock, C.A., Sarmiento, J.L., 2019. Climate change impacts on mismatches between phytoplankton blooms and fish spawning phenology. *Glob. Change Biol.* 25, 2544–2559. <https://doi.org/10.1111/gcb.14650>
- Baker, K.G., Radford, D.T., Evenhuis, C., Kuzhiumparam, U., Ralph, P.J., Doblin, M.A., 2018. Thermal niche evolution of functional traits in a tropical marine phototroph. *J. Phycol.* 54, 799–810. <https://doi.org/10.1111/jpy.12759>
- Baker, K.G., Robinson, C.M., Radford, D.T., McInnes, A.S., Evenhuis, C., Doblin, M.A., 2016. Thermal Performance Curves of Functional Traits Aid Understanding of Thermally Induced Changes in Diatom-Mediated Biogeochemical Fluxes. *Front. Mar. Sci.* 3. <https://doi.org/10.3389/fmars.2016.00044>
- Baltar, F., Bayer, B., Bednarsek, N., Deppeler, S., Escribano, R., Gonzalez, C.E., Hansman, R.L., Mishra, R.K., Moran, M.A., Repeta, D.J., Robinson, C., Sintes, E., Tamburini, C., Valentin, L.E., Herndl, G.J., 2019. Towards Integrating Evolution, Metabolism, and Climate Change Studies of Marine Ecosystems. *Trends Ecol. Evol.* S0169534719301934. <https://doi.org/10.1016/j.tree.2019.07.003>
- Barton, A.D., Irwin, A.J., Finkel, Z.V., Stock, C.A., 2016. Anthropogenic climate change drives shift and shuffle in North Atlantic phytoplankton communities. *Proc. Natl. Acad. Sci.* 1–6. <https://doi.org/10.1073/pnas.1519080113>
- Barton, S., Yvon-Durocher, G., 2019. Quantifying the temperature dependence of growth rate in marine phytoplankton within and across species. *Limnol. Oceanogr.* Ino.11170. <https://doi.org/10.1002/lno.11170>
- Beardall, J., Allen, D., Bragg, J., Finkel, Z.V., Flynn, K.J., Quigg, A., Rees, T.A.V., Richardson, A., Raven, J.A., 2009. Allometry and stoichiometry of unicellular, colonial and multicellular phytoplankton: *Tansley review*. *New Phytol.* 181, 295–309. <https://doi.org/10.1111/j.1469-8137.2008.02660.x>

- Beckmann, A., Schaum, C.-E., Hense, I., 2019. Phytoplankton adaptation in ecosystem models. *J. Theor. Biol.* 468, 60–71. <https://doi.org/10.1016/j.jtbi.2019.01.041>
- Begon, M., Townsend, C.R., Harper, J.L., 2006. *Ecology: from individuals to ecosystems*, 4th ed. Blackwell Pub, Malden, MA.
- Beman, J.M., Arrigo, K.R., Matson, P.A., 2005. Agricultural runoff fuels large phytoplankton blooms in vulnerable areas of the ocean. *Nature* 434, 211–214.
- Benavides, M., Telen, D., Lauwers, J., Logist, F., Van Impe, J., Wouwer, A.V., 2015. Parameter Identification of the Droop Model Using Optimal Experiment Design. *IFAC-Pap.* 48, 586–591. <https://doi.org/10.1016/j.ifacol.2015.05.094>
- Bennett, E., Carpenter, S., Peterson, G., Cumming, G., Zurek, M., Pingali, P., 2003. Why global scenarios need ecology. *Front. Ecol. Environ.* 1, 322–329.
- Berdahl, M., Robock, A., Ji, D., Moore, J.C., Jones, A., Kravitz, B., Watanabe, S., 2014. Arctic cryosphere response in the Geoengineering Model Intercomparison Project G3 and G4 scenarios. *J. Geophys. Res. Atmospheres* 119, 1308–1321. <https://doi.org/10.1002/2013JD020627>
- Berges, J.A., Franklin, D.J., Harrison, P.J., 2001. Evolution of an artificial seawater medium: improvements in enriched seawater, artificial water over the last two decades. *J. Phycol.* 37, 1138–1145.
- Bernhardt, J.R., Kratina, P., Pereira, A.L., Tamminen, M., Thomas, M.K., Narwani, A., 2020. The evolution of competitive ability for essential resources. *Philos. Trans. R. Soc. B Biol. Sci.* 375, 10. <http://dx.doi.org/10.1098/rstb.2019.0247>
- Bernhardt, J.R., Sunday, J.M., Thompson, P.L., O'Connor, M.I., 2018. Nonlinear averaging of thermal experience predicts population growth rates in a thermally variable environment. *Proc. R. Soc. B Biol. Sci.* 285, 10.
- Bestion, E., García-Carreras, B., Schaum, C.-E., Pawar, S., Yvon-Durocher, G., 2018a. Metabolic traits predict the effects of warming on phytoplankton competition. *Ecol. Lett.* 21, 655–664. <https://doi.org/10.1111/ele.12932>
- Bestion, E., Schaum, C.-E., Yvon-Durocher, G., 2018b. Nutrient limitation constrains thermal tolerance in freshwater phytoplankton: Nutrients alter algal thermal tolerance. *Limnol. Oceanogr. Lett.* 3, 436–443. <https://doi.org/10.1002/lol2.10096>
- Boatman, T.G., Lawson, T., Geider, R.J., 2017. A Key Marine Diazotroph in a Changing Ocean: The Interacting Effects of Temperature, CO₂ and Light on the Growth of *Trichodesmium erythraeum* IMS101. *PLoS ONE* 12, 1–20. <https://doi.org/10.1371/journal.pone.0168796>
- Bopp, L., Aumont, O., Cadule, P., Alvain, S., Gehlen, M., 2005. Response of diatoms distribution to global warming and potential implications: A global model study: Diatoms and Climate Change. *Geophys. Res. Lett.* 32, 1–4. <https://doi.org/10.1029/2005GL023653>
- Bopp, L., Resplandy, L., Orr, J.C., Doney, S.C., Dunne, J.P., Gehlen, M., Halloran, P., Heinze, C., Ilyina, T., Seferian, R., Tjiputra, J., Vichi, M., 2013. Multiple stressors of ocean ecosystems in the 21st century: projections with CMIP5 models 10, 6225–6245. <https://doi.org/10.5194/bg-10-6225-2013>

- Boyce, D., Worm, B., 2015. Patterns and ecological implications of historical marine phytoplankton change. *Mar. Ecol. Prog. Ser.* 534, 251–272. <https://doi.org/10.3354/meps11411>
- Boyd, P., Hutchins, D., 2012. Understanding the responses of ocean biota to a complex matrix of cumulative anthropogenic change. *Mar. Ecol. Prog. Ser.* 470, 125–135. <https://doi.org/10.3354/meps10121>
- Boyd, P.W., 2019. Physiology and iron modulate diverse responses of diatoms to a warming Southern Ocean. *Nat. Clim. Change* 9, 148–152. <https://doi.org/10.1038/s41558-018-0389-1>
- Boyd, P.W., Collins, S., Dupont, S., Fabricius, K., Gattuso, J.-P., Havenhand, J., Hutchins, D.A., McGraw, C., Riebesell, U., Vichi, M., Biswas, H., Ciotti, Á.M., Dillingham, P., Gao, K., Gehlen, M., Hurd, C.L., Kurihawa, H., Navarro, J., Nilsson, G., Passow, U., Portner, H.-O., 2019. SCOR WG149 Handbook to support the SCOR Best Practice Guide for ‘Multiple Drivers’ Marine Research.
- Boyd, P.W., Cornwall, C.E., Davison, A., Doney, S.C., Fourquez, M., Hurd, C.L., Lima, I.D., McMinn, A., 2016. Biological responses to environmental heterogeneity under future ocean conditions. *Glob. Change Biol.* 22, 2633–2650. <https://doi.org/10.1111/gcb.13287>
- Boyd, P.W., Rynearson, T.A., Armstrong, E.A., Fu, F., Hayashi, K., Hu, Z., Hutchins, D.A., Kudela, R.M., Litchman, E., Mulholland, M.R., Passow, U., Strzepek, R.F., Whittaker, K.A., Yu, E., Thomas, M.K., 2013. Marine Phytoplankton Temperature versus Growth Responses from Polar to Tropical Waters – Outcome of a Scientific Community-Wide Study. *PLoS ONE* 8, e63091. <https://doi.org/10.1371/journal.pone.0063091>
- Cermeño, P., Marañín, E., Harbour, D., Figueiras, F.G., Crespo, B.G., Huete-Ortega, M., Varela, M., Harris, R.P., 2008. Resource levels, allometric scaling of population abundance, and marine phytoplankton diversity. *Limnol. Oceanogr.* 53, 312–318. <https://doi.org/10.4319/lo.2008.53.1.0312>
- Chase, J.M., Leibold, M.A., 2003. *Ecological Niches: Linking Classical and Contemporary Approaches*. University of Chicago Press.
- Chattopadhyay, S.R.J., 2007. Towards a resolution of ‘the paradox of the plankton’: A brief overview of the proposed mechanisms. *Ecol. Complex.* 4, 26–33.
- Chen, B., Liu, H., 2010. Relationships between phytoplankton growth and cell size in surface oceans: Interactive effects of temperature, nutrients, and grazing. *Limnol. Oceanogr.* 55, 965–972. <https://doi.org/10.4319/lo.2010.55.3.0965>
- Chepurnov, V.A., Mann, D.G., Sabbe, K., Vyverman, W., 2004. Experimental studies on sexual reproduction in diatoms. *Int. Rev. Cytol. Surv. Cell Biol.* 237, 91–154.
- Chesson, P., 2000. Mechanisms of Maintenance of Species Diversity. *Annu. Rev. Ecol. Syst.* 31, 343–366. <https://doi.org/10.1146/annurev.ecolsys.31.1.343>
- Chesson, P., Donahue, Megan J., Melbourne, Brett A., Sears, Anna L. W., 2005. Scale Transition Theory for Understanding Mechanisms in Metacommunities, in: *Metacommunities: Spatial Dynamics and Ecological Communities*. pp. 279–306.

- Chivers, W.J., Walne, A.W., Hays, G.C., 2017. Mismatch between marine plankton range movements and the velocity of climate change. *Nat. Commun.* 8, 14434. <https://doi.org/10.1038/ncomms14434>
- Chown, S., Hoffmann, A., Kristensen, T., Angilletta, M., Stenseth, N., Pertoldi, C., 2010. Adapting to climate change: a perspective from evolutionary physiology. *Clim. Res.* 43, 3–15. <https://doi.org/10.3354/cr00879>
- Christensen, M.R., Graham, M.D., Vinebrooke, R.D., Findlay, D.L., Paterson, M.J., Turner, M.A., 2006. Multiple anthropogenic stressors cause ecological surprises in boreal lakes. *Glob. Change Biol.* 12, 2316–2322. <https://doi.org/10.1111/j.1365-2486.2006.01257.x>
- Clements, F.E., Shelford, V.E., 1939. *Bio-ecology*. J. Wiley & Sons, Inc., New York.
- Cloern, J.E., 1996. Phytoplankton bloom dynamics in coastal ecosystems: a review with some general lessons from sustained investigations of San Francisco Bay, California. *Rev. Geophys.* 34, 127–168.
- Cloern, J.E., Dufford, R., 2005. Phytoplankton community ecology: principles applied in San Francisco Bay. *Mar. Ecol. Prog. Ser.* 285, 11–28.
- Coles, J.F., Jones, R.C., 2000. Effect of temperature on photosynthesis-light response and growth of four phytoplankton species isolated from a tidal freshwater river. *J. Phycol.* 36, 7–16. <https://doi.org/10.1046/j.1529-8817.2000.98219.x>
- Collins, C.D., Boylen, C.W., 1982. Physiological Response of *Anabaena variabilis* (Cyanophyceae) to instantaneous exposure to various combinations of light intensity and Temperature. *J. Phycol.* 18, 206–211.
- Collins, M., Knutti, R., Arblaster, J., Dufresne, J.-L., Fichet, T., Gao, X., Jr, W.J.G., Johns, T., Krinner, G., Shongwe, M., Weaver, A.J., Wehner, M., Allen, M.R., Andrews, T., Beyerle, U., Bitz, C.M., Bony, S., Booth, B.B.B., Brooks, H.E., Brovkin, V., Browne, O., Brutel-Vuilmet, C., Cane, M., Chadwick, R., Cook, E., Cook, K.H., Eby, M., Fasullo, J., Forest, C.E., Forster, P., Good, P., Goosse, H., Gregory, J.M., Hegerl, G.C., Hezel, P.J., Hodges, K.I., Holland, M.M., Huber, M., Joshi, M., Kharin, V., Kushnir, Y., Lawrence, D.M., Lee, R.W., Liddicoat, S., Lucas, C., Lucht, W., Marotzke, J., Massonnet, F., Matthews, H.D., Meinshausen, M., Morice, C., Otto, A., Patricola, C.M., Philippon, G., Rahmstorf, S., Riley, W.J., Saenko, O., Seager, R., Sedláček, J., Shaffrey, L.C., Shindell, D., Sillmann, J., Stevens, B., Stott, P.A., Webb, R., Zappa, G., Zickfeld, K., Joussaume, S., Mokssit, A., Taylor, K., Tett, S., 2013. Long-term Climate Change: Projections, Commitments and Irreversibility. *Clim. Change 2013 Phys. Sci. Basis Contrib. Work. Group Fifth Assess. Rep. Intergov. Panel Clim. Change* 108.
- Collins, S., Bell, G., 2004. Phenotypic consequences of 1,000 generations of selection at elevated CO₂ in a green alga. *Nature* 431, 566–569. <https://doi.org/10.1038/nature02945>
- Collins, S., Boyd, P.W., Doblin, M.A., 2020. Evolution, Microbes, and Changing Ocean Conditions. *Annu. Rev. Mar. Sci.* 12, 13.1-13.28. <https://doi.org/10.1146/annurev-marine-010318-095311>

- Collins, S., De Meaux, J., 2009. Adaptation to Different Rates of Environmental Change in *Chlamydomonas*. *Evolution* 63, 2952–2965. <https://doi.org/10.1111/j.1558-5646.2009.00770.x>
- Cresswell, R.C., Syrett, P.J., 1982. The uptake of nitrite by the diatom *Phaeodactylum*: Interactions between nitrite and nitrate. *J. Exp. Bot.* 33, 1111–1121.
- Crowder, L., Norse, E., 2008. Essential ecological insights for marine ecosystem-based management and marine spatial planning. *Mar. Policy* 32, 772–778. <https://doi.org/10.1016/j.marpol.2008.03.012>
- Davey, M., Tarran, G.A., Mills, M.M., Ridame, C., Geider, R.J., LaRoche, J., 2008. Nutrient limitation of picophytoplankton photosynthesis and growth in the tropical North Atlantic. *Limnol. Oceanogr.* 53, 1722–1733.
- Davison, I.R., 1991. Environmental Effects on Algal Photosynthesis: Temperature. *J. Phycol.* 27, 2–8.
- Davison, I.R., 1987. Adaptation of Photosynthesis in *Laminaria saccharina* (Phaeophyta) to Changes in Growth Temperature. *J. Phycol.* 23, 273–283. <https://doi.org/10.1111/j.1529-8817.1987.tb04135.x>
- Denny, M., 2017. The fallacy of the average: on the ubiquity, utility and continuing novelty of Jensen’s inequality. *J. Exp. Biol.* 220, 139–146. <https://doi.org/10.1242/jeb.140368>
- Descamps-Julien, B., Gonzalez, A., 2005. Stable coexistence in a fluctuating environment: an experimental demonstration. *Ecology* 86, 2815–2824.
- Dickman, E.M., Newell, J.M., Gonzalez, M.J., Vanni, M.J., 2008. Light, nutrients, and food-chain length constrain planktonic energy transfer efficiency across multiple trophic levels. *Proc. Natl. Acad. Sci.* 105, 18408–18412. <https://doi.org/10.1073/pnas.0805566105>
- Dickman, E.M., Vanni, M.J., Horgan, M.J., 2006. Interactive effects of light and nutrients on phytoplankton stoichiometry. *Oecologia* 149, 676–689. <https://doi.org/10.1007/s00442-006-0473-5>
- Dowd, W.W., King, F.A., Denny, M.W., 2015. Thermal variation, thermal extremes and the physiological performance of individuals. *J. Exp. Biol.* 218, 1956–1967. <https://doi.org/10.1242/jeb.114926>
- Duarte, C.M., 2014. Global change and the future ocean: a grand challenge for marine sciences. *Front. Mar. Sci.* 1. <https://doi.org/10.3389/fmars.2014.00063>
- Dutkiewicz, S., Morris, J.J., Follows, M.J., Scott, J., Levitan, O., Dyhrman, S.T., Berman-Frank, I., 2015. Impact of ocean acidification on the structure of future phytoplankton communities. *Nat. Clim. Change* 5, 1002–1006. <https://doi.org/10.1038/nclimate2722>
- Edwards, M., Richardson, A.J., 2004. Impact of climate change on marine pelagic phenology and trophic mismatch. *Nature* 430, 881–883.
- Eggers, S.L., Lewandowska, A.M., Barcelos E Ramos, J., Blanco-Ameijeiras, S., Gallo, F., Matthiessen, B., 2014. Community composition has greater impact on the functioning of marine phytoplankton communities than ocean acidification. *Glob. Change Biol.* 20, 713–723. <https://doi.org/10.1111/gcb.12421>

- Elser, J.J., Andersen, T., Baron, J.S., Bergström, A.-K., Jansson, M., Kyle, M., Nydick, K.R., Steger, L., Hessen, D.O., 2009. Shifts in lake N: P stoichiometry and nutrient limitation driven by atmospheric nitrogen deposition. *Science* 326, 835–837.
- Elser, J.J., Bracken, M.E.S., Cleland, E.E., Gruner, D.S., Harpole, W.S., Hillebrand, H., Ngai, J.T., Seabloom, E.W., Shurin, J.B., Smith, J.E., 2007. Global analysis of nitrogen and phosphorus limitation of primary producers in freshwater, marine and terrestrial ecosystems. *Ecol. Lett.* 10, 1135–1142. <https://doi.org/10.1111/j.1461-0248.2007.01113.x>
- Eppley, R.W., 1972. Temperature And Phytoplankton Growth In The Sea. *Fish. Bull.* 70, 1063–1085.
- Falkowski, P.G., Barber, R.T., Smetacek, V., 1998. Biogeochemical controls and feedbacks on ocean primary production. *Science* 281, 200–206.
- Falkowski, P.G., Oliver, M.J., 2007. Mix and match: how climate selects phytoplankton. *Nat. Rev. Microbiol.* 5, 813–819.
- Falkowski, P.G., Owens, T.G., 1980. Light—Shade Adaptation: Two Strategies in Marine Phytoplankton. *Plant Physiol.* 66, 592–595. <https://doi.org/10.1104/pp.66.4.592>
- Feng, Y., Hare, C., Leblanc, K., Rose, J., Zhang, Y., DiTullio, G., Lee, P., Wilhelm, S., Rowe, J., Sun, J., Nemcek, N., Gueguen, C., Passow, U., Benner, I., Brown, C., Hutchins, D., 2009. Effects of increased pCO₂ and temperature on the North Atlantic spring bloom. I. The phytoplankton community and biogeochemical response. *Mar. Ecol. Prog. Ser.* 388, 13–25. <https://doi.org/10.3354/meps08133>
- Feng, Y., Hare, C.E., Rose, J.M., Handy, S.M., DiTullio, G.R., Lee, P.A., Smith, W.O., Peloquin, J., Tozzi, S., Sun, J., Zhang, Y., Dunbar, R.B., Long, M.C., Sohst, B., Lohan, M., Hutchins, D.A., 2010. Interactive effects of iron, irradiance and CO₂ on Ross Sea phytoplankton. *Deep Sea Res. Part Oceanogr. Res. Pap.* 57, 368–383. <https://doi.org/10.1016/j.dsr.2009.10.013>
- Fiksen, Ø., Follows, M.J., Aksnes, D.L., 2013. Trait-based models of nutrient uptake in microbes extend the Michaelis-Menten framework. *Limnol. Oceanogr.* 58, 193–202. <https://doi.org/10.4319/lo.2013.58.1.0193>
- Flinn, P.W., 1991. Temperature-Dependent Functional Response of the Parasitoid *Cephalonomia waterstoni* (Gahan) (Hymenoptera: Bethyridae) Attacking Rusty Grain Beetle Larvae (Coleoptera: Cucujidae). *Environ. Entomol.* 20, 872–876.
- Flynn, K.J., 2008. The importance of the form of the quota curve and control of non-limiting nutrient transport in phytoplankton models. *J. Plankton Res.* 30, 423–438. <https://doi.org/10.1093/plankt/fbn007>
- Folke, C., Carpenter, S., Walker, B., Scheffer, M., Elmqvist, T., Gunderson, L., Holling, C.S., 2004. Regime Shifts, Resilience, and Biodiversity in Ecosystem Management. *Annu. Rev. Ecol. Evol. Syst.* 35, 557–581.
- Follows, M.J., Dutkiewicz, S., Grant, S., Chisholm, S.W., 2007. Emergent Biogeography of Microbial Communities in a Model Ocean. *Science* 315, 1843–1846. <https://doi.org/10.1126/science.1138544>

- Fu, F.-X., Warner, M.E., Zhang, Y., Feng, Y., Hutchins, D.A., 2007. Effects of Increased Temperature and CO₂ on Photosynthesis, Growth, and Elemental Ratios in Marine *Synechococcus* and *Prochlorococcus* (Cyanobacteria). *J. Phycol.* 43, 485–496. <https://doi.org/10.1111/j.1529-8817.2007.00355.x>
- Fujimoto, N., Sudo, R., Sugiura, N., Inamori, Y., 1997. Nutrient-limited growth of *Microcystis aeruginosa* and *Phormidium tenue* and competition under various N:P supply ratios and temperatures. *Limnol. Oceanogr.* 42, 250–256. <https://doi.org/10.4319/lo.1997.42.2.0250>
- Gallego, I., Venail, P., Ibelings, B.W., 2019. Size differences predict niche and relative fitness differences between phytoplankton species but not their coexistence. *ISME J.* 13, 1133–1143. <https://doi.org/10.1038/s41396-018-0330-7>
- Garcia-Carreras, B., Sal, S., Padfield, D., Kontopoulos, D.-G., Bestion, E., Schaum, C.-E., Yvon-Durocher, G., Pawar, S., 2018. Role of carbon allocation efficiency in the temperature dependence of autotroph growth rates. *PNAS* 115, 7361–7368.
- Geider, R.J., 1987. Light and Temperature Dependence of the Carbon to Chlorophyll a Ratio in Microalgae and Cyanobacteria: Implications for Photophysiology and Growth of Phytoplankton. *New Phytol.* 106, 1–34.
- Geider, Richard J., MacIntyre, H.L., Kana, T.M., 1997. Dynamic model of phytoplankton growth and acclimation: responses of the balanced growth rate and the chlorophyll a:carbon ratio to light, nutrient-limitation and temperature. *Mar. Ecol. Prog. Ser.* 148, 187–200. <https://doi.org/10.3354/meps148187>
- Geider, R. J., MacIntyre, H.L., Kana, T.M., 1997. Dynamic model of phytoplankton growth and acclimation: Responses of the balanced growth rate and the chlorophyll a:carbon ratio to light, nutrient-limitation and temperature. *Mar. Ecol. Prog. Ser.* 148, 187–200. <https://doi.org/10.3354/meps148187>
- Geider, R.J., MacIntyre, H.L., Kana, T.M., 1996. A dynamic model of photoadaptation in phytoplankton. *Limnol. Oceanogr.* 41, 1–15. <https://doi.org/10.4319/lo.1996.41.1.0001>
- Geider, R.J., MacIntyre, H.L., Kana, T.M., 1998. A dynamic regulatory model of phytoplanktonic acclimation to light, nutrients, and temperature. *Limnol. Oceanogr.* 43, 679–694. <https://doi.org/10.4319/lo.1998.43.4.0679>
- Geider, R.J., Moore, C.M., Suggett, D.J., 2014. Ecology of Marine Phytoplankton, in: *Ecology and the Environment, The Plant Sciences*. Springer, New York, NY, pp. 483–531.
- Geider, R.J., Osborne, B.A., Raven, J.A., 1986. Growth, Photosynthesis and Maintenance Metabolic Cost in the Diatom *Phaeodactylum Tricornutum* at Very Low Light Levels. *J. Phycol.* 22, 39–48.
- Gienapp, P., Teplitsky, C., Alho, J.S., Mills, J.A., Merilä, J., 2008. Climate change and evolution: disentangling environmental and genetic responses. *Mol. Ecol.* 17, 167–178. <https://doi.org/10.1111/j.1365-294X.2007.03413.x>
- Giorgio, P.A. del, 1992. The relationship between ETS (electron transport system) activity and oxygen consumption in lake plankton: a cross-system calibration. *J. Plankton Res.* 14, 1723–1741. <https://doi.org/10.1093/plankt/14.12.1723>

- Godhe, A., Ryneerson, T., 2017. The role of intraspecific variation in the ecological and evolutionary success of diatoms in changing environments. *Philos. Trans. R. Soc. B Biol. Sci.* 372, 20160399. <https://doi.org/10.1098/rstb.2016.0399>
- Goldman, J.C., Carpenter, E.J., 1974. A kinetic approach to the effect of temperature on algal growth. *Limnol. Oceanogr.* 19, 756–766.
- Goldman, J.C., Ryther, J.H., 1976. Temperature-influenced species competition in mass cultures of marine phytoplankton. *Biotechnol. Bioeng.* 18, 1125–1144.
- Gonzalez, A., Holt, R.D., 2002. The inflationary effects of environmental fluctuations in source–sink systems. *Proc. Natl. Acad. Sci.* 99, 14872–14877.
- Grenney, W.J., Bella, D.A., Curl, H.C., 1973. A Theoretical Approach to Interspecific Competition in Phytoplankton Communities. *Am. Nat.* 107, 405–425.
- Grimaud, G.M., Mairet, F., Sciandra, A., Bernard, O., 2017. Modelling the temperature effect on the specific growth rate of phytoplankton: a review. *Rev. Environ. Sci. Biotechnol.* 16, 625–645. <https://doi.org/10.1007/s11157-017-9443-0>
- Grover, J.P., 1991. Resource competition in a variable environment: phytoplankton growing according to the variable-internal-stores model. *Am. Nat.* 138, 811–835.
- Gruber, N., 2011. Warming up, turning sour, losing breath: ocean biogeochemistry under global change. *Philos. Trans. R. Soc. Lond. Math. Phys. Eng. Sci.* 369, 1980–1996. <https://doi.org/10.1098/rsta.2011.0003>
- Guillard, R.R.L., Kilham, P., 1977. *The Biology of Diatoms*, 1st ed, Botanical Monographs. University of California Press.
- Guillard, R.R.L., Ryther, J.H., 1962. Studies of Marine Planktonic Diatoms: I. *Cyclotella nana* Hustedt, and *Detonula confervacea* (Cleve) Gran. *Can. J. Microbiol.* 8, 229–239. <https://doi.org/10.1139/m62-029>
- Hallegraeff, G.M., 2010. Ocean Climate Change, Phytoplankton Community Responses, and Harmful Algal Blooms: A Formidable Predictive Challenge. *J. Phycol.* 46, 220–235. <https://doi.org/10.1111/j.1529-8817.2010.00815.x>
- Han, M.-S., Furuya, K., 2000. Size and species-specific primary productivity and community structure of phytoplankton in Tokyo Bay. *J. Plankton Res.* 22, 1221–1235. <https://doi.org/10.1093/plankt/22.7.1221>
- Hare, C., Leblanc, K., DiTullio, G., Kudela, R., Zhang, Y., Lee, P., Riseman, S., Hutchins, D., 2007. Consequences of increased temperature and CO₂ for phytoplankton community structure in the Bering Sea. *Mar. Ecol. Prog. Ser.* 352, 9–16. <https://doi.org/10.3354/meps07182>
- Harley, C.D.G., Connell, S.D., Doubleday, Z.A., Kelaher, B., Russell, B.D., Sarà, G., Helmuth, B., 2017. Conceptualizing ecosystem tipping points within a physiological framework. *Ecol. Evol.* 7, 6035–6045. <https://doi.org/10.1002/ece3.3164>
- Harrison, P.J., Waters, R.E., Taylor, F.J.R., 1980. A broad spectrum artificial seawater medium for coastal and open ocean phytoplankton. *J. Phycol.* 16, 28–35.

- Heil, C.A., Revilla, M., Glibert, P.M., Murasko, S., 2007. Nutrient quality drives differential phytoplankton community composition on the southwest Florida shelf. *Limnol. Oceanogr.* 52, 1067–1078. <https://doi.org/10.4319/lo.2007.52.3.1067>
- Heitzer, A., Kohler, H.-P.E., Reichert, P., Hamer, G., 1991. Utility of Phenomenological Models for Describing Temperature Dependence of Bacterial Growth. *Appl. Environ. Microbiol.* 57, 2656–2665.
- Hinshelwood, C.N., 1947. Presidential address. Some observations on present day chemical kinetics. *J. Chem. Soc. Resumed* 694–701.
- Huertas, I.E., Rouco, M., López-Rodas, V., Costas, E., 2011. Warming will affect phytoplankton differently: evidence through a mechanistic approach. *Proc. R. Soc. Lond. B Biol. Sci.* 278, 3534–3543. <https://doi.org/10.1098/rspb.2011.0160>
- Huisman, J., Jonker, R.R., Zonneveld, C., Weissing, F.J., 1999. Competition for Light Between Phytoplankton Species: Experimental Tests of Mechanistic Theory. *Ecology* 80, 211–222. [https://doi.org/10.1890/0012-9658\(1999\)080\[0211:CFLBPS\]2.0.CO;2](https://doi.org/10.1890/0012-9658(1999)080[0211:CFLBPS]2.0.CO;2)
- Huntingford, C., Jones, P.D., Livina, V.N., Lenton, T.M., Cox, P.M., 2013. No increase in global temperature variability despite changing regional patterns. *Nature* 500, 327–330. <https://doi.org/10.1038/nature12310>
- Hutchinson, G.E., 1961. The paradox of the plankton. *Am. Nat.* 95, 137–145.
- Iglesias-Rodríguez, M.D., Brown, C.W., Doney, S.C., Kleypas, J., Kolber, D., Kolber, Z., Hayes, P.K., Falkowski, P.G., 2002. Representing key phytoplankton functional groups in ocean carbon cycle models: Coccolithophorids: Coccolithophorids in Ocean Carbon Cycle Models. *Glob. Biogeochem. Cycles* 16, 47-1-47–20. <https://doi.org/10.1029/2001GB001454>
- Interlandi, S.J., Kilham, S.S., 2001. Limiting Resources and the Regulation of Diversity in Phytoplankton Communities. *Ecology* 82, 1270–1282. <https://doi.org/10.2307/2679988>
- IPCC, 2013. Climate Change: The Physical Science Basis. Contribution of Working Group I to the Fifth Assessment Report of the Intergovernmental Panel on Climate Change [Stocker, T.F., D. Qin, G.-K. Plattner, M. Tignor, S.K. Allen, J. Boschung, A. Nauels, Y. Xia, V. Bex and P.M. Midgley (eds.)]. Cambridge University Press, Cambridge, United Kingdom and New York, NY, USA, doi:10.1017/CBO9781107415324.
- Irwin, A.J., Finkel, Z.V., Müller-Karger, F.E., Troccoli Ghinaglia, L., 2015. Phytoplankton adapt to changing ocean environments. *Proc. Natl. Acad. Sci.* 112, 5762–5766. <https://doi.org/10.1073/pnas.1414752112>
- Irwin, A.J., Oliver, M.J., 2009. Are ocean deserts getting larger? *Geophys. Res. Lett.* 36, 1–5. <https://doi.org/10.1029/2009GL039883>
- Isnanto, R.R., 2011. Comparison on Several Smoothing Methods in Nonparametric Regression. *J. Sist. Komput.* 1, 41–47.
- Jacoby, W.G., 2000. Loess: a nonparametric, graphical tool for depicting relationships between variables. *Elect. Stud.* 19, 577–613.
- James, S.C., Boriah, V., 2010. Modeling Algae Growth in an Open-Channel Raceway. *J. Comput. Biol.* 17, 895–906. <https://doi.org/10.1089/cmb.2009.0078>

- Jassby, A.D., Platt, T., 1976. Mathematical formulation of the relationship between photosynthesis and light for phytoplankton: Photosynthesis-light equation. *Limnol. Oceanogr.* 21, 540–547. <https://doi.org/10.4319/lo.1976.21.4.0540>
- Johnson, F.H., Eyring, H., Williams, R.W., 1942. The nature of enzyme inhibitions in bacterial luminescence: Sulfanilamide, urethane, temperature and pressure. *J. Cell. Comp. Physiol.* 20, 247–268. <https://doi.org/10.1002/jcp.1030200302>
- Joshi, M., Hawkins, E., Sutton, R., Lowe, J., Frame, D., 2011. Projections of when temperature change will exceed 2 °C above pre-industrial levels. *Nat. Clim. Change* 1, 407–412. <https://doi.org/10.1038/nclimate1261>
- Kamykowski, D., 1986. A survey of protozoan laboratory temperature studies applied to marine dinoflagellate behavior from a field perspective. *Contrib Mar Sci* 27, 176–194.
- Karl, D.M., Bidigare, R.R., Letelier, R.M., 2001. Long-term changes in plankton community structure and productivity in the North Pacific Subtropical Gyre: The domain shift hypothesis 22.
- Klausmeier, C.A., Litchman, E., Levin, S.A., 2007. A model of flexible uptake of two essential resources. *J. Theor. Biol.* 246, 278–289. <https://doi.org/10.1016/j.jtbi.2006.12.032>
- Klausmeier, C.A., Litchman, E., Levin, S.A., 2004. Phytoplankton growth and stoichiometry under multiple nutrient limitation. *Limnol. Oceanogr.* 49, 1463–1470. https://doi.org/10.4319/lo.2004.49.4_part_2.1463
- Kling, J.D., Lee, M.D., Fu, F., Phan, M.D., Wang, X., Qu, P., Hutchins, D.A., 2020. Transient exposure to novel high temperatures reshapes coastal phytoplankton communities. *ISME J.* 14, 413–424. <https://doi.org/10.1038/s41396-019-0525-6>
- Kordas, R.L., Harley, C.D.G., O'Connor, M.I., 2011. Community ecology in a warming world: The influence of temperature on interspecific interactions in marine systems. *J. Exp. Mar. Biol. Ecol.* 400, 218–226. <https://doi.org/10.1016/j.jembe.2011.02.029>
- Koussoroplis, A.-M., Pincebourde, S., Wacker, A., 2017. Understanding and predicting physiological performance of organisms in fluctuating and multifactorial environments. *Ecol. Monogr.* 87, 178–197. <https://doi.org/10.1002/ecm.1247>
- Kratina, P., Greig, H.S., Thompson, P.L., Carvalho-Pereira, T.S.A., Shurin, J.B., 2012. Warming modifies trophic cascades and eutrophication in experimental freshwater communities. *Ecology* 93, 1421–1430. <https://doi.org/10.1890/11-1595.1>
- Kremer, C.T., Klausmeier, C.A., 2017. Species packing in eco-evolutionary models of seasonally fluctuating environments. *Ecol. Lett.* 20, 1158–1168. <https://doi.org/10.1111/ele.12813>
- Krenek, S., Petzoldt, T., Berendonk, T.U., 2012. Coping with Temperature at the Warm Edge – Patterns of Thermal Adaptation in the Microbial Eukaryote *Paramecium caudatum*. *PLoS ONE* 7, e30598. <https://doi.org/10.1371/journal.pone.0030598>
- Kubaneck, J., Hicks, M.K., Naar, J., Villareal, T.A., 2005. Does the red tide dinoflagellate *Karenia brevis* use allelopathy to outcompete other phytoplankton? *Limnol. Oceanogr.* 50, 883–895. <https://doi.org/10.4319/lo.2005.50.3.0883>

- Kuebler, J.E., Davison, I.R., Yarish, C., 1991. Photosynthetic adaptation to temperature in the red algae *Lomentaria baileyana* and *Lomentaria orcadensis*. *Br. Phycol. J.* 26, 9–19. <https://doi.org/10.1080/00071619100650021>
- Lakeman, M.B., von Dassow, P., Cattolico, R.A., 2009. The strain concept in phytoplankton ecology. *Harmful Algae* 8, 746–758. <https://doi.org/10.1016/j.hal.2008.11.011>
- Lalli, C.M., Parsons, T.R., 2006. *Biological oceanography: an introduction*, 2. ed., reprinted. ed, Open University oceanography series. Elsevier Butterworth-Heinemann, Amsterdam.
- Lawson, C.R., Vindenes, Y., Bailey, L., van de Pol, M., 2015. Environmental variation and population responses to global change. *Ecol. Lett.* 18, 724–736. <https://doi.org/10.1111/ele.12437>
- le B. Williams, P.J., 1998. The balance of plankton respiration and photosynthesis in the open oceans. *Nature* 394, 55–57. <https://doi.org/10.1038/27878>
- Lee, J.J., McEnery, M., Pierce, S., Freudenthal, H.D., Muller, W.A., 1966. Tracer Experiments in Feeding Littoral Foraminifera. *J. Protozool.* 13, 659–670. <https://doi.org/10.1111/j.1550-7408.1966.tb01978.x>
- Lemley, D.A., Adams, J.B., Bornman, T.G., Campbell, E.E., Deyzel, S.H.P., 2019. Land-derived inorganic nutrient loading to coastal waters and potential implications for nearshore plankton dynamics. *Cont. Shelf Res.* 174, 1–11. <https://doi.org/10.1016/j.csr.2019.01.003>
- Lewington-Pearce, L., Narwani, A., Thomas, M.K., Kremer, C.T., Vogler, H., Kratina, P., 2019. Temperature-dependence of minimum resource requirements alters competitive hierarchies in phytoplankton. *Oikos* 128, 1194–1205. <https://doi.org/10.1111/oik.06060>
- Li, W., Smith, J., Piatt, T., 1984. Temperature response of photosynthetic capacity and carboxylase activity in Arctic marine phytoplankton. *Mar. Ecol. Prog. Ser.* 17, 237–243. <https://doi.org/10.3354/meps017237>
- Li, W.K., Dickie, P.M., 1987. Temperature characteristics of photosynthetic and heterotrophic activities: seasonal variations in temperate microbial plankton. *Appl. Environ. Microbiol.* 53, 2282–2295.
- Li, W.K.W., Glen Harrison, W., Head, E.J.H., 2006. Coherent assembly of phytoplankton communities in diverse temperate ocean ecosystems. *Proc. R. Soc. B Biol. Sci.* 273, 1953–1960. <https://doi.org/10.1098/rspb.2006.3529>
- Li, W.K.W., Morris, I., 1982. Temperature adaptation in *Phaeodactylum tricornutum* Bohlin: Photosynthetic Rate Compensation and Capacity. *J. Exp. Mar. Biol. Ecol.* 58, 135–150.
- Liang, Y., Koester, J.A., Liefer, J.D., Irwin, A.J., Finkel, Z.V., 2019. Molecular mechanisms of temperature acclimation and adaptation in marine diatoms. *ISME J.* 13, 2415–2425. <https://doi.org/10.1038/s41396-019-0441-9>
- Listmann, L., LeRoch, M., Schlüter, L., Thomas, M.K., Reusch, T.B.H., 2016. Swift thermal reaction norm evolution in a key marine phytoplankton species. *Evol. Appl.* 1–9. <https://doi.org/10.1111/eva.12362>
- Litchman, E., 2000. Growth of Phytoplankton Under Fluctuating Light. *Freshw. Biol.* 44, 223–235.

- Litchman, E., Edwards, K., Klausmeier, C., Thomas, M., 2012. Phytoplankton niches, traits and eco-evolutionary responses to global environmental change. *Mar. Ecol. Prog. Ser.* 470, 235–248. <https://doi.org/10.3354/meps09912>
- Litchman, E., Klausmeier, C.A., 2008. Trait-Based Community Ecology of Phytoplankton. *Annu. Rev. Ecol. Evol. Syst.* 39, 615–639.
- Litchman, E., Klausmeier, C.A., Miller, J.R., Schofield, O.M., Falkowski, P.G., 2006. Multi-nutrient, multi-group model of present and future oceanic phytoplankton communities. *Biogeosciences Discuss.* 3, 607–663.
- Litchman, E., Pinto, P. de T., Klausmeier, C.A., Thomas, M.K., Yoshiyama, K., 2010. Linking traits to species diversity and community structure in phytoplankton. *Hydrobiologia* 653, 15–28.
- Low-Décarie, E., 2017. R package “temperatureresponse.”
- Low-Décarie, E., Boatman, T.G., Bennett, N., Passfield, W., Gavalás-Olea, A., Siegel, P., Geider, R.J., 2017. Predictions of response to temperature are contingent on model choice and data quality. *Ecol. Evol.* 1–15. <https://doi.org/10.1002/ece3.3576>
- Low-Décarie, E., Fussmann, G.F., Bell, G., 2011. The effect of elevated CO₂ on growth and competition in experimental phytoplankton communities: CO₂ alters phytoplankton community dynamics. *Glob. Change Biol.* 17, 2525–2535. <https://doi.org/10.1111/j.1365-2486.2011.02402.x>
- Maddux, W.S., Jones, R.F., 1964. Some Interactions of Temperature, Light Intensity, and Nutrient Concentration During the Continuous Culture of *Nitzschia closterium* and *Tetraselmis sp.* *Limnol. Oceanogr.* 9, 79–86. <https://doi.org/10.4319/lo.1964.9.1.0079>
- Malviya, S., Scalco, E., Audic, S., Vincent, F., Veluchamy, A., Poulain, J., Wincker, P., Iudicone, D., de Vargas, C., Bittner, L., others, 2016. Insights into global diatom distribution and diversity in the world’s ocean. *Proc. Natl. Acad. Sci.* E1516–E1525.
- Marañón, E., Cermeño, P., Latasa, M., Tadonlélé, R.D., 2012. Temperature, resources, and phytoplankton size structure in the ocean. *Limnol. Oceanogr.* 57, 1266–1278. <https://doi.org/10.4319/lo.2012.57.5.1266>
- McAndrew, P.M., Bjorkman, K.M., Church, M.J., Morris, P.J., Jachowski, N., Williams, P.J., Karl, D.M., 2007. Metabolic response of oligotrophic plankton communities to deep water nutrient enrichment. *Mar. Ecol. Prog. Ser.* 332, 63–75.
- McKinnon, A.D., Duggan, S., Logan, M., Lønborg, C., 2017. Plankton Respiration, Production, and Trophic State in Tropical Coastal and Shelf Waters Adjacent to Northern Australia. *Front. Mar. Sci.* 4, 1–18. <https://doi.org/10.3389/fmars.2017.00346>
- McPeck, M.A., 2019. Limiting Similarity? The Ecological Dynamics of Natural Selection among Resources and Consumers Caused by Both Apparent and Resource Competition. *Am. Nat.* 193, E000–E000. <https://doi.org/10.1086/701629>
- Mitz, C., Thome, C., Thompson, J., Manzon, R.G., Wilson, J.Y., Boreham, D.R., 2017. A method to transform a variable thermal regime to a physiologically equivalent effective temperature. *J. Therm. Biol.* 65, 21–25. <https://doi.org/10.1016/j.jtherbio.2016.12.011>

- Montagnes, D.J.S., Morgan, G., Bissinger, J.E., Atkinson, D., Weisse, T., 2008. Short-term temperature change may impact freshwater carbon flux: A microbial perspective. *Glob. Change Biol.* 14, 2823–2838. <https://doi.org/10.1111/j.1365-2486.2008.01700.x>
- Montes-Hugo, M., Doney, S.C., Ducklow, H.W., Fraser, W., Martinson, D., Stammerjohn, S.E., Schofield, O., 2009. Recent Changes in Phytoplankton Communities Associated with Rapid Regional Climate Change Along the Western Antarctic Peninsula. *Science* 323, 1470–1473. <https://doi.org/10.1126/science.1164533>
- Moore, C.M., Suggett, D.J., Hickman, A.E., Kim, Y.-N., Tweddle, J.F., Sharples, J., Geider, R.J., Holligan, P.M., 2006. Phytoplankton photoacclimation and photoadaptation in response to environmental gradients in a shelf sea. *Limnol. Oceanogr.* 51, 936–949. <https://doi.org/10.4319/lo.2006.51.2.0936>
- Morán, X.A.G., López-Urrutia, Á., Calvo-Díaz, A., Li, W.K.W., 2010. Increasing importance of small phytoplankton in a warmer ocean. *Glob. Change Biol.* 16, 1137–1144. <https://doi.org/10.1111/j.1365-2486.2009.01960.x>
- Morel, F.M.M., 1987. Kinetics of Nutrient Uptake and Growth in Phytoplankton. *J. Phycol.* 23, 137–150.
- Mosser, J.L., Fisher, N.S., Wurster, C.F., 1972. Polychlorinated biphenyls and DDT alter species composition in mixed cultures of algae. *Science* 176, 533–535.
- Nelson, D.M., D’Elia, C.F., Guillard, R.R.L., 1979. Growth and competition of the marine diatoms *Phaeodactylum tricornutum* and *Thalassiosira pseudonana*. II. Light limitation. *Mar. Biol.* 50, 313–318. <https://doi.org/10.1007/BF00387008>
- Nixon, S.W., 1995. Coastal Marine Eutrophication: A Definition, Social Causes, and Future Concerns. *Ophelia* 41, 199–219.
- Padfield, D., Yvon-Durocher, Genevieve, Buckling, A., Jennings, S., Yvon-Durocher, Gabriel, 2015. Rapid evolution of metabolic traits explains thermal adaptation in phytoplankton. *Ecol. Lett.* <https://doi.org/10.1111/ele.12545>
- Pardew, J., Blanco Pimentel, M., Low-Decarie, E., 2018. Predictable ecological response to rising CO₂ of a community of marine phytoplankton. *Ecol. Evol.* 8, 4292–4302. <https://doi.org/10.1002/ece3.3971>
- Parkhill, J.-P., Maillet, G., Cullen, J.J., 2001. Fluorescence-based maximal quantum yield for PSII as a diagnostic of nutrient stress. *J. Phycol.* 37, 517–529.
- Pennekamp, F., Iles, A.C., Garland, J., Brennan, G., Brose, U., Gaedke, U., Jacob, U., Kratina, P., Matthews, B., Munch, S., Novak, M., Palamara, G.M., Rall, B.C., Rosenbaum, B., Tabi, A., Ward, C., Williams, R., Ye, H., Petchey, O.L., 2019. The intrinsic predictability of ecological time series and its potential to guide forecasting. *Ecol. Monogr.* 89, 1–17. <https://doi.org/10.1002/ecm.1359>
- Perruche, C., Rivière, P., Pondaven, P., Carton, X., 2010. Phytoplankton competition and coexistence: Intrinsic ecosystem dynamics and impact of vertical mixing. *J. Mar. Syst.* 81, 99–111. <https://doi.org/10.1016/j.jmarsys.2009.12.006>
- Petchey, O.L., Pontarp, M., Massie, T.M., Kéfi, S., Ozgul, A., Weilenmann, M., Palamara, G.M., Altermatt, F., Matthews, B., Levine, J.M., Childs, D.Z., McGill, B.J., Schaeppman, M.E.,

- Schmid, B., Spaak, P., Beckerman, A.P., Pennekamp, F., Pearse, I.S., 2015. The ecological forecast horizon, and examples of its uses and determinants. *Ecol. Lett.* 18, 597–611. <https://doi.org/10.1111/ele.12443>
- Peter, K.H., Sommer, U., 2012. Phytoplankton Cell Size: Intra- and Interspecific Effects of Warming and Grazing. *PLoS ONE* 7, e49632. <https://doi.org/10.1371/journal.pone.0049632>
- Pichierri, S., Accoroni, S., Pezzolesi, L., Guerrini, F., Romagnoli, T., Pistocchi, R., Totti, C., 2017. Allelopathic effects of diatom filtrates on the toxic benthic dinoflagellate *Ostreopsis cf. ovata*. *Mar. Environ. Res.* 131, 116–122. <https://doi.org/10.1016/j.marenvres.2017.09.016>
- Pittera, J., Humily, F., Thorel, M., Grulois, D., Garczarek, L., Six, C., 2014. Connecting thermal physiology and latitudinal niche partitioning in marine *Synechococcus*. *ISME J.* 8, 1221–1236. <https://doi.org/10.1038/ismej.2013.228>
- Pörtner, H.-O., 2002. Climate variations and the physiological basis of temperature dependent biogeography: systemic to molecular hierarchy of thermal tolerance in animals. *Comp. Biochem. Physiol. A. Mol. Integr. Physiol.* 132, 739–761.
- Pörtner, H.-O., Roberts, D.C., Masson-Delmotte, V., Zhai, P., Tignor, M., Poloczanska, E., Mintenbeck, K., Nicolai, M., Okem, A., Petzold, J., Rama, B., Weyer, N., 2019. IPCC Special Report on the Ocean and the Cryosphere in a Changing Climate: Summary for Policymakers (IPCC report).
- Prézelin, B.B., Hofmann, E.E., Moline, M., Klinck, J.M., 2004. Physical forcing of phytoplankton community structure and primary production in continental shelf waters of the Western Antarctic Peninsula. *J. Mar. Res.* 62, 419–460. <https://doi.org/10.1357/0022240041446173>
- Ptacnik, R., Solimini, A.G., Andersen, T., Tamminen, T., Brettum, P., Lepistö, L., Willén, E., Rekolainen, S., 2008. Diversity predicts stability and resource use efficiency in natural phytoplankton communities. *Proc. Natl. Acad. Sci.* 105, 5134–5138. <https://doi.org/10.1073/pnas.0708328105>
- R Core Team, 2016. R: A language and environment for statistical computing. R Foundation for Statistical Computing, Vienna, Austria.
- Raimbault, P., 1984. Influence of temperature on the transient response in nitrate uptake and reduction by four marine diatoms. *J. Exp. Mar. Biol. Ecol.* 84, 37–53. [https://doi.org/10.1016/0022-0981\(84\)90229-6](https://doi.org/10.1016/0022-0981(84)90229-6)
- Ras, M., Steyer, J.-P., Bernard, O., 2013. Temperature effect on microalgae: a crucial factor for outdoor production. *Rev. Environ. Sci. Biotechnol.* 12, 153–164. <https://doi.org/10.1007/s11157-013-9310-6>
- Rasconi, S., Winter, K., Kainz, M.J., 2017. Temperature increase and fluctuation induce phytoplankton biodiversity loss - Evidence from a multi-seasonal mesocosm experiment. *Ecol. Evol.* 7, 2936–2946. <https://doi.org/10.1002/ece3.2889>
- Ratkowsky, D.A., Lowry, R.K., McMeekin, T.A., Stokes, A.N., Chandler, R.E., 1983. Model for bacterial culture growth rate throughout the entire biokinetic temperature range. *J. Bacteriol.* 154, 1222–1226.

- Raven, J.A., Geider, R.J., 1988. Temperature and algal growth. *New Phytol.* 110, 441–461.
- Regan, D.L., Ivancic, N., 1984. Mixed populations of marine microalgae in continuous culture: Factors affecting species dominance and biomass productivity. *Biotechnol. Bioeng.* 26, 1265–1271. <https://doi.org/10.1002/bit.260261102>
- Rengefors, K., Kremp, A., Reusch, T.B.H., Wood, A.M., 2017. Genetic diversity and evolution in eukaryotic phytoplankton: revelations from population genetic studies. *J. Plankton Res.* 39, 165–179. <https://doi.org/10.1093/plankt/fbw098>
- Reusch, T.B.H., Boyd, P.W., 2013. Experimental Evolution Meets Marine Phytoplankton. *Evolution* 67, 1849–1859. <https://doi.org/10.1111/evo.12035>
- Rhee, G.-Y., 1982. Effects of Environmental Factors and Their Interactions on Phytoplankton Growth, in: *Advances in Microbial Ecology*. Springer, Boston, MA, US, pp. 33–74.
- Rhee, G.-Y., Gotham, I.J., 1981. The effect of environmental factors on phytoplankton growth: Temperature and the interactions of temperature with nutrient limitation: Temperature-nutrient interactions. *Limnol. Oceanogr.* 26, 635–648. <https://doi.org/10.4319/lo.1981.26.4.0635>
- Richman, S., Rogers, J.N., 1969. The Feeding of *Calanus helgolandicus* on Synchronously Growing Populations of the Marine Diatom *Ditylum brightwellii*: *Calanus* fed on Synchronously Growing *Ditylum*. *Limnol. Oceanogr.* 14, 701–709. <https://doi.org/10.4319/lo.1969.14.5.0701>
- Ricklefs, R.E., Miller, G.L., 1999. *Ecology*, 4th Edition. ed. W. H. Freeman.
- Riebesell, U., 2004. Effects of CO₂ Enrichment on Marine Phytoplankton. *J. Oceanogr.* 60, 719–729. <https://doi.org/10.1007/s10872-004-5764-z>
- Ritchie, R.J., 2008. Universal chlorophyll equations for estimating chlorophylls *a*, *b*, *c*, and *d* and total chlorophylls in natural assemblages of photosynthetic organisms using acetone, methanol, or ethanol solvents. *Photosynthetica* 46, 115–126.
- Robarts, R.D., Zohary, T., 1987. Temperature effects on photosynthetic capacity, respiration, and growth rates of bloom-forming cyanobacteria. *N. Z. J. Mar. Freshw. Res.* 21, 391–399. <https://doi.org/10.1080/00288330.1987.9516235>
- Rocap, G., Larimer, F.W., Lamerdin, J., Malfatti, S., Chain, P., Ahlgren, N.A., Arellano, A., Coleman, M., Hauser, L., Hess, W.R., Johnson, Z.I., Land, M., Lindell, D., Post, A.F., Regala, W., Shah, M., Shaw, S.L., Steglich, C., Sullivan, M.B., Ting, C.S., Tolonen, A., Webb, E.A., Zinser, E.R., Chisholm, S.W., 2003. Genome divergence in two *Prochlorococcus* ecotypes reflects oceanic niche differentiation. *Nature* 424, 1042–1047. <https://doi.org/10.1038/nature01947>
- Romero, G.Q., Gonçalves-Souza, T., Kratina, P., Marino, N.A.C., Petry, W.K., Sobral-Souza, T., Roslin, T., 2018. Global predation pressure redistribution under future climate change. *Nat. Clim. Change* 8, 1087–1091. <https://doi.org/10.1038/s41558-018-0347-y>
- Rose, J., Feng, Y., Gobler, C., Gutierrez, R., Hare, C., Leblanc, K., Hutchins, D., 2009. Effects of increased pCO₂ and temperature on the North Atlantic spring bloom. II. Microzooplankton abundance and grazing. *Mar. Ecol. Prog. Ser.* 388, 27–40. <https://doi.org/10.3354/meps08134>

- Rost, B., Zondervan, I., Wolf-Gladrow, D., 2008. Sensitivity of phytoplankton to future changes in ocean carbonate chemistry: current knowledge, contradictions and research directions. *Mar. Ecol. Prog. Ser.* 373, 227–237. <https://doi.org/10.3354/meps07776>
- Schaum, C.-E., 2014. Plastic fantastic; phenotypic plasticity, evolution, and adaptation of marine picoplankton in response to elevated pCO₂ (PhD Thesis). University of Edinburgh, UK.
- Schaum, C.-E., Barton, S., Bestion, E., Buckling, A., Garcia-Carreras, B., Lopez, P., Lowe, C., Pawar, S., Smirnov, N., Trimmer, M., Yvon-Durocher, G., 2017. Adaptation of phytoplankton to a decade of experimental warming linked to increased photosynthesis. *Nat. Ecol. Evol.* 1, 1–7. <https://doi.org/10.1038/s41559-017-0094>
- Schaum, C.-E., Buckling, A., Smirnov, N., Studholme, D.J., Yvon-Durocher, G., 2018. Environmental fluctuations accelerate molecular evolution of thermal tolerance in a marine diatom. *Nat. Commun.* 9, 1–14. <https://doi.org/10.1038/s41467-018-03906-5>
- Schaum, E., Rost, B., Millar, A.J., Collins, S., 2012. Variation in plastic responses of a globally distributed picoplankton species to ocean acidification. *Nat. Clim. Change* 3, 298–302. <https://doi.org/10.1038/nclimate1774>
- Schlüter, L., Lohbeck, K.T., Gutowska, M.A., Gröger, J.P., Riebesell, U., Reusch, T.B.H., 2014. Adaptation of a globally important coccolithophore to ocean warming and acidification. *Nat. Clim. Change* 4, 1024–1030. <https://doi.org/10.1038/nclimate2379>
- Schmidt, K., 2017. Thermal adaptation of *Thalassiosira pseudonana* using experimental evolution approaches (Ph.D.). University of East Anglia.
- Schnetger, B., Lehnert, C., 2014. Determination of nitrate plus nitrite in small volume marine water samples using vanadium(III)chloride as a reduction agent. *Mar. Chem.* 160, 91–98. <https://doi.org/10.1016/j.marchem.2014.01.010>
- Schoener, T.W., 1976. Alternatives to Lotka-Volterra competition: models of intermediate complexity. *Theor. Popul. Biol.* 10, 309–333.
- Schoolfield, R.M., Sharpe, P.J.H., Magnuson, C.E., 1981. Non-linear regression of biological temperature-dependent rate models based on absolute reaction-rate theory. *J. Theor. Biol.* 88, 719–731.
- Schulte, P.M., Healy, T.M., Fanguy, N.A., 2011. Thermal Performance Curves, Phenotypic Plasticity, and the Time Scales of Temperature Exposure. *Integr. Comp. Biol.* 51, 691–702. <https://doi.org/10.1093/icb/icr097>
- Segura, A.M., Calliari, D., Kruk, C., Conde, D., Bonilla, S., Fort, H., 2011. Emergent neutrality drives phytoplankton species coexistence. *Proc. R. Soc. B Biol. Sci.* 278, 2355–2361. <https://doi.org/10.1098/rspb.2010.2464>
- Sharp, J.H., Underhill, P.A., Hughes, D.J., 1979. Interaction (Allelopathy) between marine diatoms: *Thalassiosira pseudonana* and *Phaeodactylum tricoronatum*. *J. Phycol.* 15, 353–362.
- Shenoi, S.S.C., Nasnodkar, N., Rajesh, G., Jossia Joseph, K., Suresh, I., Almeida, A.M., 2009. On the diurnal ranges of Sea Surface Temperature (SST) in the north Indian Ocean. *J. Earth Syst. Sci.* 118, 483–496. <https://doi.org/10.1007/s12040-009-0038-1>

- Shimoda, Y., Rao, Y.R., Watson, S., Arhonditsis, G.B., 2016. Optimizing the complexity of phytoplankton functional group modeling: An allometric approach. *Ecol. Inform.* 31, 1–17. <https://doi.org/10.1016/j.ecoinf.2015.11.001>
- Shuler, C.K., Amato, D.W., Gibson, V., Baker, L., Olguin, A.N., Dulai, H., Smith, C.M., Alegado, R.A., 2019. Assessment of Terrigenous Nutrient Loading to Coastal Ecosystems along a Human Land-Use Gradient, Tutuila, American Samoa. *6* 18, 1–27.
- Siegel, P., Baker, K.G., Low-Décarie, E., Geider, R.J., 2020. High predictability of direct competition between marine diatoms under different temperatures and nutrient states. *Ecol. Evol.* 10, 7276–7290. <https://doi.org/10.1002/ece3.6453>
- Sinclair, B.J., Marshall, K.E., Sewell, M.A., Levesque, D.L., Willett, C.S., Slotsbo, S., Dong, Y., Harley, C.D.G., Marshall, D.J., Helmuth, B.S., Huey, R.B., 2016. Can we predict ectotherm responses to climate change using thermal performance curves and body temperatures? *Ecol. Lett.* 19, 1372–1385. <https://doi.org/10.1111/ele.12686>
- Smith, R.E.H., Kalff, J., 1982. Size-dependent Phosphorus Uptake Kinetics and Cell Quota in Phytoplankton. *J. Phycol.* 18, 275–284.
- Smith, S., Yamanaka, Y., Pahlow, M., Oschlies, A., 2009. Optimal uptake kinetics: physiological acclimation explains the pattern of nitrate uptake by phytoplankton in the ocean. *Mar. Ecol. Prog. Ser.* 384, 1–12. <https://doi.org/10.3354/meps08022>
- Sommer, U., 2002. Experimental systems in aquatic ecology. *Encycl. Life Sci.* 1–7.
- Sommer, U., 1991. A Comparison of the Droop and the Monod Models of Nutrient Limited Growth Applied to Natural Populations of Phytoplankton. *Funct. Ecol.* 5, 535–544. <https://doi.org/10.2307/2389636>
- Sommer, U., 1989. The Role of Competition for Resources in Phytoplankton Succession, in: Sommer, U. (Ed.), *Plankton Ecology*, Brock/Springer Series in Contemporary Bioscience. Springer Berlin Heidelberg, pp. 57–106. https://doi.org/10.1007/978-3-642-74890-5_3
- Sommer, U., 1984. The paradox of the plankton: Fluctuations of phosphorus availability maintain diversity of phytoplankton in flow-through cultures. *Limnol. Oceanogr.* 29, 633–636.
- Sommer, U., 1983. Nutrient competition between phytoplankton species in multispecies chemostat experiments. *Arch. Für Hydrobiol.* 96, 399–416.
- Staehr, P.A., Sand-Jensen, K., 2006. Seasonal changes in temperature and nutrient control of photosynthesis, respiration and growth of natural phytoplankton communities. *Freshw. Biol.* 51, 249–262. <https://doi.org/10.1111/j.1365-2427.2005.01490.x>
- Stock, C.A., Alexander, M.A., Bond, N.A., Brander, K.M., Cheung, W.W.L., Curchitser, E.N., Delworth, T.L., Dunne, J.P., Griffies, S.M., Haltuch, M.A., Hare, J.A., Hollowed, A.B., Lehodey, P., Levin, S.A., Link, J.S., Rose, K.A., Rykaczewski, R.R., Sarmiento, J.L., Stouffer, R.J., Schwing, F.B., Vecchi, G.A., Werner, F.E., 2011. On the use of IPCC-class models to assess the impact of climate on Living Marine Resources. *Prog. Oceanogr.* 88, 1–27. <https://doi.org/10.1016/j.pocean.2010.09.001>

- Stoermer, E.F., Ladewski, T.B., 1976. Apparent optimal temperatures for the occurrence of some common phytoplankton species in southern Lake Michigan. University of Michigan.
- Strzepek, R.F., Boyd, P.W., Sunda, W.G., 2019. Photosynthetic adaptation to low iron, light, and temperature in Southern Ocean phytoplankton. *Proc. Natl. Acad. Sci.* 116, 4388–4393. <https://doi.org/10.1073/pnas.1810886116>
- Suthers, I., Rissik, D., 2009. *Plankton: A guide to their ecology and monitoring for water quality*, 1st ed. CSIRO PUBLISHING, Australia.
- Suzuki, Y., Takahashi, M., 1995. Growth Response Of Several Diatom Species Isolated from Various Environments to Temperature. *J. Phycol.* 31, 880–888.
- Tatters, A., Roleda, M.Y., Schnetzer, A., Fu, F., Hurd, C.L., Boyd, P.W., Caron, D.A., Lie, A.A.Y., Hoffmann, L.J., Hutchins, D.A., 2013. Short- and long-term conditioning of a temperate marine diatom community to acidification and warming. *Philos. Trans. R. Soc. B Biol. Sci.* 368, 20120437. <https://doi.org/10.1098/rstb.2012.0437>
- Thomas, M.K., Aranguren-Gassis, M., Kremer, C.T., Gould, M.R., Anderson, K., Klausmeier, C.A., Litchman, E., 2017. Temperature-nutrient interactions exacerbate sensitivity to warming in phytoplankton. *Glob. Change Biol.* 23, 3269–3280. <https://doi.org/10.1111/gcb.13641>
- Thomas, M. K., Kremer, C.T., Klausmeier, C. a., Litchman, E., 2012. A Global Pattern of Thermal Adaptation in Marine Phytoplankton. *Science* 338, 1085–1088. <https://doi.org/10.1126/science.1224836>
- Thomas, Mridul K., Kremer, C.T., Klausmeier, C.A., Litchman, E., 2012. A Global Pattern of Thermal Adaptation in Marine Phytoplankton. *Science* 338, 1085–1088. <https://doi.org/10.1126/science.1224836>
- Tilman, D., 1987. Importance of Mechanisms of Interspecific Competition. *Am. Nat.* 129, 769–774.
- Tilman, D., 1981. Tests of Resource Competition Theory Using Four Species of Lake Michigan Algae. *Ecology* 62, 802–815. <https://doi.org/10.2307/1937747>
- Tilman, D., 1977. Resource Competition between Plankton Algae: An Experimental and Theoretical Approach. *Ecology* 58, 338–348. <https://doi.org/10.2307/1935608>
- Tilman, D., Kilham, S.S., Kilham, P., 1982. Phytoplankton community ecology: the role of limiting nutrients. *Annu. Rev. Ecol. Syst.* 13, 349–372.
- Tilman, D., Sterner, R.W., 1984. Invasions of equilibria: tests of resource competition using two species of algae. *Oecologia* 61, 197–200.
- Tilstone, G.H., Martín Míguez, B., Figueiras, F.G., Fermín, E.G., 2000. Diatom dynamics in a coastal ecosystem affected by upwelling: coupling between species succession, circulation and biogeochemical processes 205, 23–41.
- Toseland, A., Daines, S.J., Clark, J.R., Kirkham, A., Strauss, J., Uhlig, C., Lenton, T.M., Valentin, K., Pearson, G.A., Moulton, V., Mock, T., 2013. The impact of temperature on marine phytoplankton resource allocation and metabolism. *Nat. Clim. Change* 3, 979–984. <https://doi.org/10.1038/nclimate1989>

- Tozzi, S., Schofield, O., Falkowski, P., 2004. Historical climate change and ocean turbulence as selective agents for two key phytoplankton functional groups. *Mar. Ecol. Prog. Ser.* 274, 123–132.
- Trimborn, S., Brenneis, T., Sweet, E., Rost, B., 2013. Sensitivity of Antarctic phytoplankton species to ocean acidification: Growth, carbon acquisition, and species interaction. *Limnol. Oceanogr.* 58, 997–1007. <https://doi.org/10.4319/lo.2013.58.3.0997>
- Urabe, J., Togari, J., Elser, J.J., 2003. Stoichiometric impacts of increased carbon dioxide on a planktonic herbivore. *Glob. Change Biol.* 9, 818–825. <https://doi.org/10.1046/j.1365-2486.2003.00634.x>
- van Donk, E., Kilham, S.S., 1990. Temperature Effects on Silicon- and Phosphorus-Limited Growth and Competitive Interactions Among Three Diatoms. *J. Phycol.* 26, 40–50. <https://doi.org/10.1111/j.0022-3646.1990.00040.x>
- Vasseur, D.A., DeLong, J.P., Gilbert, B., Greig, H.S., Harley, C.D.G., McCann, K.S., Savage, V., Tunney, T.D., O'Connor, M.I., 2014. Increased temperature variation poses a greater risk to species than climate warming. *Proc. R. Soc. B Biol. Sci.* 281, 20132612. <https://doi.org/10.1098/rspb.2013.2612>
- Walther, G.-R., Post, E., Convey, P., Menzel, A., Parmesan, C., Beebee, T.J.C., Fromentin, J.-M., Hoegh-Guldberg, O., Bairlein, F., 2002. Ecological responses to recent climate change. *Nature* 416, 389–395. <https://doi.org/10.1038/416389a>
- Wang, X., Fu, F., Qu, P., Kling, J.D., Jiang, H., Gao, Y., Hutchins, D.A., 2019. How will the key marine calcifier *Emiliana huxleyi* respond to a warmer and more thermally variable ocean? *Biogeosciences* 16, 4393–4409. <https://doi.org/10.5194/bg-16-4393-2019>
- Ward, B., Collins, S., Dutkiewicz, S., Gibbs, S., Bown, P., Ridgwell, A., Sauterey, B., Wilson, J., Oschlies, A., 2019. Considering the role of adaptive evolution in models of the ocean and climate system (preprint). *EarthArXiv*. <https://doi.org/10.31223/osf.io/srdh3>
- Winder, M., Sommer, U., 2012. Phytoplankton response to a changing climate. *Hydrobiologia* 698, 5–16. <https://doi.org/10.1007/s10750-012-1149-2>
- Wood, A.M., Leatham, T., 1992. The Species Concept in Phytoplankton Ecology. *J. Phycol.* 28, 723–729.
- Woolway, R.I., Jones, I.D., Maberly, S.C., French, J.R., Livingstone, D.M., Monteith, D.T., Simpson, G.L., Thackeray, S.J., Andersen, M.R., Battarbee, R.W., DeGasperis, C.L., Evans, C.D., de Eyto, E., Feuchtmayr, H., Hamilton, D.P., Kernan, M., Krokowski, J., Rimmer, A., Rose, K.C., Rusak, J.A., Ryves, D.B., Scott, D.R., Shilland, E.M., Smyth, R.L., Staehr, P.A., Thomas, R., Waldron, S., Weyhenmeyer, G.A., 2016. Diel Surface Temperature Range Scales with Lake Size. *PLoS ONE* 11, e0152466. <https://doi.org/10.1371/journal.pone.0152466>
- Yoshiyama, K., Mellard, J.P., Litchman, E., Klausmeier, C.A., 2009. Phytoplankton Competition for Nutrients and Light in a Stratified Water Column. *Am. Nat.* 174, 190–203. <https://doi.org/10.1086/600113>
- Yvon-Durocher, G., Dossena, M., Trimmer, M., Woodward, G., Allen, A.P., 2015. Temperature and the biogeography of algal stoichiometry: Temperature dependence of algal stoichiometry. *Glob. Ecol. Biogeogr.* 24, 562–570. <https://doi.org/10.1111/geb.12280>



High predictability of direct competition between marine diatoms under different temperatures and nutrient states

Philipp Siegel¹ | Kirralee G. Baker¹ | Etienne Low-Décarie² | Richard J. Geider¹

¹School of Life Sciences, University of Essex Colchester Campus, Colchester, UK

²Canadian Space Agency, Saint-Hubert, QC, Canada

Correspondence

Philipp Siegel, School of Life Sciences, University of Essex Colchester Campus, Wivenhoe Park, Colchester CO4 3SQ, UK.
Email: psiegel@essex.ac.uk

Funding information

Natural Environment Research Council, Grant/Award Number: NE/P002374/1; School of Life Sciences, Essex University

Abstract

The distribution of marine phytoplankton will shift alongside changes in marine environments, leading to altered species frequencies and community composition. An understanding of the response of mixed populations to abiotic changes is required to adequately predict how environmental change may affect the future composition of phytoplankton communities. This study investigated the growth and competitive ability of two marine diatoms, *Phaeodactylum tricornutum* and *Thalassiosira pseudonana*, along a temperature gradient (9–35°C) spanning the thermal niches of both species under both high-nitrogen nutrient-replete and low-nitrogen nutrient-limited conditions. Across this temperature gradient, the competitive outcome under both nutrient conditions at any assay temperature, and the critical temperature at which competitive advantage shifted from one species to the other, was well predicted by the temperature dependencies of the growth rates of the two species measured in monocultures. The temperature at which the competitive advantage switched from *P. tricornutum* to *T. pseudonana* increased from 18.8°C under replete conditions to 25.3°C under nutrient-limited conditions. Thus, *P. tricornutum* was a better competitor over a wider temperature range in a low N environment. Being able to determine the competitive outcomes from physiological responses of single species to environmental changes has the potential to significantly improve the predictive power of phytoplankton spatial distribution and community composition models.

KEYWORDS

competition, diatoms, phytoplankton, thermal performance

1 | INTRODUCTION

Competition plays an important role in shaping biological communities in terrestrial and aquatic ecosystems (Tilman, 1987). Interspecific competition within communities occurs when two or more species possess the same or similar resource requirements

(Clements & Shelford, 1939). For phytoplankton, the most important resources are macronutrients (N, P, Si), micronutrients (trace elements), organic nutrients (vitamins), CO₂, and light (Riebesell, 2004; Tilman, Kilham, & Kilham, 1982). If demand for a resource by the organisms within an ecosystem is high, the abundance or concentration of the resource will decline. When the concentration of a resource becomes too low, it can fall below

This is an open access article under the terms of the Creative Commons Attribution License, which permits use, distribution and reproduction in any medium, provided the original work is properly cited.

© 2020 The Authors. *Ecology and Evolution* published by John Wiley & Sons Ltd.

the minimum requirement of a species to support its temperature and light-dependent maximum growth rate (μ_{\max}) and, therefore, become limiting (Andersen, 2005).

In equilibrium communities, the minimum resource concentration that supports net population growth, and for which uptake rates by the population and supply rates by the environment are in balance, is called R^* (Tilman, 1981). Assuming that all species compete for the same limiting resource and ignoring the effects of interference or apparent competition, the species with the lowest R^* should outcompete all other species and dominate a community (resource ratio theory or R^* -theory; Tilman et al., 1982). Theoretically, the number of species that can stably coexist in a system is therefore equal to the number of limiting resources, if different species are limited by different resources. The fact that most communities of primary producers usually display higher species diversity than the number of limiting resources (Cloern & Dufford, 2005; Sommer, 1984) has been termed the "Paradox of the plankton" (Hutchinson, 1961). The resolution to the paradox likely lies in the fact that natural communities are often not in equilibrium or that the ability of a species to exploit resources is not the only factor that regulates a community's diversity and the outcome of competition. Apart from limiting nutrients, species diversity is governed by other major regulating forces which can be biotic (e.g., differential grazing pressure or various forms of symbiosis such as mutualism or parasitism) or abiotic (e.g., temperature, pH, salinity) (Begon, Townsend, & Harper, 2006; Cloern & Dufford, 2005).

Whether the effect of environmental change on the outcome of competition can be predicted from the performance of isolated species and whether these predictions align with classical competition models or single species performance is unclear because experiments that examine direct species interactions along environmental gradients are scarce (Kordas, Harley, & O'Connor, 2011). Only a few studies have previously found evidence to suggest that this is possible. For example, Huisman, Jonker, Zonneveld, and Weissing (1999) showed that the ability of isolated algae species to survive on the lowest light level determined their competitive success in mixed communities. Bestion, García-Carreras, Schaum, Pawar, and Yvon-Durocher (2018) showed that phosphorus uptake rates of monocultures at different temperatures correctly predicted the competitive outcome between pairs of 6 phytoplankton species in the majority (71%) of the cases.

Simultaneous changes in multiple abiotic factors, such as those predicted to occur under climate change (e.g., rising sea surface temperatures in conjunction with changes in nutrient inputs), may also complicate predictions, as abiotic factors may interact (e.g., antagonistic or multiplicative), and organisms may respond in a way that is not accounted for from the responses to gradients of individual factors operating in isolation (Harley et al., 2017; Thomas et al., 2017). For instance, nutrient concentration was shown to interact with temperature to influence phytoplankton growth rates (Rhee & Gotham, 1981) and the cardinal temperatures (e.g., thermal optimum) of thermal performance

curves (TPCs) (Bestion, Schaum, & Yvon-Durocher, 2018; van Donk & Kilham, 1990; Thomas et al., 2017). In particular, N limitation can significantly lower the thermal optimum of the diatom *Thalassiosira pseudonana* toward colder temperatures (Thomas et al., 2017). Given this shift in thermal performance due to nutrient limitation, *T. pseudonana* may become less competitive in warm N-limited waters. In contrast, *Phaeodactylum tricornutum* is known to be a good competitor for inorganic nitrogen when this nutrient is scarce because it can take up nitrate when abundant and store it for times of depletion (Cresswell & Syrett, 1982). Thus, the outcome of interspecific competition for inorganic nutrients might be expected to depend on temperature if the interaction of nutrient limitation with temperature is species-specific. For example, *P. tricornutum* has been found to outcompete *T. pseudonana* and other species in maricultural ponds (Nelson, D'Elia, & Guillard, 1979), despite not being a dominating species in marine phytoplankton communities (Guillard & Kilham, 1977), which may be a reflection of nutrient availability or temperature characteristics in different systems. An early study on the competition between *P. tricornutum* and *T. pseudonana* showed that competition is indeed temperature-dependent and that the thermal environment influences the competitive outcome in stationary phase cultures (Goldman & Ryther, 1976). Specifically, *P. tricornutum* was found to be a good invader and dominant species under cold to intermediate temperatures (<20°C), whereas it could not establish itself as an invasive species in warmer temperatures.

Here, the interaction of temperature and nitrate availability on direct competition between *P. tricornutum* and *T. pseudonana* was investigated along a temperature gradient. To test whether temperature and nutrient status have an interactive effect on the outcome of competition, experiments were conducted in both nutrient-replete high N conditions and low N conditions (whereby nitrate limited yield). Specifically, it was hypothesized that (a) the species with the higher growth rate or carrying capacity at a given temperature and nutrient level as a monoculture would have the competitive advantage in mixed cultures and that (b) greater absolute differences in growth rate between species at a specific assay temperature would determine how quickly the poorer competitor would be displaced.

2 | MATERIAL AND METHODS

Stock cultures of *P. tricornutum* (CCMP 2561) and *T. pseudonana* (CCMP 1335) were maintained in the University of Essex algal culture collection at $15.5 \pm 1.0^\circ\text{C}$, in F/2 medium (Guillard & Ryther, 1962), prepared in artificial sea water (Berges, Franklin, & Harrison, 2001; Harrison, Waters, & Taylor, 1980), and grown on a 12:12-hr light and dark cycle at a photosynthetic photon flux density (PPFD) of approximately $60 \mu\text{mol photons m}^{-2} \text{s}^{-1}$, which is close to optimum light levels for *P. tricornutum* (Geider, Osbonie, & Raven, 1986), and approximately 30% of the optimum light level for *T. pseudonana* (Geider, MacIntyre, & Kana, 1997;

Geider, MacIntyre, & Kana, 1998). Stock cultures were transferred monthly as 1:36 dilutions.

2.1 | Competition experiments

2.1.1 | High N competition experiment

Prior to experimentation, *P. tricornutum* and *T. pseudonana* were maintained in exponential growth for 2 weeks (approximately 10–14 generations) under stock culture conditions at $15.5 \pm 1.0^\circ\text{C}$ by transferring cultures into fresh F/2 medium once cell densities reached 500,000 cells/ml for *P. tricornutum* and 250,000 cells/ml for *T. pseudonana* (equivalent to about 5% of each species' carrying capacity).

Experiments using an aluminum temperature-gradient block were conducted to assess (a) thermal performance curves (TPCs) for growth rate of monocultures of the two diatoms and (b) temperature dependence of competition between these species. The aluminum block was heated at one end and cooled at the other to generate a temperature gradient from 8.8°C at the cold end to 35°C at the hot end. The block provided 4 rows with 17 columns (assay temperatures) in each row. Temperature within each column was controlled to within 0.2°C , providing approximately 1.5°C increments along the temperature gradient. Illumination was provided from below by light emitting diodes (LEDs). PPFD was set to $150 \pm 15 \mu\text{mol photons m}^{-2} \text{s}^{-1}$, and illumination was provided on a 12:12-hr light and dark cycle.

Aliquots from stock cultures of each of the diatoms were used to inoculate 17 autoclaved borosilicate test tubes (5 ml assay volumes), which were distributed along the same 17-assay-temperature gradient described above. To assess the growth rate TPCs, in vivo chlorophyll *a* minimum fluorescence yield (F_0) was used as a proxy for biomass (see section 2.2 below). Initial cell densities were approximately 160,000 cells/ml for *P. tricornutum* and 80,000 for *T. pseudonana*, corresponding to similar F_0 values for both species. The monocultures were kept in exponential phase by diluting whenever an assay culture reached F_0 values equivalent to cell densities

corresponding to about 5% of each species' carrying capacity, approximately 500,000 cells/ml for *P. tricornutum* and 250,000 cells/ml for *T. pseudonana* (Figure 1a and Figure S1).

At the same time, to assess competition between these species, aliquots from the stock monocultures were combined to create a mixed culture with equal cell densities of 100,000 cells/ml in a 1:1 species ratio (50,000 cells of each species). The starting ratio could only be approximated, as cell densities were estimated from the relationship between cell density and F_0 determined at 15.5°C , but fluorescence per cell is not constant as it varies between species and with assay temperature. This mixed culture was then used to inoculate 34 autoclaved borosilicate test tubes (5 ml assay volumes), which were distributed in duplicates along the same 17-assay-temperature gradient to assess the acute effect of temperature on competition. After mixed cultures had been established and distributed across the temperature gradient, 200 μl was removed daily from each mixed culture tube and preserved with Lugol's solution for cell frequency counts, that is, relative species abundances of the mixed cultures over time. 200 μl of fresh F/2 medium was added to keep the culture volume constant. As with the monocultures, F_0 measured daily was used as an index of community biomass. The mixed cultures were kept in exponential growth by diluting when F_0 reached values corresponding to about 5% of the carrying capacity.

After a further 2 weeks, the monocultures from each assay temperature that had been used to assess the growth rate TPCs of the two species were mixed together in an equal cell density ratio to investigate the effect of thermal acclimation on competition. Here, 2 mixed cultures to monitor competition were created at each assay temperature and aliquots were sampled daily to monitor changes in relative species frequencies.

Following completion of the competition experiment, triplicate monocultures of each species were grown across the gradient to increase the total replication for determining the TPC for growth rate of each monoculture to $n = 4$. However, in the final analysis, one of the *T. pseudonana* growth replicates was omitted as an outlier because the TPC was significantly different to the remaining three replicates (Figure S2a).

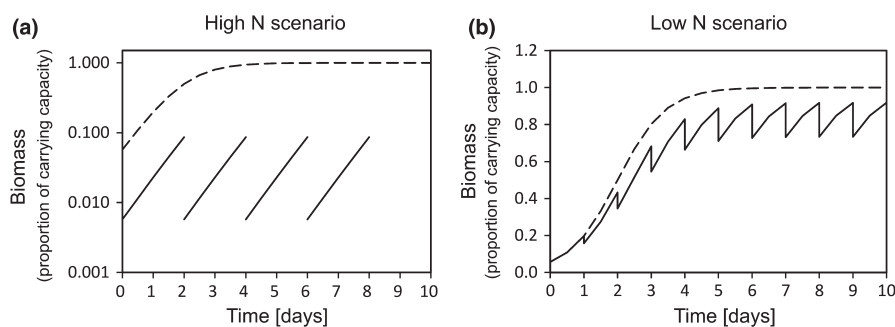


FIGURE 1 Simulation of semicontinuous cultures for obtaining and maintaining (a) nutrient-replete (high N scenario) and (b) nutrient-limited (low N scenario) cultures. Simulation assumes cultures are already acclimated to the nutrient-replete growth under defined temperature, irradiance, etc. Assumes logistic growth with the nutrient-replete growth rate = 1.4 d^{-1} , and carrying capacity = 1. Dilution is approximately 10-fold in the high N scenario and 1.25-fold in the low N scenario. Solid lines are the culture density. Dashed line is the culture density that would be obtained in a batch culture undergoing logistic growth. Note that (a) is on a log scale to represent that high N exponential cultures were kept at low densities far from reaching stationary phase, whereas (b) is on a linear scale

The above experimental design enabled the examination of (a) the TPCs for growth of *P. tricorntutum* ($n = 4$) and *T. pseudonana* ($n = 3$) and (b) the acute interspecific competition along the temperature gradient in the 2 weeks following the transfer from their $15.5 \pm 1.0^\circ\text{C}$ source environment ($n = 2$) and of cultures acclimated for 2 weeks to temperatures of $8.8\text{--}35^\circ\text{C}$ ($n = 2$).

2.1.2 | Low N competition experiment

Cultures were acclimated as a batch culture for 2 weeks in low N F/2 medium (starting concentration $55 \mu\text{M}$ in comparison to $882 \mu\text{M}$ in full F/2). As shown in Figure S3, this NO_3 concentration reduced carrying capacity and ensured that cultures would reach the stationary growth phase at cell densities that did not saturate the fast repetition rate fluorometry (FRRf) signal. After acclimation, two monoculture replicates of each species were inoculated from early stationary phase stock cultures and grown in 5-ml volumes across the 17 assay temperatures in the temperature-gradient thermoblock ($9.1\text{--}33.8^\circ\text{C}$) in the low N ($55 \mu\text{M}$) F/2 medium. The light regime was kept consistent with that used for the high N competition experiment and once again set to a PPFD in the range of $150 \pm 15 \mu\text{mol photons m}^{-2} \text{s}^{-1}$ on a 12:12-hr light and dark cycle.

The cultures were maintained in semicontinuous growth by removing 20% of the culture volume (1 ml) daily (used for determining cell abundance and nitrate concentration) and replacing this volume with fresh medium to maintain a total volume of 5 ml. This way cultures could be grown until cell abundance (yield) was limited by the concentration of nitrate provided in the growth medium and daily population growth rate was set by the dilution rate (Figure 1b). Although the daily sampling regime was different from the high N scenario to account for the necessities of culturing microorganisms in nutrient-limited conditions, the results of the two nutrient scenarios can be compared as the same species were used and cultures were treated otherwise equally during the competition experiment.

The removed 1 ml samples were centrifuged at $5,000 \text{ g}$ for 7 min at 4°C . A subsample of the supernatant ($300 \mu\text{l}$) was transferred to a flat-bottom 96-well plate (Thermo Scientific Nunclon, USA) and stored at -20°C to measure the sum of nitrate plus nitrite (NO_x) at a later time (see section 2.4 below). The cell pellet was resuspended in the remaining volume ($700 \mu\text{l}$), fixed with formaldehyde (final concentration 1%), and stored at -20°C until cell abundances were estimated with flow cytometry (see section 2.5 below).

After growing in monocultures for 2 weeks, inorganic nitrogen concentrations in all treatments were depleted below the detection limit of the NO_x assay (i.e., $<0.5 \mu\text{M}$; see Figure S4). At this point, the fluorescence signals had stabilized or were declining, indicating that the yield was N-limited (see Figure S5). Following this determination, one of the two monocultures of each species at each assay temperature was used to inoculate two mixed cultures for the competition phase of the experiment. Each mixed culture tube received 2 ml assay volumes from each monoculture, for a total volume of 4 ml, which was then topped up with 1 ml of low N F/2 medium

to maintain a constant assay volume of 5 ml (competition replicates across assay temperatures at this point in time $n = 2$). The need to use 2 ml assay volume of each monoculture to not break with the 20% daily dilution had the consequence that the desired 1:1 species ratio at the start of mixed cultures could not always be reached. As in the high N experiments, $200 \mu\text{l}$ of the sampled volume was preserved daily with Lugol's solution for cell frequency counts. The remaining $800 \mu\text{l}$ volume was treated the same way as low N monocultures, with samples being centrifuged, and $300\text{-}\mu\text{l}$ aliquots stored for NO_x analysis.

One week later, the second N-limited semibatch monoculture replicate of each species was used to inoculate another set of two mixed cultures tubes at each assay temperature for a second duplicate competition experiment (increasing the amount of competition replicates to $n = 4$). Mixed cultures were kept in the same semicontinuous regime as monocultures with 20% of sample volume being harvested and replaced with fresh medium on a daily basis.

The above experimental design enabled the examination of (a) the thermal niche of *P. tricorntutum* ($n = 2$) and *T. pseudonana* ($n = 2$) under low N conditions and (b) the acute interspecific competition along the temperature gradient at the onset of N limitation ($n = 2$) and of cultures that were cultured in isolation for an additional 7 days at $9.1\text{--}33.8^\circ\text{C}$ ($n = 2$).

2.2 | Chlorophyll fluorescence

In vivo chlorophyll *a* minimum fluorescence F_0 (minimum fluorescence yield), used as a proxy for biomass, and photosynthetic efficiency F_v/F_m were measured daily via FRRf with a FastTracka II fluorometer and Fast Act laboratory system (both CTG Ltd). Photosynthetic efficiency was calculated via the formula $(F_m - F_0)/F_m$ (F_m = maximum fluorescence yield) by the FastPro software (version 1.0.55) used to attain and record FRRf measurements. Peak excitation was at 435 nm and fluorescence emission measured at 680 nm (with a 25 nm bandwidth). The measuring protocol was set to 24 sequences per acquisition with a 100 ms sequence interval and a 20 s acquisition pitch.

Measurements were taken on cells that were dark acclimated for 30 min at their assay temperature, and profiles of fluorescence emission were fitted within the Fast Pro 8 software (version 1.0.55) (Chelsea Technologies).

2.3 | Mixed population species frequency counts

Frequency counts for the high N and low N experiment were carried out to monitor the relative abundance of each species in the mixed populations over time. Flow cytometry could not be used to discriminate between the two species as their forward scatter (FSC) and chlorophyll *a* fluorescence overlapped. As such, Lugol's preserved cells were allowed to settle to the bottom of the well-plate wells (approximately 3 hr) before frequency counts were performed using an

Olympus inverted microscope at 200× magnification. In each fixed sample, a minimum of 400 cells was counted in order to calculate a *P. tricornutum*-to-*T. pseudonana* cell abundance ratio.

2.4 | NO_x assay (total nitrite/nitrate analysis)

NO_x, the sum of nitrite and nitrate, concentration was measured using the method of Schnetger and Lehnert (2014) to track the monocultures to nitrogen depletion before mixing them together for the low N competition experiment. The 300 μl frozen aliquots were defrosted on ice, and a 150 μl volume was transferred to a fresh 96 well-plate, and 75 μl of the NO_x reagent was added. The reagent was mixed with the assay volume by pipetting up and down several times and incubated at 45 ± 5°C for 60 min before measuring absorbance at 540 nm in a FLUOstar Omega plate reader (BMG Labtech).

2.5 | Flow cytometry

For the low N experiment only, flow cytometry data were used to confirm that cell densities had stabilized, despite *F*₀ fluorescence declining, as cell physiology continued to adjust to N limitation. Cellular chlorophyll content is known to decline under N limitation (Parkhill, Maillet, & Cullen, 2001), and as a consequence, the ratio of *F*₀ to cell density will also decline (Figure S6). Because cellular physiology was stable in exponentially growing cultures of the high N experiment, flow cytometry was not required.

Previously collected samples (as described above in section 2.1.2) were defrosted on ice and quantified with an Accuri C6 flow cytometer (BD Biosciences) equipped with a blue laser (488 nm). Diatom populations were discriminated based on chlorophyll *a* fluorescence (>670 nm) and forward scatter (FSC). FSC was used as a proxy for cell size to observe potential changes across assay temperatures after 15 days of monoculture growth in the low N medium. After counting cells within 45 μl of sample volume per sample, population statistics were calculated using particle counts within gates with the supplied BD Accuri C6 Analysis Software (Version 1.0.264.21).

2.6 | Data analysis

2.6.1 | Growth rates and carrying capacities

Growth rates (μ) in high N medium (starting nitrate concentration of 882 μM) were calculated for each monoculture replicate and dilution phase as the slope of the linear regression of the natural log of *F*₀ over time (Figure S1). The growth rate calculated for the 1st dilution phase was not used for further analysis as the cultures had not yet acclimated to assay conditions. Growth rates from all subsequent dilution phases were used to fit the TPC models (see section 2.6.2 below).

The initial exponential growth rates during the nutrient-replete phase in low N semicontinuous cultures (with a starting nitrate concentration of 55 μM) were calculated using FRRf data from the first 4 days of culturing before the exponential increase in *F*₀ slowed (see Figures S5 and S7). Growth rates were calculated with Equation (1) as.

$$\mu = k + \ln\left(\frac{1}{0.8}\right) \quad (1)$$

where k is the slope of $\ln(F_0)$ over time, and $\ln\left(\frac{1}{0.8}\right)$ (natural logarithm of 100% medium (i.e., 1.0) over 80% medium (i.e., 0.8)) was added to k to account for the dilution by the daily volume removed (1 ml) from the 5 ml culture.

Cell densities increased to a maximum by day 5 that was sustained thereafter (see Figure S8). The carrying capacity, K , under the imposed dilution rate of 0.22 d⁻¹, was calculated for each replicate and at each assay temperature from the average cell densities measured after experimental day 4.

2.6.2 | Thermal performance curves

All twelve equations available in the R package “temperatureresponse” (Low-Décarie et al., 2017) were fitted to the temperature-dependent data of growth and carrying capacities obtained from monocultures of *P. tricornutum* and *T. pseudonana* (Table S1). For the growth model fitting in high N cultures, data from all dilution phases, except dilution phase 1, which was regarded as the growth phase in which the cultures acclimated to assay conditions, were used. The average growth rate across dilution phases was calculated for each species and replicate at each assay temperature, and the temperature dependence was modeled based on these average growth rates. For the low N scenario, thermal performances were modeled on the acute growth rates obtained from the first 4 days of low N growth (Figure S7) and on the thermal response of carrying capacities across assay temperatures (Figure S8).

The most appropriate equation for each species was selected based on a visual inspection of the data in combination with Akaike's information criterion (AIC) values (see Figure S9). Visual inspection was necessary as AIC values alone did not always predict the equation that best described the temperature-dependent data, especially at suboptimal temperatures. For *P. tricornutum*, Equation (2) from Ratkowsky, Lowry, McMeekin, Stokes, and Chandler (1983) was found to be the best model across all replicates.

$$\text{Rate} = [a \cdot (T - T_{\min})]^2 \cdot [1 - \exp(b \cdot (T - T_{\max}))]^2 \quad (2)$$

For *T. pseudonana*, Equation (3) from Montagnes, Morgan, Bissinger, Atkinson, Weisse (2008) was found to best describe the thermal performance.

$$\text{Rate} = a + b \cdot T + c \cdot T^2 \quad (3)$$

where T in both equations is the assay temperature at which growth rate and carrying capacity were measured.

The fitted TPCs were used to obtain the optimum temperature for growth (T_{opt}), the maximum growth rate (μ_{max}) at this temperature, and the low and high temperatures at which $\mu = 0.5\mu_{max}$ (CT_{50min} and CT_{50max}). Single parameters of nonlinear model fits can be found in Tables S2-S4.

To investigate whether the thermal niche differed significantly between (a) the two species, and (b) two nutrient scenarios, a two-way MANOVA was used to examine the 4 dependent variables (T_{opt} , CT_{50min} , CT_{50max} , and μ_{max}). The two independent variables were "species" (levels: *P. tricornutum* and *T. pseudonana*) and "nutrient scenario" (levels: high N and low N). Sample size was $n = 11$ (4 *P. tricornutum* replicates in high N, and 2 in low N, as well as 3 *T. pseudonana* replicates in high N and 2 in low N), and significance levels were set to a p -value of 0.05. By conducting a MANOVA, we could access all pairwise comparisons to determine which cardinal temperatures (a) changed significantly in the overall thermal niche and (b) were affected by a "species" and "nutrient scenario" interaction.

To test whether the thermal dependency of carrying capacities under low N conditions differed between the two species, individual one-way ANOVAs were conducted with "species" as the independent variable on the four dependent parameters T_{opt} , CT_{50min} , CT_{50max} , and maximum carrying capacity (K_{max}). MANOVA testing was not possible due to the replication number of $n = 2$ for the monocultures grown in low N conditions. p -values of the single ANOVAs were adjusted for multiple testing with a Bonferroni correction and reported as q -values.

2.6.3 | Predicted competition coefficients

Competition coefficients across assay temperatures in high N and low N conditions were predicted from the mean growth rates (Equation 4a) or mean carrying capacities (Equation 4b) of each species calculated from the fitted TPCs.

$$\text{Predicted competition coefficient } (T) = (\mu_1)_T - (\mu_2)_T \quad (4a)$$

where $(\mu_1)_T$ and $(\mu_2)_T$ are the growth rates of species 1 and species 2 at temperature T .

$$\text{Predicted competition coefficient } (T) = (K_1)_T - (K_2)_T \quad (4b)$$

where $(K_1)_T$ and $(K_2)_T$ are the carrying capacities of species 1 and 2 at temperature T .

Since competition coefficients are traditionally calculated from growth rates (e.g., Low-Décarie, Fussmann, & Bell, 2011; Segura et al., 2011), coefficients calculated from carrying capacities must be treated with caution, as the relationship between K and competitive outcome is not established for steady-state nutrient-limited conditions. Higher K does not necessarily signify better competition ability. Under steady-state nutrient limitation, it is R^* that determines

competitive outcome (Tilman, 1981), but because the NO_x concentrations were below the detection limit of our assay, we could not measure R^* in our experiment.

The predicted temperature dependence of competition coefficients was modeled with a local estimated scatter plot smoothing (LOESS) from the R core package "stats" (R Core Team, 2016). LOESS fits a smoothing curve into data that is distributed on a scatter plot to graphically represent the relationship between an independent and a dependent variable. It is a suitable method for visualizing complex nonlinear relationships. The final smoother curve is the result of many local regression curves fit together (Isnanto, 2011; Jacoby, 2000). As such, it is a tool for predicting specific points on a regression, such as the inflexion point of competition, and to explore data. To display the strength of how closely our LOESS smoother followed the calculated competition coefficients, we reported R^2 -values and residual standard errors (RSE) in the results.

2.6.4 | Observed competition coefficients

Changes in the ratio of the abundances of the two species through time (Figures S10 and S11) were used to calculate observed competition coefficients. The competition coefficient was calculated as the slope of the change in the natural logarithm of species frequency over time. Competition coefficients were calculated with Equation (5) for mixed high N cultures and mixed low N cultures.

$$\text{Competition coefficient} = \frac{\ln \left(\frac{N_{P.tricornutum}:N_{T.pseudonana}(t)}{N_{P.tricornutum}:N_{T.pseudonana}(0)} \right)}{t} \quad (5)$$

where N = species abundance, and t = time. At the temperature at which competition coefficients are 0, stable coexistence of the two species is expected.

As described above (Section 2.1), each nutrient scenario had 4 competition replicates across the temperature gradient. In the final analysis of competition under high N conditions, the acute and acclimated competition replicates were pooled because we did not find an effect of temperature acclimation and could not observe a significant difference in the temperatures at which the competitive advantage switched from *P. tricornutum* to *T. pseudonana* ($F_{1,2} = 4.34$, $p = .173$) (Figure S12, and Table S5). Due to a lack of an effect of temperature acclimation on the progression of competition across temperatures, we did not structure the competition replicates into acclimated and nonacclimated in the low N scenario and focussed on culturing the monocultures to N limitation, pooling the four competition replicates as well.

In order to determine whether nutrient regime significantly changed the temperature at which *P. tricornutum* and *T. pseudonana* coexisted (i.e., the inflexion point temperature at which the competition coefficient equalled 0), we conducted a one-way ANOVA with the temperature of competition inflexion as the response variable and "nutrient regime" as the independent variable. Significance levels were set to a p -value of .05.

All data analysis and calculations mentioned above were carried out with the statistical software R (version 3.3.1) (R Core Team, 2016).

3 | RESULTS

3.1 | Differences in temperature and nutrient response between species in monoculture

When *P. tricornutum* and *T. pseudonana* were grown as monocultures, the thermal niches of the two species differed significantly from one another irrespective of nitrogen conditions (2-way-MANOVA, $F_{1,7} = 103.49$, $p < .001$) (Figure 2, Table S6). The contrasting thermal niches between the two species were evident in differing cardinal temperatures (CT_{50min} , T_{opt} , CT_{50max}) (Figure 3a) and μ_{max} (Figure 3b). *Phaeodactylum tricornutum* occupied a cooler thermal niche than *T. pseudonana*, characterized by lower cardinal temperatures (Figure 3a), and could not sustain growth when temperature was in excess of 30°C (Figure 2). In contrast, *T. pseudonana* occupied a warmer thermal niche and was struggling to grow toward the coolest tested assay temperatures. In the range of 10°C and below, the growth rate of *T. pseudonana* approached 0 d⁻¹, indicating that the thermal tolerance minimum of this *T. pseudonana* strain was being reached (Figure 2).

N limitation altered the thermal niche of both species (Figures 2 and 3). The 2-way MANOVA confirmed that nitrate levels had a significant effect on the cardinal temperatures of the TPCs of the

two monocultures ($F_{1,7} = 9.59$, $p < .05$). However, the two diatoms responded differently to a reduction in N and consequently there was a significant interaction between “N regime” and “species” ($F_{1,7} = 17.84$, $p < .01$). Specifically, the thermal niche for *P. tricornutum* became slightly more narrow (increase in CT_{50min} by 0.31°C), and μ_{max} at T_{opt} increased by 14%. In contrast, the thermal niche of *T. pseudonana* widened (CT_{50min} dropping by 2.38°C), and the μ_{max} of *T. pseudonana* getting reduced by 17% (isolated ANOVA results within the MANOVA test for each cardinal temperature can be found in Tables S7-S10).

Similar to the growth rate results, carrying capacities also displayed a unimodal nonlinear response along the assay-temperature gradient and monocultures reached higher carrying capacities the closer the assay temperatures were to the species' T_{opt} (Figure 4a). All of the cardinal temperatures for carrying capacity TPCs differed significantly from one another between species (T_{opt} : $F_{1,2} = 545.9$, $q < 0.01$; CT_{50min} : $F_{1,2} = 78.28$, $q = 0.05$; CT_{50max} : $F_{1,2} = 743.1$, $q < 0.01$) (Figure 5a). Similar to the growth trends in the high N scenario, these significant differences arose because the thermal niche of *T. pseudonana* was shifted more toward warm temperatures than *P. tricornutum*. Despite differences in the thermal niches, the maximum carrying capacity at T_{opt} did not differ significantly between species ($F_{1,2} = 6.96$, $q = 0.48$) (Figure 4b). Individual test statistics for the single one-way ANOVAs can be found in the Supplementary Material (Tables S11-S14).

After 15 days of growing the monocultures in the low N medium, cell size showed a U-shaped trend across assay temperatures with cell size increasing toward the coldest and warmest tested assay temperatures

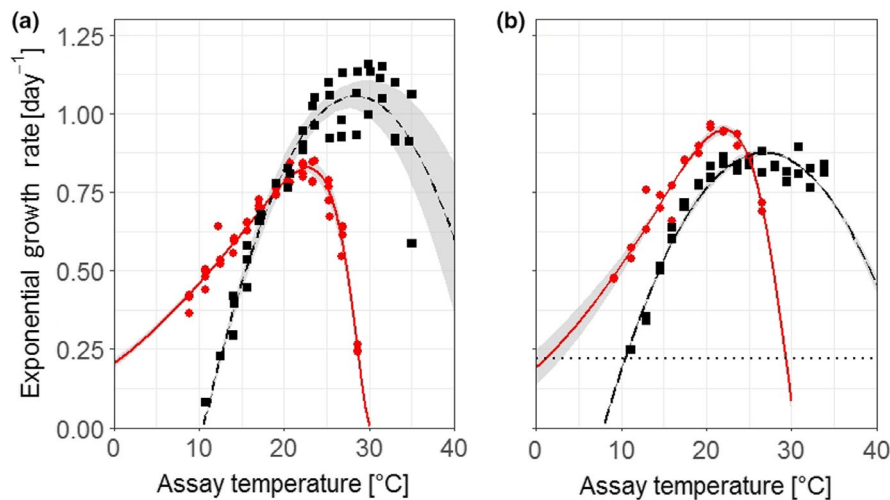


FIGURE 2 Average temperature response curves depicting (a) acclimated growth rates of *Phaeodactylum tricornutum* (red circles and solid line) and *Thalassiosira pseudonana* (black squares and dashed line) under high nitrate conditions ($n = 4$ and 3 respectively) and (b) the initial acute growth rate (days 0–4) under low N conditions ($n = 2$ for both species). Shaded area denotes standard deviation of the average model calculated from replicate model fits. Symbols in (a) represent the growth rates from distinct biological replicates and were calculated from the average growth rates across dilution steps after the diatoms had acclimated to growth under assay conditions. Dotted line in (b) indicates $\ln(1/0.8)$, the daily dilution rate that was imposed by the sampling regime in these semicontinuous cultures; cell abundance would have declined in cultures with growth rates below this value which equates to a growth rate of 0.22 d^{-1} . Raw data used to calculate growth rates in the high nitrate ($882 \mu\text{M NO}_3^-$) medium (a) can be seen in Figure S1, and data used to calculate growth rates in the low N ($55 \mu\text{M NO}_3^-$) medium (b) can be seen in Figure S7. Nonlinear model outputs of the single replicate models used to calculate the average model can be found in Tables S2 and S3, and single model fits on the individual growth replicates can be found in Figure S2a,b

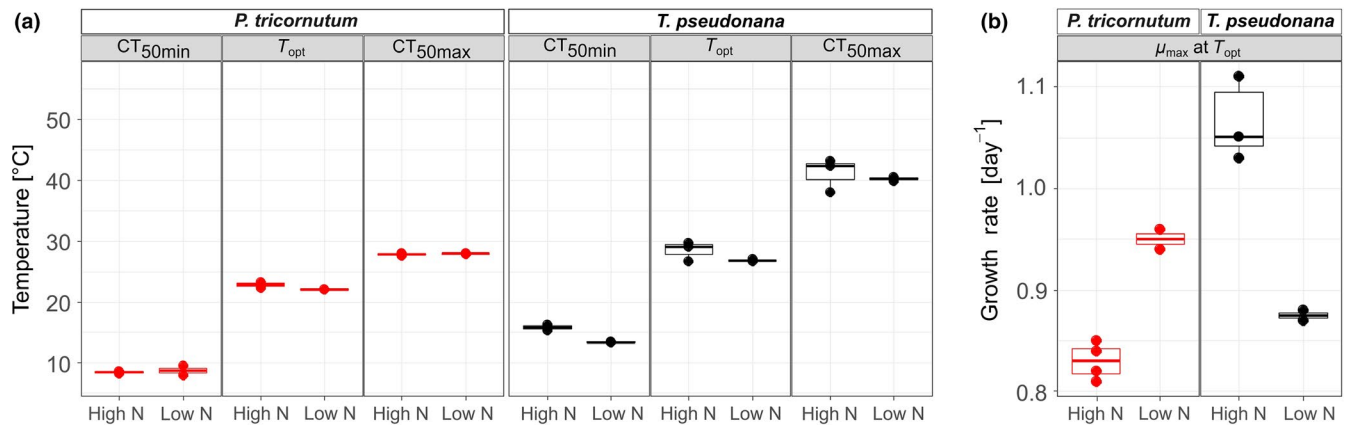


FIGURE 3 Comparison of (a) cardinal temperatures and (b) maximum growth rates from thermal performance curve model fits for growth rates between *Phaeodactylum tricornutum* and *Thalassiosira pseudonana* under high N and low N growth conditions. For *Phaeodactylum tricornutum*, $n = 4$ in high N and $n = 2$ in low N. For *Thalassiosira pseudonana*, $n = 3$ in high N and $n = 2$ in low N

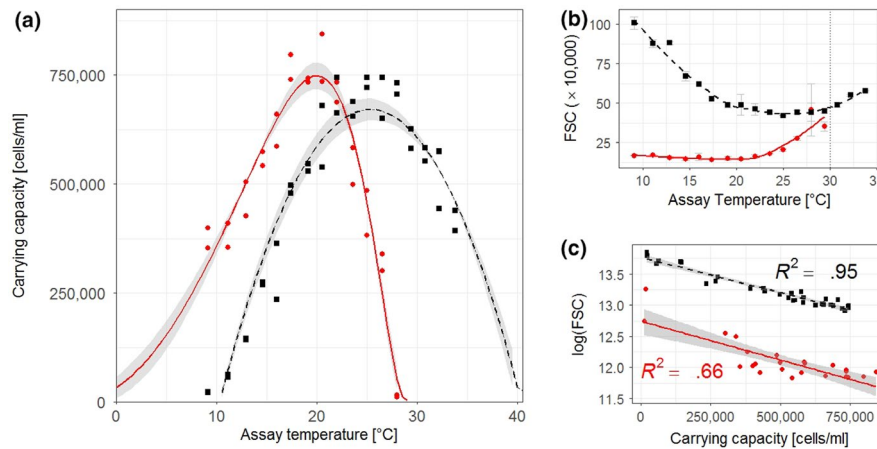


FIGURE 4 (a) Temperature response curves of carrying capacity of *Phaeodactylum tricornutum* (red circles and solid line) and *Thalassiosira pseudonana* (black squares and dashed line) under nitrogen depleted conditions in the N-limited phase of semicontinuous culturing in the low N medium ($n = 2$ for both species). Shaded area denotes standard deviation of the average model calculated from replicate model fits. Symbols show the carrying capacities from distinct biological replicates across the assay-temperature range. Raw data used to calculate carrying capacities can be seen in Figure S8. Nonlinear model outputs of the single replicate models used to calculate the average model can be found in Table S4, and single model fits on the individual growth replicates can be found in Figure S2c. (b) Forward scatter (FSC) from flow cytometry data of the low N experiment across assay temperatures. FSC measurements depicted here were taken on the last day of replicate monocultures before they were mixed together for the competition experiment. The purpose of the solid and dashed LOESS lines is to visualize the U-shaped trend of the data across assay temperatures ($R^2 = 0.85$, and $RSE = 4.503$ for *Phaeodactylum tricornutum*; $R^2 = 0.97$, and $RSE = 3.378$ for *Thalassiosira pseudonana*). LOESS was not used as a model to predict the relationship between temperature and cell size. Dotted line at 30°C indicates the critical maximum temperature for *Phaeodactylum tricornutum* beyond which it could not sustain growth. (c) Correlation between carrying capacity K and $\log(\text{FSC})$ for both species. Solid and dashed lines are linear models of the regression

(Figure 4b). There was a strong negative linear correlation between the logarithm of cell size and K (Figure 4c), with the smallest cell sizes being observed at assay temperatures closest to each diatom's T_{opt} , meaning that cell size increased toward the diatoms' physiological limits.

3.2 | Competition across assay temperatures

Monoculture TPCs were used to predict competition across assay temperatures. Under high N conditions, LOESS (represented by the solid

black line in Figure 6a, $R^2 = 0.998$, and $RSE = 0.021$) predicted an inflexion point at 18.8°C (i.e., a competition coefficient equal to 0), indicating that *P. tricornutum* was predicted to outcompete *T. pseudonana* from the coldest assay temperature up to 18.8°C. N limitation was predicted to alter the competition across assay temperatures whereby the inflexion point would shift horizontally across the temperature axis to 24.6°C (5.9°C warmer than under high N conditions; solid black line in Figure 6b, $R^2 = 0.996$, and $RSE = 0.026$). Because K also showed a response across the assay-temperature gradient, it was possible to make a second prediction of competition in the low N scenario based on K .

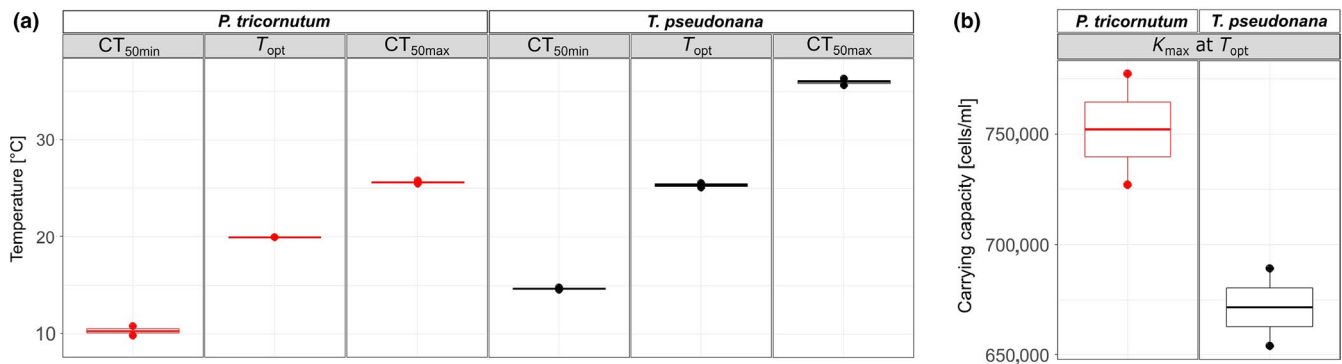


FIGURE 5 Comparison of (a) cardinal temperatures and (b) maximum carrying capacities from thermal performance curve model fits for carrying capacities between *Phaeodactylum tricornutum* and *Thalassiosira pseudonana* in low N conditions ($n = 2$ for both species)

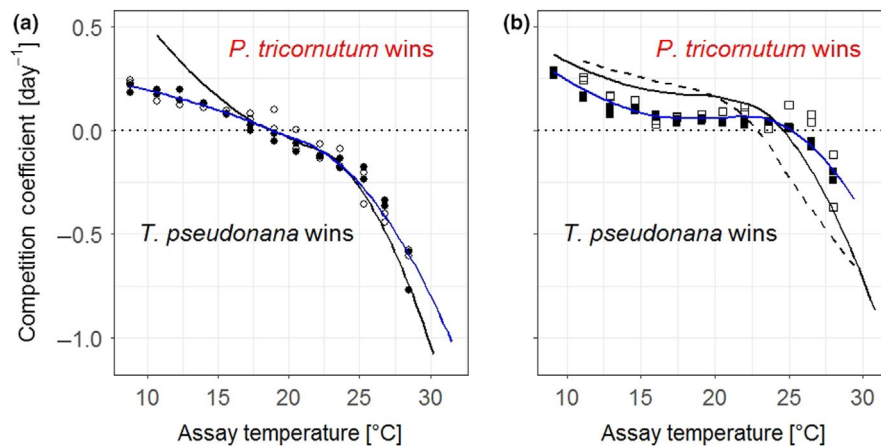


FIGURE 6 Predicted (black lines) and observed (symbols) competition coefficients between *Phaeodactylum tricornutum* and *Thalassiosira pseudonana* across assay temperatures in (a) high N conditions and (b) low N conditions. A coefficient of 0 indicates no competitive advantage for either species and predicts stable coexistence under the assay conditions. At coefficients greater than 0, *Phaeodactylum tricornutum* has the competitive advantage, and at coefficients below 0, *Thalassiosira pseudonana* has the advantage. The further the competition coefficient deviates from 0, the stronger is the competition between the two species. In (a), the solid black line indicates predictions for competition coefficients made from high N monoculture growth rates. The solid blue line is the LOESS smooth to visualize the progression of all observed high N competition coefficients across temperatures ($R^2 = 0.97$, $RSE = 0.047$). Observed coefficients were calculated from changes in species frequencies over time in mixed cultures (data from Figure S10), calculated with Equation (5). Closed symbols represent the competition coefficients that were started when stock cultures were transferred to the temperature-gradient block, open symbols those that were started 2 weeks later to investigate the potential effects of temperature acclimation. In (b), solid black line indicates predictions made from the initial exponential growth rate in low N medium for monocultures, whereas the dashed line indicates predictions made from monoculture carrying capacities across the temperature gradient. The solid blue line is the LOESS smooth to visualize the progression of all observed low N competition coefficients across temperatures ($R^2 = 0.86$, $RSE = 0.051$). Observed coefficients were calculated from changes in species frequencies over time in mixed cultures (data from Figure S11), calculated with Equation (5). Closed symbols represent competition replicates that were started at the onset of N limitation, and open symbols those that were started from monocultures that were cultured under N limitation for an additional 7 days

Competition coefficients calculated from K predicted the switch at 22.9°C (4.2°C warmer than under high N conditions; dotted black line in Figure 6b, $R^2 = 0.992$, and $RSE = 0.039$). Competition was predicted to be strongest at assay temperatures where the growth rates or carrying capacities in monocultures exhibited greatest divergence between species. Naturally, a species would lose the competition at an assay temperature where it could not sustain growth as an isolated species, having reached its physiological limits. Between the upper and lower temperature thresholds where both species could grow, the competitive outcomes were determined by the thermal growth performances of the species in isolation.

When the two diatoms were mixed together and competed against one another, the observed competition coefficients displayed a similar progression across assay temperatures as the predictions. In high N conditions, inflexion points occurred at $18.8 \pm 1.2^\circ\text{C}$ (predicted at 18.8°C) (Figure 6a). As predicted, *P. tricornutum* won competitions across temperatures colder than the inflexion point, whereas *T. pseudonana* won competitions at temperatures warmer than the inflexion point. When the nitrate concentration was reduced, the competitive switch occurred at a warmer temperature, as predicted from the temperature dependencies of low N growth rates and carrying capacities (Figure 6b). The average temperature for the

inflexion point in low N medium was 6.5°C greater than in high N medium and differed significantly ($F_{1,6} = 83.11, p < .001$) (Table S15). The inflexion point was located at $25.3 \pm 0.6^\circ\text{C}$ (predicted at 24.6°C when growth rate was used to calculate the competition coefficients or 22.9°C when carrying capacity was used for the prediction). Pooling of mixed culture replicates for the final analysis due to a lack of a temperature acclimation signal in the high N scenario did not affect our interpretation of the conclusion that the competitive shift occurred at higher temperatures in the low N scenario.

3.3 | Predictability of change in competitive ability

In both nutrient scenarios, the predicted and observed competition coefficients were strongly correlated (R^2 -values of 0.76–0.98), indicating that competition coefficients were very predictable from growth in monocultures (Table 1).

Progression of predicted and observed competition coefficients across temperatures was very similar, yet deviations existed between predictions and observations. For example in high N conditions, observed coefficients tended to be lower than predictions across the five lowest assay temperatures, and therefore, observed competition was not as strong as predicted across the assay temperatures where *P. tricornutum* outcompeted *T. pseudonana* (competition coefficient > 0). Likewise, across the temperatures at which *T. pseudonana* was predicted to win (competition coefficient < 0), the strength of the competition coefficients was slightly overestimated and predicted to be more negative than observed values (Figure 6a).

In low N conditions, the predicted and observed coefficients aligned less strongly than in high N conditions, but correlation was still high (see R^2 in Table 1). Predictions were more accurate when they were made from low N growth rates than from carrying capacities (Figure 6b). As with the high N experiment, the predicted coefficients were typically stronger than the observed. In addition, both low N predictions underestimated the temperature of the inflexion

point and predicted the competitive advantage to switch at a lower assay temperature than it did in the experiment, therefore, underestimating the temperature range at which *P. tricornutum* was the better competitor.

4 | DISCUSSION

In this study, competition between *P. tricornutum* and *T. pseudonana* was determined primarily by the growth performance of these species under specified thermal and nutrient regimes in isolation and indicated that they did not interact strongly in mixed populations. The results provide support for our hypotheses as we show that in relatively simple systems, prediction of competitive outcomes from isolated species performance across a thermal gradient is possible. The amount of N present in the mixed cultures influenced the competition across the temperature gradient and showed that alterations in nutrient concentrations have the potential to change the outcomes of competition with all else being constant. Further aligning with our hypothesis, the better growing species in isolation had the competitive advantage in mixed cultures, with the switch in competitive advantage occurring at or close to the temperature where the TPCs of the two species intercepted. The poorer competitor also lost the competition quicker when the absolute differences between monoculture thermal performances were the largest.

4.1 | Reduced nitrogen impacts competition across temperatures

Under low N conditions, we observed *P. tricornutum* to be the better competitor across most of the tested assay temperatures. Although N uptake rates were not measured in this experiment, the increased competitive success of *P. tricornutum* in low N conditions, and a warmer inflexion temperature of competitive advantage as a result

TABLE 1 Parameters for linear models ($y = ax + b$) correlating predicted (x) and observed competition coefficients (y) across assay temperatures

Correlation	Linear model parameters					p-value of correlation
	R^2 of correlation	Slope \pm 95%-confidence interval	y-Intercept \pm 95%-confidence interval	df	t-value	
High N growth rates with competition coefficients (n = 13)	0.98	1.37 ± 0.13	0.06 ± 0.04	11	22.60	<.001*
Low N growth rates with competition coefficients (n = 14)	0.93	1.73 ± 0.29	-0.01 ± 0.05	12	13.09	<.001*
Low N carrying capacity with competition coefficients (n = 13)	0.76	1.96 ± 0.72	-0.05 ± 0.11	11	5.98	<.001*

Note: Significant correlations (alpha level of 0.05) that conclude a relationship between predictions and observations are marked in bold and with an asterisk.

thereof, could be attributed to its previously reported high affinity and high uptake rates for nitrogen (Goldman & Ryther, 1976; Grover, 1991; Sharp, Underhill, & Hughes, 1979). This may have facilitated *P. tricornutum* to win competitions across most of the N-limited temperature gradient, including at assay temperatures up to 3.2°C warmer than predicted (22.9°C prediction from K across temperatures compared to warmest observed inflexion point in low N conditions at 26.1°C). To confirm that the increased competitive success can be explained through better nitrogen uptake rates and storage abilities, future experiments should quantify N uptake rates of the two species under the assay conditions described in this study. Its good nitrogen uptake ability could help *P. tricornutum* to win competitions under N-limiting conditions at temperatures where other species can normally reach higher carrying capacities or grow faster when N is not limiting. However, the high N affinity of *P. tricornutum* may be nullified in conditions where N content of surface waters is high. For *T. pseudonana*, the reduction in μ_{\max} and shift of T_{opt} toward colder temperatures in low N conditions was in accordance with Grimaud, Mairet, Sciandra, and Bernard (2017) and confirmed the effect of nitrogen concentration on *T. pseudonana* growth rates. This change in thermal performance indicates that *T. pseudonana* may become less competitive in warm N-limited waters, but its competitive ability should be reinstated following the introduction of N into a system, for example, in coastal up-welling zones.

Despite presumed better nitrogen uptake abilities, *P. tricornutum* did not win all competitions across the whole assay-temperature gradient in low N conditions. This may be due to the fact that good N uptake ability was offset toward the warm assay temperatures by physiological limits for growth of this diatom. Past research has identified R^* across temperatures as a U-shaped function (Lewington-Pearce et al., 2019; Tilman, Mattson, & Langer, 1981), and warmer temperatures were found to increase nitrogen demand in phytoplankton (Toseland et al., 2013). Toward the growth limits, the minimum nutrient requirements for a species rise rapidly within a small temperature range as cells become stressed and need a larger internal nutrient content (cell quota) to survive while other physiological limits become more important (Rhee & Gotham, 1981; Thomas et al., 2017; Tilman, 1981). The circumstance that cell size was also found to display a U-shaped trend with assay temperatures could have reinforced the observed patterns of competition across the assay-temperature gradient. Cell size is known to play a role in competitive success and species dominance because larger, slower growing cells tend to have lower nutrient uptake rates relative to smaller cells with more beneficial surface-area-to-volume ratios (Gallego, Venail, & Ibelings, 2019; Litchman & Klausmeier, 2008; Smith & Kalff, 1982). This study provides further support of this relationship, whereby cells growing toward their physiological limits (thermal extremes) were larger and grew slower, thus potentially amplifying the rate at which a species was losing competitions close to its physiological limits. As surface temperatures are expected to increase in aquatic systems worldwide, this temperature dependence of R^* and cell size might play a crucial role for population dynamics under warming scenarios in future marine and freshwater ecosystems (Bernhardt, Sunday, &

O'Connor, 2018; Lewington-Pearce et al., 2019). Approaching physiological limits through warming might shift abiotic conditions in a direction in which a competitor might be at a loss although it is generally better at taking up nutrients in more moderate environments. Such an environmental change toward more critical conditions might offset the ability of a species to reduce nutrients to a concentration that is lower than the R^* of a direct competitor (McPeck, 2019).

The observed changes in species frequencies over time in the low N scenario may have been due to interspecific differences in the capacity for surge uptake. Greater capacity for surge uptake is commonly defined as higher values of the maximum velocity of nutrient uptake (V_{\max} in the Michaelis–Menten equation), induced in phytoplankton as a physiological adjustment to nutrient limitation (Morel, 1987). The species with the greater capacity to increase V_{\max} will sequester nutrients quicker, effectively depriving them from the competitor with a lower capacity to increase V_{\max} . In our low N experiment, daily additions of fresh medium were followed by extensive phases of nutrient starvation when this added nitrate was fully taken up. Because we did not measure nitrate uptake kinetics, we cannot conclude from our experiments whether the outcome of competition depended on the ability to sequester nitrate quickly after N addition or the ability to live off the lowest nitrate concentrations (interspecific differences in the half saturation constant for uptake, K_m of the Michaelis–Menten curve). The growth rates calculated from the increase in fluorescence during the first few days of the low N monocultures might be indicative of surge uptake playing a role in the competitive success under low N conditions. The predictions of competitive outcomes from the exponential growth phase in low N medium did align closer with the observed competitions than the predictions from carrying capacities (see Figure 6b). However, using fluorescence-based growth rates or maximum K under low N conditions as predictors of competition can be regarded as proxies at best. Confirmation of a role for surge uptake in competition between these two species requires further experiments. The determination of N uptake rates and residual nitrate concentrations using more sensitive methods (e.g., stable isotopes) may help improve predictions of competitive success.

4.2 | Predictability of competition under environmental change

In this study, monoculture responses of phytoplankton were found to be good predictors of competitive outcomes. Previously, they also have been identified as good predictors of phytoplankton biogeography (Barton, Irwin, Finkel, & Stock, 2016; Thomas, Kremer, Klausmeier, & Litchman, 2012). Whether such culture-based measurements are ultimately suitable for forecasting shifts in phytoplankton communities in response to environmental change and whether the findings can be generalized for other species pairs or taxa remains to be tested. Predictability of competitive outcomes in complex communities still presents a major challenge (Pennekamp et al., 2019).

As the species in this study did not appear to influence one another in mixed cultures, it is likely that allelopathic interactions did not play a role in this competition scenario. Indeed, monoculture performance would cease to be a good predictor of competitive ability if one species had a toxic effect on the other in a two species competition. For example, dinoflagellates can inhibit growth of competitors by releasing toxins (e.g., Kubanek, Hicks, Naar, & Villareal, 2005), and some diatoms excrete chemicals that inhibit growth of other diatoms (Pichierri et al., 2017). A slower growing species might be able to gain a competitive advantage through the excretion of allelopathic substances upon sensing another species in its surrounding. Such species-specific interactions may explain some of the uncertainty in modeling natural phytoplankton communities. Furthermore, TPCs for growth of the same species were found to vary slightly from laboratory to laboratory even when similar protocols were employed (Boyd et al., 2013). These differences could be driven in part by data quality and model fitting (Low-Décarie et al., 2017), but they still raise concerns that predictability of competition response, which is dependent on thermal niche parameters and μ_{max} , only remain valid within a specific setting. In addition, adaptive changes in nutrient requirements or physiological parameters could change competitive abilities and reduce predictability. Elucidating the role of evolutionary change and whether long-term interactions are affected by genotypic variability will therefore play a crucial role in understanding future phytoplankton community structure (Bernhardt et al., 2020).

Our observations in monocultures were suitable for predicting the inflexion points of competition. However, the predictions across the whole temperature range commonly overestimated the magnitude of competition coefficients, and this increased the further the coefficients were from 0 (see Figure 6). The mismatch between predicted and observed coefficients at the extreme temperatures may be due to the fact that light microscopy counts could not distinguish between viable and nonviable cells. The outcome being that cell frequency counts overestimated the number of reproducing cells of the losing competitor and incorrectly tipping the competition coefficient in its favor. Future studies could employ the use of a cell viable stains to discriminate between live and dead cells (e.g., Baker et al., 2018) when conducting cell frequency counts.

4.3 | Wider implications of the study

The nitrogen loads to many coastal waters are predicted to increase in the future due to agricultural runoff or other human activities (Beman, Arrigo, & Matson, 2005; Nixon, 1995), and surface waters are expected to become more stratified as warming increases (Bestion, Schaum, et al., 2018). The findings that competitive outcomes change across temperatures and are dependent on the amount of N present in the experimental system imply that environmental changes and alterations of marine environments will affect how phytoplankton communities will be structured in the future. Changes in species interactions could then have subsequent effects on ecosystem functioning since distinctively structured communities

cycle nutrients and carbon differently or have varying nutritional value for higher trophic levels (Falkowski, Barber, & Smetacek, 1998; Litchman, Klausmeier, Miller, Schofield, & Falkowski, 2006; Schaum, Rost, Millar, & Collins, 2012).

Regardless of the importance for natural ecosystems, the finding that competitive outcomes could be well predicted in a simplified system could be of relevance for large scale pond maricultures or other algae biotechnological settings where simple model communities or monocultures are established for harvest or extraction of secondary metabolites. The ability to predict what the population composition would be under a defined set of abiotic parameters could help to control growth dynamics or purity of a culture (Regan & Ivancic, 1984). By being able to predict composition, parameters can be altered to potentially stabilize mixed cultures or purify them through changing temperature or nutrient loading.

5 | CONCLUSION

The current study demonstrated that competition between two diatoms could be well predicted in a controlled laboratory system. The aquatic environments where these algae naturally occur are however exposed to fluctuations in light, nutrients, temperature, as well as changes in species composition due to migrations and water currents. In order to achieve higher comparability with natural environments, further investigations should focus on the effects of temperature variations and other abiotic fluctuations and their effects on competition between these two diatoms. Other species combinations and more complex communities could also be investigated to understand how general the current findings are. The ability to predict where inflexion points of species interactions lie across gradients and when multiple environmental stressors interact will bring the scientific community closer to understanding nonlinear ecosystem responses and help to potentially find strategies to mitigate changes that are predicted to occur under future environmental scenarios.

ACKNOWLEDGMENTS

The authors would like to thank all the laboratory technicians at the University of Essex that contributed to the setup of this work and the running of laboratory facilities, specifically Tania Cresswell-Maynard, Amanda Clements, John Green, and Dr. Phil Davey. The work was made possible through the University of Essex School of Life Sciences start-up grant of Etienne Low-Décarie. Kirralee G. Baker was supported by NERC grant NE/P002374/1 awarded to Richard Geider. The authors would also like to thank two anonymous reviewers for their invaluable improvements to this manuscript.

CONFLICT OF INTEREST

None declared.

AUTHOR CONTRIBUTIONS

Philipp Siegel: Conceptualization (lead); Data curation (lead); Formal analysis (lead); Investigation (lead); Methodology (lead);

Project administration (lead); Validation (lead); Visualization (lead); Writing-original draft (lead); Writing-review & editing (lead). **Kirralee G. Baker:** Data curation (supporting); Formal analysis (supporting); Investigation (supporting); Methodology (supporting); Project administration (supporting); Validation (supporting); Writing-original draft (supporting); Writing-review & editing (supporting). **Etienne Low-Décarie:** Conceptualization (supporting); Data curation (supporting); Formal analysis (supporting); Funding acquisition (lead); Supervision (lead); Validation (supporting); Visualization (supporting); Writing-original draft (supporting); Writing-review & editing (supporting). **Richard J. Geider:** Conceptualization (supporting); Data curation (supporting); Formal analysis (supporting); Funding acquisition (supporting); Investigation (supporting); Methodology (supporting); Supervision (supporting); Validation (supporting); Visualization (supporting); Writing-original draft (supporting); Writing-review & editing (supporting).

DATA AVAILABILITY STATEMENT

Collected data and R script used for the analysis of the publication can be downloaded via the publicly accessible repository "Knowledge Network for Biocomplexity" under <https://knb.ecoinformatics.org/view/urn:uuid:11f6dc8a-91cc-4c9d-8cf0-00366b3b0374>.

ORCID

Philipp Siegel  <https://orcid.org/0000-0002-1755-083X>

Kirralee G. Baker  <https://orcid.org/0000-0003-3008-2513>

Etienne Low-Décarie  <https://orcid.org/0000-0002-0413-567X>

Richard J. Geider  <https://orcid.org/0000-0003-3276-047X>

REFERENCES

- Andersen, R. A. (2005). *Algal culturing techniques* (1st ed., p. 596). Cambridge, MA: Elsevier Academic Press.
- Baker, K. G., Radford, D. T., Evenhuis, C., Kuzhiumparam, U., Ralph, P. J., & Doblin, M. A. (2018). Thermal niche evolution of functional traits in a tropical marine phototroph. *Journal of Phycology*, 54(6), 799–801. <https://doi.org/10.1111/jpy.12759>
- Barton, A. D., Irwin, A. J., Finkel, Z. V., & Stock, C. A. (2016). Anthropogenic climate change drives shift and shuffle in North Atlantic phytoplankton communities. *Proceedings of the National Academy of Sciences of the United States of America*, 201519080, <https://doi.org/10.1073/pnas.1519080113>
- Begon, M., Townsend, C. R., & Harper, J. L. (2006). *Ecology: From individuals to ecosystems* (4th ed., p. 738). Malden, MA: Blackwell Pub.
- Beman, J. M., Arrigo, K. R., & Matson, P. A. (2005). Agricultural runoff fuels large phytoplankton blooms in vulnerable areas of the ocean. *Nature*, 434(7030), 211–214. <https://doi.org/10.1038/nature03370>
- Berges, J. A., Franklin, D. J., & Harrison, P. J. (2001). Evolution of an artificial seawater medium: Improvements in enriched seawater, artificial water over the last two decades. *Journal of Phycology*, 37(6), 1138–1145. <https://doi.org/10.1046/j.1529-8817.2001.01052.x>
- Bernhardt, J. R., Kratina, P., Pereira, A. L., Tamminen, M., Thomas, M. K., & Narwani, A. (2020). The evolution of competitive ability for essential resources. *Philosophical Transactions of the Royal Society B: Biological Sciences*, 375, 20190247. <https://doi.org/10.1098/rstb.2019.0247>
- Bernhardt, J. R., Sunday, J. M., & O'Connor, M. I. (2018). Metabolic theory and the temperature-size rule explain the temperature dependence of population carrying capacity. *American Naturalist*, 192(6), 687–697. <https://doi.org/10.1086/700114>
- Bestion, E., García-Carreras, B., Schaum, C.-E., Pawar, S., & Yvon-Durocher, G. (2018). Metabolic traits predict the effects of warming on phytoplankton competition. *Ecology Letters*, 21(5), 655–664. <https://doi.org/10.1111/ele.12932>
- Bestion, E., Schaum, C.-E., & Yvon-Durocher, G. (2018). Nutrient limitation constrains thermal tolerance in freshwater phytoplankton: Nutrients alter algal thermal tolerance. *Limnology and Oceanography Letters*, 3(6), 436–443. <https://doi.org/10.1002/lol2.10096>
- Boyd, P. W., Rynearson, T. A., Armstrong, E. A., Fu, F., Hayashi, K., Hu, Z., ... Thomas, M. K. (2013). Marine phytoplankton temperature versus growth responses from polar to tropical waters – Outcome of a scientific community-wide study. *PLoS One*, 8(5), e63091. <https://doi.org/10.1371/journal.pone.0063091>
- Clements, F. E., & Shelford, V. E. (1939). *Bio-ecology* (1st ed., p. 400). New York, NY: J. Wiley & Sons, Inc. <https://doi.org/10.5962/bhl.title.6424>
- Cloern, J. E., & Dufford, R. (2005). Phytoplankton community ecology: Principles applied in San Francisco Bay. *Marine Ecology Progress Series*, 285, 11–28. <https://doi.org/10.3354/meps285011>
- Cresswell, R. C., & Syrett, P. J. (1982). The uptake of nitrite by the diatom *Phaeodactylum*: Interactions between nitrite and nitrate. *Journal of Experimental Botany*, 33(137), 1111–1121. <https://doi.org/10.1038/s41396-018-0330-7>
- Falkowski, P. G., Barber, R. T., & Smetacek, V. (1998). Biogeochemical controls and feedbacks on ocean primary production. *Science*, 281(5374), 200–206. <https://doi.org/10.1126/science.281.5374.200>
- Gallego, I., Venail, P., & Ibelings, B. W. (2019). Size differences predict niche and relative fitness differences between phytoplankton species but not their coexistence. *ISME Journal*, 13(5), 1133–1143. <https://doi.org/10.1038/s41396-018-0330-7>
- Geider, R. J., MacIntyre, H. L., & Kana, T. M. (1997). Dynamic model of phytoplankton growth and acclimation: Responses of the balanced growth rate and the chlorophyll a:carbon ratio to light, nutrient-limitation and temperature. *Marine Ecology Progress Series*, 148, 187–200. <https://doi.org/10.3354/meps148187>
- Geider, R. J., MacIntyre, H. L., & Kana, T. M. (1998). A dynamic regulatory model of phytoplanktonic acclimation to light, nutrients, and temperature. *Limnology and Oceanography*, 43(4), 679–694. <https://doi.org/10.4319/lo.1998.43.4.0679>
- Geider, R. J., Osbonie, B. A., & Raven, J. A. (1986). Growth, photosynthesis and maintenance metabolic cost in the diatom *Phaeodactylum tricornutum* at very low light levels. *Journal of Phycology*, 22(1), 39–48. <https://doi.org/10.1111/j.1529-8817.1986.tb02513.x>
- Goldman, J. C., & Ryther, J. H. (1976). Temperature-influenced species competition in mass cultures of marine phytoplankton. *Biotechnology and Bioengineering*, 18(8), 1125–1144. <https://doi.org/10.1002/bit.260180809>
- Grimaud, G. M., Mairet, F., Sciandra, A., & Bernard, O. (2017). Modeling the temperature effect on the specific growth rate of phytoplankton: A review. *Reviews in Environmental Science & Biotechnology*, 16(4), 625–645. <https://doi.org/10.1007/s11157-017-9443-0>
- Grover, J. P. (1991). Resource competition in a variable environment: Phytoplankton growing according to the variable-internal-stores model. *American Naturalist*, 138(4), 811–835. <https://doi.org/10.1086/285254>
- Guillard, R. R. L., & Kilham, P. (1977). *The biology of diatoms* (1st ed., p. 497). Oakland, CA: Botanical Monographs. University of California Press.
- Guillard, R. R. L., & Ryther, J. H. (1962). Studies of marine planktonic diatoms: I. *Cyclotella nana* Hustedt, and *Detonula confervacea* (Cleve) Gran. *Canadian Journal of Microbiology*, 8(2), 229–239. <https://doi.org/10.1139/m62-029>

- Harley, C. D. G., Connell, S. D., Doubleday, Z. A., Kelaher, B., Russell, B. D., Sarà, G., & Helmuth, B. (2017). Conceptualizing ecosystem tipping points within a physiological framework. *Ecology and Evolution*, 7(15), 6035–6045. <https://doi.org/10.1002/ece3.3164>
- Harrison, P. J., Waters, R. E., & Taylor, F. J. R. (1980). A broad spectrum artificial seawater medium for coastal and open ocean phytoplankton. *Journal of Phycology*, 16, 28–35. <https://doi.org/10.1111/j.0022-3646.1980.00028.x>
- Huisman, J., Jonker, R. R., Zonneveld, C., & Weissing, F. J. (1999). Competition for light between phytoplankton species: Experimental tests of mechanistic theory. *Ecology*, 80(1), 211–222. [https://doi.org/10.1890/0012-9658\(1999\)080\[0211:CFLBPS\]2.0.CO;2](https://doi.org/10.1890/0012-9658(1999)080[0211:CFLBPS]2.0.CO;2)
- Hutchinson, G. E. (1961). The paradox of the plankton. *American Naturalist*, 95(882), 137–145. <https://doi.org/10.1086/282171>
- Isnanto, R. R. (2011). Comparison on several smoothing methods in non-parametric regression. *Jurnal Sistem Komputer*, 1(1), 41–47.
- Jacoby, W. G. (2000). Loess: A nonparametric, graphical tool for depicting relationships between variables. *Electoral Studies*, 19, 577–613. [https://doi.org/10.1016/S0261-3794\(99\)00028-1](https://doi.org/10.1016/S0261-3794(99)00028-1)
- Kordas, R. L., Harley, C. D. G., & O'Connor, M. I. (2011). Community ecology in a warming world: The influence of temperature on interspecific interactions in marine systems. *Journal of Experimental Marine Biology and Ecology*, 400(1–2), 218–226. <https://doi.org/10.1016/j.jembe.2011.02.029>
- Kubaneck, J., Hicks, M. K., Naar, J., & Villareal, T. A. (2005). Does the red tide dinoflagellate *Karenia brevis* use allelopathy to outcompete other phytoplankton? *Limnology and Oceanography*, 50(3), 883–895. <https://doi.org/10.4319/lo.2005.50.3.0883>
- Lewington-Pearce, L., Narwani, A., Thomas, M. K., Kremer, C. T., Vogler, H., & Kratina, P. (2019). Temperature-dependence of minimum resource requirements alters competitive hierarchies in phytoplankton. *Oikos*, 128(8), 1194–1205. <https://doi.org/10.1111/oik.06060>
- Litchman, E., & Klausmeier, C. A. (2008). Trait-based community ecology of phytoplankton. *Annual Review of Ecology Evolution and Systematics*, 39, 615–639. <https://doi.org/10.1146/annurev.ecolsys.39.110707.173549>
- Litchman, E., Klausmeier, C. A., Miller, J. R., Schofield, O. M., & Falkowski, P. G. (2006). Multi-nutrient, multi-group model of present and future oceanic phytoplankton communities. *Biogeosciences Discuss*, 3(3), 607–663. <https://doi.org/10.5194/bg-3-585-2006>
- Low-Décarie, E., Boatman, T. G., Bennett, N., Passfield, W., Gavalás-Olea, A., Siegel, P., & Geider, R. J. (2017). Predictions of response to temperature are contingent on model choice and data quality. *Ecology and Evolution*, 7(23), 10467–10481. <https://doi.org/10.1002/ece3.3576>
- Low-Décarie, E., Fussmann, G. F., & Bell, G. (2011). The effect of elevated CO₂ on growth and competition in experimental phytoplankton communities: CO₂ alters phytoplankton community dynamics. *Global Change Biology*, 17(8), 2525–2535. <https://doi.org/10.1111/j.1365-2486.2011.02402.x>
- McPeck, M. A. (2019). Limiting similarity? The ecological dynamics of natural selection among resources and consumers caused by both apparent and resource competition. *American Naturalist*, 193(4), E92–E115. <https://doi.org/10.1086/701629>
- Montagnes, D. J. S., Morgan, G., Bissinger, J. E., Atkinson, D., & Weisse, T. (2008). Short-term temperature change may impact freshwater carbon flux: A microbial perspective. *Global Change Biology*, 14(12), 2823–2838. <https://doi.org/10.1111/j.1365-2486.2008.01700.x>
- Morel, F. M. M. (1987). Kinetics of nutrient uptake and growth in phytoplankton. *Journal of Phycology*, 23, 137–150. <https://doi.org/10.1111/j.1529-8817.1987.tb04436.x>
- Nelson, D. M., D'Elia, C. F., & Guillard, R. R. L. (1979). Growth and competition of the marine diatoms *Phaeodactylum tricornutum* and *Thalassiosira pseudonana*. II. Light limitation. *Marine Biology*, 50(4), 313–318. <https://doi.org/10.1007/BF00387008>
- Nixon, S. W. (1995). Coastal marine eutrophication: A definition, social causes, and future concerns. *Ophelia*, 41, 199–219. <https://doi.org/10.1080/00785236.1995.10422044>
- Parkhill, J.-P., Maillet, G., & Cullen, J. J. (2001). Fluorescence-based maximal quantum yield for PSII as a diagnostic of nutrient stress. *Journal of Phycology*, 37(4), 517–529. <https://doi.org/10.1046/j.1529-8817.2001.037004517.x>
- Pennekamp, F., Iles, A. C., Garland, J., Brennan, G., Brose, U., Gaedke, U., ... Petchey, O. L. (2019). The intrinsic predictability of ecological time series and its potential to guide forecasting. *Ecological Monographs*, 89(2), 1–17. <https://doi.org/10.1002/ecm.1359>
- Pichierri, S., Accoroni, S., Pezzolesi, L., Guerrini, F., Romagnoli, T., Pistocchi, R., & Totti, C. (2017). Allelopathic effects of diatom filtrates on the toxic benthic dinoflagellate *Ostreopsis cf. ovata*. *Marine Environment Research*, 131, 116–122. <https://doi.org/10.1016/j.marenvres.2017.09.016>
- R Core Team (2016). *R: A language and environment for statistical computing*. Vienna, Austria: R Foundation for Statistical Computing.
- Ratkowsky, D. A., Lowry, R. K., McMeekin, T. A., Stokes, A. N., & Chandler, R. E. (1983). Model for bacterial culture growth rate throughout the entire biokinetic temperature range. *Journal of Bacteriology*, 154(3), 1222–1226. <https://doi.org/10.1128/JB.154.3.1222-1226.1983>
- Regan, D. L., & Ivancic, N. (1984). Mixed populations of marine microalgae in continuous culture: Factors affecting species dominance and biomass productivity. *Biotechnology and Bioengineering*, 26(11), 1265–1271. <https://doi.org/10.1002/bit.260261102>
- Rhee, G.-Y., & Gotham, I. J. (1981). The effect of environmental factors on phytoplankton growth: Temperature and the interactions of temperature with nutrient limitation: Temperature-nutrient interactions. *Limnology and Oceanography*, 26(4), 635–648. <https://doi.org/10.4319/lo.1981.26.4.0635>
- Riebesell, U. (2004). Effects of CO₂ enrichment on marine phytoplankton. *Journal of Oceanography*, 60(4), 719–729. <https://doi.org/10.1007/s10872-004-5764-z>
- Schaum, E., Rost, B., Millar, A. J., & Collins, S. (2012). Variation in plastic responses of a globally distributed picoplankton species to ocean acidification. *Nature Climate Change*, 3(3), 298–302. <https://doi.org/10.1038/nclimate1774>
- Schnetger, B., & Lehnert, C. (2014). Determination of nitrate plus nitrite in small volume marine water samples using vanadium(III)chloride as a reduction agent. *Marine Chemistry*, 160, 91–98. <https://doi.org/10.1016/j.marchem.2014.01.010>
- Segura, A. M., Calliari, D., Kruk, C., Conde, D., Bonilla, S., & Fort, H. (2011). Emergent neutrality drives phytoplankton species coexistence. *Proceedings of the Royal Society B-Biological Sciences*, 278(1716), 2355–2361. <https://doi.org/10.1098/rspb.2010.2464>
- Sharp, J. H., Underhill, P. A., & Hughes, D. J. (1979). Interaction (Allelopathy) between marine diatoms: *Thalassiosira pseudonana* and *Phaeodactylum tricornutum*. *Journal of Phycology*, 15, 353–362. <https://doi.org/10.1111/j.1529-8817.1979.tb00705.x>
- Smith, R. E. H., & Kalff, J. (1982). Size-dependent phosphorus uptake kinetics and cell quota in phytoplankton. *Journal of Phycology*, 18, 275–284. <https://doi.org/10.1111/j.1529-8817.1982.tb03184.x>
- Sommer, U. (1984). The paradox of the plankton: Fluctuations of phosphorus availability maintain diversity of phytoplankton in flow-through cultures. *Limnology and Oceanography*, 29(3), 633–636. <https://doi.org/10.4319/lo.1984.29.3.0633>
- Thomas, M. K., Aranguren-Gassis, M., Kremer, C. T., Gould, M. R., Anderson, K., Klausmeier, C. A., & Litchman, E. (2017). Temperature-nutrient interactions exacerbate sensitivity to warming in phytoplankton. *Global Change Biology*, 23(8), 3269–3280. <https://doi.org/10.1111/gcb.13641>

- Thomas, M. K., Kremer, C. T., Klausmeier, C. A., & Litchman, E. (2012). A global pattern of thermal adaptation in marine phytoplankton. *Science*, 338(6110), 1085–1088. <https://doi.org/10.1126/science.1224836>
- Tilman, D. (1981). Tests of resource competition theory using four species of lake Michigan algae. *Ecology*, 62(3), 802–815. <https://doi.org/10.2307/1937747>
- Tilman, D. (1987). Importance of mechanisms of interspecific competition. *American Naturalist*, 129(5), 769–774.
- Tilman, D., Kilham, S. S., & Kilham, P. (1982). Phytoplankton community ecology: The role of limiting nutrients. *Annual Review of Ecology and Systematics*, 13, 349–372. <https://doi.org/10.1146/annurev.es.13.110182.002025>
- Tilman, D., Mattson, M., & Langer, S. (1981). Competition and nutrient kinetics along a temperature gradient: An experimental test of a mechanistic approach to niche theory. *Limnology and Oceanography*, 26(6), 1020–1033. <https://doi.org/10.4319/lo.1981.26.6.1020>
- Toseland, A., Daines, S. J., Clark, J. R., Kirkham, A., Strauss, J., Uhlig, C., ... Mock, T. (2013). The impact of temperature on marine phytoplankton resource allocation and metabolism. *Nature Climate Change*, 3(11), 979–984. <https://doi.org/10.1038/nclimate1989>
- van Donk, E., & Kilham, S. S. (1990). Temperature effects on silicon- and phosphorus-limited growth and competitive interactions among three diatoms. *Journal of Phycology*, 26(1), 40–50. <https://doi.org/10.1111/j.0022-3646.1990.00040.x>

SUPPORTING INFORMATION

Additional supporting information may be found online in the Supporting Information section.

How to cite this article: Siegel P, Baker KG, Low-Décarie E, Geider RJ. High predictability of direct competition between marine diatoms under different temperatures and nutrient states. *Ecol Evol.* 2020;00:1–15. <https://doi.org/10.1002/ece3.6453>